2015

Collagen Crosslinking Reagent Utilized to Modify the Mechanical Properties of the Soft Palate in Equine Snoring and Apnea Applications

Stephanie L. Hunt
University of Kentucky, stephanie.louise.hunt@gmail.com

STUDENT AGREEMENT:

I represent that my thesis or dissertation and abstract are my original work. Proper attribution has been given to all outside sources. I understand that I am solely responsible for obtaining any needed copyright permissions. I have obtained needed written permission statement(s) from the owner(s) of each third-party copyrighted matter to be included in my work, allowing electronic distribution (if such use is not permitted by the fair use doctrine) which will be submitted to UKnowledge as Additional File.

I hereby grant to The University of Kentucky and its agents the irrevocable, non-exclusive, and royalty-free license to archive and make accessible my work in whole or in part in all forms of media, now or hereafter known. I agree that the document mentioned above may be made available immediately for worldwide access unless an embargo applies.

I retain all other ownership rights to the copyright of my work. I also retain the right to use in future works (such as articles or books) all or part of my work. I understand that I am free to register the copyright to my work.

REVIEW, APPROVAL AND ACCEPTANCE

The document mentioned above has been reviewed and accepted by the student's advisor, on behalf of the advisory committee, and by the Director of Graduate Studies (DGS), on behalf of the program; we verify that this is the final, approved version of the student's thesis including all changes required by the advisory committee. The undersigned agree to abide by the statements above.

Stephanie L. Hunt, Student

Dr. Thomas Hedman, Major Professor

Dr. Abhijit Patwardhan, Director of Graduate Studies

COLLAGEN CROSSLINKING REAGENT UTILIZED TO MODIFY THE MECHANICAL PROPERTIES OF THE SOFT PALATE IN EQUINE SNORING AND APNEA APPLICATIONS

THESIS

A thesis submitted in partial fulfillment of the
requirements for the degree of Master of Science in
Biomedical Engineering in the College of Engineering
at the University of Kentucky

By

Stephanie Louise Hunt

Lexington, Kentucky

Director: Dr. Thomas Hedman, Professor of Biomedical Engineering

Lexington, Kentucky

2015

ABSTRACT OF THESIS

COLLAGEN CROSSLINKING REAGENT UTILIZED TO MODIFY THE MECHANICAL PROPERTIES OF THE SOFT PALATE IN EQUINE SNORING AND APNEA APPLICATIONS

Snoring is a sleep disruption that can lead to obstructive sleep apnea (OSA), which interrupts breathing by obstructing the airway. Injecting a protein crosslinker, such as genipin, into the soft palate could decrease the severity of snoring and OSA by stiffening the soft palate. Equine soft palates modeled human palates due to a high incidence of awake snoring and apnea.

The pilot *in vivo* study treated six horses with two 100 mM injections of the buffered genipin reagent. The efficacy phase horses underwent respiratory audio recordings to document snoring changes using Matlab and ImageJ in the time and frequency domains. Histological analysis was completed on the safety phase palates post treatment.

All horses were successfully treated with the genipin injections. At least one horse showed high frequency amplitude reductions, and all horses had low frequency amplitude reductions, correlating to a reduction in palatal displacement and snoring loudness. One efficacy horse appears to have been completely cured. The histological analysis presented tissue damage, mucosal tissue damage, and mild inflammation due to palate expansion and errant injections.

Different injection volumes and techniques should be investigated next. Applying this treatment to human studies for snoring and OSA applications is the ultimate goal.

KEYWORDS: Obstructive sleep apnea, snoring, soft palate stiffening, sound analysis of snoring, biomechanical testing of soft tissue

Stephanie Hunt

December 2, 2015

COLLAGEN CROSSLINKING REAGENT UTILIZED TO MODIFY THE MECHANICAL PROPERTIES OF THE SOFT PALATE IN EQUINE SNORING AND APNEA APPLICATIONS

By

Stephanie Louise Hunt

Dr. Thomas Hedman

Director of Thesis

Dr. Abhijit Patwardhan

Director of Graduate Studies

December 2, 2015

Date

ACKNOWLEDGMENTS

I would like to thank everyone who has helped and motivated me throughout my Master's studies. First, I would like to thank my advisor, Dr. Thomas Hedman, for setting a high standard of scholarship and excellence in biomedical engineering research to which I aspire. I also need to thank Dr. Hedman for his timely and instructive comments throughout the entire thesis development, allowing me to complete this project. I would like to thank my committee members, Dr. Patwardhan and Dr. Puleo, as well, for their advice and direction along the way.

Additionally, I would like to thank my lab mates at Orthopeutics, LP/Crosscoat Medical, LLC for their help with my project, especially Dr. Jonathan Kuo, Dr. Matt Brown, and Dr. Sharath Sundararaj. I need to thank the many professionals who have provided their expertise along the way as well, including Dr. Kimberly Sprayberry, Dr. Brett Woodie, and Dr. Fabio Aristizabal. Finally, I need to thank Dr. Natanya Nieman and Dr. Andy Roberts for helping me find horses to enroll horses in my study. Without the help from these professionals, this thesis would not have been conceivable.

Finally, I would like to thank my family and friends for supporting and motivating me throughout this entire process. I especially need to thank my dad, Rick Hunt, for encouraging me to pursue engineering many years ago. It was their continuous support and dedication that made this journey possible.

TABLE OF CONTENTS

LIST OF TABLES

LIST OF FIGURES

1. Introduction

Snoring is a highly prevalent condition that affects people of all ages, caused by the vibration of the tissues in the airway of the nose and throat, especially the soft palate. Conditions leading to snoring are exacerbated by obesity, allergies, aging, medication use, or alcohol consumption. Snoring can lead to sleep cycle disruptions for the snorer and their family, sleep deprivation, daytime lethargy, and drowsiness [1-4]. In some instances, snoring can advance into a more serious, and sometimes life threatening condition, obstructive sleep apnea (OSA). In OSA, breathing is interrupted during sleep by physical obstruction of the airway caused by excessive compliance of the soft palate and abnormalities in the geometry of air passages. Repeated trauma to the soft palate caused by snoring can increase its passive deformability and damage its muscle fibers and peripheral nerve fibers, increasing the chance of obstruction. OSA can lead to respiratory and cardiovascular complications, such as high blood pressure, stroke, heart failure, diabetes and depression [1-5].

Current treatments for snoring and OSA follow a 4-phase path. The first step is simple lifestyle changes, such as weight loss or changing eating or drinking habits. The second phase consists of over the counter medications, oral devices and nasal dilators. One common example of over the counter products is nasal snoring strips. The third phase consists of non-surgical devices, such as the continuous positive air pressure machine (CPAP) that provides continuous air to the patient to counter the narrowing of the air passage. The final phase consists of various surgical treatments aimed at either removal of offending tissues or stiffening the soft palate through the formation of scar tissue. Examples of common surgical procedures include radiofrequency ablation, injection of sclerosants, uvulectomy surgery, and the Pillar procedure [1,4,5,6-15].

The treatments for both snoring and OSA are relatively unsuccessful. A majority of the current surgery procedures rely on stiffening the soft palate to increase damping, and therefore to improve airflow induced vibrations. Typically, the stiffening is the result of fibrosis formation, which is an inflammatory wound-healing response resulting in fibroblast activation and production of a poorly organized extracellular matrix [6-15]. Short-term results are promising for these treatments; however, fibrosis contributes to mechanical degradation of the overloaded soft palate, leading to eventual loss of treatment benefits. Generally, the collagen network created in fibrotic lesions is not the same type of collagen originally present in the tissue, leading to degradation of the

mechanical properties and reduction of the tissue's durability, or fatigue resistance [8,15-17]. Additionally, the tissue-material interfaces produced in some procedures can cause micro-motion, wear, particle-release, inflammatory or cellular responses and tissue damage [13-16]. Treatments that rely on heat denaturation of the target tissue can produce inferior mechanical properties, substandard molecular and micro-structural geometries and loss of initial treatment-related benefits [6-12]. With less than ideal results from current treatments, along with an increasing number of patients diagnosed with snoring and OSA, a new treatment is necessary that can stiffen the soft palate while improving the mechanical properties of the tissue.

The hypothesis of this study was that an injection of a non-toxic protein cross-linking reagent into the soft palate would augment the mechanical properties and reduce deformation and vibration of the palate when subjected to physiologic air flow, thus decreasing severity of snoring and the likelihood of airway collapse, while also increasing the tissue's resistance to mechanical degradation. Instead of creating scar tissue that degrades over time, crosslink augmentation stabilizes the tissue while preserving the microstructural and compositional integrity. More specifically, this method can modify the viscoelastic, elastic-plastic, and durability properties by increasing the strength, stiffness, fatigue resistance and energy required to permanently deform or fail the tissue [18-26]. Compared to other treatments, protein crosslinking is less intrusive, less expensive, faster (same-day benefit), and less harsh in regards to induction of inflammatory responses.

An alternative to animal model research was unsuccessful in simulating the multi-faceted conditions leading to soft palate degradation, tissue vibration and air passage obstruction. Likewise, the inflammatory and immunogenic responses and the mechanically activated cellular responses to a non-physiologically altered matrix cannot be simulated to an acceptable level in a non-living model. Therefore, equine soft palates were used as a relevant model to represent human snoring and OSA due to a high incidence of awake snoring and apnea, otherwise known as dorsal displacement of the soft palate, or DDSP. This disease is a naturally occurring soft palate disorder caused by the displacement of the caudal edge of the soft palate, which interferes with normal airflow through the nasopharynx, producing mechanical property deficiencies, snoring, and temporary obstruction of the airway. DDSP occurs in 10 to 20% of competitive horses; however, this is only an estimate because horses with this malady are often

quietly euthanized [27]. Current treatments include the tie-forward procedure, laser staphylectomy, myectomy, and the Cornell Collar that focus on immobilizing the larynx or stiffening the soft palate to prevent displacement of the soft palate, all of which have about a 50-60% success rate [27-33].

The hypotheses of this study were tested through *in vivo* and *in vitro* methods using equine soft palates as a relevant model for human snoring and OSA. A pilot equine *in vivo* study tested the efficacy and safety of genipin injection treatment of the soft palate. The *in vitro* mechanical testing study used cadaveric equine soft palates to determine the effects of the genipin treatment on the mechanical properties of the soft palate. Together, these studies provided a glimpse into the potential treatment benefits of injecting a genipin crosslinking reagent into the soft palate for treatment of human snoring and OSA, as well as equine DDSP.

Prior to starting any work on the current study, a previous *in vitro* equine soft palate study was completed by Dr. Jonathan Kuo and his team from Orthopeutics, LP in Lexington, KY that was used to determine the concentrations of the genipin treatment used in both the pilot *in vivo* study and the *in vitro* mechanical testing study. Kuo et al. designed and constructed a custom wind tunnel, equipped with a mounting clamp that mimicked the support provided to the soft palate by the hard palate and connective tissues, to simulate the equine respiratory tract as shown in Figure 1.1 The wind tunnel system produced transient and steady state wind flow up to 14 meters/second over the mounted soft palate to simulate breathing conditions. A laser reflection transducer (Keyence LK-081, Itaska, IL) was mounted above the samples to measure the displacement amplitudes and vibration frequency and amplitudes of the specimens. Three different concentrations for genipin injection were tested, including 50 mM, 100 mM and 150 mM. Additionally, untreated controls and 0.33% genipin soaked samples were tested to serve as baselines for untreated tissue and maximum genipin crosslinked tissue, respectively. Changes in displacement and frequency were measured and compared between treated and untreated samples. The genipin injected soft palates resulted in localized crosslinking around the injection side. The 50 mM, 100 mM and 150 mM genipin concentration injection had 44%, 46% and 64% respective decrease in transient displacement of the soft palate compared to the untreated samples. For steady state displacements (vibration amplitudes), there was a 36%, 23%, and 42% decrease compared to the control samples for the 50 mM, 100 mM, and 150 mM genipin

concentration injections, respectively. The genipin injections covered 40%, 49% and 51% of the soft palate for the 50 mM, 100 mM, and 150 mM genipin concentration injections, respectively, based on the area of crosslinking region, which appears blue due to the genipin reaction.

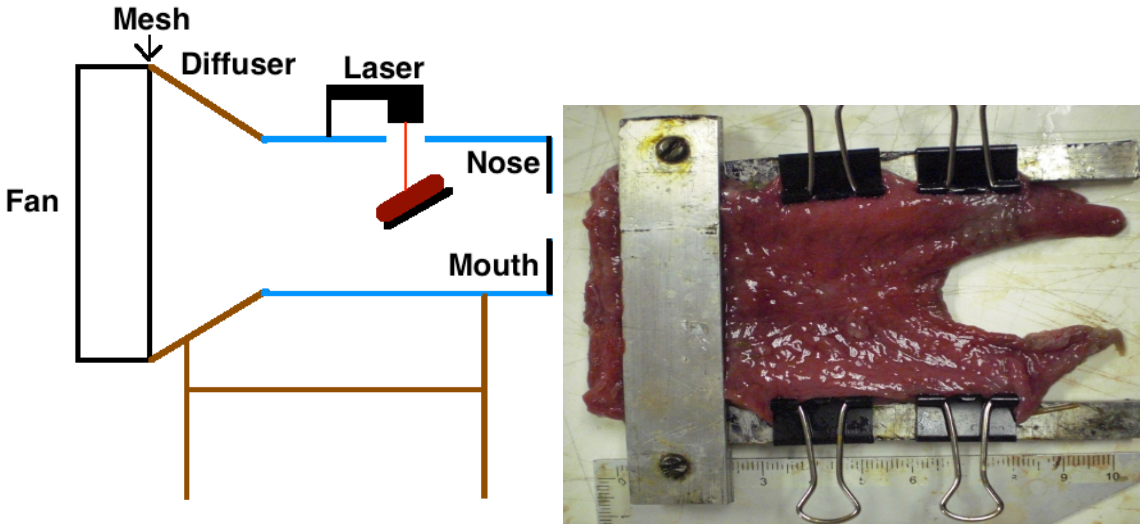

Figure 1.1: The wind tunnel was custom designed to mimic the equine breathing flow (left). It consisted of a fan that blew wind over the soft palate to measure changes in the displacements using a laser displacement measurement system. The wind tunnel supported the soft palate (right) similar to how the hard palate and connective tissue support it in the horse's airway.

Based on the results of the wind tunnel study, the 100 mM concentration of genipin injections was used for the *in vivo* study for a variety of reasons. First, the 100 mM concentration showed a decrease in both deformation and vibration of the palate. Also, it treated about half of the palate, as demonstrated by the area of the blue genipin crosslinking region. The amount of area covered by the genipin was important in the equine studies because the soft palate is larger, thus more coverage is needed to effectively treat the tissue. Finally, a previous safety study completed by Orthopeutics, LP, showed no adverse acute reactions at the 100 mM genipin concentration when injecting it into the equine soft palate *in vivo*. Overall, the 100 mM concentration for the genipin injections showed the most promise to produce a noticeable treatment effect for horses afflicted with DDSP.

For the equine soft palate mechanical testing study, the 50 mM genipin concentration was chosen because it was the preferred concentration for potential human snoring and OSA applications. The 50 mM concentration was picked because it had minimal toxicity based on previous studies while demonstrating a similar effect in the

wind tunnel as higher concentrations. Also, no DMSO was required to solubilize the genipin at a lower concentration.

The pilot equine *in vivo* study consisted of two phases: the efficacy phase, which tested the success of the genipin injections for treating DDSP, and the safety phase, which tested the short-term biological effects of the genipin injections on the soft palate. The efficacy phase consisted of three horses diagnosed with DDSP, while the safety phase consisted of three horses with no apparent breathing disorders. The efficacy phase horses underwent dynamic endoscope examinations and respiratory audio recordings prior to and after the soft palate injections to qualitatively and quantitatively measure the effects of the genipin treatment. The respiratory audio recordings were analyzed using Matlab in the time domain and frequency domain to determine if there were any changes in the snoring loudness or frequency of DDSP associated with the genipin treatment. At the completion of the study, the soft palates from the safety phase horses were harvested for histological analysis using hematoxylin and eosin (H&E) stain to determine any presence of inflammation or fibroplasia infiltrates.

The mechanical testing study used cadaveric equine soft palates to test the effect of the genipin treatment on the mechanical properties of the tissue. Three test groups, including untreated control samples, buffer-only injected samples, and buffered genipin treated samples, underwent three mechanical tests using a universal testing machine. Each sample underwent a cyclical loading (hysteresis), stress relaxation and tensile loading to failure test in order to determine quantitative changes between the treated samples and untreated samples. First cycle hysteresis, change in hysteresis, hysteresis ratio, stress relaxation, relaxation modulus, normalized relaxation modulus, ultimate tensile stress and strain, toe region slope, Young's modulus, yield point stress and strain, toughness, energy, and resilience were calculated from the results of the mechanical tests. Statistical analysis was completed using the F-test, Student's *t*-test and the Mann-Whitney U non-parametric test to determine any statistically significant differences between the three test groups.

2. Background

2.1 Snoring and Obstructive Sleep Apnea

2.1.1 Overview

Snoring is a respiratory sound generated primarily by inspiration in the upper airway during sleep [1]. The functions of the upper airway, which is the part of the respiratory system between the nostrils and trachea, include air warming, humidification, pathways for olfaction, coordination of ventilation with swallowing, protection from aspiration of food, and primary defense against infection [2]. These functions are controlled by the neuromuscular systems under both voluntary and involuntary control [2]. Snoring is worsened by alcohol consumption, weight gain, sedative medications, sleep deprivations, and supine sleeping positions. The symptoms of snoring include drooling, dry mouth and restless sleep [3]. Additionally, patients experience excessive daytime sleepiness (EDS), which is measured by the Epworth Sleepiness Scale (ESS) [3]. Overall, snoring affects people of all ages, occurring in 35-45% of men and 15-28% of women [4]. However, it is more prevalent in the elderly, occurring in 28-67% of elderly men and in 20-54% of elderly women [4].

Obstructive sleep apnea (OSA) is a potentially life threatening condition caused by repetitive partial or complete collapse of the upper airway during sleep. OSA occurs when an imbalance persists between the forces dilating and occluding the pharynx due to insufficiencies in luminal patency and airway stability, including slowly varying vascular pressure and tissue elasticity and quickly varying muscular effects [1,34]. OSA is a gradually progressive disease caused by a variety of factors, including palatal denervation, a thickened soft palate, an enlarged tongue volume, a receding jaw, an enlarge uvula or a lack of muscle tone in the throat [1-4]. Additionally, a lack of rigidity caused by a decrease in mechanical properties of the pharyngeal tissues can also lead to airway occlusion, including the upper airway muscles, larynx and soft palate [34]. These conditions lead to apneas - a cessation of breathing, or hypopneas - reduced breathing phases [1]. During sleep, the upper airway is particularly vulnerable because the reflexes are relaxed, leaving the airway susceptible to collapse, leading to OSA conditions [2,4]. OSA occurs in about 2-11% of the population aged 16 or older, or approximately 10 million individuals. Men are twice as likely to experience OSA than women. Additionally, OSA is more common in Pacific Islanders, Hispanic Americans, and African Americans [1,4,5].

OSA is characterized by a loud snore alternating with 20- to 30- second intervals of silence, terminated by loud snorts, gasps, moans or other vocalizations, and sometimes in conjunction with brief awakenings and body movements [3]. Additionally, 18-31% of patients experience nocturnal dyspnea, or a sensation of choking or suffocating, in relationship with OSA [3]. Nocturnal symptoms of OSA consist of intermittent snoring, nocturnal enuresis, witnessed apneas, dyspnea, drooling, dry mouth, bruxism, restless sleep/frequent arousals, gastroesophageal reflux and nocturia [1,4]. Daytime symptoms include daytime sleepiness, diminished intellectual performance, personality changes, morning headaches, diminished quality of life, depression, anxiety, irritability, and sexual dysfunction [1,4]. Excessive body weight and genetic factors play a role in OSA, as well [1,4]. As OSA worsens, it leads to more serious respiratory and cardiovascular complications, including hypertension, cardiovascular disease, stroke, obesity, insulin resistance, and myocardial infarction [1,3,5].

OSA is diagnosed according to the apnea hypopnea index (AHI), physical examinations, and patient symptoms [1,3]. AHI is defined as the number of apneas plus the number of hypopneas per hour of sleep. Typically, if a patient experiences more than five respiratory collapses per hour (AHI ≥ 5), they are diagnosed with OSA. OSA is then categorized based on severity: mild OSA from 5 ≤ AHI < 20; moderate OSA from 20 ≤ AHI < 40; and severe OSA with AHI ≥ 40 [1,3]. Diagnosing sleep apnea through symptoms alone is only successful about 50% of the time; therefore, sleep endoscopic examinations or polysomnography tests are utilized for a more accurate diagnosis [3,5]. Sleep endoscopic examinations are completed using a flexible endoscope to view the nasal passage while a patient is sleeping. There are a few disadvantages associated with endoscopic examinations that interfere with the validity of the test, including reduction of the cross-section of the airway by the endoscope, arousal reactions due to mechanical stimulus, to visual obstruction by phlegm, and to simultaneous assessment of only one level of the airway [1]. A polysomnography test, which is the current ‘gold standard’ for diagnosing OSA, is a sleep study completed overnight that observes various sleep irregularities. However, sleep studies are expensive and time consuming, which dissuades patients from undergoing them [3]. In both techniques, an apnea is identified as the cessation of airflow for at least ten seconds [6]. Additionally, according to the American Academy of Sleep Medicine Task Force, hypopnea is defined as either greater than 50% reduction in airflow, or less than 50% reduction in airflow associated

with a desaturation of greater than 3%, or a moderate reduction in airflow with associated arousal by electroencephalogram (EEG) [35].

2.1.2 Current Treatments

Current treatments for snoring and OSA range from conservative options to apparatus therapies to invasive surgeries, all of which have respective advantages and disadvantages. The goal of all snoring treatments is to reduce or stop vibration of the relevant airway structures, while the goals of OSA treatments are to enlarge the airway or to alter mechanical properties of the pharyngeal tissues to prevent collapse and eliminate apneas, hypopneas, and other related symptoms [1,34,36]. The first treatment option for both snoring and OSA are conservative treatments, which consist of weight reduction, optimization of sleep hygiene, avoidance of certain sleeping positions, and cessation of certain medication, alcohol and tobacco use [1,37].

The next phase consists of oral devices and apparatus therapies. One common oral device is mandibular repositioning appliance (MRA), which manually moves the mandible forward to improve the upper airway patency [37]. Typically, the MRA has a 50-70% success rate for mild to moderate severe OSA [1]. In general, the oral devices are bulky and uncomfortable, leading to hypersalivation, xerostomy, jaw pain, dental pain and permanent teeth misalignments [1,4].

The most widely used apparatus therapy is the continuous positive airway pressure (CPAP) machine, which delivers a continuous flow of air through a nasal mask, creating a constant pressure during the respiratory cycle to eliminate obstructive apneas, as shown in Figure 2.1 [4]. The CPAP machine works by counteracting the negative transmural pressure that promotes collapse and narrowing of the floppy-toned upper airway pharyngeal musculature by pneumatically splinting open the upper airway via the application of a positive pressure across the airway walls to prevent narrowing or collapse [37]. With a potential success rate of 98%, the CPAP machine is the ‘gold standard’ therapy in OSA treatments; however, there are patient compliance issues resulting in only 60-80% of patients using it due to common side effects, including nasal congestion, rhinorrhea, dryness, sneezing, complaints of machine noise, loss of mask seal against face, and intolerance to the level of positive pressure [1-5].

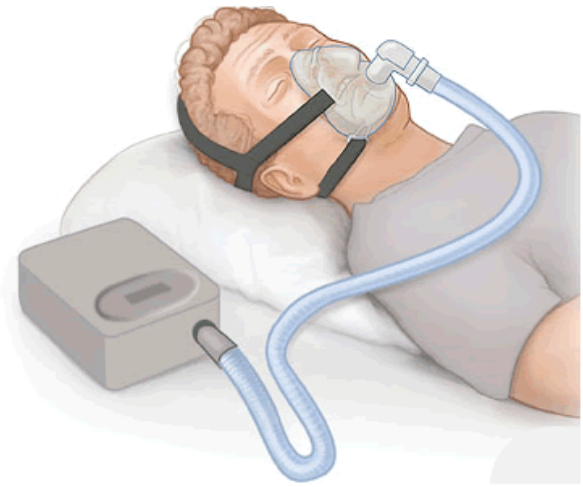

Figure 2.1: The CPAP machine is an external device used to treated OSA and severe snoring. The machine is bulky and noisy, causing sleep cycle disruptions for the patient and their family.

Nasal surgery options are typically used in conjunction with the CPAP machine to assist in snoring reduction and OSA. Common nasal surgeries include: septoplasty, septorhinoplasty, turbinate reduction, and endoscopic sinus surgery [5]. Overall, nasal surgeries are successful at reducing snoring 34-69% of the time and OSA 20% of the time in combination with the CPAP machine [4].

When simple lifestyle changes and apparatus therapies fail, surgical procedures focus on altering the soft palate and surrounding tissues for treatment of snoring and OSA. The uvulopalatopharyngoplasty (UPPP) consists of ablating the excessive tissue of posterior margin of the soft palate, uvula, and lateral pharyngeal wall with a laser, cautery or cold knife to relieve oropharyngeal obstruction and to increase stiffness through postoperative scarring [4,36,38]. Typically, the UPPP procedure is completed in conjunction with a tonsillectomy [4]. In general, there is a long-term success rate of 70% for snoring and of 50% for OSA [5]. The success of the treatment relies on the amount of soft palate tissue resected. Excessive resection can cause palatal malfunction, and conservative resection can still produce snoring or OSA symptoms [38]. The procedure is considered to be relatively painful with high morbidity and mortality rates and common side effects, including post-op bleeding, voice changes, nasopharyngeal stenosis, persistent dry throat, swallowing abnormalities, respiratory distress and palatal incompetence [4,5,38].

Another surgery treatment is the laser-assisted uvulopalatoplasty (LAUP), which reduces snoring by trimming the palate and surrounding tissues and by increasing the

stiffness through postoperative scarring [36]. The procedure consists of ablation of the palate, velum, and uvula using a carbon dioxide laser under local anesthesia [4]. Overall, the side effects are minor with the biggest complaint being severe pain and potential ineffectiveness [4]. The effectiveness was reported as 69% successful at 9 months and as 55% successful at 59 months post treatment. In general, success rates deteriorated from 70% to 30% over time, with differences in laryngeal anatomy being the biggest reason for failure [5]. In some cases, treatments can be repeated every six weeks to improve effectiveness [5].

Many surgical treatments focus on stiffening the soft palate to prevent vibration and obstruction, such as radiofrequency thermotherapy, the injection of sclerosants, the Pillar procedure, and laser soft palate stiffening. Radiofrequency thermotherapy is accomplished by using radiofrequency energy to create thermal lesions with subsequent fibrosis leading to stiffening and some shrinkage of the palate and tongue base [5]. This outpatient procedure works best for mild to moderate OSA, with effectiveness being related to the total energy delivered and to the location of the lesions that increase scar tissue [5,35]. Common complications include pain, dryness, or recurrence of snoring [35]. Similarly, the injection of sclerosants stiffens the palate by injecting chemicals, such as sodium tetradecyl sulphate, into the tissue to induce scarring and stiffening of the palate [5]. Again, complications include pain, dryness, foreign body sensation, and recurrence of snoring [36].

The Pillar procedure consists of inserting palatal implants into the soft palate to reduce vibration and narrowing of the soft palate by increasing the stiffness of the palate [5,36]. Three small, rectangular implants, made of a woven polyester material, are inserted into the soft palate in a parallel orientation for the treatment of OSA [36]. Initially, the treatment reduces AHI in patients with mild to moderate OSA as long as the implant stays in place. However, over time, the effectiveness decreases because the fibrotic encapsulation around the implants leads to tissue degradation [36]. The most common side effect of the Pillar procedure is the extrusion of the implant at a rate of 0-25% due to chronic inflammatory responses and fibrous capsule formation. This side effect is remedied by replacing the implant [36].

Comparably, the laser soft palate stiffening procedure stiffens the palate using a low power Nd:YAG laser of 1.44 micrometer as an alternative treatment to the UPPP surgery. This procedure is less invasive than the UPPP because it is a form of

"electrosurgery" that works by visibly shrinking the soft palate by breaking intrinsic collagen crosslinking to shrink the collagenous matrix, with an average 3.0 mm immediate reduction in length [38]. Histopathology results show no inflammation or necrosis, with submucosal fibrosis and scarring produced about 1-1.5 mm deep [38]. The immediate response is mucosal shrinking, followed by a gradual tissue stiffening over time with the formation of tissue fibrosis [38]. Long-term effectiveness for this particular treatment have not been studied fully, but similar to other methods that stiffen the palate through scar tissue formation, it can be assumed that the effectiveness will decrease over time due to mechanical degradation in the soft palate.

Other treatments for snoring and OSA include skeletal facial corrections and tracheotomy surgeries. The maxillomandibular advancement is a type of skeletal facial correction that works by repositioning the jaw to allow for more airflow to prevent obstruction [36]. A tracheotomy is an opening in the windpipe that alleviates breathing obstructions [4,39]. Tracheotomy surgeries are generally viewed to be a mutilating intervention because it creates an unsightly hole in the trachea [4]. In general, these two treatments are the only treatments considered to be 100% effective at preventing OSA, and are reserved for patients with severe OSA that are unsuitable for CPAP or other surgical options due to severe life-threatening conditions or failure of previous surgical approaches [4].

2.1.3 Acoustic Analyses of Snoring and Sleep Apnea

A review of the literature was conducted to determine common techniques for detecting and analyzing snoring and OSA sounds. Relevant techniques could then be applied to the equine *in vivo* study to record and analyze snoring sounds. Beck et al. characterized snoring in the article title, "The acoustic properties of snoring." In Beck's study, snoring was simulated in a canine model by placing a balloon above the larynx and inflating it to create various levels of obstruction to simulate OSA [40]. Beck then analyzed the snoring sounds from 75-2000 Hz in the time domain and frequency domain. The canine snoring sounds resulted in complex waveforms in the low frequency range associated with intermittent airway closure. The biggest difference between Beck's study and the current study is the animal model. Beck's study used a canine model that had an induced airway obstruction, whereas the equine model used in the present study experienced a naturally occurring form of OSA and snoring. Regardless of the animal model, Beck's study reiterated the idea that complex snoring waveforms in

the low frequency range are associated with airway obstruction, meaning that respiratory recordings and analysis in the low frequency range are a viable way to determine differences in snoring patterns.

Another article titled, “Is there a relationship between sound intensity and frequency and OSAS severity?” by Acar et. al. explored the correlation between snoring loudness and OSA severity through snoring analysis. Acar’s study consisted of patients with various degrees of OSA, ranging from mild to severe [41]. This study analyzed the snoring sounds using the fast Fourier transform function (FFT), and snoring was quantified using average snoring sound intensity level (SSIL) and the maximal frequency (Fmax). Acar determined that SSIL and Fmax increased with age, in females, and in patients with severe OSA. Additionally, Acar concluded that SSIL and Fmax are strongly correlated with AHI, and thus the severity of OSA. Acar’s study showed that the FFT is a preferred way to analyze snoring sounds because it allows various peaks to be determined. Acar also indicated that higher frequency peaks are characteristic of OSA snoring, which can be carried over for the equine snoring analysis used in the present study. In contrast, Acar’s study focused on determining specific parameters associated with OSA, while the present study focused more on comparing a pre treatment frequency domain curve against a post treatment frequency domain curve.

Another article by Azarbarzin and Moussavi, titled, “Snoring sounds variability as a signature of obstructive sleep apnea,” worked to determine an association between snoring sounds and the degree of OSA. Azarbarzin and Moussavi recorded snoring sounds from patients with varying degrees of OSA and analyzed them using the time domain and frequency domain [42]. In their study, the apneic events had a pattern of high amplitude bands followed by apneic gaps without breathing in the time domain graphs. These concepts can be used in the present equine *in vivo* study to determine the location of an obstruction caused by DDSP in the time domain.

2.2 Dorsal Displacement of the Soft Palate

2.2.1 Overview

Equine soft palates were used as a relevant model to represent the multi-faceted conditions leading to soft palate degradation, tissue vibration and air passage obstruction in snoring and OSA due to a high incidence of a pathology involving awake snoring and apnea, known as dorsal displacement of the soft palate, or DDSP. This

disease is a naturally occurring soft palate disorder caused by the displacement of the caudal edge of the soft palate, which interferes with normal airflow through the nasopharynx. The disorder most commonly occurs when the head is in a flexed position, or when the horse is fatigued during hard exercise [43]. The displacement can usually be self-corrected by the animal by swallowing or by readjusting the head position, however, it can occur several times during a single race or training session, causing interruptions to normal breathing and consequently a significant decrease in performance.

Horses breathe completely through their nostrils, meaning that they cannot breathe through their mouths [43]. The soft palate is a musculomembranous tissue that extends from the hard palate to the esophageal pharynx, separating the oral cavity from the nasopharynx [44]. The epiglottis projects through the caudal notch, or free border, of the palate [44]. Together, the soft palate and epiglottis form a seal to block off the nasal cavity from the oral cavity. The free border of the palate should remain beneath the epiglottis at all times, except during swallowing or coughing [44]. DDSP occurs when the caudal edge of the soft palate displaces dorsally relative to the epiglottis, partially blocking the nasal passage and creating air turbulence during inspiration and, primarily, expiration, as demonstrated in Figure 2.2 [44]. When displaced, the soft palate reduces the cross-sectional area of the nasopharnyx, causing an obstruction. The caudal edge of the palate vibrates as air flows past it, producing a “gurgling” or “snoring” noise in 50-80% of affected horses [29-33,44-46]. When the soft palate is displaced, minute ventilation decreases by 13%, and maximal oxygen consumption decreases by 10% [45]. Swallowing or head movements can return the palate to the normal position after displacement [44]. In permanent cases, the palate is continuously displaced [27].

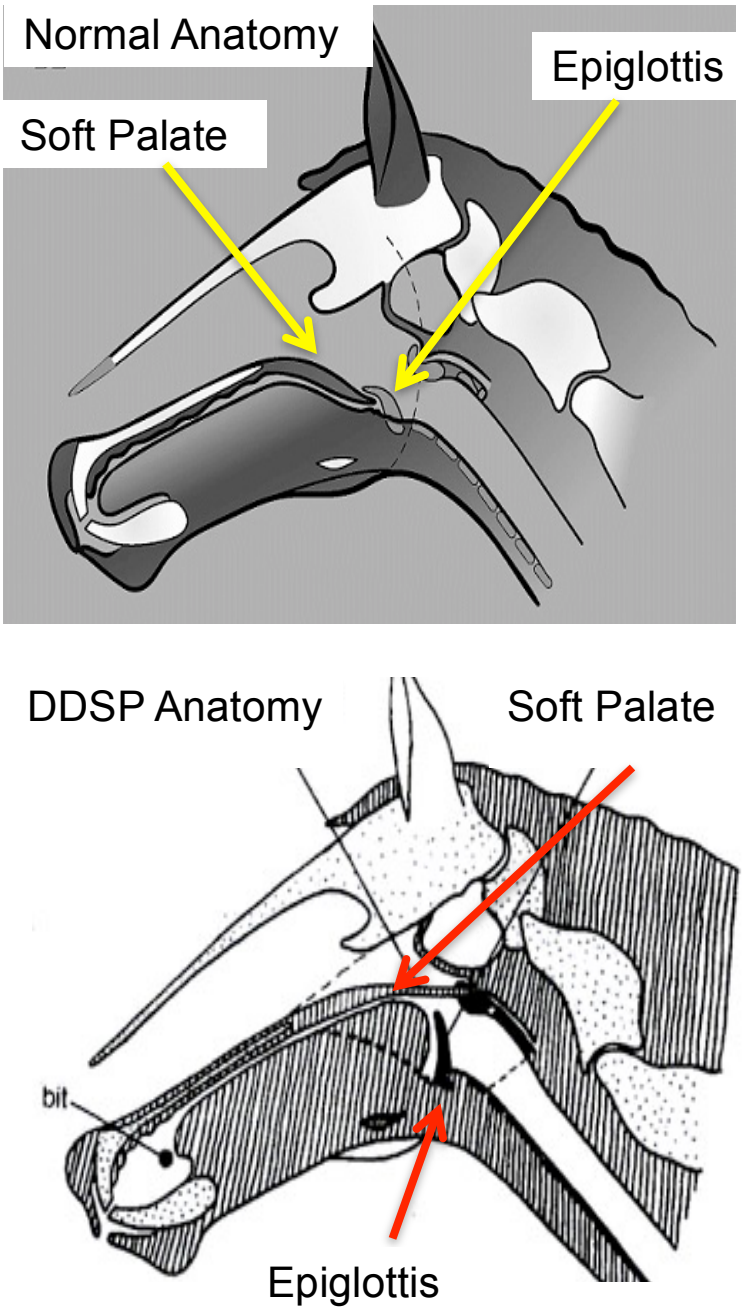

Figure 2.2: The normal airway anatomy (top) of a horse allows air to pass freely past the soft palate, which is tucked underneath the epiglottis. In DDSP (bottom), the soft palate is displaced above the epiglottis, blocking the airway as the horse exhales.

DDSP occurs in 10-40% of competitive horses, especially Thoroughbreds and Standardbred racehorses [27-33]. There is no known correlation between age of the horse and predisposition to DDSP, although younger horses seem more prone to the malady [27,32]. Since the soft palate acts as a seal for the larynx, any factor that disrupts the seal can cause the soft palate to displace. Therefore, retraction of the

tongue can cause caudal displacement of the larynx, forcing the soft palate above the epiglottis [24]. Structural abnormalities or physical obstruction due to masses, granulomas or cysts can also interfere with soft palate position, causing DDSP [27,46]. In certain cases, hyper activation of the muscles responsible for the movement of the larynx can cause the larynx to retract, thus displacing the palate. This condition manifests in horses that are overly excitable or nervous [46].

DDSP is diagnosed through clinical observations and dynamic endoscopic examinations. A loud "gurgling" or "snoring" noise, as well as the fluttering of the cheeks as air is diverted beneath the displaced palate, are common symptoms of DDSP. Additionally, affected horses demonstrate exercise intolerance, often described by trainers as "choking down" or "swallowing their tongue" due to the temporary airway obstruction [27].

Resting endoscopic evaluations are not useful in detecting DDSP because the soft palate rarely displaces at rest; however, resting endoscopic evaluations are utilized to assess the nasopharyngeal function and to rule out other upper airway disorders [27]. DDSP is diagnosed with a dynamic endoscopic examination performed on a treadmill or over ground. The dynamic endoscope mimics showing or racing conditions that induce the displacement as close as possible. For example, the horse is equipped with the typical tack and/or devices utilized during showing or racing. An endoscope is advanced through the nostril to the pharynx, then the horse is exercised at various speeds and intensities until fatigue to induce DDSP conditions [27]. In some instances, the frequency of swallowing increases immediately prior to displacement [27]. Additionally, some horses experience a billowing of the caudal portion of the soft palate, causing palatal instability, preceding displacement [27]. DDSP is diagnosed if the soft palate displaces dorsally to the epiglottis for longer than eight seconds during the dynamic endoscopic evaluations [27].

2.2.2 Current Treatments

Because there are a variety of conditions that lead to DDSP, potential treatments vary significantly, from simple external devices or tack adjustments to complex surgical procedures. The simplest treatment for DDSP is a tongue-tie during exercise, in which the tongue is physically tied to the lower jaw using a leather strap or fabric strip. The tongue is indirectly connected to the larynx, so tying it prevents caudal retraction of the

larynx, and thus applying dorsal pressure to the soft palate in order to prevent displacement [44,46,47]. Tying the tongue does not always prevent displacement, and in some cases, multiple tongue-ties are required to prevent displacement. Similarly, changing the tack can help with the management of DDSP. Commonly used tack options include a Z-bit or a leverage bit to hold the head and neck in certain positions to decrease the possibility of displacement [27,44]. Also, figure 8 nosebands are often used to prevent air from flowing into the orthopharynx by applying ventral pressure to the soft palate [46]. Finally, an external device can be added to assist in prevention of DDSP. As shown in Figure 2.3, the Cornell Collar applies pressure to the caudal aspect of the basihyoid bone and ventral aspect of the thyroid cartilage to pull the larynx more rostral, reducing the possibility of soft palate displacement [47].

Figure 2.3: The Cornell Collar is an external device that applies pressure to the basihyoid bone to elevate the larynx and reduce potential soft palate displacements.

When conservative treatments fail at preventing DDSP, more invasive surgical procedures are sometimes attempted. Surgical treatments range from muscle transection to soft palate shortening to soft palate stiffening. Overall, surgical treatments have a 58-78% success rate [48].

A sternothyrohyoid myectomy transects the “strap” muscles via a bilateral partial tenomyectomy to increase upper airway pressure and to provide stability to the

nasopharyngeal structures. The “strap” muscles, which are responsible for caudal retraction of the larynx, include the sternohyoideus, sternothyroideus and omohyoideus muscles, commonly referred to as sternothyrohyoid muscles [44,47]. One potential benefit of this procedure is that it can be performed under light anesthesia with the horse remaining standing. Similarly, there is a relatively short recovery period of about 14 days with minimal complications [27,44,46]. Overall, the sternothyrohyoid myectomy has a reported 58-73% success rate [27,46,49,50].

A staphylectomy consists of removing a portion of the caudal margin of the soft palate to prevent airway obstruction [44]. Although the staphylectomy is a relatively straightforward procedure, it can have severe complications and a 4-6 week recovery period. If the soft palate is cut too short, it may allow food and water contents to enter the nasopharynx during swallowing, leading to coughing, sneezing, or aspiration pneumonia [46]. The success rate of 40-60% is based on the reduction of the amount of tissue blocking the airway when the soft palate displaces [46,49].

The laryngeal tie-forward procedure mimics the effects of the Cornell Collar by permanently positioning the larynx dorsally to the basihyoid bone by suturing the larynx to the bone [27]. This procedure attempts to correct DDSP by reducing caudal movement of the larynx [50]. Post-operatively, there are minimal complications, and horses can return to work within 10-14 days [27]. Overall, there is about a 60-80% success rate, with failure typically being the result of breakdown of the suture [49,50].

Similar to treatment in human snoring and OSA, one common treatment for DDSP is stiffening the soft palate through laser treatments or palatal sclerotherapy. In laser palatoplasty, the caudal edge of the soft palate is stiffened though laser induced fibrosis during an outpatient procedure [27]. Minimal inflammatory complications occur post-operatively, and most horses can return to work within one month [27]. Similarly, caudal soft palate photothermoplasty stiffens the caudal edge of the soft palate by creating a large area of fibrosis through laser ablation of strips of the oral mucosa and submucosa [48]. Overall, stiffening the soft palate through various laser treatments had an immediate success rate of 60-92% to prevent DDSP [48-50]. Likewise, to stiffen the palate using sclerotherapy, a sclerosing agent, such as sodium tetradecyl sulfate, is injected into the submucosal layer of the soft palate to induce fibrosis [49]. Overall, a small study showed that sclerotherapy is a relatively simple procedure with minimal side effects and a short-term success rate of about 75% [49]. In general, the short-term

results show that stiffening the soft palate through the formation of scar tissue can prevent displacement and vibration of the palate; however, long-term results show that fibrous formation degrades the soft palate and is mechanically insufficient compared to healthy tissue, leading to treatment failure [48-50].

A common approach to DDSP treatment is a combination of two or more procedures. Composite surgeries offer the benefit of minimizing anesthesia and surgery, while increasing the chances for DDSP prevention [51]. One common composite surgery is the Llewellyn procedure, which combines the myectomy with a staphlectomy to transect the sternothyrohoid muscles and shorten the caudal edge of the soft palate. The Llewellyn procedure has an initial 60-92% success rate, but similar to the previous procedures, it becomes less effective over time due to degradation of the soft palate [49,50].

2.2.3 Review of Equine Soft Palate Stiffening, Testing, and Sound Analysis

A review was completed of literature associated with stiffening the equine soft palate for prevention of DDSP to compare and contrast the procedure and results with the present study. One study, completed by Munoz et al, was titled, “Histological and biomechanical effects of palatal sclerotherapy in the horse using sodium tetradecyl sulfate.” Munoz et al. used healthy horses to inject tetradecyl sulfate into the distal portion of the soft palate to stiffen it [52]. During the injections, a bubble was created at the injection site, leading to hard nodule formation in at least one of the horses [52]. A study by Alkabes et al. titled, “Evaluation of the effects of transendoscopic diode laser palatoplasty on clinical, histologic, magnetic resonance imaging, and biomechanical findings,” was also reviewed. Alkabes’ study, which used healthy horses, stiffened the soft palate through scar tissue formation via the laser palatoplasty procedure [53]. Alkabes treated the horses with either a low-dose or a high-dose laser treatment, with edemas forming initially in each horse. Over time, the edema decreased, and scarring of the soft palate increased [53]. Similar to the present study, both reviewed studies aimed to stiffen the soft palate to prevent DDSP. However, both of these studies relied to some extent on scar tissue formation, whereas the current study relies on crosslinking. Another major difference between the present study and these two studies is that the horses used in these studies were not diagnosed with DDSP and had normal soft palates. Using horses with normal soft palates could lead to very different results

when compared to using horses with abnormal soft palates, due the pre-existing degradation and instability of the DDSP afflicted soft palate.

Both of the studies in the literature analyzed the soft palate tissue through histological analysis and biomechanical testing. Munoz evaluated the tissue using H&E staining, and did not find any significant necrosis, inflammation, or fibrosis in the treated or control palates [52]. Alkabes analyzed the tissue using H&E staining, and discovered inflammation caused by infiltration of lymphocytes and plasma cells. The high-dose laser treated horses also had multiple fibrotic bands present [53]. Similar to the present study, both of these studies used H&E staining for the histological analysis. As predicted, Alkabes' study showed presence of fibrotic tissue formation, which is not the intended target in the current study that aims to stiffen and to strengthen the soft palate through crosslinking.

The studies in the literature also biomechanically evaluated the treated tissues. Munoz tested each sample in tension until failure at a rate of 10 mm/s to determine the slope of the deformation curve, tensile stress and tensile strain [52]. In Munoz's study, 80% of the samples failed near the grips with no significant differences in stiffness, tensile strain or stress between the treated and control samples [52]. Alkabes examined the samples in compression using a deformation rod connected to a 100-g load cell at a rate of 3 mm/s [53]. Alkabes' study showed a decrease in the elastic modulus of the high-dose laser treated horses compared to the control horses [53]. For the present study, compression testing was not used because the equine soft palate experiences minimal compressive loads; therefore, Alkabes' biomechanical testing was not relevant to the present study. On the other hand, Munoz's biomechanical testing was similar to the present study because they tested the samples in tension to find Young's Modulus, tensile stress and tensile strain. However, the current study loaded the samples at a slower rate of 1 mm/s as described in the procedure in Section 3.3.4, rather than the rate of 10 mm/s used in Munoz's study. One major issue with Munoz's biomechanical testing was that a majority of the samples failed near the grips rather than in the middle; consequently, steps were taken in the current study to neck down the samples to half of their original width to ensure failure in the middle of the sample.

Three articles were reviewed to compare techniques for recording and analyzing respiratory sounds in horses. The first paper by Derksen et al was titled, "Spectrum analysis of respiratory sounds in exercising horses with experimentally induced laryngeal

hemiplegia or dorsal displacement of the soft palate." Derksen induced DDSP in horses and recorded the respiratory sounds using a tape recorder positioned 4 cm from the horse's nostril [53]. Abnormal respiratory noises were easily recorded in exercising horses in Derksen's study, proving that it would be possible to record respiratory noises in the present study to determine differences in snoring before and after treatment.

Two articles by Franklin et al. were reviewed because they analyzed respiratory noises in horses with breathing disorders. These articles were titled, "Spectral analysis of respiratory noise in horses with upper airway disorders," and "The displaced equine soft palate as a source of abnormal respiratory noise during expiration." Franklin's studies recorded abnormal respiratory noises through an *in vivo* study with exercising horses diagnosed with DDSP and through an *in situ* study using cadaveric equine heads to simulate DDSP conditions [55,56]. In each of Franklin's studies, the respiratory audio was recorded using a microphone placed halfway between the horse's nostrils to avoid interference noises at a sampling rate of 10 kHz [55,56]. Both of these studies analyzed respiratory recordings by breaking the signals into individual inspiratory and expiratory segments and transforming them into the frequency domain using the fast Fourier transform (FFT) to determine an expiration to inspiration ratio for comparison with control horse respiratory audio [55,56]. One of the biggest differences was that Franklin compared the control horse respiratory audio to the DDSP horse respiratory audio using the expiration to inspiration ratio. In the present study, the amplitude peaks were compared in the pre treatment and post treatment frequency domain graphs instead. For both the *in vivo* and *in situ* study, the snoring frequencies occurred in a low frequency range from 50-150 Hz, while a common 'DDSP peak' existed in the range from 20 to 80 Hz that could be potentially used to diagnose DDSP [55,56]. A very important finding from the Franklin studies was the existence of a 'DDSP peak' seen in all horses with DDSP, as well as in the cadaveric horse heads. This finding provided a potential metric to use in the current study to determine the success of the genipin treatments based on the appearance or disappearance of the 'DDSP peak' in the 20-80 Hz range.

2.3 Genipin Crosslinking

2.3.1 Overview

Protein crosslinking is used to modify mechanical properties of biomaterials by augmenting the native collagenous crosslinks by adding additional crosslinking bonds

through direct injection of crosslinking agents [57,58]. Native collagenous crosslinks connect lysine or hydroxylysine residues within tropocollagen molecules or between different molecules [58]. Exogenous crosslinks can be added to create intrahelical crosslinks between the tropocollagen molecules within individual helical strands or to create interhelical crosslinks between adjacent molecules. Additionally, intermicrofibrillar crosslinks can be formed between two adjacent microfibrils if the distance between the microfibrils is smaller than the length of the crosslinking agent [58], or in the case of self-polymerizing crosslinkers such as glutaraldehyde and genipin, if the distance between potential binding sites is smaller than the chain length of the crosslinker.

One of the most commonly used crosslinkers is glutaraldehyde, but it has many adverse side effects, including acute toxicity and calcification of the treated collagen [59]. Therefore, other alternatives are being used as crosslinking reagents. Genipin is a naturally occurring, minimally toxic crosslinker extracted from geniposide, a major ingredient in the fruit from the *Gardenia jasminoides* plant, which grows in Central Asia [57]. Genipin is commonly used with a phosphate buffered saline (PBS) solution to crosslink biomaterials and implants [57]. Genipin reacts with the free amino groups of lysine, hydroxylysine or arginine within biological tissue to produce a covalent bond, and a blue coloration with the simplest primary amine, methylamine. The genipin-methylamine monomer is formed through a nucleophilic attack by methylamine on the olefinic carbon at C-3 of genipin, followed by the opening of the dihydropyran ring and attack of the resulting aldehyde group by the secondary amino group. The blue pigments are formed through oxygen radical-induced polymerization and dehydrogenation of several intermediary pigments [60]. As a result, after crosslink fixation, the tissue turns a dark blue, with the darkness of the blue coloration reflecting the density of the genipin crosslink bonds in the tissue [61]. Genipin crosslinking forms intrahelical, interhelical crosslinks, or intermicrofibrillar crosslinks [58]. Fixation by genipin crosslinking depends on the amount of genipin and the type of tissue. As the genipin diffuses through the tissue, the fixation reaction occurs immediately. If a limited amount of genipin is present, complete fixation can occur in a few minutes, but if a larger amount of genipin is present, unreacted genipin can continue to diffuse and react with available amines throughout the adjacent tissue such that complete fixation can take hours. In general, fixation is usually complete within 24 hours [61].

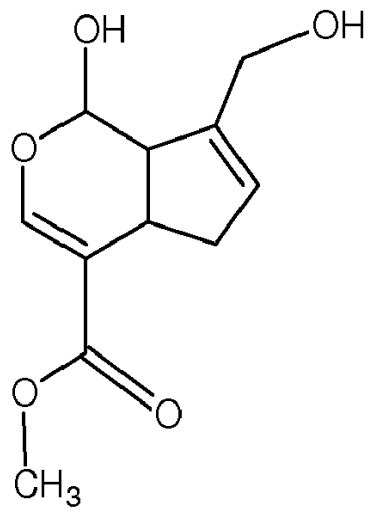

Figure 2.4: Molecular structure of genipin.

Using genipin as a crosslinking agent creates stable collagenous matrices, making the tissue less susceptible to enzymatic degradation [57,59-62]. Similarly, genipin treatment causes a three-fold reduction in fatigue induced mechanical degradation of the tissue [62]. Additionally, compared to glutaraldehyde, genipin crosslinking induces a smaller inflammatory reaction and calcium concentration in the fixed tissue [60,61,64].

2.3.2 Mechanical Properties and Biocompatibility

Crosslinking a tissue with genipin alters the strength, stiffness, and other mechanical properties of the tissue. Genipin treated tissues sometimes experience an increase in tensile strength and modulus caused by an increase in crosslinking density [59,63]. Additionally, genipin crosslinking produces inter-fibrillar crosslinks, which may reduce the ability of the collagen fibers to slide past each other. Therefore, the tissue can be less extensible, which could decrease the overall strain and increase the stiffness of the tissue, depending on the degree of crosslinking and the structure of the tissue [58,59,65]. Finally, genipin crosslinking also increases the tear resistance by 40% and the number of fatigue cycles to achieve failure [62].

Biocompatibility studies have shown that genipin crosslinking is 2000-3000 times less cytotoxic than glutaraldehyde [60,64]. Additionally, genipin exposure is not associated with any abnormal symptoms in the liver or kidney, or in hematological or histological analysis [64]. However, genipin crosslinking is sensitive to pH changes, with the degree of genipin crosslinking concentrations varying at different pH values.

Genipin crosslinking at a basic pH is greater than crosslinking at a neutral pH, which is greater than crosslinking at an acidic pH [61]. In general, the higher the pH, the more reactive the genipin is for crosslinking [61].

2.3.3 Other uses

Genipin has successfully crosslinked many other collagenous tissues. It is being investigated for the treatment of osteoarthritis by preventing chemical degradation and mechanical wear of articular cartilage [65]. Also, it has been used to treat injuries to the tendon and ligaments of horses [62]. Likewise, genipin crosslinking has been investigated for treatment of the pericardium, aortic valves, spinal discs, cellular scaffolds, knee meniscus injuries, tendons, and ligaments [57,62]. Traditionally, genipin has been used for herbal medications, Chinese medicine, treatments of jaundice, and various inflammatory and hepatic diseases [63]. Also, the dark blue pigment can be derived through the reaction of genipin with an amino acid and used in the fabrication of food dyes [60,61].

3. Methods

3.1 Pilot *in vivo* Study Preparation

3.1.1 Study Design

The purpose of the *in vivo* study was to determine the safety and efficacy of injecting the equine soft palate with a genipin reagent. The study was broken down into two parts: a safety phase and an efficacy phase. The safety phase utilized three control horses to test the biological effects of the genipin reagent injections, while the efficacy phase utilized three DDSP horses to test the success of reducing soft palate vibrations and displacements with the genipin reagent injections.

To set up the experiment, Dr. Kimberly Sprayberry, DVM from Cal Poly San Luis Obispo, provided expert advice for the *in vivo* study. Dr. Sprayberry helped by answering specific questions about the injection method, finding the DDSP horses, and quantifying the snoring sounds. Working with Dr. Sprayberry, the requirements for the pre treatment examinations were set to include both a dynamic endoscope examination and a breathing audio recording to confirm DDSP diagnoses and to record the abnormal breathing patterns, respectively. To view the questions and answers in full, see Appendix A1.

Dr. Brett Woodie, DVM, MS, Dipl. ACVS from Rood and Riddle Equine Hospital, assisted with diagnosing the DDSP horses through dynamic endoscope examinations. Dr. Woodie also recommended enrolling horses older than two years old to ensure full development of the soft palate.

For the sound analysis portion of the study, Dr. Abhijit Patwardhan, Ph.D., a professor from the Department of Biomedical Engineering at the University of Kentucky with considerable signal-processing expertise, helped guide the appropriate steps. Dr. Patwardhan advised to record all respiratory audio in a non lossy format, such as Windows Media Audio (WMA), to avoid automatic data compression of the audio signal by the digital voice recorder, which was important because the distinguishing parameters between the pre-treatment recordings and the post-treatment recordings were unknown at the start of the study. The goals for the sound analysis, outlined with Dr. Patwardhan's assistance, were to objectively measure the snoring volume and to differentiate between low frequency and high frequency amplitudes in order to determine shifts in the post-treatment audio amplitudes from the pre-treatment audio amplitudes.

3.1.2 Voice Recorder Design

In order to quantify the DDSP snoring noise, a digital voice recorder was utilized to record the horses while exercising. The recordings were then analyzed using the time domain and the frequency domain in Matlab to determine any irregular breathing patterns and any changes in loudness or frequency of the snoring sounds. The audio recording mechanism consisted of a digital voice recorder, a microphone, and a sturdy base.

The digital voice recorder had a few specific requirements. First, it had to pick up sounds in a difficult environment with background noise and wind present. It was crucial that voice activated recording (VAR) feature, which is common in most recording devices, could be disabled. This feature causes the recorder to only record when it detects frequencies associated with human speech, and since the recorder needed to pick up breathing noise, the VAR feature had to be disabled. Likewise, the recorder had to record in WMA or a similar non lossy recording format. Finally, the ideal recorder needed to have a microphone jack, a rechargeable battery, and an USB import jack. The RCA VR5330R digital voice recorder was chosen because it fit all of the aforementioned requirements. The recorder was set to record in the high quality (HQ)

setting at a sampling rate of 8000 Hz. The specifications for the digital voice recorder are in Appendix A2.

The original recording device design consisted of a headstall with a wire attached to support the microphone as shown in Figure 3.1. The actual device was created using wooden shims, duct tape and vet wrap. Two wooden shims were secured together with duct tape to create a sturdy base for the recorder. Then, the microphone wire was run along the length of the wooden shims with the microphone secured at one end. The wooden shims and microphone cord were fully wrapped in vet wrap to cover all rough edges of the wood and to protect the microphone cord. The voice recorder was attached on the opposite end of the microphone by wrapping vet wrap around the carrying case, ensuring to leave enough room to insert the recorder. The entire device was attached to the halter or bridle using zip ties. Two to three zip ties were secured on either end of the recorder, making sure it was securely attached. The recorder was firmly attached on the front of the head or side of the head depending on the horse's tack with the microphone as close to one nostril as possible to minimize background noise as shown in Figure 3.2. The microphone placement was uniform for each individual horse throughout the study.

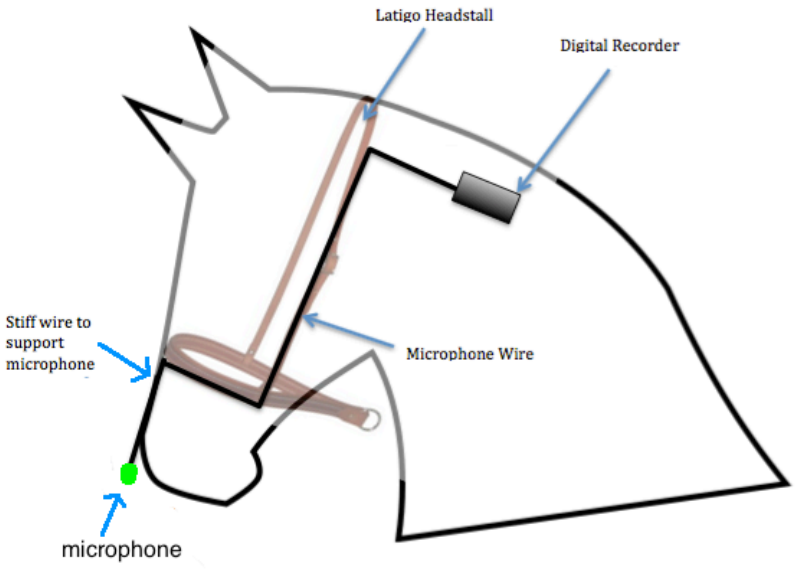

Figure 3.1: The recording device schematic consisted of a headstall or halter with a sturdy wire to support the microphone, which was placed near the horse's nostril. The digital recorder was attached to the horse's neck or further up the halter.

Figure 3.2: The recording device was created with wooden shims and vet wrap and attached to either the side or front of the horse's tack using zip ties to hold it firmly in place. The microphone placement was consistent for each individual horse throughout the study.

The recorder's design integrity was tested using eight non-study horses. These horses were exercised at a variety of speeds with numerous outdoor situations, including windy and calm days, to test the effectiveness of the device to record all breathing noises. For all of the test horses, the recorder was attached to the halter on the side of the head with the microphone near the nostril, and the horse was exercised at a walk, trot and canter. The recordings were then studied to ensure that a variety of breathing noises could be heard.

3.1.3 Study Enrollment

Before enrolling any horses in the study, a consent form and a donation form were created. The consent form was used for the efficacy phase horses because the original owner maintained ownership throughout the study. The donation form was used for the safety phase horses because the owner relinquished ownership to Orthopeutics, LP for the study. Both forms described the study in detail, including the background of genipin, the procedure, and the associated risks. Additionally, the forms requested information about the owner, the horse, and the horse's veterinary history. The consent form required further information describing the horse's DDSP history, including the date of DDSP onset, the frequency of displacement, the loudness of DDSP snoring, and previous surgeries related to DDSP. It was required that all horses had a completed

consent or donation form on file prior to starting the study. See Appendix A3 for the consent form and Appendix A4 for the donation form.

The efficacy phase horses were located by calling or emailing a list of over 300 qualified equine veterinarians in Kentucky provided by Dr. Sprayberry to help locate three horses diagnosed with DDSP. The requirements for the DDSP horses were that they must be at least two years old, be either thoroughbreds or Standardbred racehorses, and be free of any breathing abnormalities except for DDSP. Ideally, the DDSP horses would not have any previous surgeries or treatments for DDSP that would affect the structural or biological composition of the soft palate. See Appendix A5 for the sample transcript of the emails and phone calls made to the veterinarians.

The safety phase control horse requirements included having no breathing issues, being older than two years old, and being thoroughbreds, Standardbred racehorses, or similar breeds. Originally, the plan was to purchase cheap yearling thoroughbreds that were not eligible to enter the thoroughbred sale for racing, and that were designated for euthanasia by their owners. However, per Dr. Woodie's recommendation, horses younger than two years old were not enrolled in the study because their soft palates may not be fully developed at an immature age. Therefore, donated horses or purchased horses meeting the requirements were accepted as control horses.

Once all of the horses were enrolled, pre treatment examinations were completed. First, each efficacy phase horse underwent either a dynamic endoscope examination or provided previous documentation of a DDSP diagnosis from within one calendar year of the projected study start date. Dr. Woodie completed the dynamic endoscopic examinations using either a treadmill located at Rood and Riddle Equine Hospital or using a portable dynamic endoscope at a remote location.

The second stage of the pre treatment testing was to record each DDSP horse while exercising to document abnormal respiratory noises. The goal was to record any roars, snores, vibrations, or breathing gaps associated with soft palate displacement. Each horse was recorded for 20 minutes at a walk, trot, and canter to ensure adequate snoring and palate displacements.

3.1.4 Reagent Preparation

The genipin reagent used in the treatment consisted of two parts contained in two different vials: the genipin powder and the buffer solution. The reagent was a 100 mM concentration of genipin powder in a 10% Dimethyl sulfoxide (DMSO), 45 mM 3-[4-(2-Hydroxyethyl)-1-piperazyl]propane sulfonic acid phosphate (EPPS-P) buffered solution. Assistance in preparing the reagent components was received from Dr. Matthew Brown of Orthopeutics, LP/Crosscoat Medical, LLC in Lexington, KY.

To prepare the genipin vials, the vials, caps and lids were sterilized using autoclave sterilization. Then, 45.24 ± 0.05 mg of cGMP genipin powder (CAS# 6902-77-8) from Wilshire Technologies was placed into each vial with a disposable scoop to create a 100 mM buffer solution. The rubber cap was placed in the bottle and crimped shut. A total of 12 vials of genipin powder were prepared and shipped to STERIS Isomedix Services for terminal gamma irradiation for sterilization.

To prepare the 45 mM EPPS-P buffer solution with 10% DMSO added, the vials, caps and lids were sterilized using autoclave sterilization. Then 22.5 mL of 100 mM EPPS-P buffer, 22.5 mL of deionized water, and 5 mL of DMSO were combined into a bottle, through a 0.2µm sterile filter in a sterile hood. Then, 2 mL of the buffer solution was distributed into 12 sterile vials. The DMSO was added to the buffer to increase solubility of the genipin. Phosphate was added to the EPPS solution initially to catalyze the genipin crosslinking reaction.

Adding 2 mL from one buffer vial to one genipin power vial would produce 2 mL of the 100 mM buffered genipin reagent. One reagent vial was sufficient for two 1 mL injections for the soft palate. Appendix A6 shows the calculations for the genipin powder and buffer solution.

3.2 Pilot *in vivo* Study

3.2.1 Study Logistics

Due to grant requirements, the pilot *in vivo* study had to be completed in an Association for Assessment and Accreditation of Laboratory Animal Care International (AALAC) and Office of Laboratory Animal Welfare (OLAW) approved facility. Therefore, the *in vivo* study was conducted at Sinclair Research Center (SRC), in Columbia Missouri. All of the study horses had to be shipped to SRC, and the efficacy phase

horses had to be shipped back from SRC upon study completion. All six horses arrived to SRC by September 15, 2014, allowing for a one-week acclimation phase**.** Overall, the study lasted three weeks**,** with one week of acclimation, one injection day, three observation recovery days, and one week of post study recovery.

3.2.2 Equine Arrival and Acclimation

Upon arrival at SRC, SRC personnel performed full veterinary examinations on each horse. During the one-week acclimation phase, the horses were individually housed in appropriately sized box stalls within an enclosed large animal facility according to floor space criteria provided by the USDA animal welfare requirements. Horses were fed grain supplied by their owners as directed, and given unlimited access to fresh water and hay *ad libitum*. The horses were hand walked twice per day for exercise. Generalized exams and observations were completed twice a day throughout the course of the study.

3.2.3 Soft Palate Treatment

Dr. Fabio Aristizabal, DVM from UC Davis, completed all soft palate injections. SRC veterinarians monitored the horses throughout the injection process**.** Dr. Thomas Hedman, Ph.D. of Orthopeutics, LP/Crosscoat Medical, LLC and SRC personnel were also present to assist and to observe the procedures.

To begin the injections, a SRC veterinarian examined each horse. After receiving a clean bill of health, the horse was sedated with the appropriate dose of intravenous detomidine and butorphanol according to the animal's weight. The horse was then led into a stockade and given ample time to ensure full sedation. Then, a 1-meter long, 9 mm-outer diameter fiberoptic endoscope was inserted into one nostril and advanced into the larynx. Dr. Aristizabal examined the soft palate to ensure there were no abnormalities. Approximately 10 to 20 mL of 2% lidocaine was then sprayed onto the surface of the caudal margin of the soft palate through the injection port of the endoscope to induce topical local anesthesia.

Concurrently, the genipin buffered reagent was prepared. For each injection, 2 mL of the 45 mM EPPS-P buffer solution with 10% DMSO was injected into one vial of the genipin powder. The solution was then shaken vigorously for about ten minutes until

all of the particles were fully dissolved. Throughout the procedure, the buffer and genipin vials were stored at room temperature.

After allowing several minutes for the lidocaine to take effect, the soft palate injections were completed. The endoscope was advanced through one nostril to the soft palate, and a transendoscopic injection needle was passed through the endoscope's biopsy port and positioned over the area on the opposite side of the soft palate to inject the reagent. Each horse was injected with two 1 mL injections of the genipin buffered reagent in the 5:00 and 7:00 positions on the soft palate, with the epiglottis occupying the 6:00 position, as shown in Figure 3.3. The first horse received two 1.5 mL injections of the genipin buffered reagent due to accidentally injecting too much reagent. After ensuring the needle was in the correct position, 1.5 mL of the reagent was drawn up into the syringe, and the needle was primed. The transendoscopic needle maintained a loading volume of 0.5 mL in the tube, so it was crucial to load 1.5 mL of the reagent solution into the syringe to ensure the desired 1 ml of the reagent was injected into the soft palate. The needle was then pushed forward into the tissue with a quick, controlled thrust in order to penetrate the epidermal covering of the palate. Once the needle was placed in the proper location in the soft palate, the reagent was injected using 1 mL of air. The endoscope was then removed and reinserted through the other nostril for the second injection. After both injections were complete, the horse was led back into the stall for recovery. This procedure was repeated for all six horses.

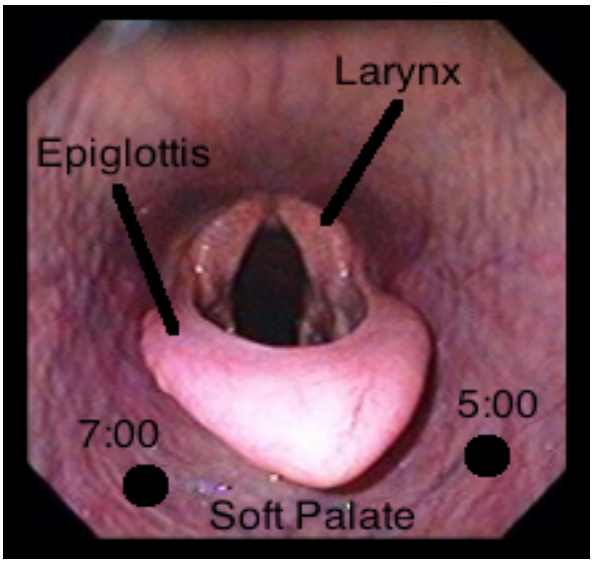

Figure 3.3: The 5:00 and 7:00 injection positions are represented by the black dots on the soft palate when viewed through an endoscope inserted from the nasal cavity of the horse.

For the first 72 hours post treatment, the horses were monitored around the clock with veterinary examinations every hour. Food and water were withheld until the horse was fully recovered from the sedation. The horses remained at SRC for one-week post treatment to allow for full recovery before traveling.

The three safety phase horses were euthanized seven days post treatment, and their soft palates were harvested. The horses were sedated with Detomidine (0.02 mg/kg) and Butorphanol (0.03 mg/kg) intravenously. Fatal Plus (1mL/4.5 kg) was injected for final euthanasia. The soft palates were harvested, stored on dry ice**,** and shipped to Orthopeutics, LP in Lexington, KY for further analysis. The horses were properly disposed of by SRC.

The three efficacy phase horses were returned to their owners 12 days post-treatment for post-treatment examinations.

3.2.4 Post Treatment Examinations

Two weeks post treatment, the efficacy phase horse owners reported on the exercise tolerance, breathing sounds, and general well-being of each horse compared to pre treatment conditions.

Post treatment dynamic endoscope examinations were conducted on the efficacy phase horses. Additionally, respiratory recordings were completed post treatment for 20 minutes at full speed for each individual horse. The dynamic endoscope examinations and the breathing recordings were delayed until approximately six weeks post treatment to allow the horses to be trained back into the same exercise condition as demonstrated in the pre treatment examinations

3.2.5 Respiratory Audio Analysis

The sound analysis was completed using MATLAB. As per Dr. Patwardhan's suggestions, the sound analysis was broken down into the time domain and frequency domain in low frequency ranges and high frequency ranges. The specific steps to analyze the breathing audio were determined as follows. First, have a DDSP professional classify the snoring sound for validation. Then, create a data set with control and DDSP horse breathing. Next, analyze the audio in the time domain and frequency domain. Finally, complete blind testing to determine the results of the

program. Figure 3.4 represents the respiratory audio analysis steps completed using Matlab.

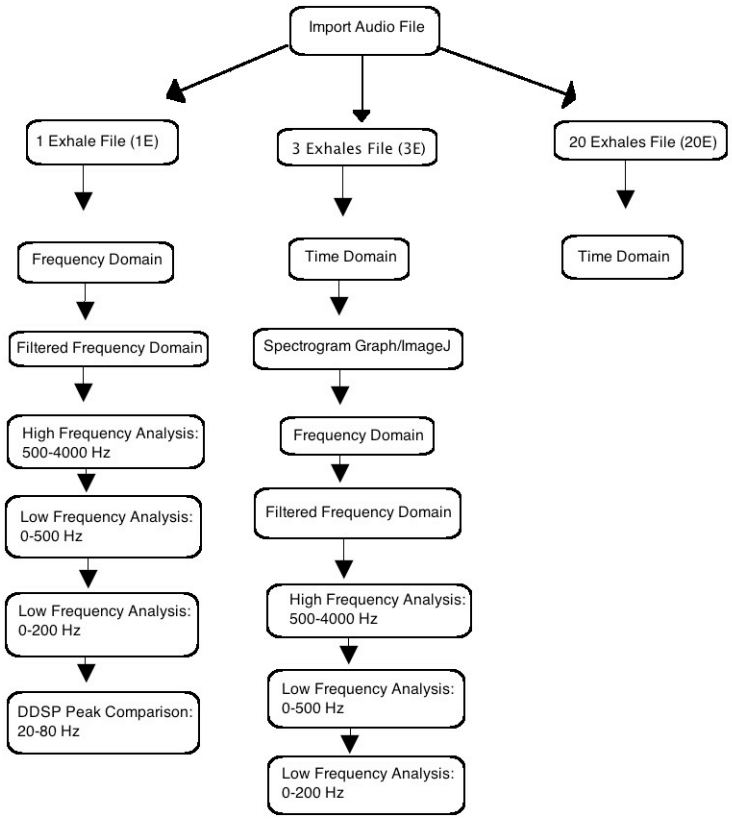

Figure 3.4: Each sound file was broken down into 1, 3 and 20 exhale groups for analysis in the time domain and frequency domain in Matlab.

The audio samples were about 20 minutes long, recording from the time when the recorder was attached until it was removed. Therefore, the samples were cut down using Audacity 2.1.1 (Computer Program, 2015), an audio editor and recording program, to remove the excess audio that was not required, leaving only the audio from the horse exercising at full speed. Each recording was approximately five minutes long after removing the excess audio. Then, the time locations of palate displacements were determined by noting where loud snores or where gaps in breathing occurred. The loud snores and breathing gaps indicated a palate displacement because the wind pipe was obstructed. Using the palate displacement time locations, the samples were further broken down into 1, 3, and 20 exhale recordings for various analyses. The one exhale (1E) recordings were analyzed using the frequency domain only. The three exhales (3E)

recordings were analyzed using the time domain, spectrograms, and the frequency domain. The 20 exhales (20E) recordings were analyzed using the time domain.

Individual programs were created in Matlab (Mathworks Matlab, R2014a Student Version) to analyze 1E, 3E, and 20E recordings, with the 3E program shown as an example in Appendix A7. After the programs were finalized and validated using control respiratory recordings, the pre treatment and post treatment sound recordings for each horse in the efficacy phase of the pilot *in vivo* study were analyzed. For all programs, the first step was to import the desired files. Then, the length and time of the files were determined.

Next, the 3E and 20E programs analyzed the files in the time domain. The time domain was used to locate any gaps in the breathing pattern caused by a soft palate obstruction. Additionally, the pattern and amplitudes of each exhale was compared for pre and post-treatment recordings. To do this, the moving average was used to filter the data, which is done by creating a series of averages for different divisions and shifting it along the full data set to filter the file. For each audio file, the divisions used for averaging were one-fourth of the entire data set, with a=1 and b= [¼ ¼ ¼ ¼] for the filter function in Matlab. Then, the time domain for pre treatment recordings and post treatment recordings were plotted in one window for easy comparisons with time on the x-axis and amplitude on the y-axis.

Then, the 3E programs plotted spectrogram graphs to visually determine changes in sound amplitude across all frequency ranges. Spectrogram graphs were not plotted for the 1E programs because there was insufficient data with only a single exhale shown in the spectrogram. Additionally, the 20E spectrogram graphs were not plotted because they did not provide any additional information compared to the 3E spectrogram graphs. The spectrograms were plotted using the spectrogram function with a window (nwin) of 1024 samples and an overlap (noverlap) of 768 samples. For each graph, the x-axis represented time, the y-axis represented frequency, and the color intensity represented amplitude from -40 to -120 V as demonstrated in Figure 3.5. The spectrogram graphs for pre treatment and post treatment recordings were plotted in one window for comparison.

After creating the spectrogram graphs in Matlab, the total red area representing high amplitudes was analyzed using ImageJ software to determine the percent

difference between pre and post treatment recordings. To do this, the Matlab spectrogram was saved as a JPEG and imported into ImageJ. Once imported, the graph was split into three 8-bit images representing the red, green and blue color channels. When separating color channels, a filter is applied to the image to differentiate red, green and blue colors. For example, for the green color channel, a filter is applied that blocks any green pixel from passing through, causing it to appear white in the final picture. The filter allows any pixel that is not green to pass through, representing it as black or as a shade of gray. Therefore, the green channel best mapped the red high amplitude pixels in the spectrogram graph because the red area appeared as black after the channel filter was applied as illustrated in Figure 3.6. Then, the threshold was adjusted using the default values to intensify the pixels, which fall into the intensity range from 0 to 160. Pixels with an intensity of 0 represented black and an intensity of 255 represented white [65]. Finally, the total area and percent area of the number of pixels were calculated through the analyze particles feature in ImageJ. These steps were completed for all the pre treatment and post treatment spectrograms, and a detailed protocol is shown in Appendix A8. The percent difference was calculated to determine the change in the total area of the high amplitude red squares in the spectrogram graphs using Equation 1.

$$\%Difference = \frac{Post\ Treatment\ Area - Pre\ Treatment\ Area}{Pre\ Treatment\ Area}\ x\ 100\% \quad (Eq.1)$$

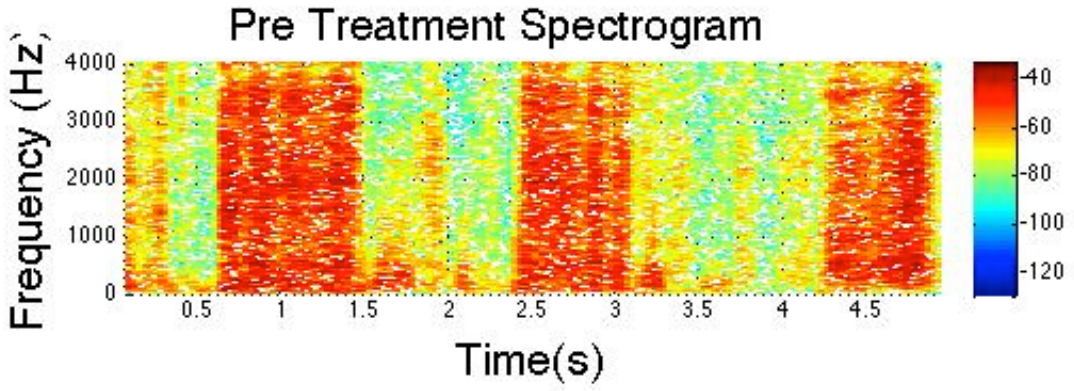

Figure 3.5: An example spectrogram graph shows the various colors present with red representing the high amplitude noises and blue representing the low amplitude noises.

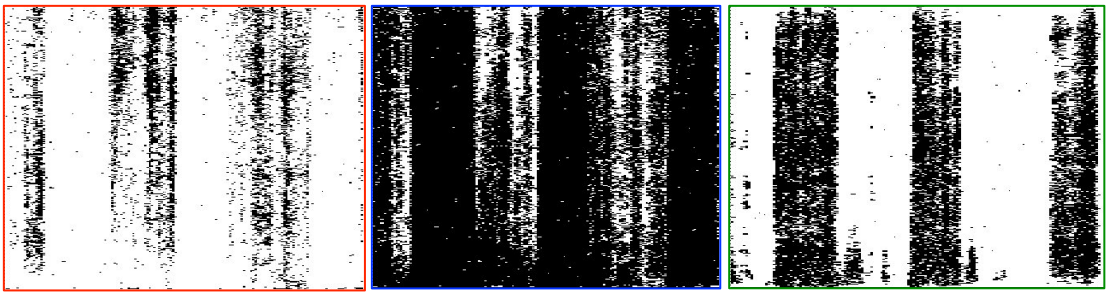

Figure 3.6: The red (left), blue (middle), and green (right) channel graphs produced by ImageJ display the different color pixels depending on which filter is applied to the original image. In this case, the green channel best represents the shape of red squares in the original spectrogram graph.

Finally, the 1E and 3E programs were analyzed using the frequency domain. First, the recordings were transformed into the frequency domain using the fast Fourier transform (FFT). Once in the frequency domain, the entire pre treatment and post treatment graphs were plotted with frequency on the x-axis and amplitude on the y-axis. Then, the frequency domain signals were filtered using the moving average to remove noise. The original frequency domain graph and the filtered graph were plotted on a single graph for comparison for both the pre treatment and post treatment files.

The high amplitude frequency range was analyzed in relation to palatal displacement “whistling” noises. The filtered signals for the pre and post treatment audio was plotted from 500 to 4000 Hz. The low-end frequency was set to 500 Hz because that was the cutoff frequency for the laser non-contact displacement measuring system used in the wind tunnel study. With a data collection rate of 8 kHz, the Nyquist frequency for the samples was 4000 Hz, so that was used as the maximum point in the graph.

The low amplitude frequency range was analyzed in relation to snoring loudness because typical snoring sounds occur below 200 Hz. First, frequency domain graphs were created from 0 to 500 Hz because frequencies less than 500 Hz would contain the sounds related to snoring caused by vibration of the soft palate according to Dr. Patwardhan. Also, 500 Hz was the cutoff frequency for the laser system used during the wind tunnel study. Next, the frequency domain graphs were plotted from 0 to 200 Hz because 200 Hz is the typical maximum frequency used for human snoring analysis [39,40]. Then, the frequency domain graphs were plotted form 0 to 100 Hz to correspond with palatal vibrations. For the low frequency domain graphs, the area under the curve was used to determine the percent difference between the pre-treatment

and post-treatment audio recordings. The area under the curve was calculated using the trapz function in Matlab and plotted on the corresponding graph as demonstrated by Figure 3.7. Percent difference was calculated using Equation 1.

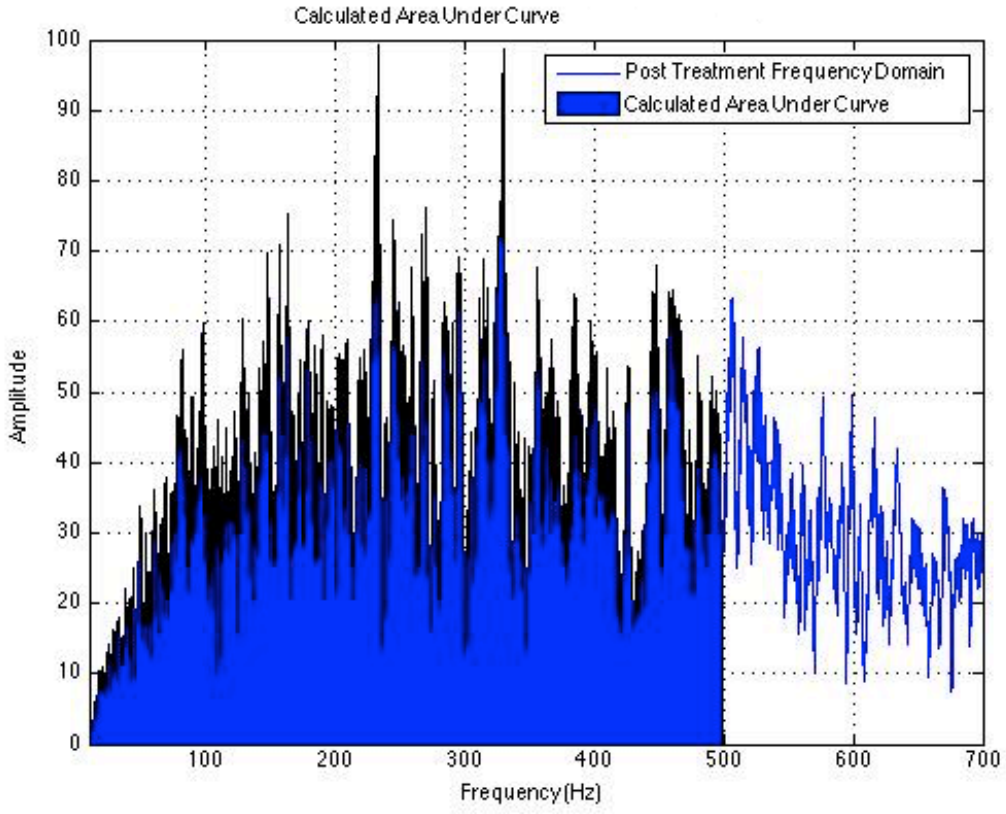

Figure 3.7: For each pre treatment and post treatment frequency domain graph, the area under the curve was calculated and highlighted as demonstrated in the graph above.

Finally, as previously mentioned, a study completed by Franklin et al. discovered a peak in the frequency domain corresponding to DDSP. Based on their results, the peak appeared at 41±21Hz for the *in vitro* horses and 53±24 Hz for *in vivo* study horses with DDSP, as shown in Figure 3.8 [55]. Therefore, the 1E frequency domain graphs were analyzed from 20 Hz to 80 Hz to include the average 'DDSP Peak' location plus one standard deviation on either side. Only 1E was analyzed in this range to best compare to the results from the previous study, which only analyzed one exhale at a time. These graphs were used to determine if the 'DDSP Peak' existed before or after treatment with the genipin injections in relation to the study completed by Franklin et al.

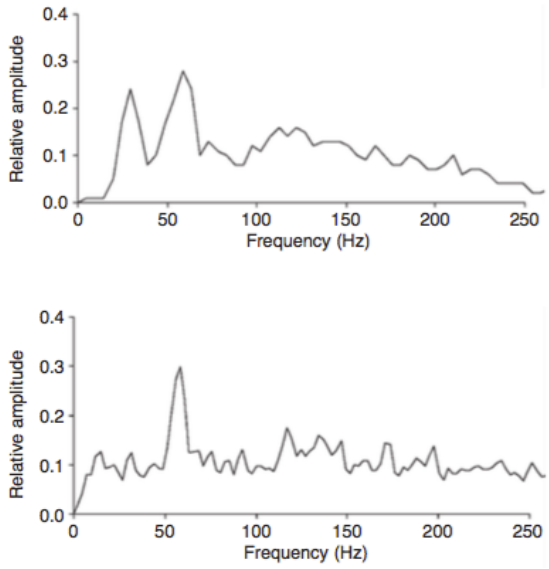

Figure 3.8: The DDSP peak occurs in the 20-80 Hz range in the frequency domain as demonstrated by the peaks from the cadaveric *in vitro* DDSP study results (top) and the *in vivo* study results (bottom) [55].

3.2.6 Histological Analysis

The three soft palates harvested from the safety phase horses were thawed for 24 hours and sectioned for histological analysis. Each palate was cut in half along the median, and then three sections were cut perpendicular to the median from each lateral half palate, producing six samples for each palate for a total of 18 samples. Two samples from treated regions of tissue as determined by the visual observation of the blue coloration due to genipin crosslinking, and one sample from an apparently untreated region of tissue were sectioned from each soft palate half. Figure 3.9 shows the specific sections used for each palate. Samples were taken from the internal portion of the sample along the sagittal plane so that each histology slice would contain both the oral and respiratory mucosal layer. A suture was placed in each sample on the opposite side of the cutting plane. The samples were labeled according to the original location on the soft palate and placed in beakers with 100 mL of 10% formalin for six days. Then, the samples were packaged into separate 50 mL tubes of 70% ethanol and shipped via FedEx ground to IDEXX BioResearch Pathology Services (IDEXX) in Columbia, MO for histological analysis.

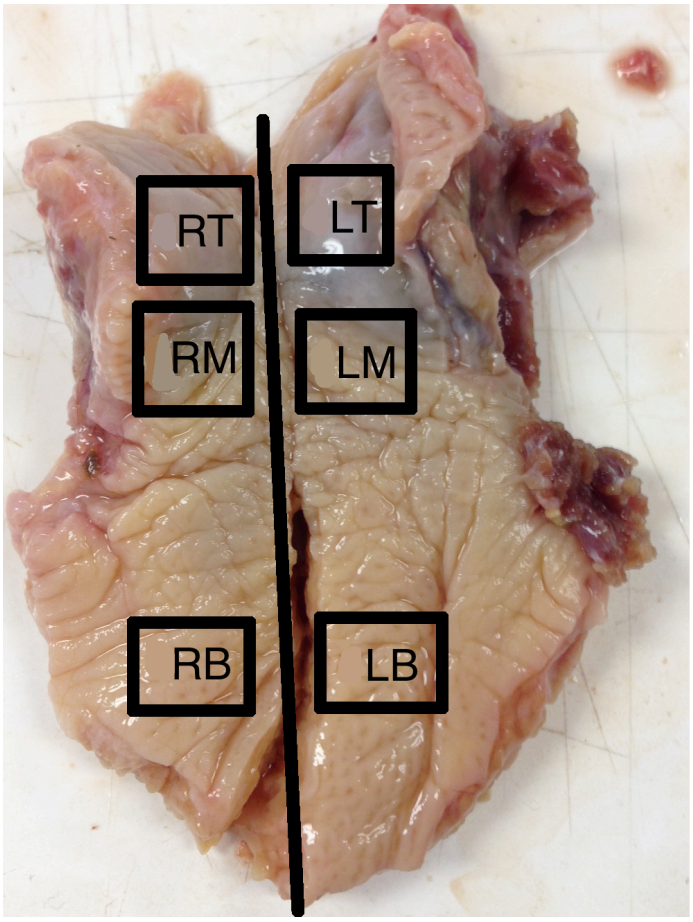

Figure 3.9: Each soft palate was divided in half and then three sections were cut from each half in the general areas shown in the figure. At least one of the samples from each side was cut from a perceived untreated section of the palate.

Dr. Cynthia Besch-Williford, a licensed veterinary pathologist, at IDEXX completed the histological analysis. All biopsies were sectioned in the sagittal plane such that both mucosal surfaces along with the submucosal and muscular components were represented. Tissues were processed for paraffin infiltration, blocked, sectioned, stained with H&E and examined microscopically. Observed microscopic changes were described as to the extent and grade of inflammation and fibroplasia using terms including minimal, mild, moderate, and marked.

3.3 Soft Palate Mechanical Testing

3.3.1 Study Preparation

The soft palate mechanical testing study was completed to determine any mechanical property changes in the soft palate after injecting it with 50 mM genipin solution. The genipin was mixed with a saline solution that would be available in most

hospital or laboratory settings. Phosphate was added to the solution to catalyze the reaction.

A total of 12 cadaveric equine soft palates were separated into four sections and put into three testing groups: control (no injection), buffer-only injection or genipin injection. The samples were mechanically tested to compare the hysteresis, stress relaxation and tensile properties of each sample.

3.3.2 Reagent Preparation

The genipin powder was premeasured and placed into individual glass vials. Each vial contained 22.6 ± 0.5 mg of genipin (CAS#6902-77-8) from Wilshire Technologies in order to create a concentration of 50 mM when mixed with 2 mL of the buffer solution. A total of 10 vials were created.

To make the buffer solution, saline was combined with phosphate to create a 50 mM phosphate solution. First, the 0.9% saline was made by adding 9.0 grams of NaCl (CAS#7647-14-5) to 1000 mL of deionized water and shaking vigorously until fully dissolved. Then, 19.0 grams of sodium phosphate tribasic dodecahydrate (CAS# 10101-89-0) was added to the 1000 mL saline solution, creating saline with a 50 mM phosphate concentration. See Appendix B1 for full calculations for the genipin and buffer solution.

3.3.3 Sample Preparation

Twelve frozen cadaveric equine soft palates were received from Conboy Enterprises, Inc. in Lexington, KY. The soft palates included the entire upper respiratory tract, including the trachea, larynx, epiglottis, soft palate, and the surrounding bones, muscles, tendons and ligaments. The palates were thawed for 24 hours. After thawing, the soft palates were excised from the surrounding tissue. To remove, the tissue above the palate was cut in half along the median to expose the epiglottis and soft palate. The epiglottis was placed below the notch in the soft palate. Then, the palate was removed by cutting along the outside edge of the palate. The edges of the V-notch of the palate were removed by cutting along the bones. Once the palate was removed, it was examined and trimmed to ensure only the soft palate was present. The other tissue was discarded appropriately. See Appendix B2 for the soft palate extraction protocol supplemented with pictures.

The soft palate was then divided into four samples, cut along the V-notch of the palate. First, the soft palate was divided along the midline, and then two samples, approximately 2 cm wide, were cut along the V-notch, or free edge, of the palate. The samples cut from the first spot next to the free edge of the palate were labeled as tops, and the samples cut closer to the hard palate were labeled as bottoms, as demonstrated in Figure 3.10. The samples were divided among the three groups according to the chart in Figure 3.11.

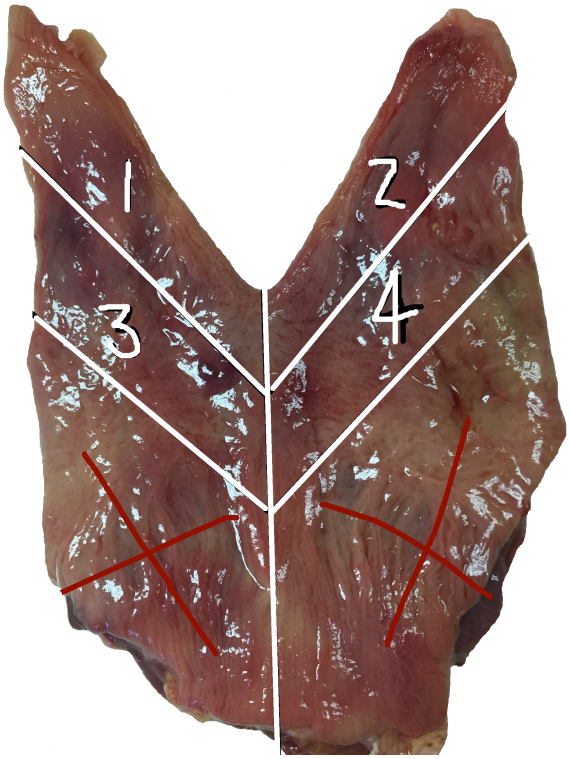

Figure 3.10: The two samples, #1 and #2, sectioned from the free edge of the palate were labeled as tops. Section #3 and #4 were labeled as bottoms. The excess tissue near the hard palate was discarded.

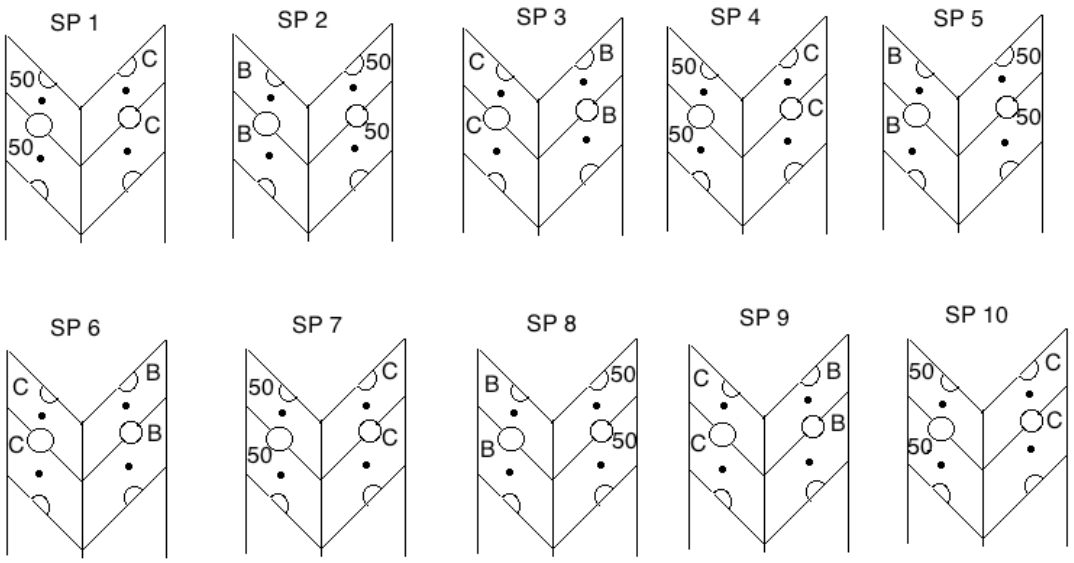

	Left Top	Left Bottom	Right Top	Right Bottom	Total
50	4	4	3	3	14
C	3	3	4	4	14
B	3	3	3	3	12
Total	10	10	10	10	40

• Injection Site
○ Punch Site
50: 50 mmol Section
C: Control Section
B: Buffered Section

Figure 3.11: Each soft palate sample was divided into a test category based on the schematic above. The test categories were rotated among the palates to randomize the groupings.

Samples in the control group were wrapped in a saline soaked paper towel, sealed in a plastic bag filled halfway with saline to maintain tissue moisture, and put on a shaker plate at room temperature. Samples in the buffer group were injected with 0.5 mL of the buffer solution using a 22 g, 1” needle. The injections were administered about halfway down the length of the sample. The needle was inserted at an angle of approximately 30 degrees from the horizontal. The reagent was delivered with uniform pressure over five seconds. The sample was wrapped in a saline soaked paper towel, placed in a sealable plastic bag halfway filled with saline, and put on a shaker plate at room temperature. Samples in the genipin group were injected with 0.5 mL of the genipin reagent using a 22 g, 1” needle. The injections were administered about halfway down the length of the sample. The needle was inserted at an angle of approximately 30 degrees from the horizontal as demonstrated in Figure 3.12. The reagent was delivered with uniform pressure over five seconds. The sample was wrapped in a saline soaked paper towel, placed in a sealable plastic bag halfway filled with saline, and put

on a shaker plate at room temperature. Pre-treatment sample height, length, and width, as well as injection time were recorded.

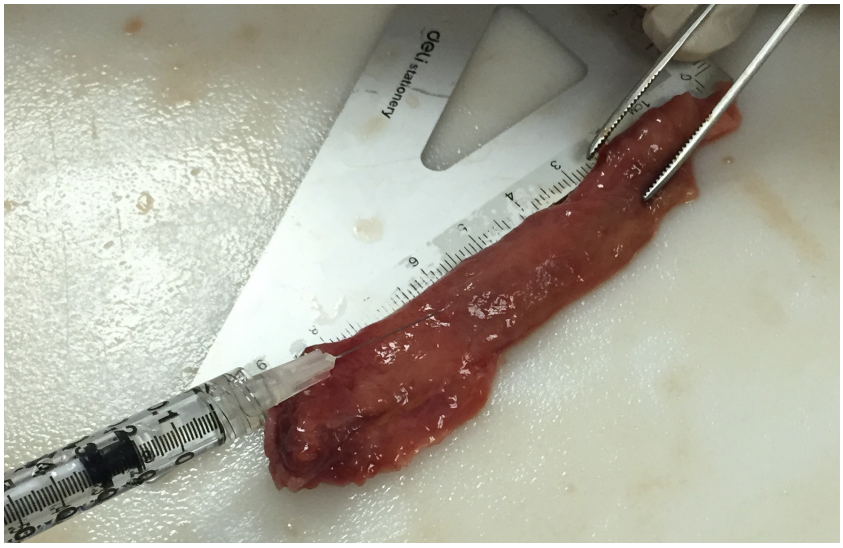

Figure 3.12: The needle was placed about halfway down the length of the sample. The reagent was uniformly injected as the needle was pulled back out of the sample to ensure even coverage and to prevent pillowing of the palate.

All samples remained on the shaker plate overnight for 12-15 hours at room temperature to allow the genipin plenty of time to diffuse. After incubation, all samples were necked down to approximately 1 cm wide by 1 cm long in the middle using a circular metal punch as seen in Figure 3.13. Necking height, length, and width were recorded.

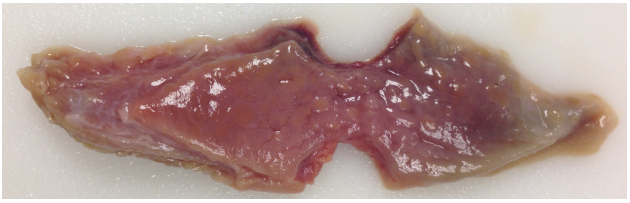

Figure 3.13: After incubating overnight, the soft palate samples were necked down to ensure failure in the middle during the tensile test.

3.3.4 Mechanical Testing Protocol

All samples were mechanically tested using a materials test system (Test Resources 100R1000) via a protocol including hysteresis, stress relaxation and tensile loading to failure tests, as shown in Appendix B3. The sample was loaded into the tensile testing machine and secured using the grips at a gauge length of 42 mm. To

prevent slippage, both ends of the tissue were wrapped in a Chem-Wipe to reduce wetness and increase grip.

The hysteresis test was performed first. A force of 10 N was loaded onto the sample. The test resources machine was then set up to perform a hysteresis test of 20 cycles with a displacement of +/- 3mm from the starting point at a rate of 5 mm/s. The time (s), stroke (mm), load (N), torque (N-mm) and angle (deg) were recorded at a sampling rate of 50 Hz.

The stress relaxation test was performed next. Again, a force of 10 N was applied to the sample. The sample was then held at that constant displacement for five minutes. Upon completion of the five minutes, the force was reduced to zero, and the sample rested for one minute. Again, the time (s), stroke (mm), load (N), torque (N-mm) and angle (deg) were recorded at a sampling rate of 25 Hz.

Finally, the tensile test to failure was performed. Starting from 0 N, the machine loaded the tissue in tension until failure at 1 mm per second. The time (s), stroke (mm), load (N), torque (N-mm) and angle (deg) were recorded at a sampling rate of 50 Hz. After the genipin samples failed, the approximate percent of blue fibers in the failure region was noted by looking at the surface fibers of the torn region.

3.3.5 Mechanical Testing Analysis

Hysteresis was calculated as the area between the loading up and loading down curves for each sample. To determine the change in hysteresis and the hysteresis ratio, the time (s), stroke (mm) and load (N) data from the mechanical test was utilized. The starting point was used to offset the stroke data to find the absolute displacements. For example, if the starting point was -42 mm, the stroke data was offset by 42 mm. Then, strain was determined by dividing the displacement by gauge length. Finally, stress in MPa was calculated by dividing the load by the cross-sectional area of the tissue.

To determine the 1st and 20th cycles of the hysteresis plot, the cyclical loading was plotted with load in Newton on the y-axis and time in seconds on the x-axis as shown in Figure 3.14. The first cycle was determined to be from the first local minimum to the second local minimum as shown in red. The last cycle was determined to be from the 19th local minimum to the 20th local minimum as shown in black. Then, the corresponding local minimum points were extracted and graphed to create the individual

cycle hysteresis curves with stress on the y-axis and strain on the x-axis. For the first cycle, the stress and strain were plotted from corresponding values at the 1st local minimum point to the 2nd local minimum point as shown in Figure 3.15. For the last cycle, the stress and strain were plotted from corresponding values at the 19th local minimum point to the 20th local minimum point as shown in Figure 3.15, as well. Finally, the entire hysteresis curve was plotted with strain on the x-axis and stress on the y-axis as shown in Figure 3.17. The 1st and 20th cycles were highlight in red and black respectively.

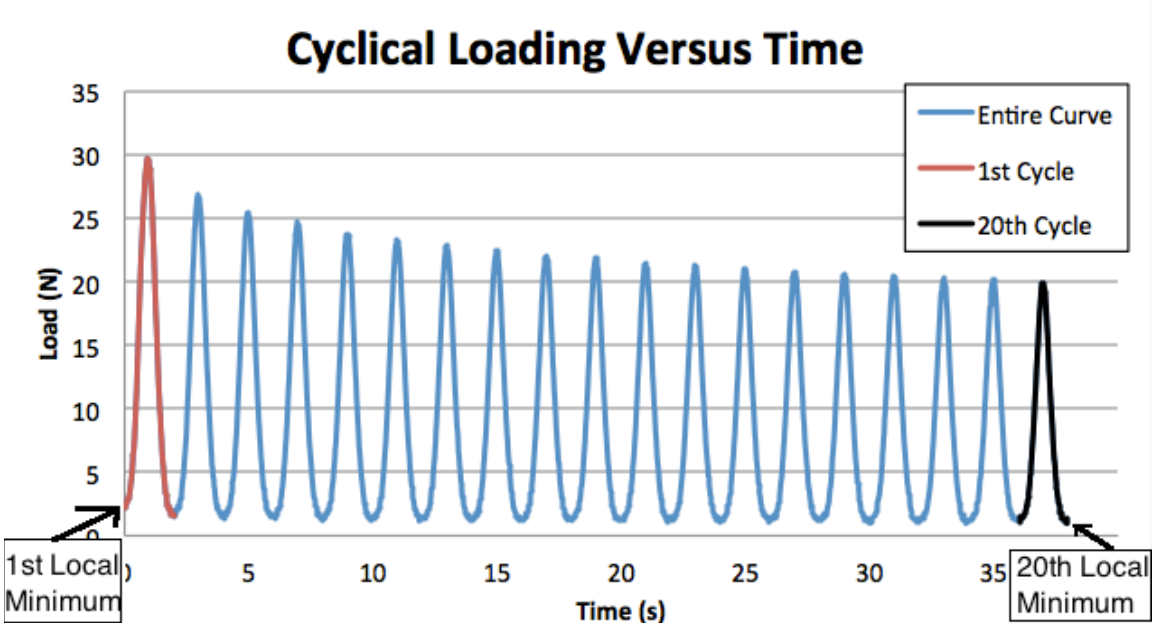

Figure 3.14: To determine the location of the 1st and 20th cycles of the hysteresis curve, the loading cycles versus time were plotted. The 1st cycle was taken from the 1st local minimum to the 2nd local minimum, and the 20th cycle was calculated form the 19th local minimum to the 20th local minimum.

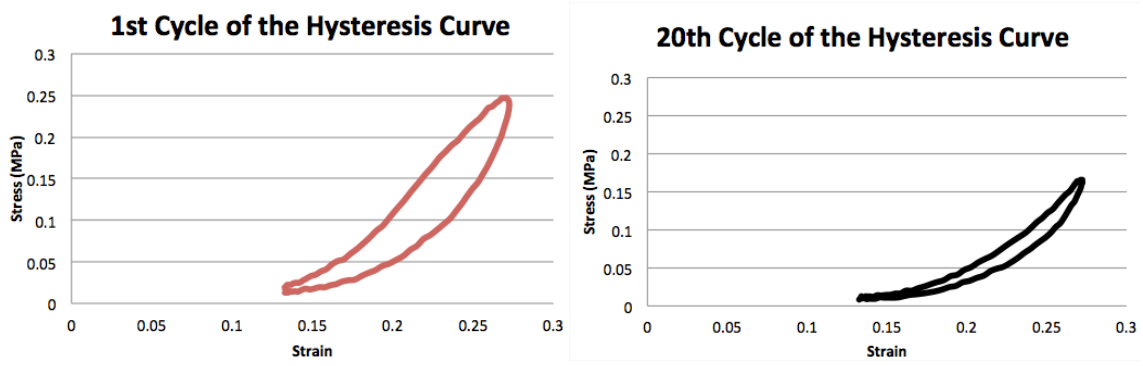

Figure 3.15: The 1st and 20th cycles were plotted in relation to stress and strain to determine the hysteresis.

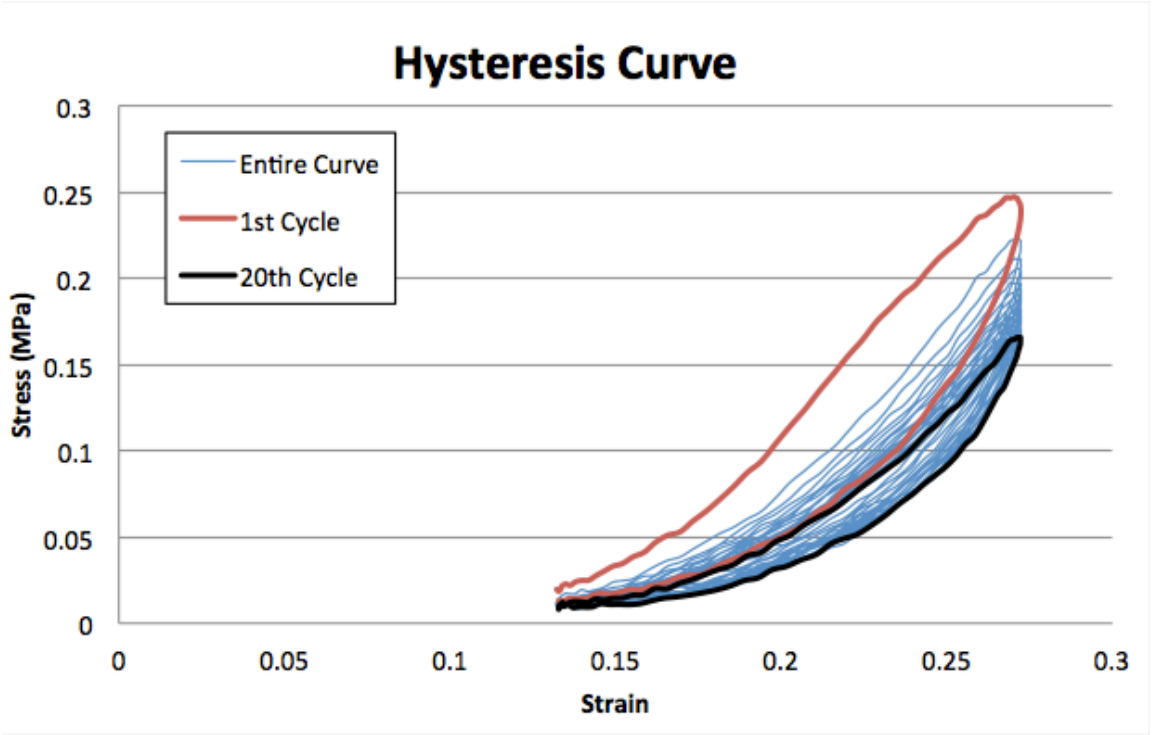

Figure 3.16: The entire hysteresis curve was plotted with the 1st and 20th cycles highlighted to see their relation to the rest of the cycles.

Finally, the contribution toward the hysteresis calculation for each individual set of adjacent data points was calculated using Equation 2, with stress point 1 and stress point 2 representing the individual stress points throughout the hysteresis cycling.

$$Individual\ Hysteresis = \left(\frac{Stress\ Point\ 1 + Stress\ Point\ 2}{2}\right) * (Strain\ 2 - Strain\ 1) \quad \text{(Eq. 2)}$$

Once all of the individual hysteresis values were calculated, the total hysteresis for the loading curve and the total hysteresis for the unloading curve were calculated for the 1st load-unload cycle. The total hysteresis for the loading curve was calculated by adding together all of the individual hysteresis values from the 1st local minimum to the 1st cycle maximum. The total hysteresis for the unloading curve was calculated by adding together all of the individual hysteresis values form the 1st cycle maximum to the 2nd local minimum. Then, the difference between the loading curve total hysteresis and the unloading curve hysteresis was calculated to determine the area between the curves. This was repeated for the 20th cycle. Finally, the change in hysteresis between the 1st and 20th cycles was calculated by subtracting the 20th cycle hysteresis from the 1st cycle hysteresis. Additionally, the hysteresis ratio was calculated by dividing the 20th cycle

hysteresis by the 1st cycle hysteresis. Examples of hysteresis calculations are shown in Appendix B4.

Using the load (N), time (s), and stroke (mm) data from the stress relaxation test, the stress relaxation was calculated as the decrease in stress over a five-minute period. First, the offset displacement was added to the stroke to find total displacement, and then the displacement divided by the gauge length was used to determine the strain. Next, stress in MPa was calculated by dividing the load by the cross-sectional area. Using the stress in MPa and time in seconds, the stress relaxation curve was plotted as demonstrated in Figure 3.17. Then, stress relaxation was calculated by subtracting the minimum stress value from the maximum stress value. Next, relaxation modulus was calculated by dividing the stress by the constant strain according to Equation 3, and then the overall relaxation modulus was determined by subtracting the minimum modulus value from the maximum modulus value. Finally, normalized relaxation modulus was calculated by normalizing the strain used in Equation 3 by dividing the individual sample strain by the average strain for each test group.

$$Relaxation\ Modulus\ (t) = \frac{\sigma(t)}{\varepsilon} \quad \text{(Eq. 3)}$$

Examples of the stress relaxation test calculations are shown in Appendix B5.

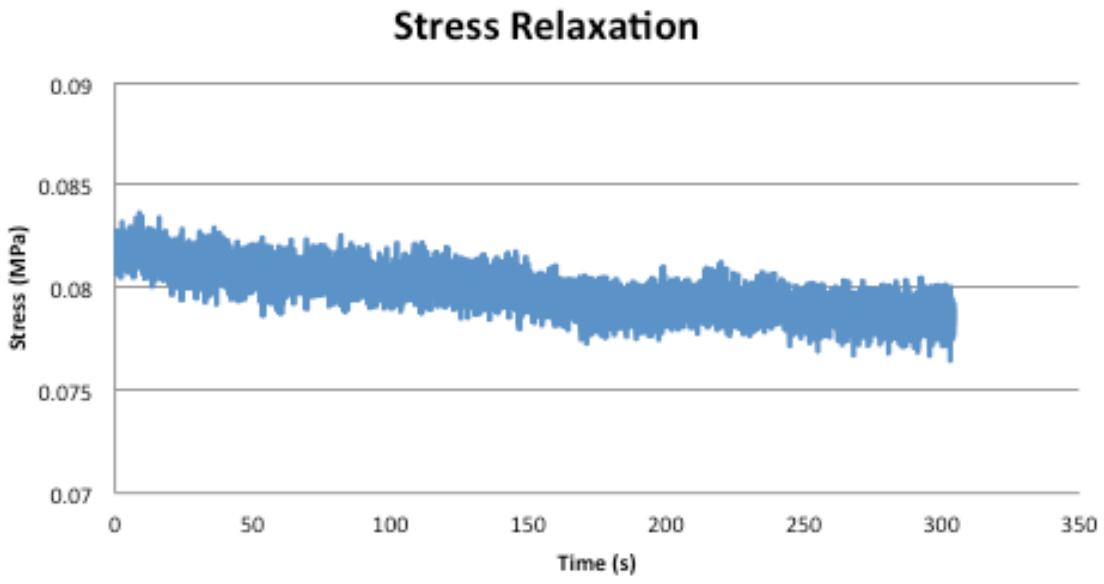

Figure 3.17: The stress relaxation graph for each sample was plotted to demonstrate the relaxation of the specimen over time.

The tensile test to failure data was utilized to calculate a variety of elastic-plastic parameters using stroke (mm) and load (N), including ultimate tensile stress, ultimate tensile strain, Young's modulus, toe region slope, yield point stress, yield point strain, toughness and resilience. Using the stroke (mm) from the mechanical testing data, the values were offset based on the starting stroke. For example, if the test begins at -42 mm, the stroke values were offset by 42 mm to get the actual deformation of the specimen. Then the strain was calculated by dividing the deformation by the gauge length. Using the load (N) data from the mechanical test, stress was calculated by dividing it by the smallest cross-sectional area of the specimen. The maximum stress was used to determine the ultimate tensile stress. The ultimate tensile strain was the strain at the maximum stress point. The ultimate tensile stress and strain occurred at the maximum point in the graph as illustrated in Figure 3.18 by the black arrow.

Next, the stress versus strain graph was plotted with stress on the y-axis and strain on the x-axis to find the next parameters as demonstrated in Figure 3.18. First, the toe region was calculated by plotting the points from the first non-zero stress value to 0.05 MPa and adding a polynomial trend line raised to the 2^{nd} power. The toe region slope, which measured the straightening of the collagen fibers as they began to experience load, was the slope of the toe region trend line as shown in purple. Next, the start of the linear region was determined by moving 50 values past the last value of the toe region. The linear region was determined to be the next 150-200 values past the starting point, as long as there was no obvious break in linearity in the graph as shown in green. A linear trend line was plotted for this region. Young's modulus, which measured the stiffness of the tissue, was considered to be the slope of the linear region trend line.

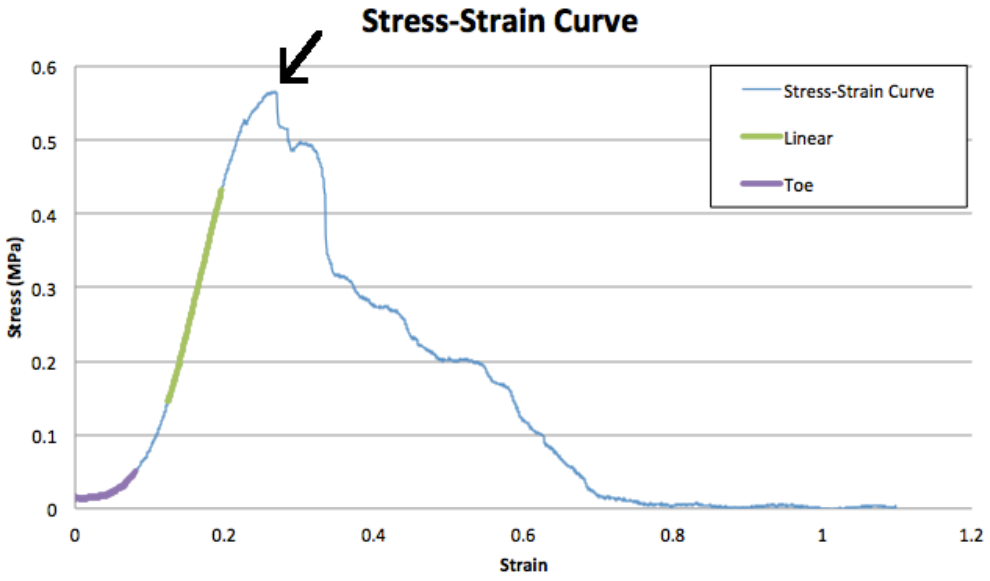

Figure 3.18: The ultimate tensile stress and strain were determined by the maximum location on the graph as illustrated by the black arrow. The toe region slope and Young's modulus were also determined from the toe region and linear region, respectively.

Then, the linear region trend line was offset by 0.2% strain, and the resulting line was plotted. From the intersection of the offset strain line and the stress-strain curve, the yield point was calculated as the point that the tissue begins to plastically deform leading to permanent tissue damage as shown in Figure 3.19. The x and y values at the yield point were the yield strain and yield stress as demonstrated by the black arrow. The toughness was defined as the ability to deform the tissue up to the fracture point, and the area under the entire stress-strain curve calculated it as demonstrated by the orange highlighting in Figure 3.20. From the toughness value, the energy required to deform the tissue was calculated by multiplying the toughness by the cross-sectional area. Likewise, the resilience was defined as the ability of a material to absorb energy when it is deformed elastically, and it was calculated by determining the area under the stress-strain curve up to the yield point as shown by the red highlighting in Figure 3.21 [66-68]. Examples of the tensile test to failure calculations are shown in Appendix B6.

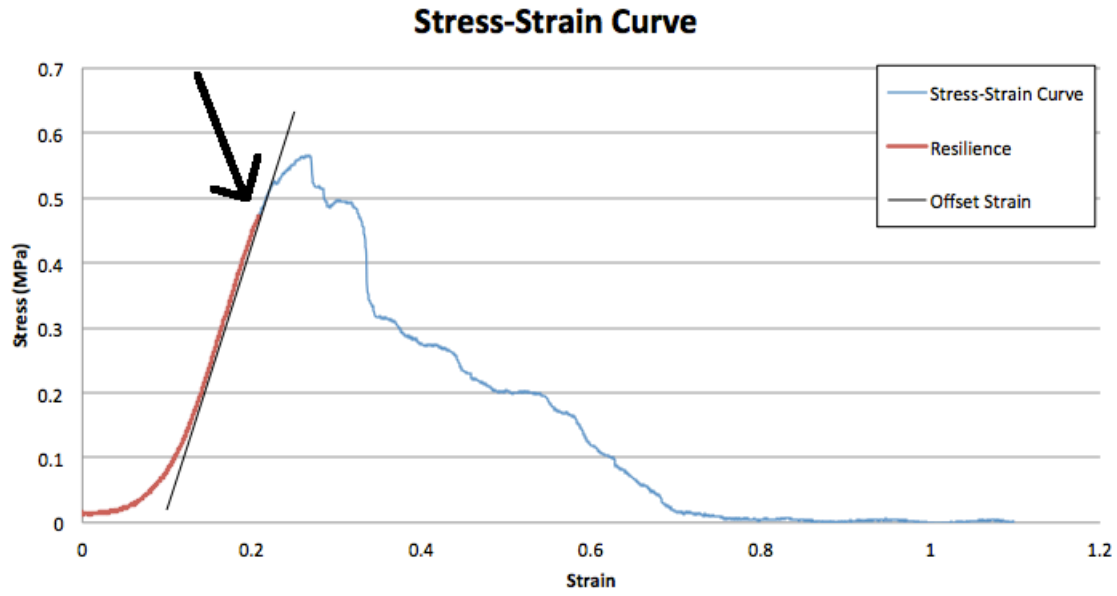

Figure 3.19: The yield point was determined by offsetting the linear region line by 0.2% strain and calculating the intersection point of the two lines, as demonstrated by the arrow in the graph.

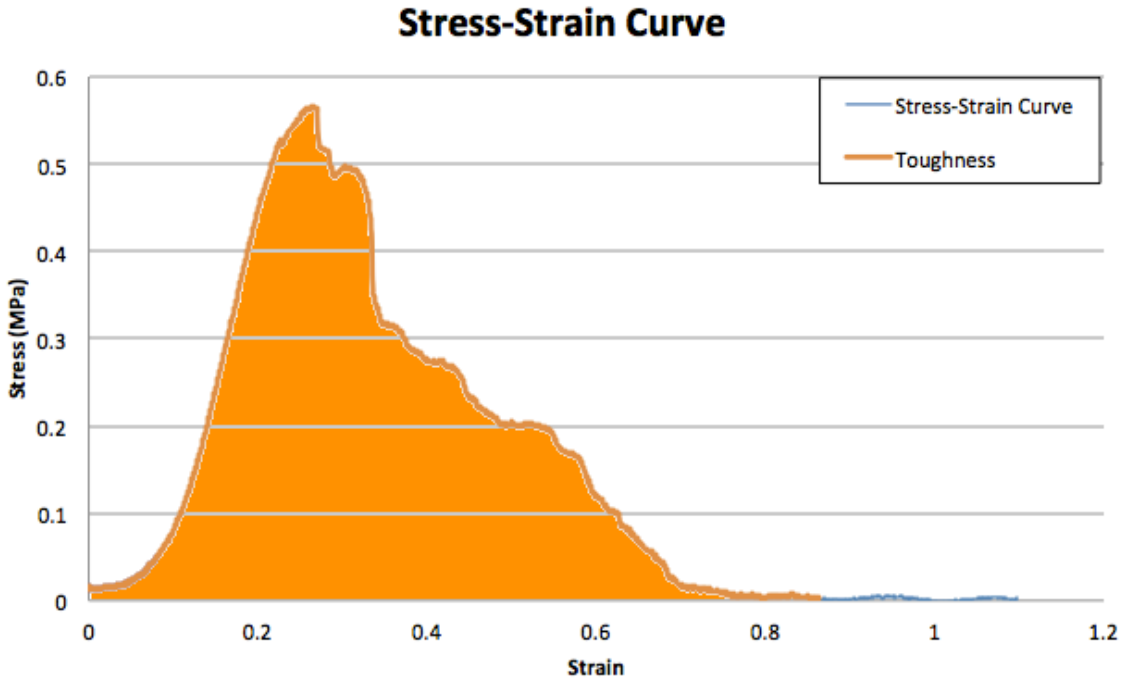

Figure 3.20: Toughness was calculated by the area under the stress-strain curve as represented in orange.

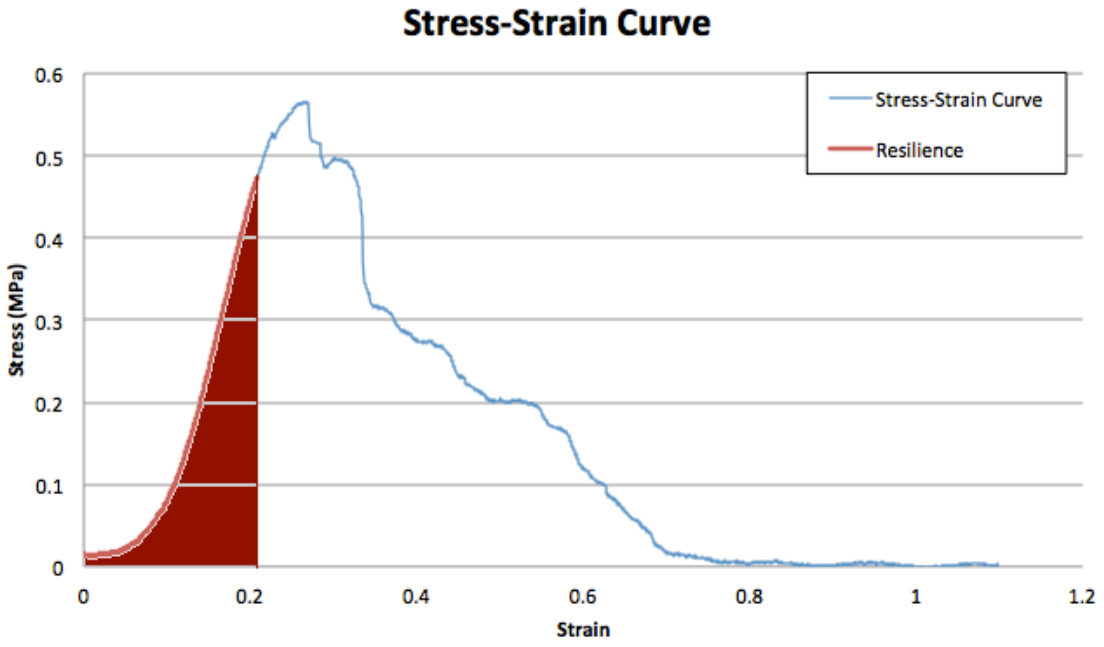

Figure 3.21: Resilience was calculated as the area under the stress strain curve up to the yield point as highlighted in red.

After all of the parameters were calculated for each sample, the outliers, determined by the three-sigma rule, were removed from the data set. Any samples that had results more than three standard deviations away from the mean were noted as outliers in that category. If a sample had more than five total outliers across all categories, the sample was determined to be an overall outlier and removed from the analysis.

The averages and standard deviations for each parameter were calculated for individual control, buffer, and genipin groups. Likewise, each group was broken down into the tops group and the bottoms group, corresponding to the position of the sample relative to the soft palate as previously demonstrated in Figure 3.10, and the averages and standard deviations for each parameter were also calculated. Percent differences between the parameters of the different groups were computed using Equation 4.

$$\%Difference = \frac{(average\ group1\ parameter - average\ group2\ parameter)}{average\ group1\ parameter} * 100 \quad \text{(Eq. 4)}$$

Any parameters with a percent difference greater than 30% were noted.

Statistical analysis was completed to determine if the means of the different groups were statistically significant. The first group compared was the control samples

versus the buffer treated samples, comparing the top samples only, the bottom samples only, and all of the samples combined. This was used to verify that there was no significant difference in the mechanical properties caused by the buffer treatment alone. The same statistical comparisons were compared for the buffer samples versus the genipin treated samples. This comparison was used to determine any significant differences in the mechanical properties as a result of the genipin treatment. Either a two-sample *t*-test with independent sample groups or a non-parametric Mann-Whitney test was completed based on the results of the F test.

The two-sample *t*-test with independent groups determined whether the means of two groups were different. To complete a two-sample *t*-test, the following assumptions were made [70]:

- The two groups were independent variables.
- Each observation within the group was independent of the other observations in the group.
- The variables followed a normal distribution with the same variance.

The Mann-Whitney test compared the median differences between the two groups. The assumptions followed for the Mann-Whitney were [70]:

- The two groups were independent of one another.
- The results were ordinal.
- The samples within each group were independent.
- The variables did not have to be normally distributed.

To decide the appropriate statistical analysis test for each group, the F-test was completed to determine if the sample variances of the two populations were equal. Equation 5 was used to calculate the F statistic [70].

$$F = \frac{(\frac{df_1 * S_1^2}{\sigma_1^2})/df_1}{(\frac{df_{12} * S_2^2}{\sigma_2^2})/df_2} \quad (Eq. 5)$$

Then, the F_{crit} value was determined using an F-table. If the F value was greater than the F_{crit} value, the variances were considered to be different. If the F value was less than the F_{crit} value, the variances were considered to be the same. For the comparisons that

passed the F-test, a *t*-test was completed because all assumptions of the *t*-test could be met. For comparisons that failed the F-test, a Mann-Whitney test was completed because the sample variances were determined to be different resulting in not being able to meet all of the *t*-test assumptions.

4. Results and Discussion

This section discusses the results of the pilot equine *in vivo* study and the soft palate mechanical testing study. Throughout this chapter, the results from the wind tunnel study conducted previously by Dr. Kuo, as discussed in Chapter 1, are referenced in relation to the results of the *in vivo* and mechanical testing studies.

4.1 Pilot *in vivo* Study Results

This section goes into further detail about the results of the pilot equine *in vivo* study, including the outcomes of dynamic endoscope examinations and the respiratory audio recordings.

4.1.1 Voice Recorder Design Testing

Prior to conducting tests on the *in vivo* study horses, the recorder design integrity was tested using eight non-study horses to verify that the recorder could distinguish a variety of breathing noises in various exercising conditions. All eight of the non-study horses were equipped with the recorder on the side of the halter and exercised at a walk, trot, and canter as shown in Figure 4.1. The recordings took place in windy conditions and in calm conditions. The recorder was able to pick up a variety of exhales, snorts, coughs, and other respiratory noises. Additionally, the design of the recorder was sturdy enough to withstand being smacked against a gate by one of the horses. Overall, the recorder was determined to be successful because it could pick up a variety of noises in different environmental conditions, as well as withstand physical abuse by the horses throwing or moving their heads.

Figure 4.1: The recording device was tested on non-study horses to ensure the integrity of the device at a walk, trot and canter.

4.1.2 Study Enrollment

Despite DDSP being relatively prevalent in racehorses, most afflicted horses are quietly euthanized, making it difficult to find the three horses to enroll in the study. Dr. Sprayberry provided a list of over 300 qualified equine veterinarians in Kentucky that were called or emailed to potentially help find horses with DDSP. From that list, only a handful of local veterinarians were willing to help locate horses with DDSP. Overall, the process took six months to find just three DDSP horses to enroll in the study.

The first horse enrolled was a 7-year-old thoroughbred mare that was previously diagnosed with DDSP via a dynamic endoscope examination. She displaced frequently at a walk, trot, and canter. She had no previous surgeries or treatments for DDSP. She was a pet with no previous racing history. This horse was withdrawn from the study, due to logistical issues and feasibility concerns about the study.

The next horse enrolled was a 7-year-old thoroughbred gelding, BH. At 2 years old, he underwent a preventative tieback surgery despite having a normal epiglottis and soft palate at the time. At 3 years old, the tieback was released, and he began displacing a few months later. At that point, he was diagnosed with DDSP and retired from racing. A tie forward procedure was completed at 5 years old. At 6 years old, the

edge of his soft palate was trimmed with a laser. Currently, he has been turned out to pasture due to frequent displacement of his soft palate. BH has no surgical or treatment options left for DDSP.

The third horse was TH, a 3-year-old Standardbred gelding. TH was not previously diagnosed with DDSP, but he exhibited all of the classic symptoms, including roaring, snoring, and exercise intolerance. During races, TH would produce a loud roaring noise and then stop, gasping for air. TH did not undergo any surgeries, but he did unsuccessfully try the Cornell Collar. TH was actively being raced in Standardbred harness races at the start of the study.

The final horse was MV, a 2-year-old Standardbred mare. MV was never formally raced, but she was in training to be a Standardbred harness racehorse. During training, MV often would roar and experience shortness of breath.

One donated control was a 25-year-old quarter horse gelding with no history of breathing abnormalities. The other donated control was a 17-year-old quarter horse gelding with no history of breathing abnormalities. The final control horse was purchased from a horse dealer in KY. This control was a 6-year-old quarter horse mix gelding with no history of breathing abnormalities.

After all six horses were enrolled in the study; horse identification numbers were assigned as shown in Table 4.1

Table 4.1: Identification numbers assigned to safety and efficacy phase horses enrolled in the study.

Horse ID	Animal Name	Gender	Age	Study Phase
1	BH	Gelding	8	Efficacy - DDSP
2	TH	Gelding	3	Efficacy - DDSP
3	MV	Filly	2	Efficacy - DDSP
4	Donation #1	Gelding	16	Safety – Control
5	Donation #2	Gelding	23	Safety – Control
6	Purchased Horse	Gelding	6	Safety - Control

4.1.3 Pre Treatment Examinations

An outside veterinarian completed a dynamic endoscope examination on Horse #1 using a dynamic endoscope within the last year. The report of the study concluded that Horse #1 had a completely paralyzed and thickened left arytenoid. Also, the left arytenoid was partially scarred and located out of the way due to a previous tieback surgery that was released. DDSP occurred readily, and the palate was displaced through 90% of the examination. The epiglottis was moderately flaccid and normal sized. See Appendix C1 for full pre treatment endoscopic examination for Horse #1.

Horse #2 and Horse #3 were both examined for DDSP by Dr. Woodie using a dynamic endoscope as demonstrated in Figure 4.2. Horse #2 was evaluated using the equine treadmill at Rood and Riddle Equine Hospital, in Lexington, KY. Horse #2 was diagnosed as having a normal upper airway at rest. While pacing at high-speed exercise, Horse #2 displaced his palate and was diagnosed with DDSP. Horse #3 was evaluated using a portable dynamic endoscope at Red Mile Racetrack, in Lexington, KY. See Appendix C2 for complete diagnosis from the pre treatment endoscopic examination for Horse #2.

Figure 4.2: Dynamic endoscope examinations were completed using an equine treadmill for Horse #2 (left) and a portable dynamic endoscope at a remote location for Horse #3 (right).

The pre treatment respiratory recording for Horse #1 was completed on a lunge line at a walk, trot, and canter for 20 minutes. The recorder was attached to the left side of his halter with the microphone placed near his nostril as shown in Figure 4.3. During the recording, Horse #1 did not displace or make any abnormal breathing sounds at a walk or trot. However, at a canter, Horse #1 snored frequently and experienced exercise

intolerance. At least once, Horse #1 came to a complete stop and snorted loudly to correct his displaced palate. The audio recordings for Horse #1 had excess wind noise because of slight movement of the halter during exercise.

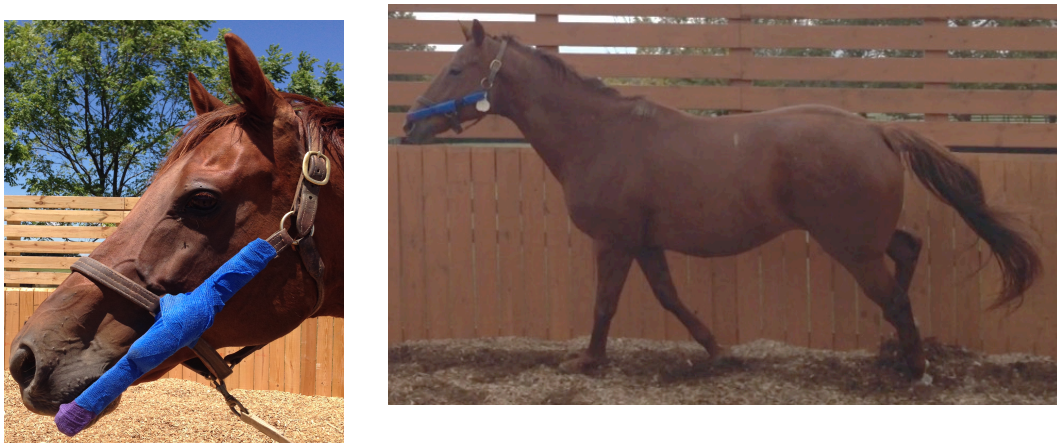

Figure 4.3: Attaching the recording device to the side of the halter allowed the audio recordings for Horse #1 to be recorded. During the recordings, the recorder moved slightly with the movement of the halter.

Horse #2 was recorded while exercise harness racing for 20 minutes. Per his owner, Horse #2 was pacing at his top racing capabilities. Due to interference with the bridle and riding equipment, the recorder was attached to the front of his bridle with the microphone near his nostrils as shown in Figure 4.4. During the recording, Horse #2 snored loudly throughout the exercising, with increased snoring towards the end of the race.

Figure 4.4: The recording device was attached to the front of Horse #2's bridle to record his respiratory noises.

Horse #3 was recorded while exercise harness racing, as well. The trainer completed a full practice race with Horse #3 for 20 minutes. Again, due to potential

interference with the tack, the recorder was attached to the front of her bridle with the microphone near her nostrils as shown in Figure 4.5. During the pre treatment recording, Horse #3 snored while trotting at high speeds and had multiple occasions where her breathing was completely interrupted for about ten second intervals.

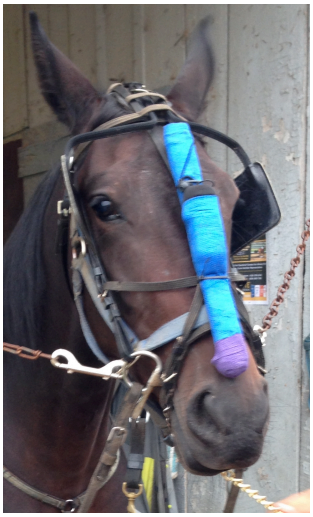

Figure 4.5: For Horse #3, the recording device was attached to the front of the bridle to record any respiratory noises.

4.1.4 Soft Palate Treatment

Even for an experienced veterinarian, injecting the soft palate proved to be a difficult procedure. The soft palate is a flimsy material, making it difficult to insert the needle and maintain the correct position to administer the reagent. Therefore, the injections were completed so that the needle trajectory crossed the center of the soft palate to help maintain the correct needle position. When the endoscope was inserted into the right nostril, the 7:00 palate injection was completed on the left side, and when the endoscope was inserted into the left nostril, the 5:00 palate injection was completed on the right side. A digital display video endoscope was unable to be obtained for this study, so a simple endoscope with only a standard viewing port was used for the injections. Dr. Aristizabal had to look through the 1-meter long viewing port, which is similar to looking through the body tube of a microscope, to see the injection location and needle placement. As one would expect, looking through a 1-meter long tube made the injection area very small and challenging to see, thus increasing the difficulty of placing the needles in the correct position, as shown in Figure 4.6. If a digital display video endoscope had been available, some of the difficulties associated with this type of injection would have been greatly reduced.

Also, the 1-meter long transendoscopic injection needle required a 0.5 mL loading dose to fill the needle tube plus an additional 1 mL of the reagent to advance the desired amount into the soft palate. The 1 ml advancing substance was overlooked when preparing for the study and extra reagent was not available. Therefore, Dr. Aristizabal suggested to use a column of approximately 1 mL of air to push the entire reagent volume into the soft palate as demonstrated in Figure 4.7. Dr. Aristizabal had previously used air to advance reagents for other equine applications in peripheral tissues, and he did not believe it would cause any issues. Due to the compressibility of air under pressure, using 1 mL of air to advance the reagent would result in less than 1 mL of reagent being injected. During each of the soft palate injections the soft palate readily expanded to accommodate the extra volume, causing a 'pillow' filled with the reagent and perhaps a small volume of air to form at the injection site. This was most likely due to the fact that the soft palate has insufficient elasticity to withstand the injection without incurring moderate tissue damage as further discussed in Section 4.1.7.

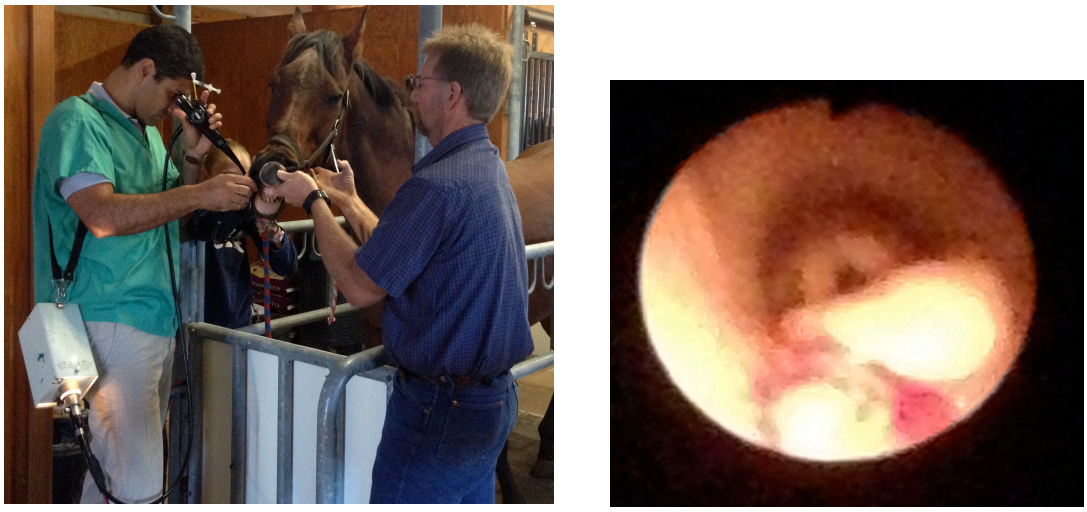

Figure 4.6: The endoscope had a viewing window that allowed the soft palate to be viewed (left). However, because the endoscope was 1 meter long, the soft palate appeared very small (right). When viewing the soft palate in real time, it appeared clear and in focus. The image on the right is only out of focus because it was taken with a camera through the endoscope port.

Figure 4.7: The reagent was advanced into the soft palate using a column of air after ensuring the needle was in the correct position.

The protocol called for each horse to receive two 1 mL injections of the genipin buffered reagent into the 5:00 and 7:00 positions on the soft palate. Five of the six horses received two 1 mL injections in these positions. Horse #5 was the first horse treated, and he received two 1.5 mL injections by mistake because the full amount was accidentally injected into the soft palate. Also, during the first injection for Horse #1, the needle slipped out of the soft palate as the reagent was being delivered, causing it to be sprayed topically on the soft palate. Horse #1 then received two more 1 mL injections into the 5:00 and 7:00 positions. All individual horse injection details and notes are included in Table 4.2

Table 4.2: Notes from soft palate treatment and volume of reagent injected for each horse.

Injection Order	Horse ID	Injection Spot	Volume Injected (mL)	Procedure Notes
1	5	5:00	1.5	• Injected too much reagent by mistake
2		7:00	1.5	
3	4	5:00	1.0	• Very tough palate – difficult to insert needle
4		7:00	1.0	
5	1	5:00	1.0	• 1 mL of reagent sprayed topically on soft palate • Very flimsy soft palate • Palate displaced during injection
6		7:00	1.0	
7	3	5:00	1.0	• Normal palate
8		7:00	1.0	
9	2	5:00	1.0	• Very soft and flimsy soft palate
10		7:00	1.0	
11	6	5:00	1.0	• Injected both 5:00 and 7:00 locations from one nostril
12		7:00	1.0	

Post treatment, the horses were examined every hour for 72 hours. Initially, a few of the horses cleared their throat or coughed, but not excessively. Horse #3 experienced mild hypersalivation and a reduced appetite 24 hours post treatment as shown in Figure 4.8. These symptoms subsided within 24 hours. Otherwise, all of the horses recovered unremarkably. Table 4.3 in Appendix C3 lists the post treatment clinical observations for each horse in more detail.

Figure 4.8: Horse #3 experienced hypersalivation for 24 hours post treatment, as noted by the white foam coming from the horse's mouth.

Seven days after treatment, the safety phase control horses were sedated with Detomidine (0.02 mg/kg) and Butorphanol (0.03 mg/kg), and euthanized with Fatal Plus (1 mL/4.5 kg). Their soft palates were then removed, stored on dry ice and shipped to Orthopeutics, LP for analysis. The animal carcasses were appropriately disposed of by SRC. Twelve days after treatment, the efficacy phase horses were returned to their owners for post treatment examinations.

4.1.5 Post Treatment Examinations

Immediately after returning home, follow up phone calls were made to the efficacy phase horse owners for updates on the well being, breathing sounds, and exercise tolerance. Per Horse #1's owner, Horse #1 was recovering well and showing no signs of abnormal noises. Horse #1 had not been exercised, so the status of abnormal noises and exercise intolerance were unknown. In general, Horse #2 was recovering well and showing no signs of abnormal noises at rest. However, when exercising at high speeds, Horse #2 showed variable results. Sometimes when exercised, he would breathe normally with no abnormal noises or noticeable displacements. Other times, he would snore throughout his entire exercise session and displace his soft palate at the end during high speed exercising. Overall, Horse #3

recovered well from the genipin treatment and demonstrated no abnormal breathing sounds or exercise intolerance.

Approximately one month after treatment, the efficacy phase horses underwent post treatment dynamic endoscope examinations and respiratory audio recordings. Post treatment, Horse #1 underwent a portable dynamic endoscope examination by Dr. Woodie at a walk, trot and canter on a lunge line. At rest, Horse #1 had a paralyzed and thickened left arytenoid and evidence of a previous left ventriculocordectomy. Horse #1 did not displace his palate at rest. While exercising, he did not displace his soft palate or make any abnormal respiratory noises at a walk, trot or canter. He did experience intermittent epiglottic entrapment. For the full post treatment diagnosis, see Appendix C1.

The post treatment dynamic endoscopic examination was completed on Horse #2 while exercise harness racing using a portable dynamic endoscope. At rest, the soft palate and upper airway were within normal limits. During high-speed exercise, he displaced his soft palate. For full post treatment diagnosis, see Appendix C2.

Horse #3 did not have a post treatment dynamic endoscope examination completed due to logistical issues. Horse #3 resides over two hours away and the owner was unable to make the round trip to bring the horse to Lexington, KY for the examination.

Respiratory audio recordings were completed on all three horses post treatment. For the post treatment audio recording for Horse #1, the halter was again placed on the left side of the halter with the microphone near the nostril. Horse #1 was lunged at a walk, trot and canter for 20 minutes. During this time, the Horse #1 did not make any abnormal respiratory noises or snoring. Also, Horse #1 did not show any exercise intolerance or stop exercising because of palatal displacements.

Horse #2 had a post treatment audio recording completed while exercise harness racing with the recorder attached to the center of the bridle with the microphone near the nostril. During the post treatment audio, Horse #2 did not displace his soft palate, however, audible snoring noises were still present towards the end of his race. Per his owner, Horse #2 paced his fastest mile to date, showing an improvement in exercise intolerance.

The post treatment respiratory recording for Horse #3 was completed during an exercise harness race at full trotting speed. The recorder was attached to the center of bridle with the microphone near the nostril. During the post audio treatment, Horse #3 did not make any abnormal respiratory noises or experience any breathing issues. Based on the breathing recording, Horse #3 did not displace her palate or show any exercise intolerance after the genipin treatment.

Based on the dynamic endoscopic examinations and the audio respiratory recordings, two of the three horses have showed improvement in snoring loudness and palatal displacement. Horse #1 and #3 both exercised post treatment with no abnormal breathing noises or exercise intolerance. Horse #2 showed inconsistent results with limited improvement in snoring loudness. Therefore, it appears that the genipin treatment reduced snoring loudness and palatal displacement; however, more research should be completed to determine the appropriate dosage and concentration to produce desirable results in all horses.

4.1.6 Respiratory Audio Analysis

In the pre treatment and post treatment respiratory recordings, the horses were exercised for the same amount of time and at the same exertion rate to remove as many discrepancies as possible between the recordings. To analyze the respiratory audio files, the samples were cut down using Audacity 2.1.1 (Computer Program, 2015), an audio editor and recording program, to remove the extraneous noises associated with attaching and detaching the recorder and warming the horse up. The resulting audio files consisted of about five minutes of the horses exercising at maximum speed. For Horse #1, full speed was cantering on a lunge line; for Horse #2, full speed was high-speed pacing while harness racing; and for Horse #3, full speed was high-speed trotting while harness racing. Then, the points of palatal displacements or snoring were noted for each sound file, as listed in Table 4.4. For Horse #1, the clearest pre treatment snoring sounds occurred between 0:59-1:06 minutes. For Horse #2, the clearest pretreatment snoring sounds appeared during the 5:05-5:50 minute range with snoring occurring with each exhale. For Horse #3, the clearest pretreatment displacement locations were from 2:45-2:59 minutes because there was a time interval when the horse completely stopped breathing during this span. Using the location of the palatal displacements, the audio files were further broken down into one exhale (1E), three

exhales (3E) and 20 exhales (20E) sections that contained the DDSP snoring or breathing gaps when present.

Table 4.4: DDSP snoring locations for each horse with clear snores highlighted in bold

Audio File	Snoring Locations (in mins)
Horse #1: Pre Treatment	**0:59-1:06**; 2:43-2:50; 4:27-4:33; 5:34-5:49
Horse #1: Post Treatment	None
Horse #2: Pre Treatment	0:24; 0:56; 2:51; 3:54; 4:28; 4:53-4:59; **5:05-5:50**
Horse #2: Post Treatment	1:10-1:12; 1:36-1:39; 4:17-4:24; 5:03-5:05
Horse #3: Pre Treatment	0:19; 0:58-1:00; 2:30; **2:45-2:59**; 5:32-5:34
Horse #3: Post Treatment	2:32*; 3:09* *Possible snoring noises, but difficult to be conclusive with respiratory audio alone

Next, the 3E and 20E audio files were analyzed using custom program codes developed in Matlab in the time domain. The 3E files were used to compare amplitudes between pre treatment and post treatment audio files. For each graph, the pre treatment audio recordings are shown in red and the post treatment audio recordings are shown in blue. As shown in Figure 4.9, Horse #1 has about the same amplitude peaks for the pre treatment and post treatment breathing, however, the breathing pattern is much more uniform post treatment. This is also true for Horse #2 and Horse #3, who demonstrated smaller amplitude peaks in the post treatment graphs as shown in Figures 4.10 and 4.11, respectively. The reduction in amplitude for all three horses relates to a reduction in snoring loudness. In all three time domain graphs, there is also evidence of an approximately 10 Hz oscillation in the pre treatment exhales. For Horse #1 and Horse #3, this low frequency vibration is not present in the post treatment exhales, which corresponds to a decrease in palatal snoring. Additionally, for Horse, #1, the breathing rate post treatment is twice as fast as the breathing rate pre treatment. Since the audio files were taken at approximately the same time into the warm up routine, it could be assumed that the horse is able to work harder post treatment, thus increasing his breathing rate. Overall, the time domain graphs for all three horses support the dynamic endoscope examination results because they show a decrease in snoring loudness and an increase in exercise tolerance based on the decrease in amplitude peaks and the increased breathing rates. Horse #1 and Horse #3 no longer experience any DDSP symptoms, which is evident in their time domain graphs because there is a decrease in post treatment amplitude peaks and a decrease in the 10 Hz oscillations associated with palatal vibration. For Horse #2, there was a decrease in amplitude peaks; however, the 10 Hz oscillations are still present in the post treatment time domain graph, supporting the results of the dynamic endoscopic examination with a reduction in snoring loudness but the presence of palatal vibrations.

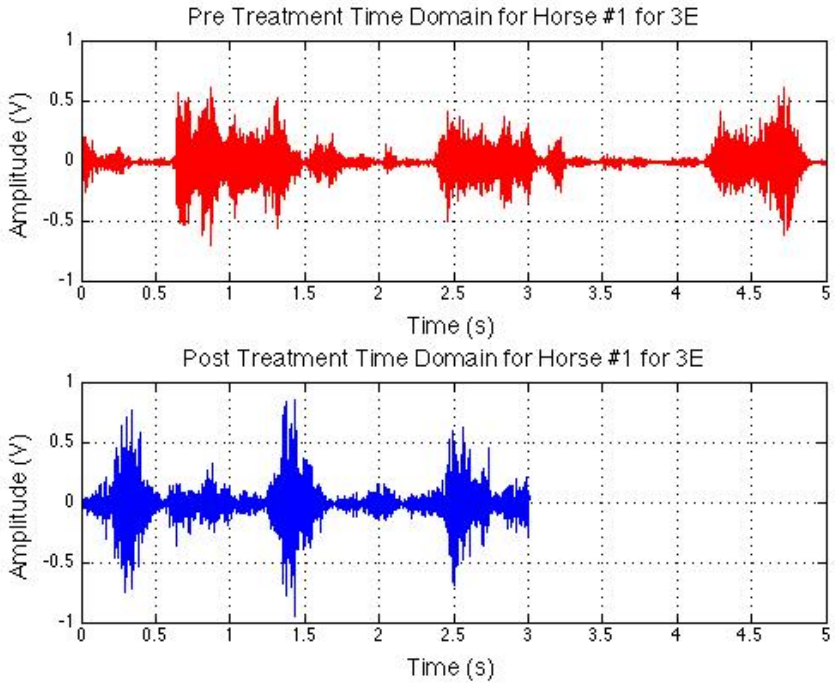

Figure 4.9: The time domain graph for Horse #1 for 3E shows a reduction in the 10 Hz oscillations, as well as an ability to work harder based on the faster breathing rate.

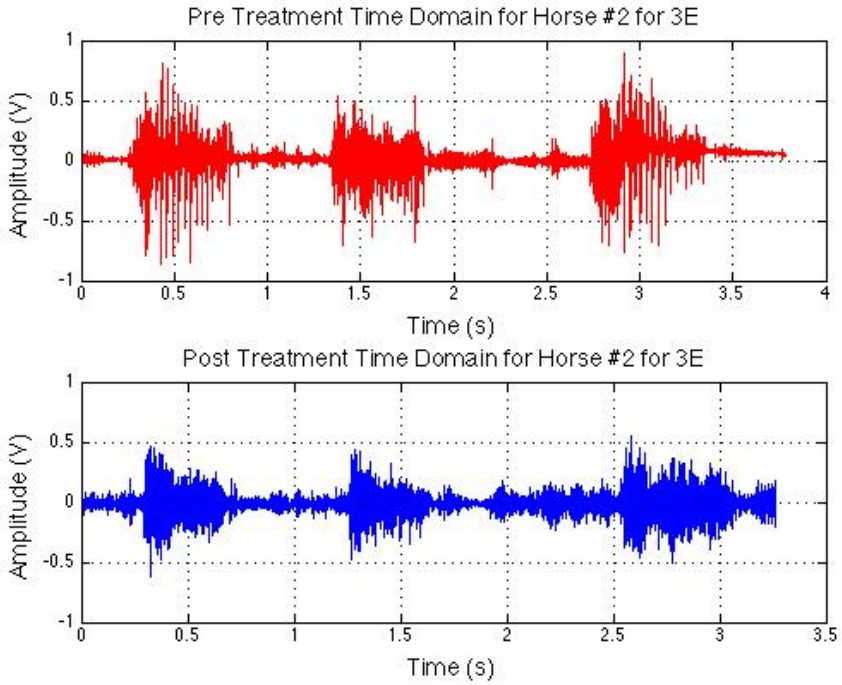

Figure 4.10: Horse #2 demonstrates a reduction in the amplitudes in the post treatment time domain graph, relating to a reduction in snoring loudness.

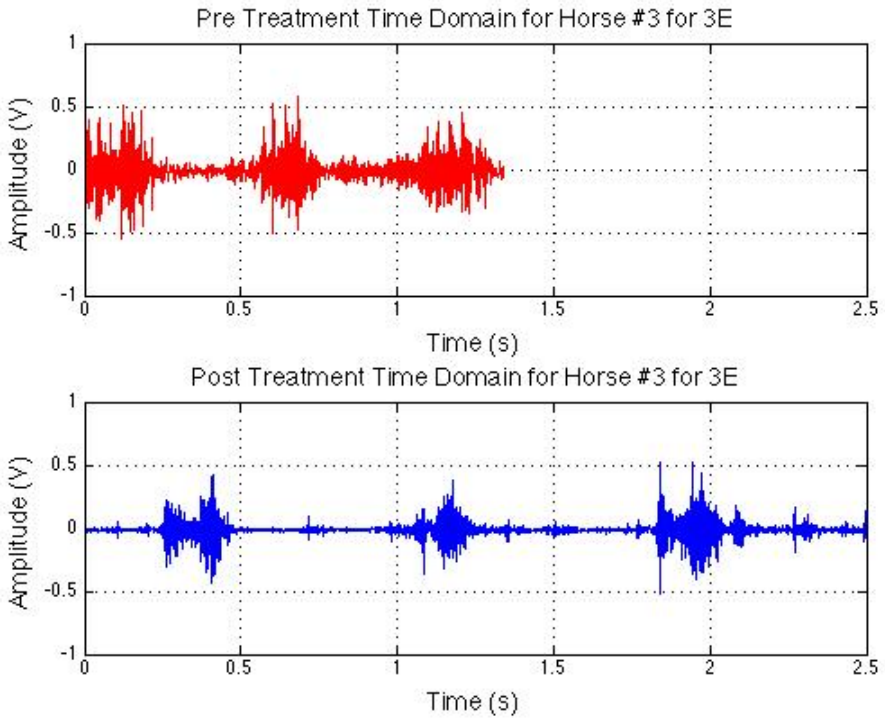

Figure 4.11: The post treatment time domain graph for Horse #3demonstrated a decrease in both the amplitude peaks and the 10 Hz oscillations, relating to a reduction in snoring loudness and palatal vibrations.

The 20E files were analyzed to determine any irregularities in the breathing pattern because the larger number of exhales allowed patterns to be easily noticed. In general, for all three horses, the pre treatment time domain graphs were not uniform in amplitude peak heights. Additionally, in the pre treatment graphs, there is evidence of irregular breathing patterns, with short inhales, long exhales, and gaps caused by airway obstruction, as demonstrated in particular by Horse #1 in Figure 4.12. For all horses, each individual exhale in the pre treatment graphs is much longer, causing the breathing rate to be slower than in the post treatment graphs. This is especially evident for Horse #2, as seen in Figure 4.13. Horse #3 also shows evidence of a large breathing gap in the pre treatment audio between 10 and 12 seconds as shown in Figure 4.14. Any gaps in the breathing pattern indicate apneic events, as previously described in the study by Azarbarzin and Moussvi [42]. In the post treatment graphs, breathing patterns are more regular with a uniform peak height for all three horses. Also, any breathing gaps caused by airway obstruction are also non-existent. Overall, the 20E time domain graphs are useful to determine the location of soft palate displacements as indicated by the gaps in the breathing pattern.

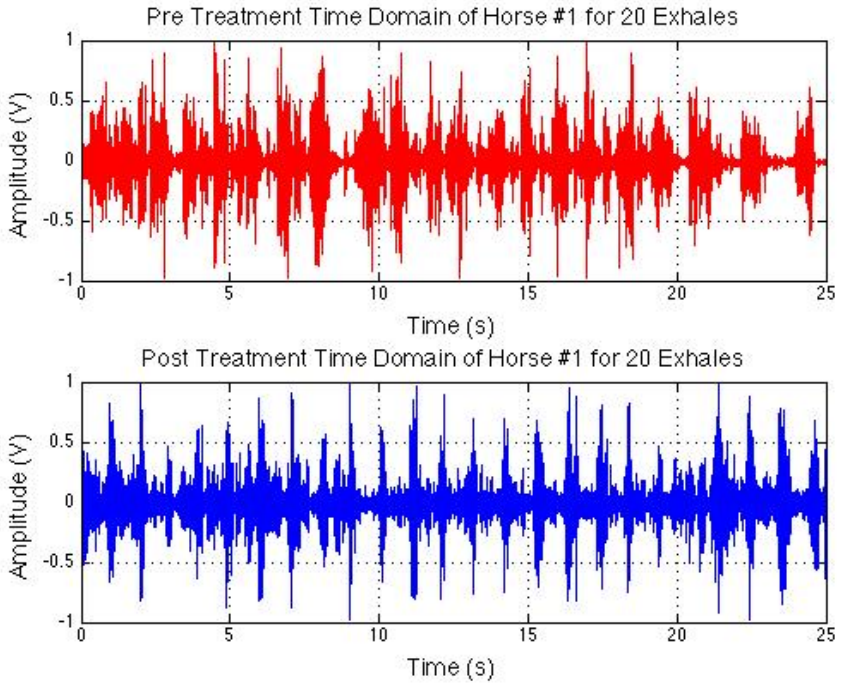

Figure 4.12: The 20E time domain graphs for Horse #1 show varying lengths of inhales and exhales in the pre treatment graph. In the post treatment graph, the breathing rhythm is more uniform.

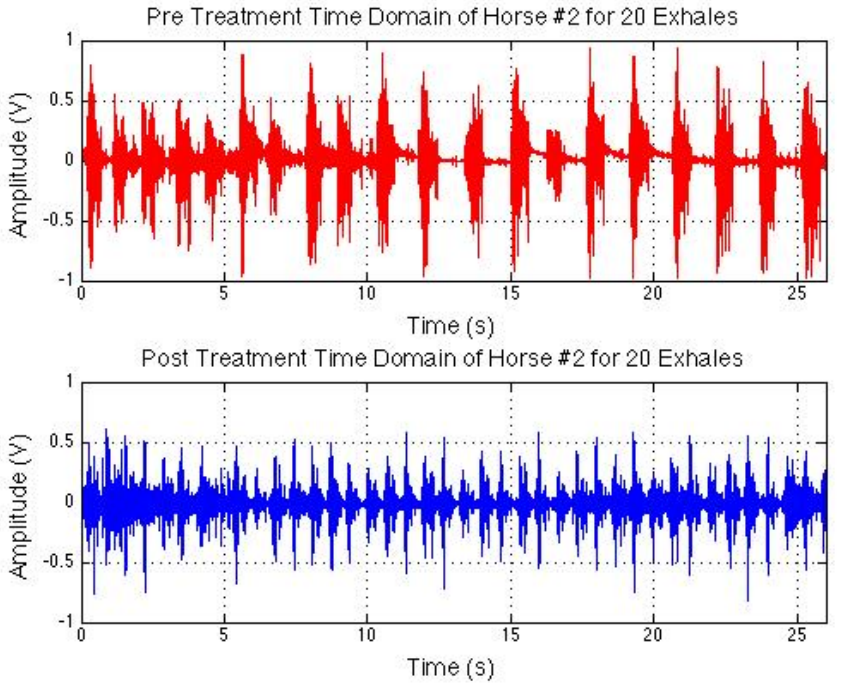

Figure 4.13: For Horse #2, the 20E pre treatment time domain graph has a much slower breathing rate due to each exhale requiring more force to overcome palatal vibration. The post treatment graph has a faster, more uniform, breathing rate.

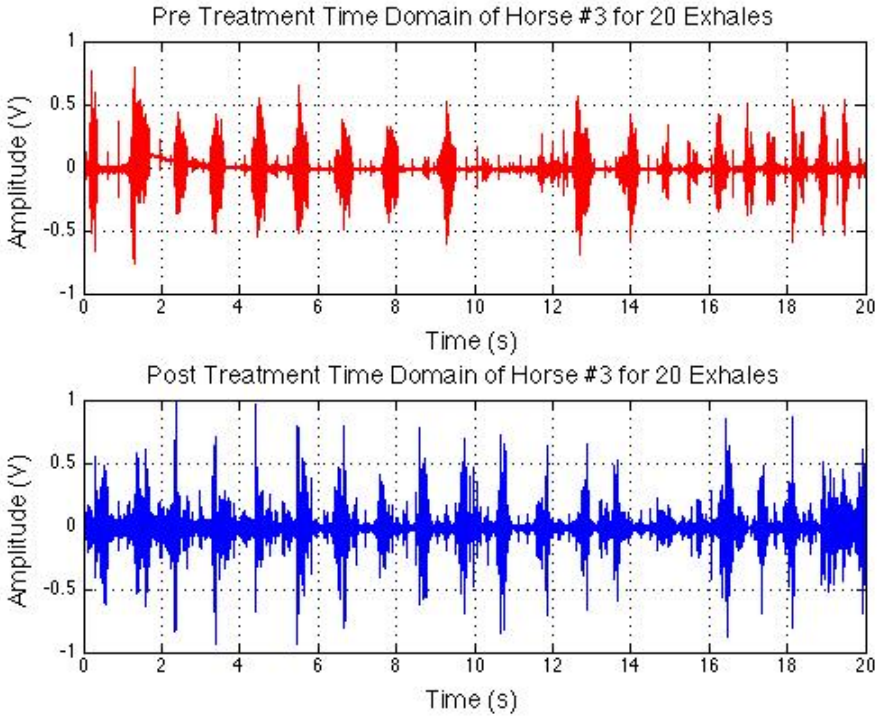

Figure 4.14: The 20E pre treatment time domain graph for Horse #3 has a large gap from 10-12 seconds, corresponding to an airway obstruction. In the post treatment graph, there is no evidence of any palatal obstructions.

Then, spectrogram graphs were created in Matlab using the 3E audio files. The spectrograms showed changes in amplitude across a variety of frequencies. For the spectrograms, the x-axis represented time, the y-axis represented frequency, and the red squares represented high amplitudes at -40 V while the blue squares represented low amplitudes at -120 V. Horse #1 and Horse #3 both showed a noticeable reduction in the quantity of high amplitude red squares in the high frequency range in the post treatment spectrogram graph compared to the pre treatment graph as demonstrated in Figure 4.15 and Figure 4.17, respectively. Additionally, Horse #3 had a reduction in the area of red squares in the low frequency range. Horse #2 did not have an obvious decrease in the number of red squares representing high amplitudes for any frequency between the pre treatment and post treatment spectrogram graphs as shown in Figure 4.16. Based on the spectrogram graphs, the genipin treatment seemed to have caused a decrease in amplitude in the high frequency range, which corresponds to a decrease in palatal vibration and whistling. This is supported by the results of the dynamic endoscope examinations and owner reports that had a reduction of DDSP symptoms for Horse #1 and Horse #3.

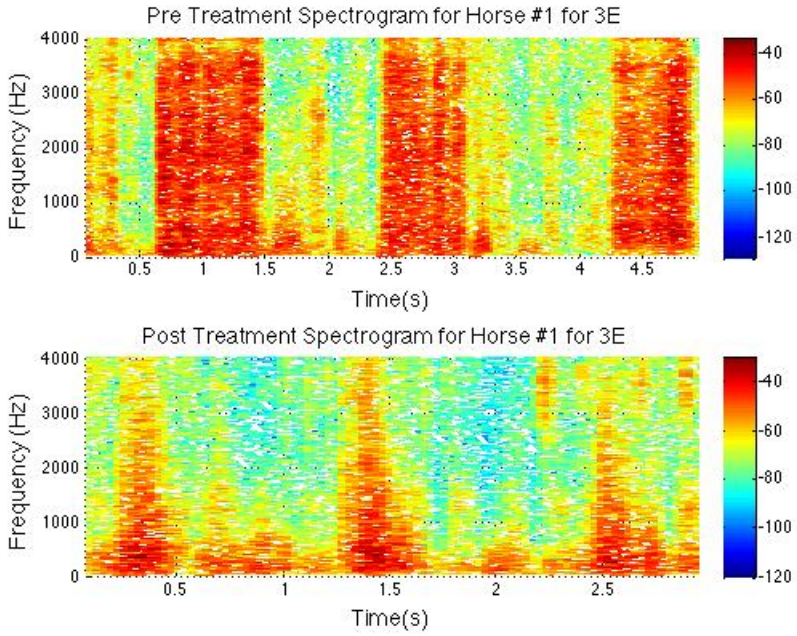

Figure 4.15: The spectrogram for Horse #1 shows a reduction in high amplitude red squares in the high frequency range in the post treatment graph (bottom) compared to the pre treatment graph (top).

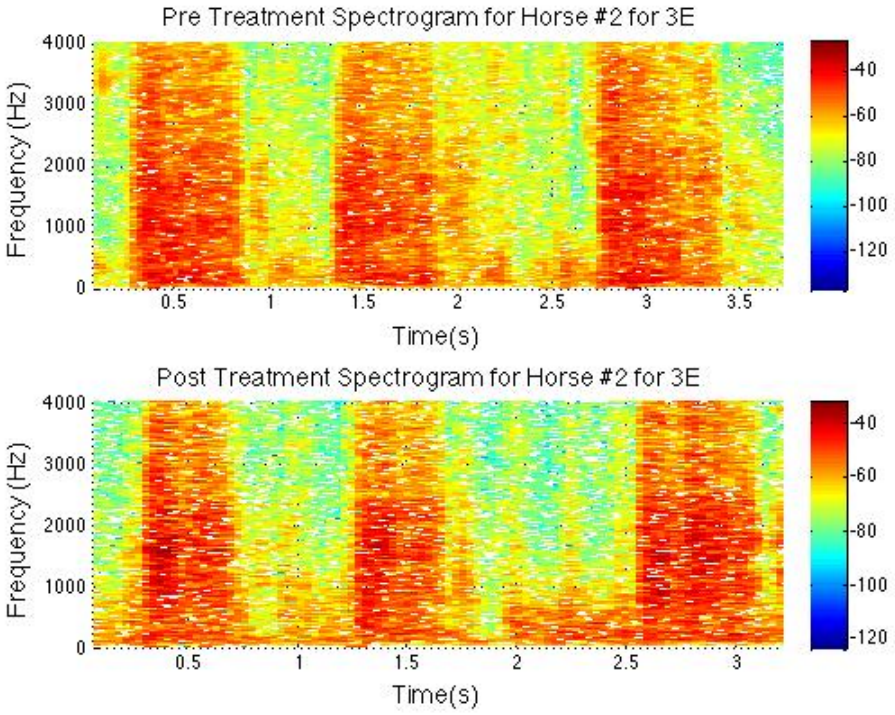

Figure 4.16: The pre treatment (top) and post treatment (bottom) spectrogram graphs for Horse #2 did not show an obvious difference in the area of high amplitude red squares for any frequency range.

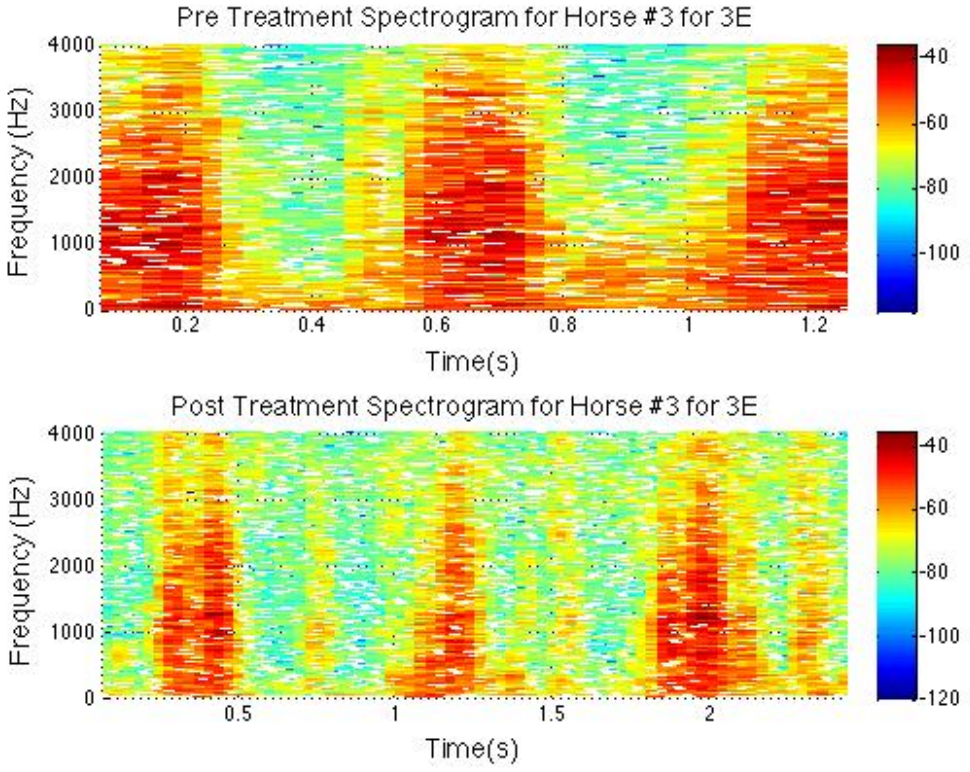

Figure 4.17: The pre treatment spectrogram graph (top) showed more high amplitude red squares than the post treatment spectrogram graph (bottom) across all frequency ranges for Horse #3.

Using ImageJ image analysis software, the area of high amplitude red squares was calculated and compared pre and post treatment to determine the percent differences. Each spectrogram graph was loaded into ImageJ and analyzed using the green color channel to count the number of red squares. The green color channel was used because it best represented the area of the red squares due to the filter applied when separating the channels. The green color channel graphs for each spectrogram are shown in Figures 4.18, 4.19 and 4.20 with the pre treatment and post treatment spectrogram graphs represented. Using the color channel graphs, the area of red squares was calculated by counting the number of black particles in the green color channel graphs, as summarized in Table 4.5. Figure 4.21 shows the differences for each horse in the area of red squares, representing high amplitude sounds across all frequencies. Using these values, the percent difference between the area of red squares in the pre treatment spectrogram and the post treatment spectrogram was calculated for each horse and plotted in Figure 4.22. On average, there was a 39% decrease in the number of red squares in the post treatment respiratory recordings

compared to the pre treatment respiratory recordings. Horse #1 and #3 both had a reduction of greater than 50% in the number of high amplitude squares relating to a reduction in sounds associated with snoring an palatal displacement, which correlates with the observations made at the post treatment evaluations and with the horse owner post treatment assessments.

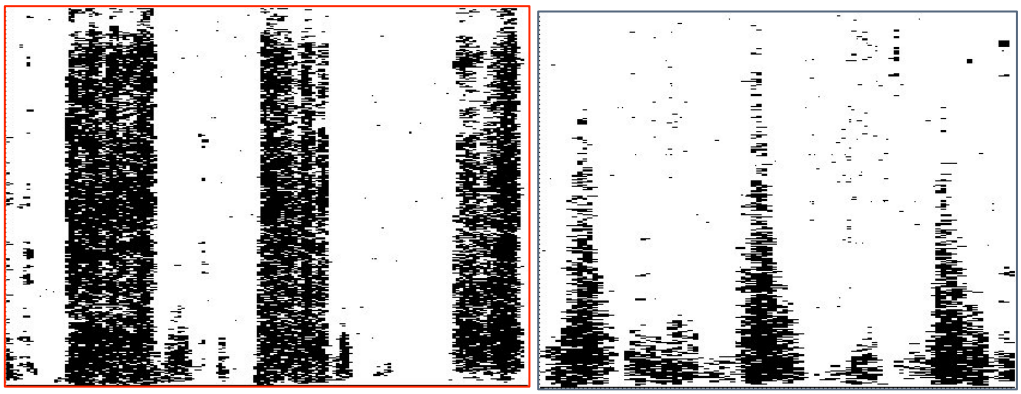

Figure 4.18: The green color channel graphs from Image J representing the pre treatment spectrogram (left) and post treatment spectrogram (right) for Horse #1 showed a decrease in high frequency amplitudes.

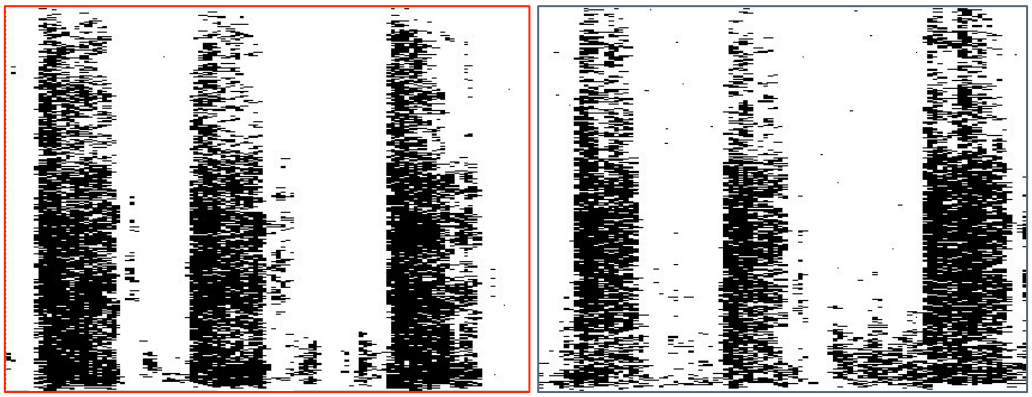

Figure 4.19: The green color channel graphs from Image J representing the pre treatment spectrogram (left) and post treatment spectrogram (right) for Horse #2 showed a slight decrease in the area of red squares.

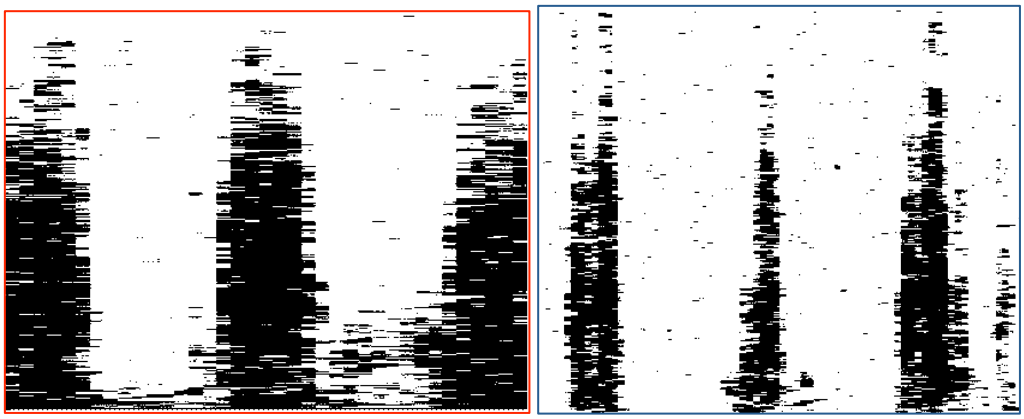

Figure 4.20: The green color channel graphs from Image J representing the pre treatment spectrogram (left) and post treatment spectrogram (right) for Horse #3 showed a decrease in the area of red squares across all frequency ranges.

Table 4.5: The ImageJ results included the total area of red squares as well as the percent area. Using these values, the percent difference was calculated for the pre treatment and post treatment spectrograms for each horse.

Audio File	Total Area	Percent Area Red	Percent Difference in area of red squares in post treatment spectrogram
Horse #1: Pre Treatment	48605	32.33%	60.20% decrease
Horse #1: Post Treatment	19400	12.87%	
Horse #2: Pre Treatment	45344	30.16%	7.54% decrease
Horse #2: Post Treatment	41612	27.89%	
Horse #3: Pre Treatment	54399	23.13%	50.01% decrease
Horse #3: Post Treatment	27196	11.56%	

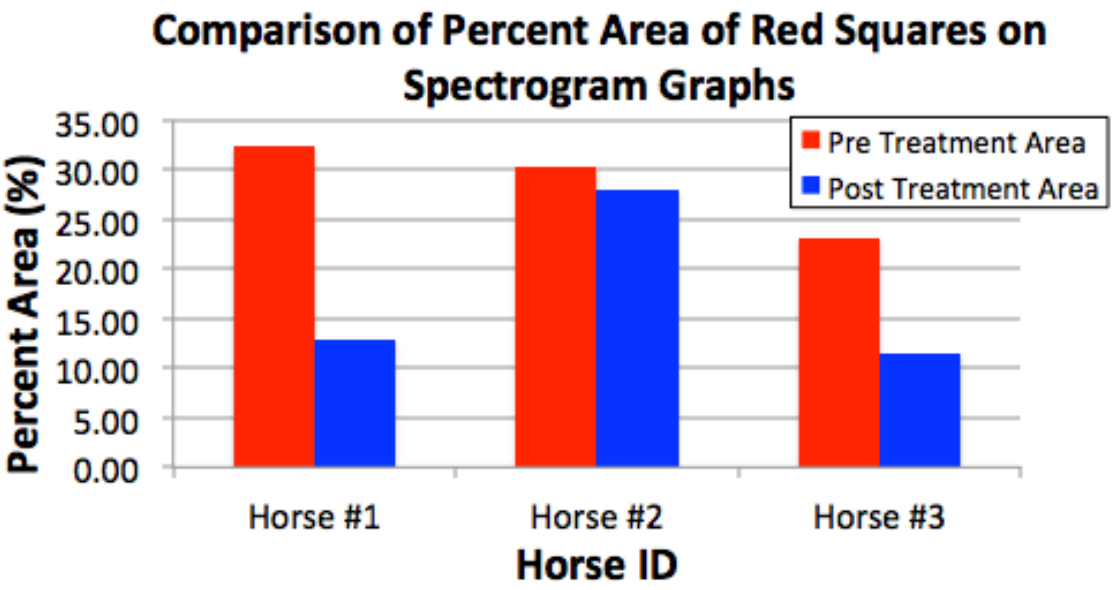

Figure 4.21: For each horse, the percent area of red squares decreased after treating the soft palate with the genipin reagent as shown in the bar graph.

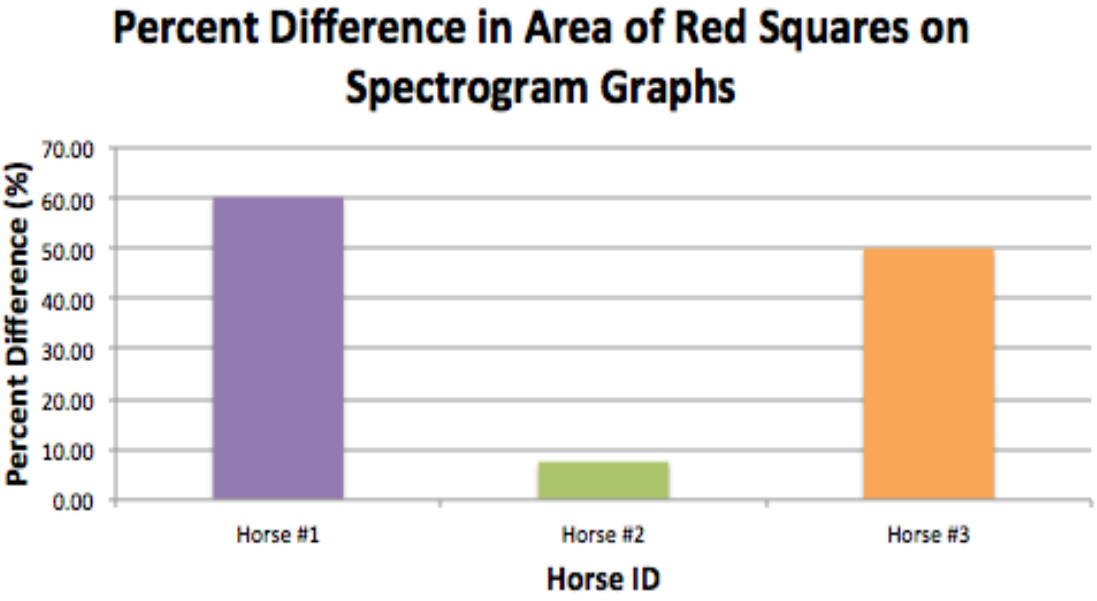

Figure 4.22: Each horse had at least a 5% decrease in the area of red squares in the post treatment recording compared to the pre treatment recording.

Finally, the 1E and 3E audio files were analyzed using the frequency domain in the high frequency and low frequency ranges. The one exhale (1E) and three exhale (3E) sections were chosen based on the location of DDSP snores and palatal displacements as described in Table 4.4. The 1E sound files were used to see the

changes in the frequency domain between pre and post treatment audio files for just a single exhale at a time. The 3E sound files were used to see the post treatment changes as an average of a few exhales at a time. For both the 1E and 3E graphs, the entire frequency range between 0 Hz and 4000 Hz were evaluated first in order to see the general frequency distribution of each audio segment with the pre treatment audio recordings in red and the post treatment audio recordings in blue as shown in Figures 4.23-4.28. Comparing the 1E graphs to the 3E graphs for the pre treatment and post treatment files, the shapes of the graphs are generally the same for all three horses. Also, based on visual examination alone, it appeared that there was a reduction in higher frequency amplitudes for the post treatment audio files, as demonstrated in Figures 4.23 and 4.24. Additionally, there seems to be a decrease in amplitudes in the lower frequency range as shown in Figures 4.25-4.28, corresponding to a reduction in snoring loudness.

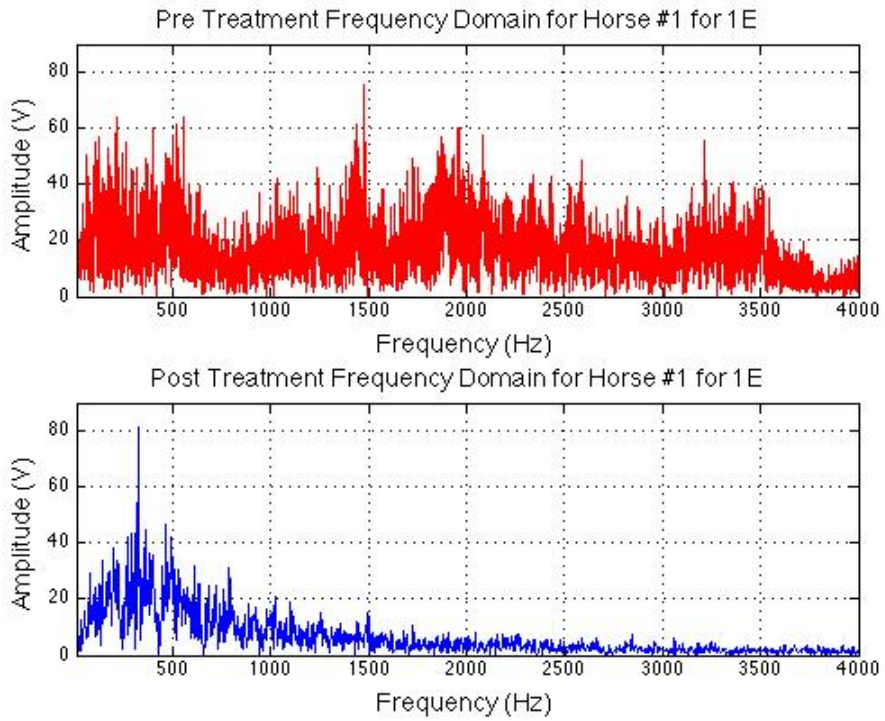

Figure 4.23: The frequency domain graphs for the pre treatment and post treatment audio recordings for Horse #1 show a general reduction in amplitudes, especially in the high frequency range, for the 1E files.

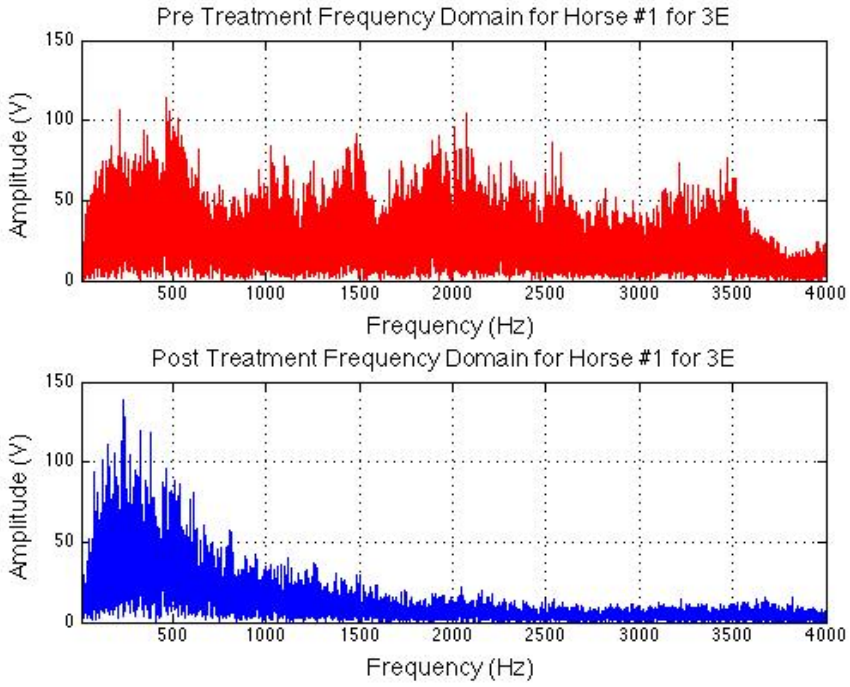

Figure 4.24: The frequency domain graphs for the pre treatment and post treatment audio recordings for Horse #1 show a large reduction in amplitudes, especially in the high frequency range, for the 3E files.

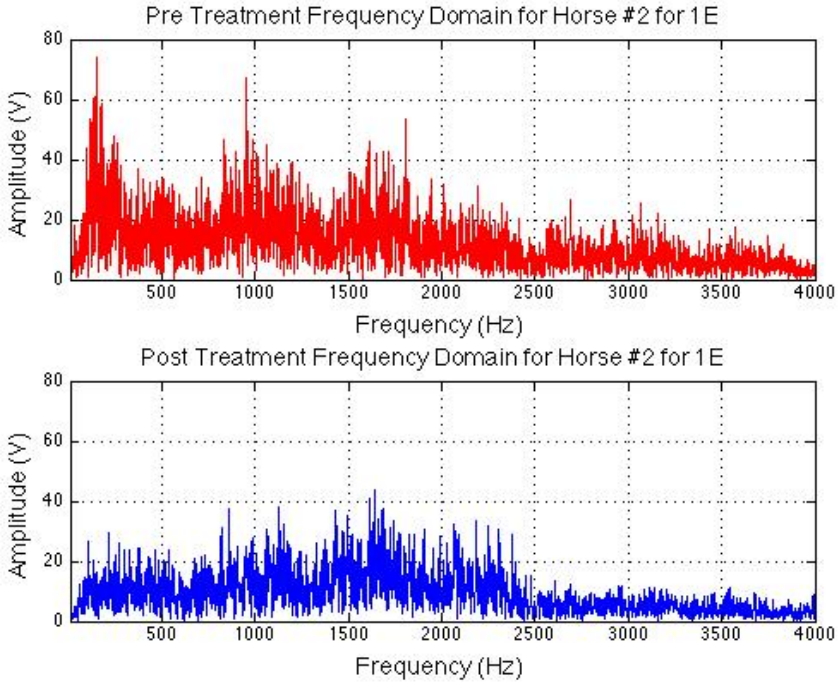

Figure 4.25: For Horse #2, the pre and post treatment frequency domain graphs show a general decrease in amplitude for the 1E files, especially in the low frequency range.

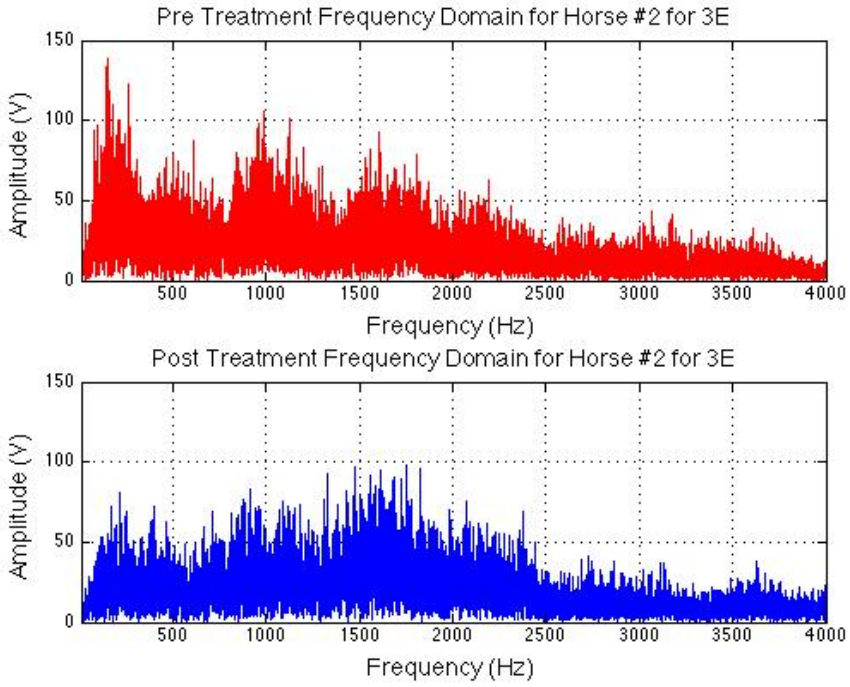

Figure 4.26: In the 3E files, the frequency domain graphs also show a general reduction in amplitude for the post treatment files for Horse #2, especially in the low frequency domain.

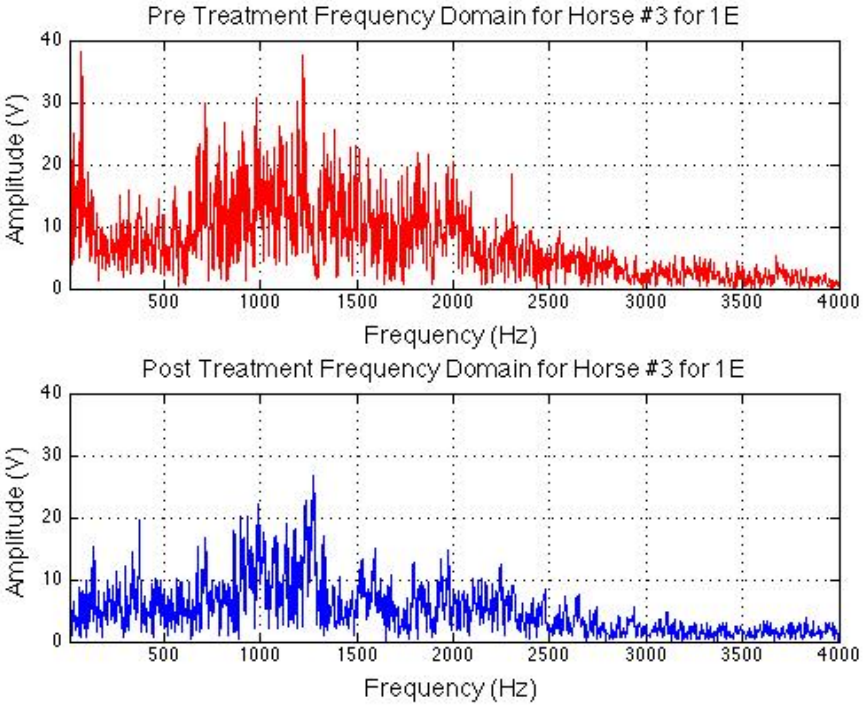

Figure 4.27: In general, Horse #3 had a reduction in amplitudes of the frequency domain graphs from pre treatment to post treatment for the 1E files, particularly in the low frequency range.

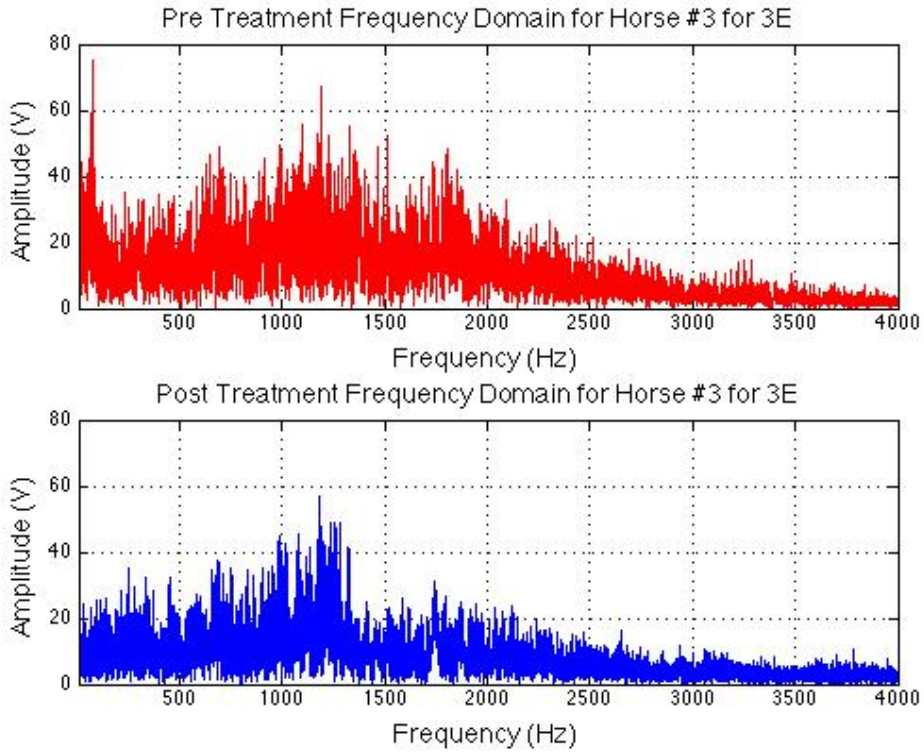

Figure 4.28: Again, the 3E file graphs for Horse #3 show a general reduction in amplitude for the post treatment frequency domain graph from the pre treatment graph, particularly in the low frequency range.

The frequency domain graphs were filtered using the moving average to aid in the quantitative analysis by removing any background noise or outlier peaks. The filtered frequency domain graphs, in pink, were plotted over top of the original data, in black, to display the changes in the graphs. As predicted, the large outlier peaks were removed when filtered using the moving average for all 1E and 3E frequency domain graphs, as shown in Figures 4.29-4.34 below.

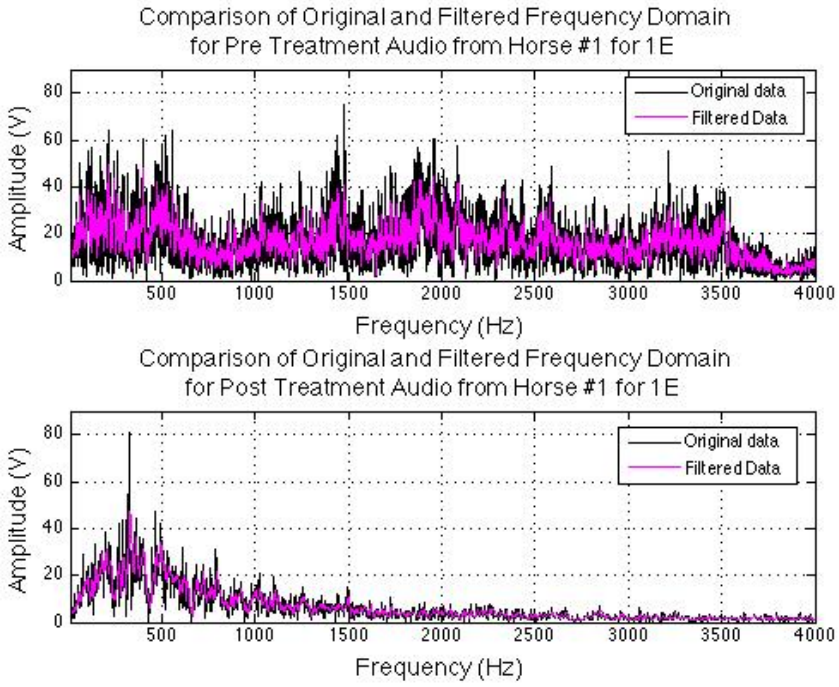

Figure 4.29: Using the moving average to filter the frequency domain graphs, the large outlier peaks were smoothed in the1E pre treatment and post treatment graphs for Horse #1.

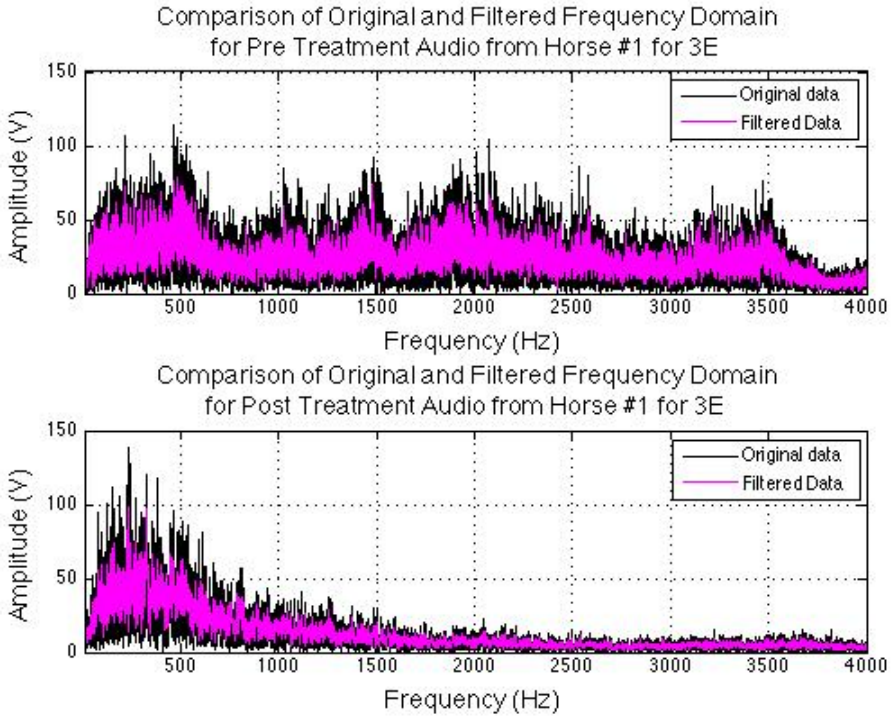

Figure 4.30: The moving average filter removed the large outlier peaks and background noise for Horse #1 in the 3E pre treatment and post treatment graphs.

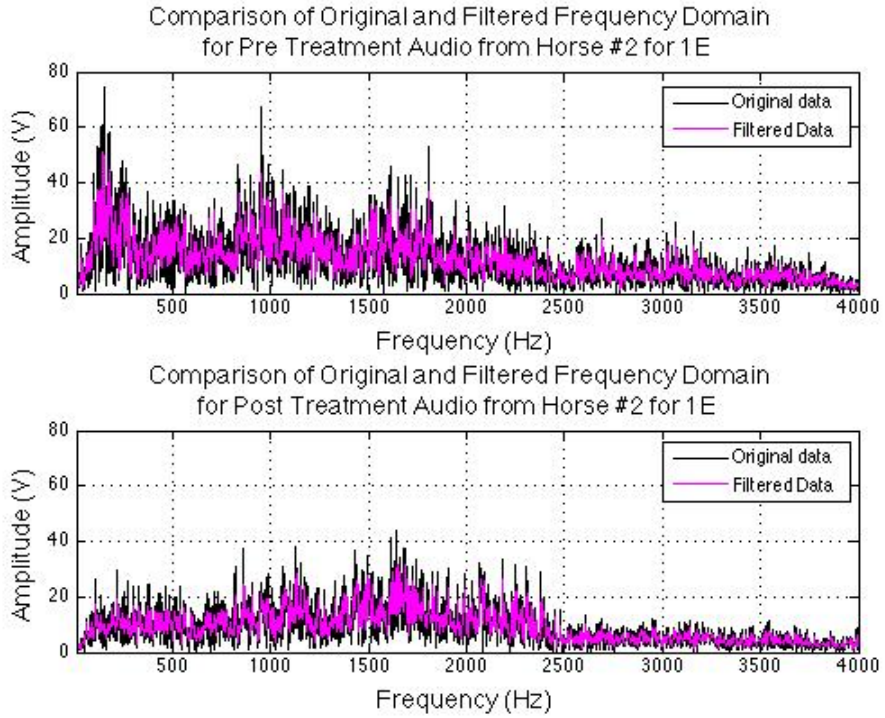

Figure 4.31: For Horse #2, smoothing the frequency domain graphs using the moving average method diminished the large outlier peaks in the 1E pre treatment and post treatment graphs.

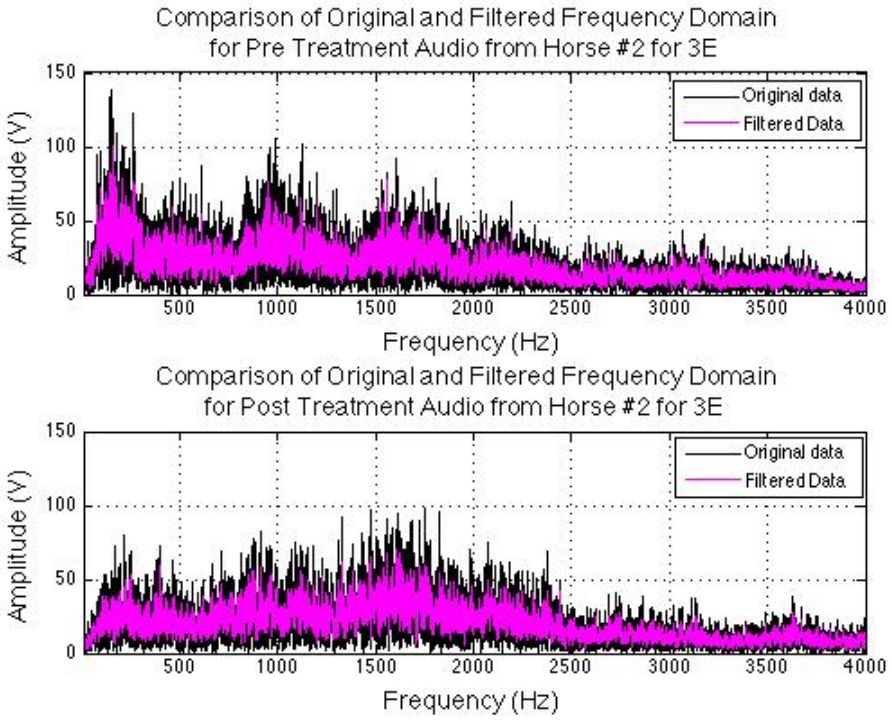

Figure 4.32: For the 3E pre treatment and post treatment graphs for Horse #2, the large outlier peaks were reduced after filtering.

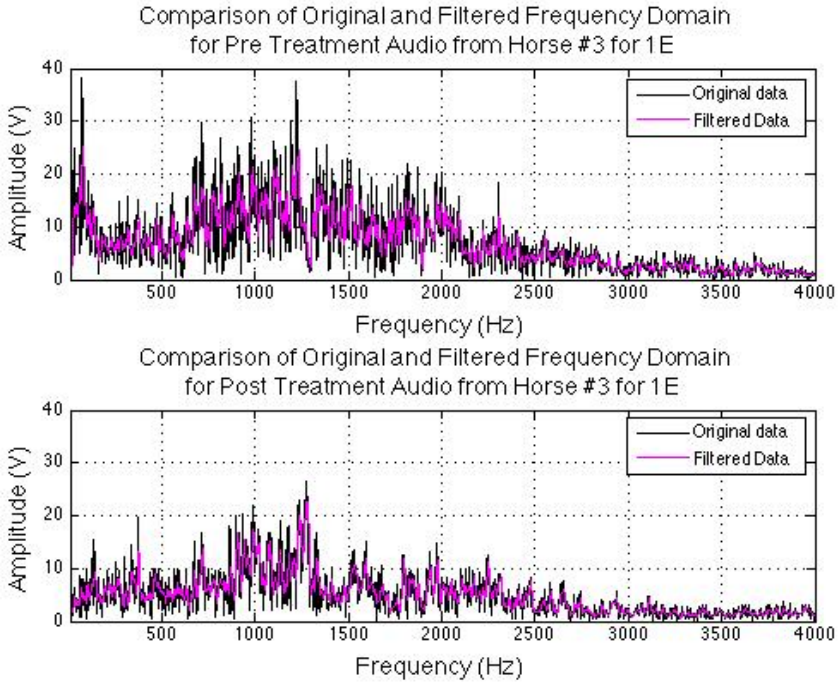

Figure 4.33: Filtering the frequency domain graphs for Horse #3 using the moving average method removed the outlier peaks from the 1E pre treatment and post treatment audio files.

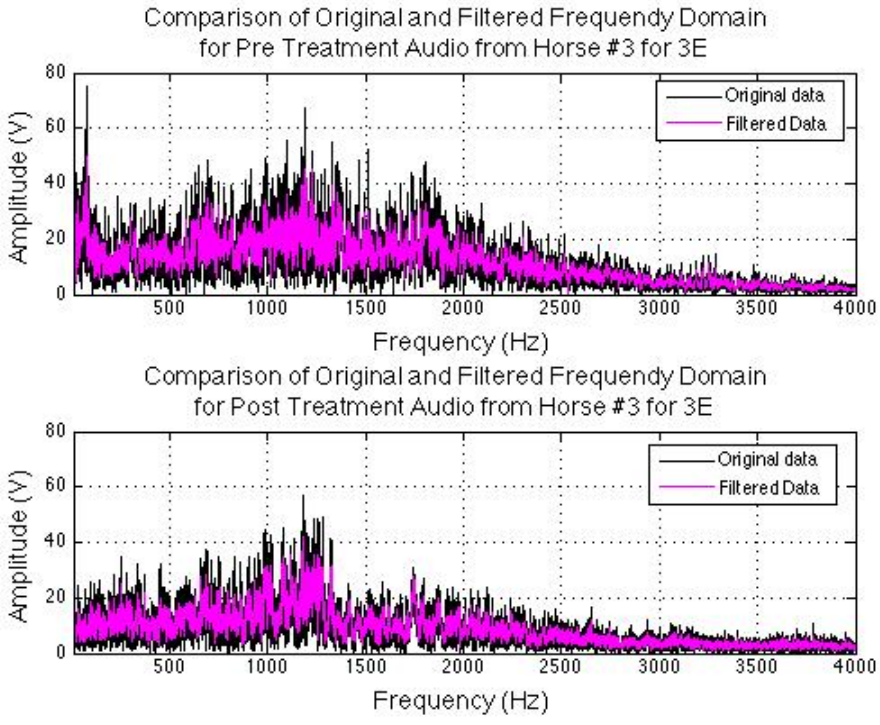

Figure 4.34: For the 3E pre treatment and post treatment audio files, the moving average method removed the outlier peaks for Horse #3.

After filtering, the frequency domain graphs were broken down into the high frequency range from 500 to 4000 Hz for 1E files and 3E files. The high frequency domain analysis started at 500 Hz because that was the cut off frequency for the laser used in the wind tunnel study. The Nyquist frequency, which is the minimum rate that a signal can be sampled without introducing errors, was 4000 Hz, making that the maximum point in the frequency domain. For all graphs, the pre treatment audio is shown in red and the post treatment audio is shown in blue. Horse #1 showed a substantial decrease in amplitudes in the high frequency range as shown in Figure 4.35. Horse #2 did not have any obvious decreases in the high frequency range as demonstrated in Figure 4.36. Horse #3 exhibited a slight decrease in amplitudes in the high frequency range, but not nearly as drastic as the reduction for Horse #1 as seen in Figure 4.37. Since Horse #1 has been clinically evaluated to no longer having DDSP after the genipin treatment based on the dynamic endoscope testing, the reduction in the high frequency whistling noises could be associated with the elimination of palatal displacement in the equine model. This is further supported by the high frequency range results for Horse #2 because that horse did not have any reduction in the high frequency range amplitude, and that horse still has clinically validated DDSP based on the post treatment dynamic endoscopic examination. Horse #3 did not undergo a post treatment dynamic endoscope, but based on owner reports, the horse is not experiencing any DDSP symptoms, which supports that the decrease in high frequency amplitudes is associated with a reduction in palatal displacement.

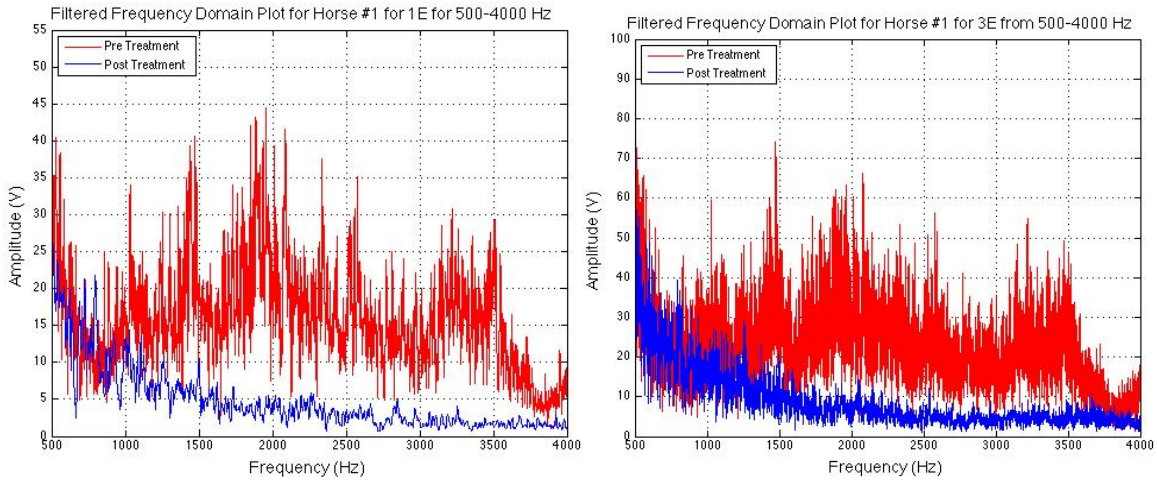

Figure 4.35: The frequency domain graphs from 500-4000 Hz for Horse #1 show a substantial decrease in amplitudes in the high frequency range after the genipin treatment for both the 1E graph (left) and 3E graph (right).

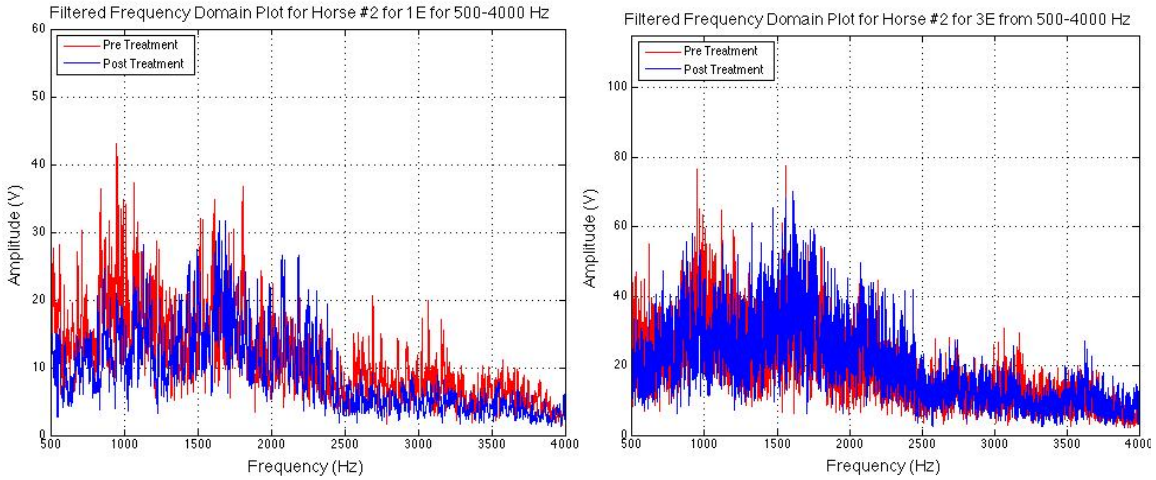

Figure 4.36: Horse #2 shows a slight reduction in the 1E graph (left) in the post treatment amplitudes in the high frequency range, but no reduction in the 3E graph (right), indicating that the selection of exhales can influence the outcome.

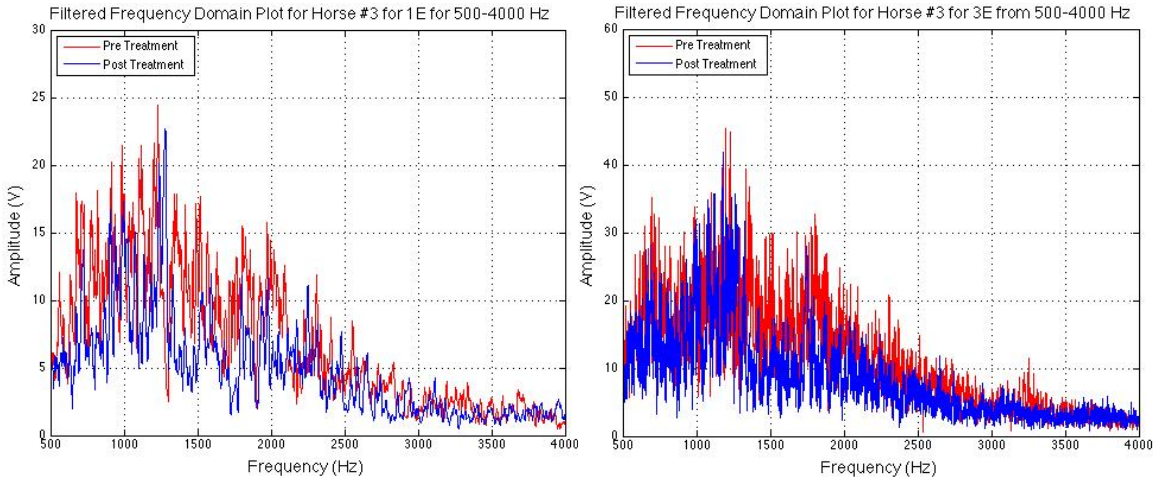

Figure 4.37: Horse #3 had a slight decrease in amplitudes in the high frequency range as shown by the 1E graph (left) and the 3E graph (right).

The filtered frequency domain files were examined in various low frequency ranges to determine the reduction in amplitude peaks correlating to a decrease in snoring loudness and soft palate vibrations. The ranges used were 0-500 Hz, 0-200 Hz and 0-100 Hz, correlating to various frequency ranges commonly used to analyze snoring sounds. The areas under the frequency domain curve were calculated as a representation of the spectral density of the audio file, and then the percent difference was determined to quantify a difference between the pre treatment and post treatment amplitude files. The trapz function in Matlab was used to determine the area under the curve for the 1E and 3E files, and the specific area used for each frequency range was

highlighted as shown in Figures 4.38-4.43. The pre treatment graph is shown in red and the post treatment graph is shown in dark blue. The area under the curve (AUC) from 0-500 Hz is shaded in light blue, the AUC from 0 -200 Hz is highlighted in green, and the AUC from 0-100 is colored in yellow.

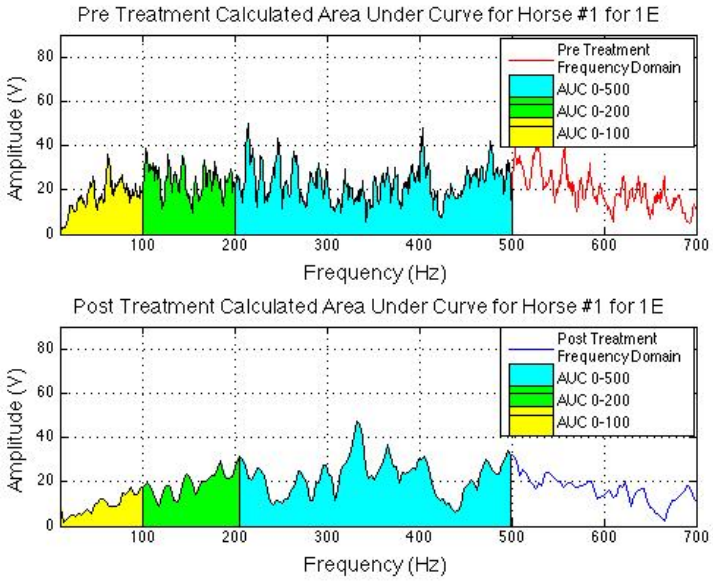

Figure 4.38: The areas under the curve for the Horse #1 for the 1E pre treatment (top) and post treatment (bottom) files were calculated for the various frequency ranges.

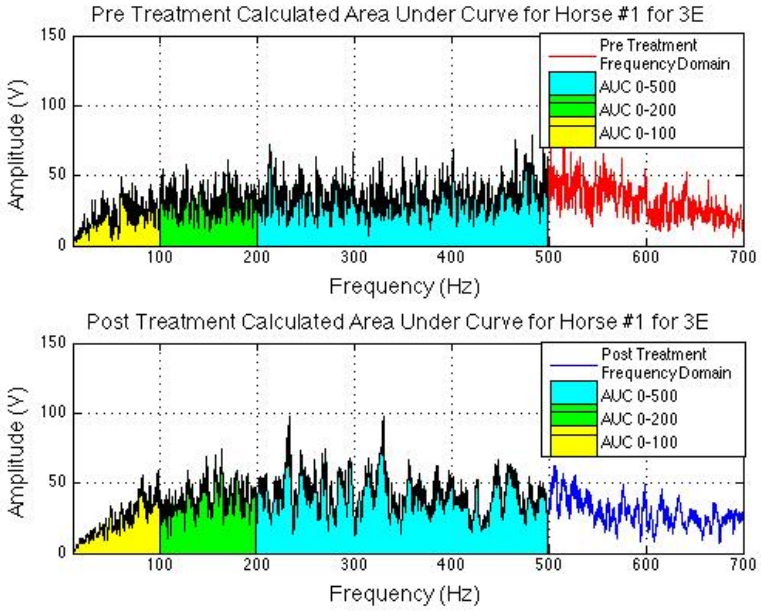

Figure 4.39: The areas under the curve for the Horse #1 for the 3E pre treatment (top) and post treatment (bottom) files were calculated for the various frequency ranges.

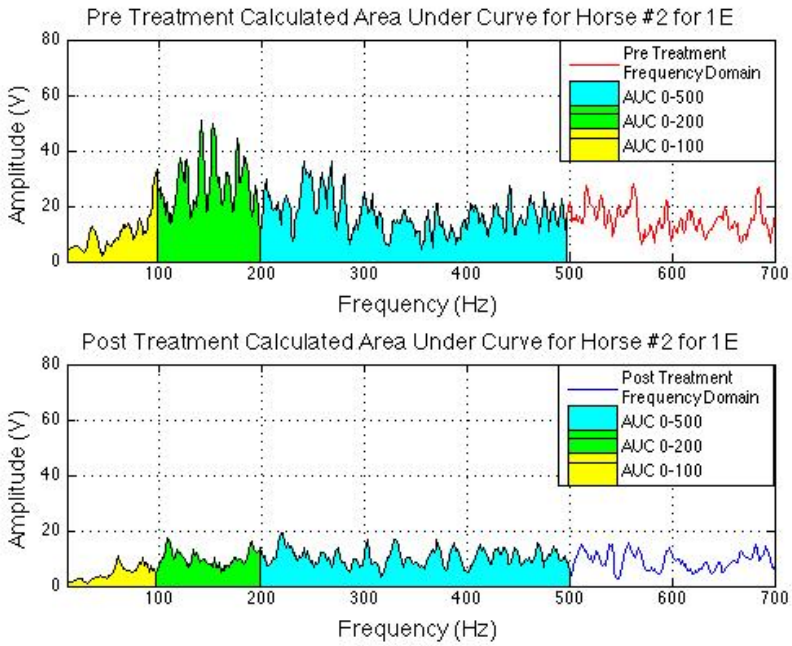

Figure 4.40: The areas under the curve for the Horse #2 for the 1E pre treatment (top) and post treatment (bottom) files were calculated for the various frequency ranges.

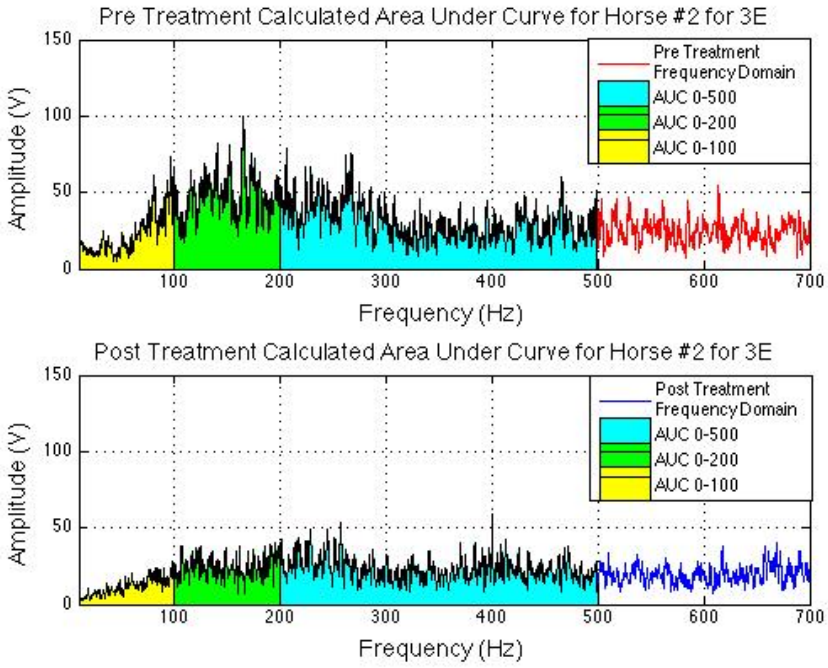

Figure 4.41: The areas under the curve for the Horse #2 for the 3E pre treatment (top) and post treatment (bottom) files were calculated for the various frequency ranges.

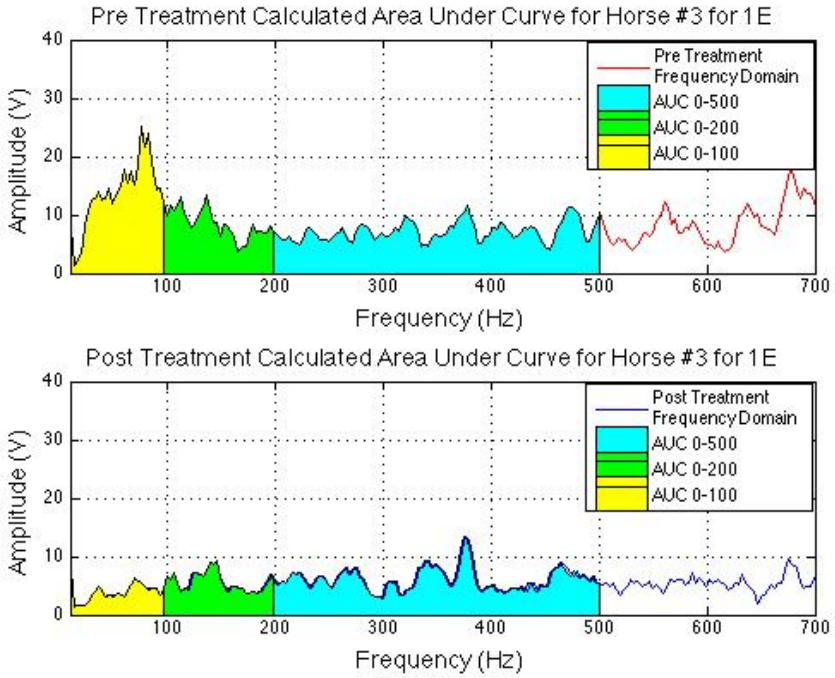

Figure 4.42: The areas under the curve for the Horse #3 for the 1E pre treatment (top) and post treatment (bottom) files were calculated for the various frequency ranges.

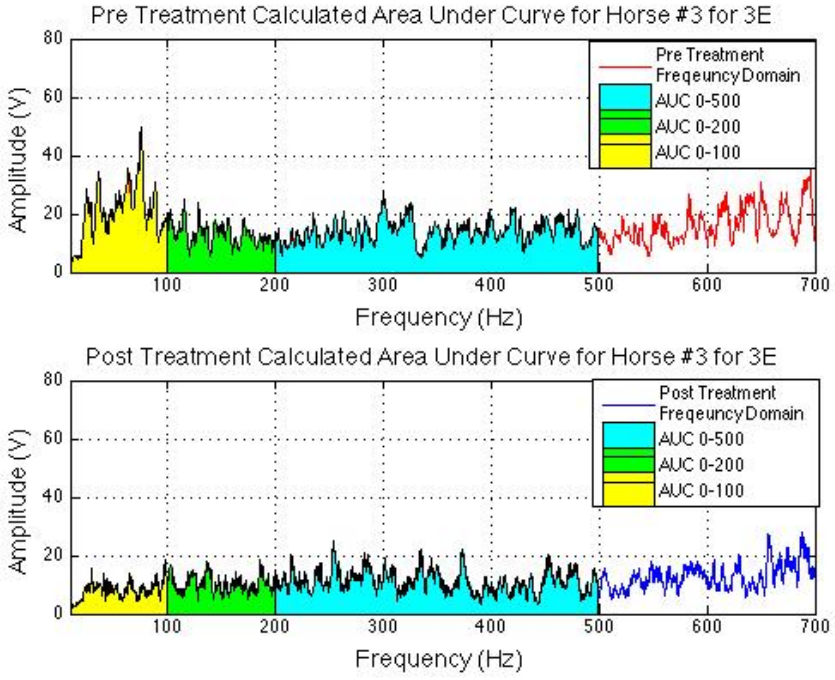

Figure 4.43: The areas under the curve for the Horse #3 for the 3E pre treatment (top) and post treatment (bottom) files were calculated for the various frequency ranges.

The filtered frequency domain files were examined in the low frequency range from 0 to 500 Hz. A limit of 500 Hz was chosen because it was the cutoff frequency for the laser used in the wind tunnel study. In the graphs, the pre treatment audio data is shown in red, and the post treatment data is shown in blue. As demonstrated by all three horses, there is a reduction in the low frequency range amplitudes between 0-500 Hz. Horse #1 also shows a decrease in amplitudes, but it is less evident in the 3E graph than in the 1E graph as shown in Figure 4.44. Horse #2 and Horse #3 show a definitive reduction that is evident in both the 1E graphs and 3E graphs, as demonstrated in Figures 4.45 and 4.46. The reduction in low frequency domain amplitudes supports the reduction in steady-state displacements, or vibration amplitudes, as seen in the wind tunnel study.

As previously shown in Figures 4.38-4.43, the area under the frequency domain curves was determined for each audio file as a representation of the spectral density of the audio file. Table 4.6 highlights the calculated areas under the curves, and the associated percent difference between the pre treatment values and post treatment values for each individual horse. Figure 4.47 and 4.48 show the differences in the areas under the curve between the pre treatment and post treatment audio files for the 1E and 3E files, respectively. Finally, Figure 4.49 plots the percent differences between the area under the curve for the pre treatment file and post treatment file for each horse in the 1E and 3E files. Overall, for the 1E files, there was an average 31.6% reduction in amplitudes from 0-500 Hz. For the 3E files, there was an average 15.6% reduction in amplitudes form 0-500 Hz. In the 3E files, Horse #1 had a slight increase in the area under the curve for the post treatment curve. Based on clinical observations, Horse #1 no longer experiences any DDSP related snoring, so the increase in area under the curve for the post treatment audio file could be the result of background noise that was not fully filtered out or due to increased airflow because of an elevated level of exercise available to the horse now that the breathing disorder has been corrected. The reduction in amplitudes in the low frequency range from 0-500 Hz relates to a decrease in snoring loudness, which further supports the wind tunnel study results that showed an average 23% reduction in steady state soft palate vibration amplitudes for the 100 mM genipin concentration injections.

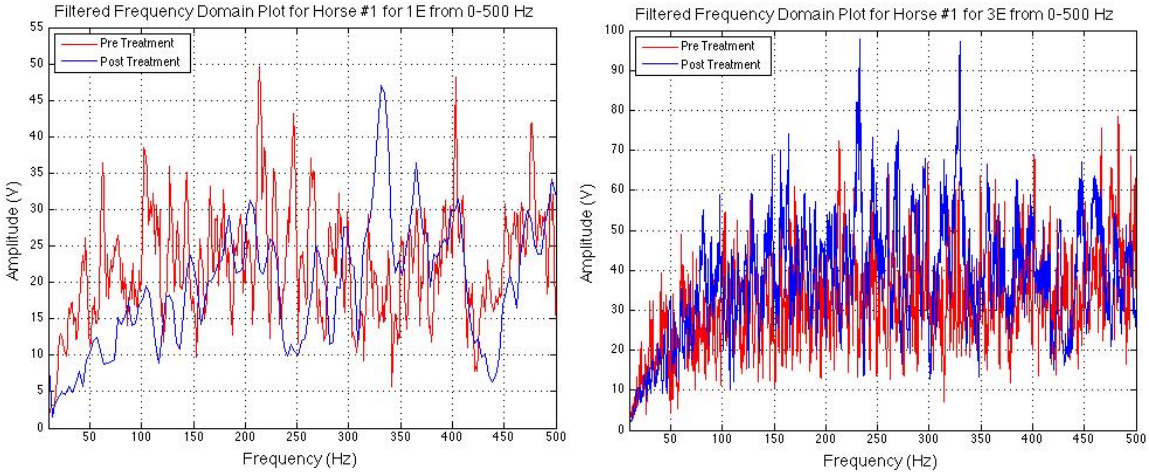

Figure 4.44: Horse #1 shows a post treatment reduction in amplitudes in the 1E graph (left) in the frequency domain graph from 0-500 Hz, with a less obvious reduction in amplitudes in the 3E graph (right). A majority of the reduction in amplitudes occurs in the frequencies below 200 Hz.

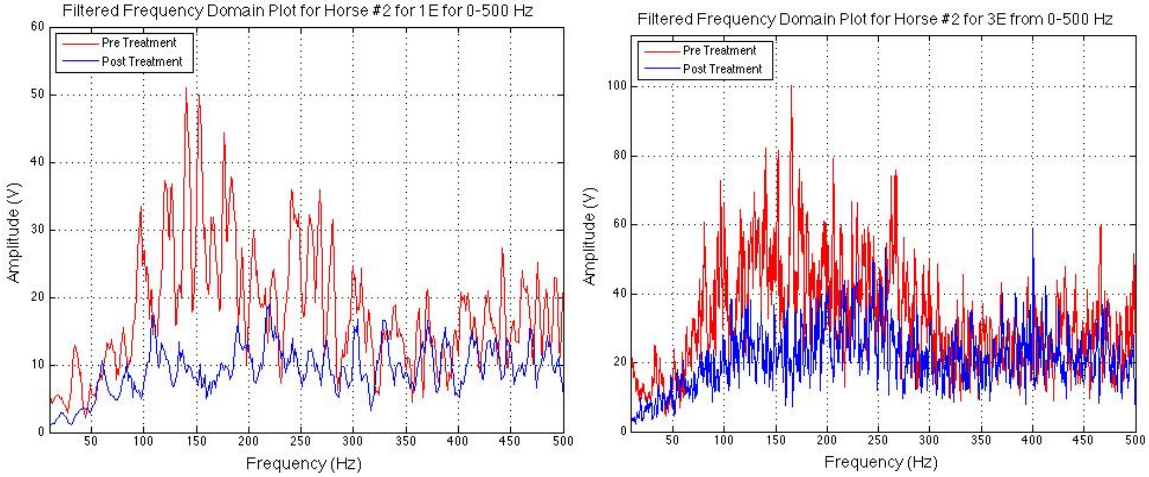

Figure 4.45: For Horse #2, there is a large reduction in amplitudes in both the 1E (left) and 3E (right) post treatment curves compared to the pre treatment curves, with the greatest amplitude decrease occurring below 200 Hz.

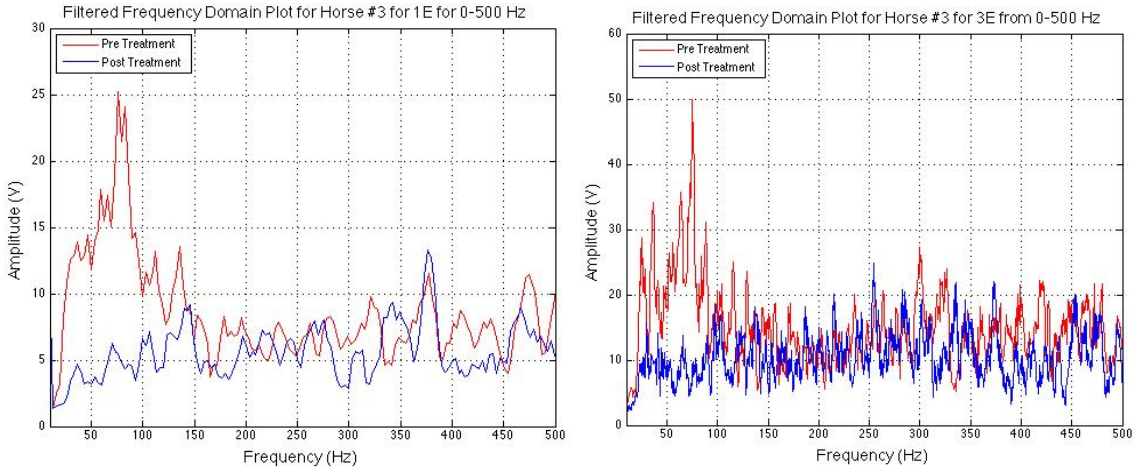

Figure 4.46: The 1E (left) and 3E (right) post treatment amplitudes demonstrated a slight reduction from the pre treatment amplitudes, especially below 150 Hz, for Horse #3.

Table 4.6: This table shows the spectral density of the audio data represented by the areas under the curve in the frequency domain for the 1E and 3E audio files from 0-500 Hz and the percent differences calculated between the pre treatment and post treatment graphs.

Audio File	$\sum_{\omega=0}^{\omega=500} A_{1E}\Delta\omega$ A_{1E}=Audio Amplitude for 1E	1E %Difference between Pre and Post Treatment Audio	$\sum_{\omega=0}^{\omega=500} A_{3E}\Delta\omega$ A_{3E}=Audio Amplitude for 3E	3E %Difference between Pre and Post Treatment Audio
Horse #1: Pre Treatment	1.10E+04	12.46% decrease	1.56E+04	19.29% increase
Horse #1: Post Treatment	9.62E+03		1.86E+04	
Horse #2: Pre Treatment	9.12E+03	48.74% decrease	1.62E+04	35.15% decrease
Horse #2: Post Treatment	4.68E+03		1.05E+04	
Horse #3: Pre Treatment	4.33E+03	33.46% decrease	7.42E+03	30.90% decrease
Horse #3: Post Treatment	2.88E+03		5.13E+03	

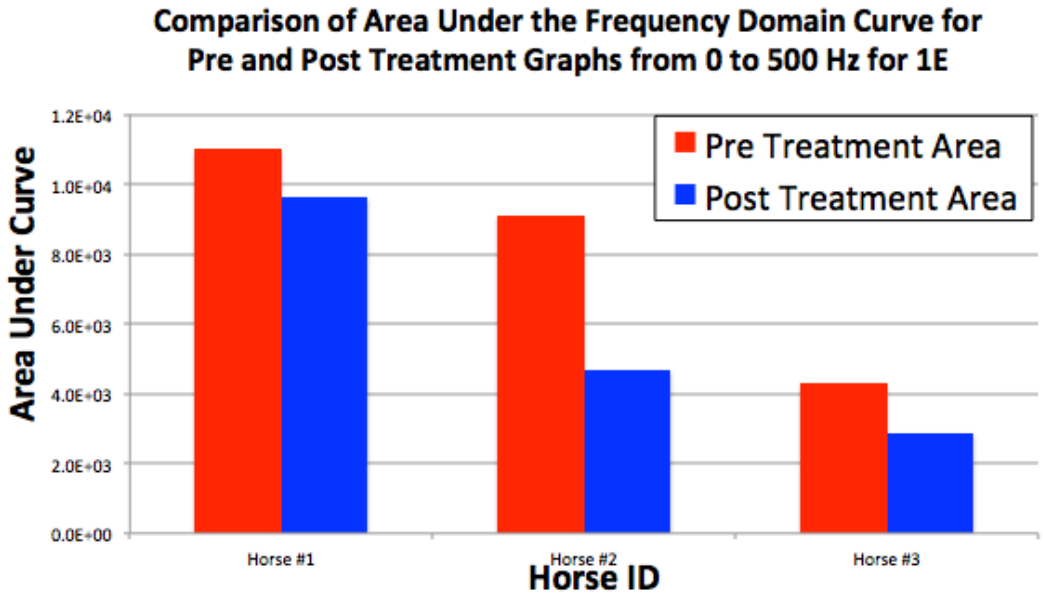

Figure 4.47: The spectral density of the audio data represented by the areas under the frequency domain curve demonstrate a reduction in post treatment amplitudes for all horses from 0-500 Hz for the 1E files, relating to a reduction in snoring loudness and soft palate vibrations.

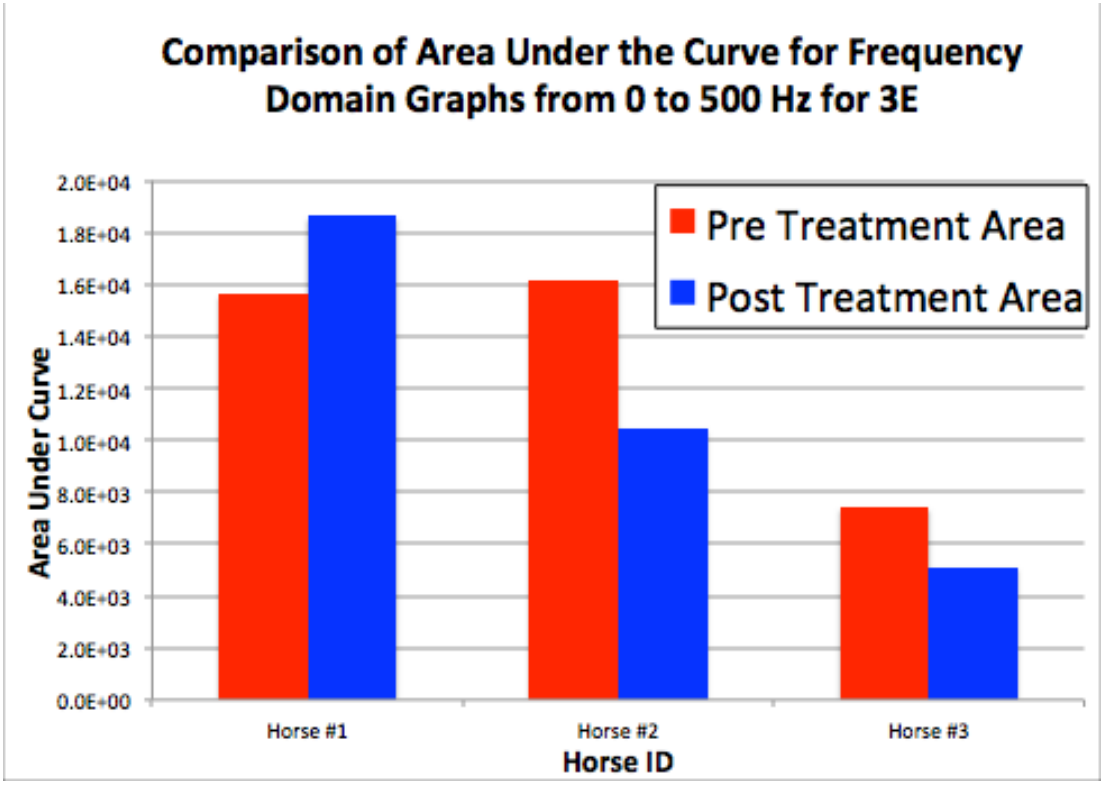

Figure 4.48: The spectral density of the audio data represented by the areas under the frequency domain curve demonstrate a reduction in post treatment amplitudes for two horses from 0-500 Hz for the 3E files, relating to a reduction in snoring loudness and soft palate vibrations. Although no longer experiencing DDSP symptoms, Horse #1 had an increase in amplitudes for the 3E file from 0-500 Hz, which could be attributed to an increase in breathing rate post treatment.

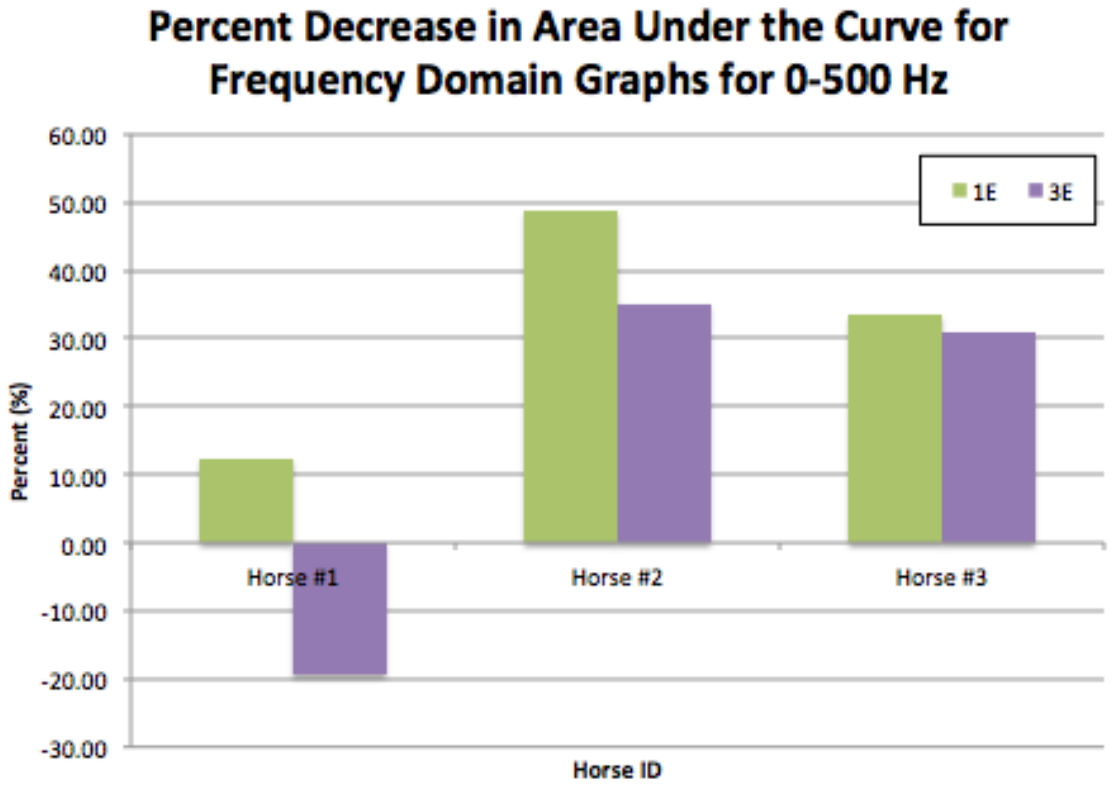

Figure 4.49: Comparing the percent differences in the amplitudes of the pre treatment and post treatment spectral densities for the 1E and 3E files from 0-500 Hz, shows an average 31.6% decrease for the 1E file and 15.6% decrease for the 3E files.

Similarly, the audio data was analyzed in the low frequency range from 0 to 200 Hz for the 1E and 3E files. A cutoff of 200 Hz was used because the common frequency range to analyze human snoring sounds is from 0 to 200 Hz, which is associated with snoring and the soft palate vibrations, as previously stated. In all graphs, the pre treatment audio files are represented in red and the post treatment audio files are represented in blue. In general, all three horses experienced a decrease in the amplitudes of frequency domain graphs from 0 to 200 Hz in the 1E files. For Horse #1 the reduction in amplitudes was noticeable in the 1E graph, but less noticeable in the 3E graph, as shown in Figure 4.50. Most of the reduction in amplitudes for Horse #1 occurred below 100 Hz, which is associated specifically with a reduction in soft palate vibrations. Horse #2 and Horse #3 both reflected large reductions in amplitude from 0 to 200 Hz for the 1E and 3E files as demonstrated in Figures 4.51 and 4.52, relating to a reduction in snoring loudness and soft palate vibrations.

The areas under the pre treatment and post treatment frequency curves were calculated for each horse, as a representation of the spectral density of the audio data, and the percent difference between the two was determined. As previously shown, Figures 4.38-4.43 highlight the areas under the curves that were calculated, and these results are displayed in Table 4.7. Figure 4.53 and 4.54 show the areas under the curve for pre treatment and post treatment graphs for each horse for the 1E files and 3E files, respectively. Finally, Figure 4.55 plotted the percent differences between the pre treatment and post treatment audio files for each horse for the 1E and 3E files. Overall, there was an average 47.2% decrease in amplitude for the 1E post treatment audio files, and an average 25.4% decrease in amplitude for the 3E post treatment audio files. Again, Horse #1 experienced a slight increase in the post treatment area under the curve from 0-200 Hz for the 3E file, most likely due to an increase in breathing rate because of a reduction in exercise exertion after curing his breathing disorder. Based on the reduction of the amplitudes in the 0-200 Hz frequency range, it can be concluded that all three horses experienced a decrease in snoring loudness due to the correlation with human snoring frequencies. This conclusion is in agreement with the individual reports from the owners who stated that all three horses had a decrease in snoring loudness while exercising. Also, it is supported by the dynamic endoscope results from Horse #1, who was diagnosed as no longer having DDSP after the genipin treatment.

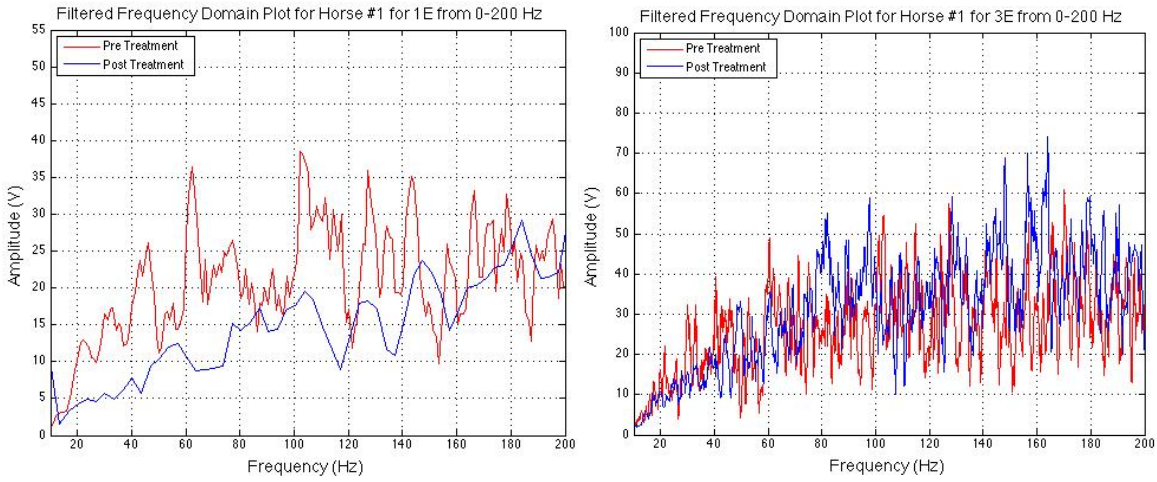

Figure 4.50: The areas under the pre treatment and post treatment curves for Horse #1 show a reduction in amplitude from 0-200 Hz for the 1E files (left) and for the 3E files (right), especially in the frequency range below 100 Hz relating to a reduction in soft palate vibration.

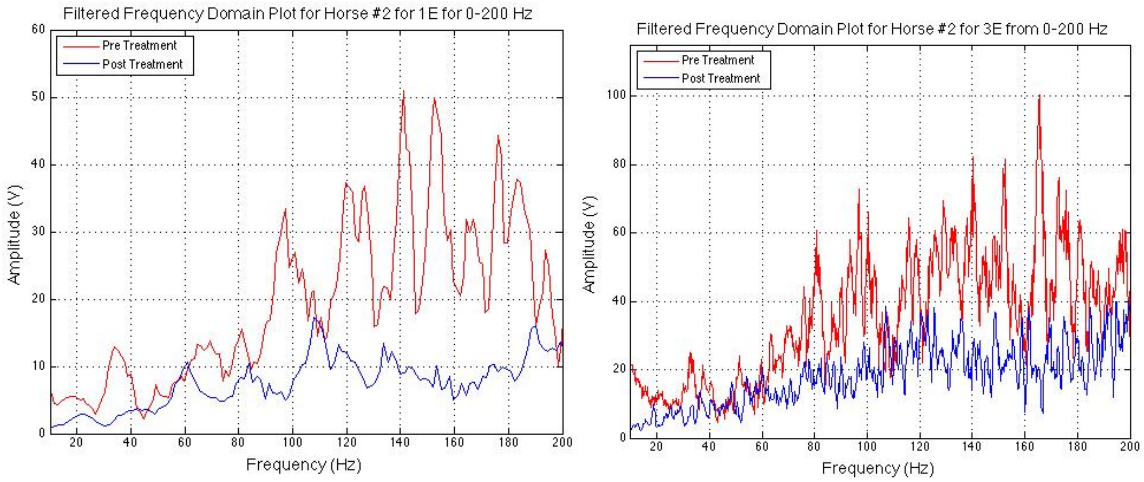

Figure 4.51: The areas under the pre treatment and post treatment curves for Horse #2 show a large reduction in amplitude for the 1E files (left) and 3E files (right) from 0-200 Hz, relating to a reduction in snoring loudness and soft palate vibration.

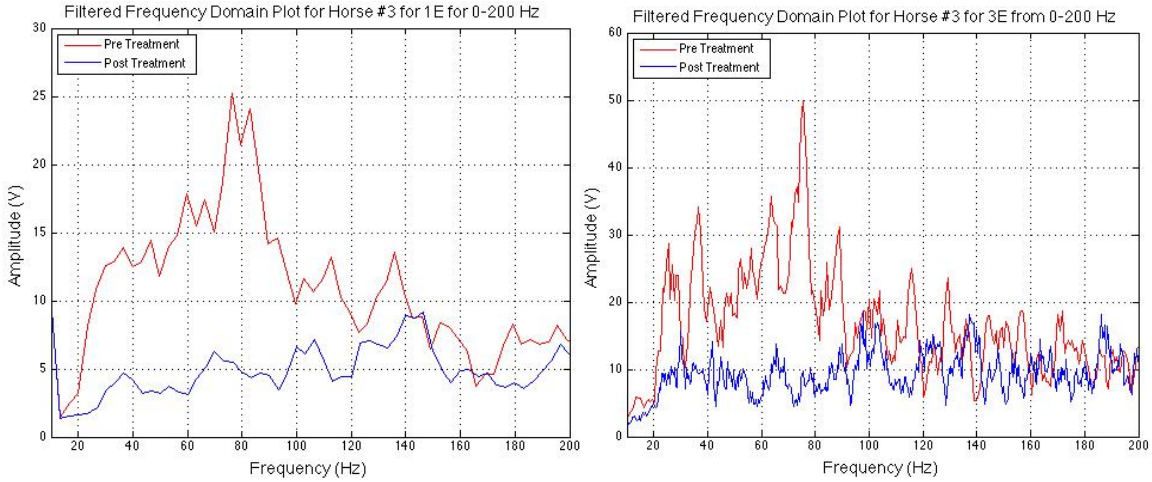

Figure 4.52: The areas under the pre treatment and post treatment curves for Horse #3 demonstrate a reduction in amplitude for the 1E files (left) and 3E files (right) from 0-200 Hz, especially in the range from 0-100 Hz, representing a reduction in soft palate vibration.

Table 4.7: This table shows the spectral density of the audio data represented by the areas under the curve in the frequency domain for the 1E and 3E audio files from 0-200 Hz and the percent differences calculated between the pre treatment and post treatment graphs.

Audio File	$\sum_{\omega=0}^{\omega=200} A_{1E}\Delta\omega$ A_{1E}=Audio Amplitude for 1E	1E %Difference between Pre and Post Treatment Audio	$\sum_{\omega=0}^{\omega=200} A_{3E}\Delta\omega$ A_{3E}=Audio Amplitude for 3E	3E %Difference between Pre and Post Treatment Audio
Horse #1: Pre Treatment	4.09E+03	27.04% decrease	5.06E+03	18.11% increase
Horse #1: Post Treatment	2.99E+03		5.98E+03	
Horse #2: Pre Treatment	4.01E+03	62.11% decrease	6.99E+03	49.94% decrease
Horse #2: Post Treatment	1.52E+03		3.50E+03	
Horse #3: Pre Treatment	2.17E+03	52.36% decrease	3.19E+03	44.29% decrease
Horse #3: Post Treatment	1.03E+03		1.78E+03	

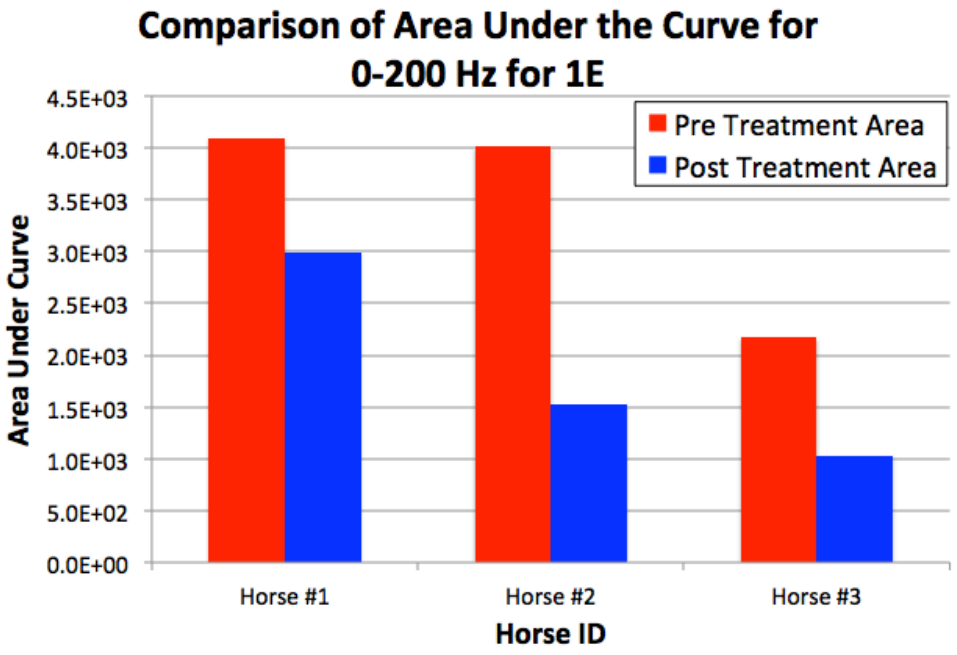

Figure 4.53: All three horses experienced a reduction in the amplitudes for the areas under the frequency domain curves, which represented spectral density, from 0-200 Hz for the 1E graphs, relating to a reduction in snoring loudness and palatal vibrations.

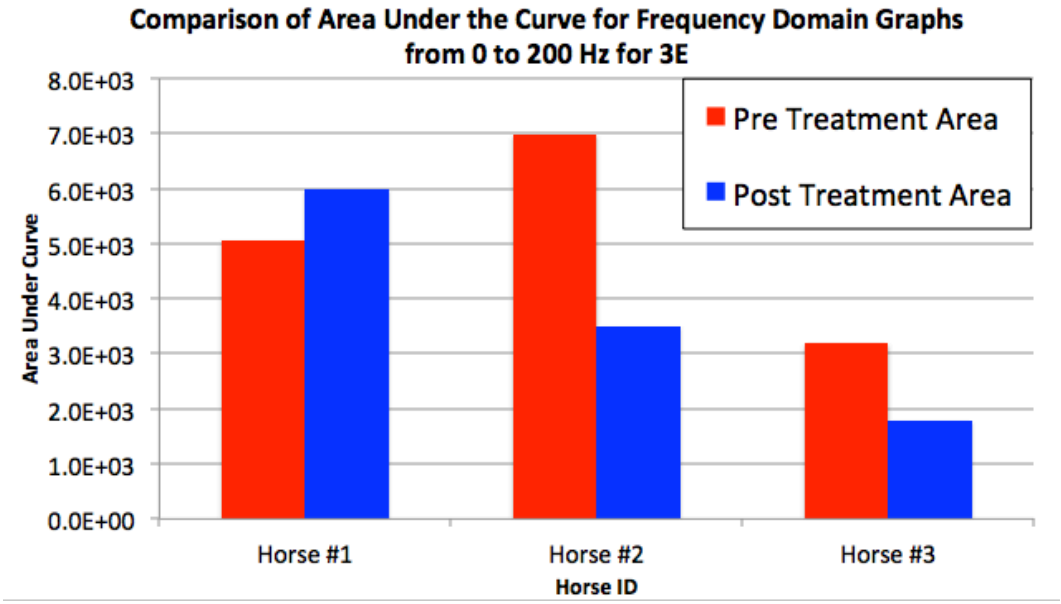

Figure 4.54: Two of the three horses experienced a reduction in the amplitudes for the areas under the frequency domain curves, which represented spectral density, from 0-200 Hz for the 3E graphs, relating to a reduction in snoring loudness and palatal vibrations. Horse #1 had a slight increase in the post treatment amplitudes.

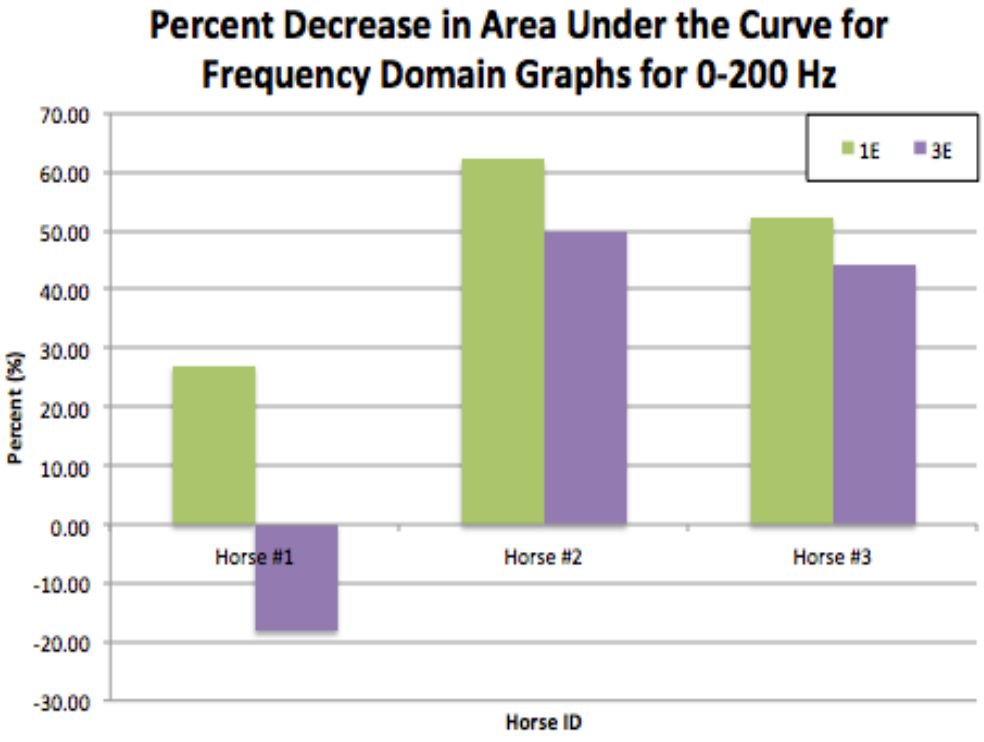

Figure 4.55: Comparing the percent differences in the amplitudes of the pre treatment and post treatment spectral densities for the 1E and 3E files from 0-200 Hz, shows an average 47.2% decrease for the 1E file and 25.4% decrease for the 3E files.

Additionally, the audio data was analyzed in the low frequency range from 0 to 100 Hz for the 1E and 3E files to correlate to vibrations associated with the soft palate. Snoring sounds detected by trained individuals are typically heard in the 0-50 Hz range, thus analyzing the audio files from 0-100 Hz would correspond to snoring loudness, as well. In all graphs, the pre treatment audio files are represented in red and the post treatment audio files are represented in blue. In general, all three horses experienced a decrease in the amplitudes of frequency domain graphs from 0 to 100 Hz in the 1E files. For Horse #1, the reduction in amplitudes were noticeable in the 1E graph, but less noticeable in the 3E graph, as shown in Figure 4.56. Horse #2 and Horse #3 both reflected large reductions in amplitude from 0 to 100 Hz for the 1E and 3E files as demonstrated in Figures 4.57 and 4.58, relating to a reduction in snoring loudness and soft palate vibrations. The largest reduction in amplitudes for Horse #1 and Horse #3 happened below 50 Hz, which corresponds to a reduction in soft palate vibration that occurs around 25 Hz. These results coincide with the post treatment dynamic endoscope examinations and owner updates that report these horses as no longer experiencing any DDSP symptoms, including soft palate displacements and snoring.

The areas under the pre treatment and post treatment frequency curves were calculated for each horse, as a representation of the spectral density of the audio data, and the percent difference between the two curves was determined for the 0-100 Hz frequency range. As previously shown, Figures 4.38-4.43 highlight the areas under the curves that were calculated, and these results are displayed in Table 4.8. Figure 4.59 and 4.60 show the areas under the curve for pre treatment and post treatment graphs for each horse for the 1E files and 3E files, respectively. Finally, Figure 4.61 plots the percent differences between the pre treatment and post treatment audio files for each horse for the 1E and 3E files. Overall, there was an average 55.0% decrease in amplitude for the 1E post treatment audio files, and an average 35.6% decrease in amplitude for the 3E post treatment audio files. Again, Horse #1 experienced a slight increase in the post treatment area under the curve from 0-100 Hz for the 3E file, most likely due to an increase in breathing rate because of a reduction in exercise exertion after curing his breathing disorder. Based on the reduction of the amplitudes in the 0-100 Hz frequency range, it can be concluded that all three horses experienced a decrease in snoring loudness due to the correlation with human snoring frequencies. Additionally, based on the reduction in amplitudes below 50 Hz, it can be determined that the horses also had a reduction in soft palate vibrations. These conclusions agree

with the individual owner reports and the dynamic endoscope examination results that showed a reduction in snoring loudness and palate vibration for two of the horses while exercising. Although, Horse #2 still experienced intermittent DDSP symptoms post treatment, his frequency domain graph from 0-100 Hz still shows a reduction in snoring loudness and palatal vibrations. In this case, the 56.9% reduction in the 1E file and 53.80% reduction in the 3E file for Horse #3 may not have been sufficient to completely rid all of the DDSP snoring and palate displacement symptoms.

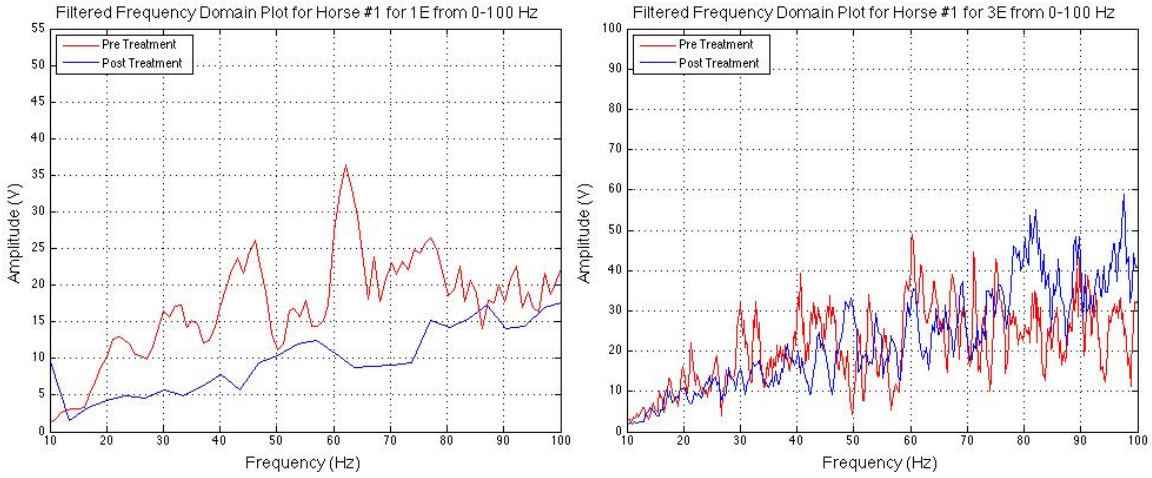

Figure 4.56: The areas under the frequency domain curve for the 1E (left) file shows a reduction in amplitudes from the pre treatment to the post treatment graphs, relating to a reduction in snoring loudness for Horse #1. The 3E (right) file shows a reduction in frequencies below 50 Hz, relating to a reduction in soft palate vibrations.

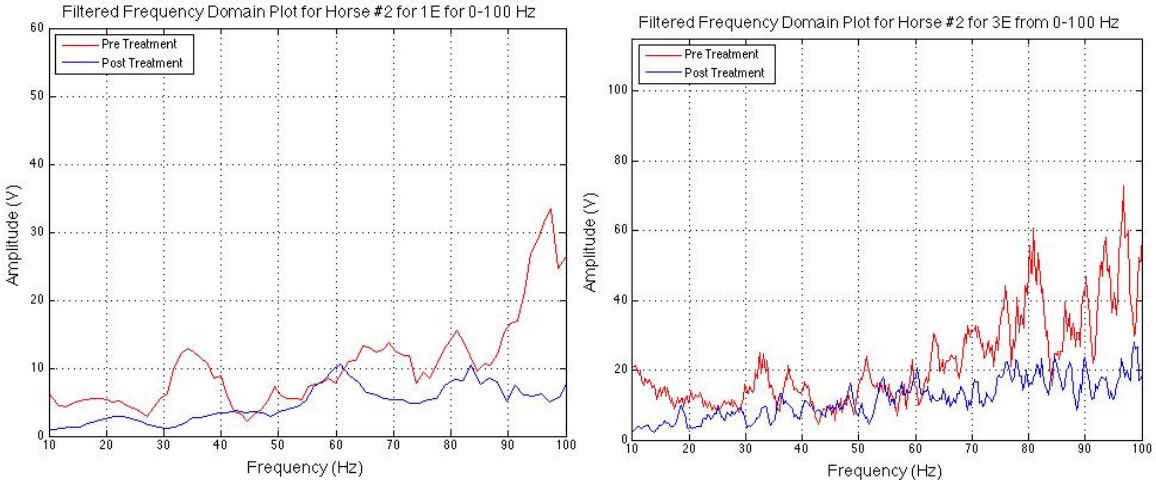

Figure 4.57: The areas under the frequency domain curve for the 1E (left) and 3E (right) files show a reduction in amplitudes from the pre treatment to the post treatment graphs, relating to a reduction in snoring loudness for Horse #2.

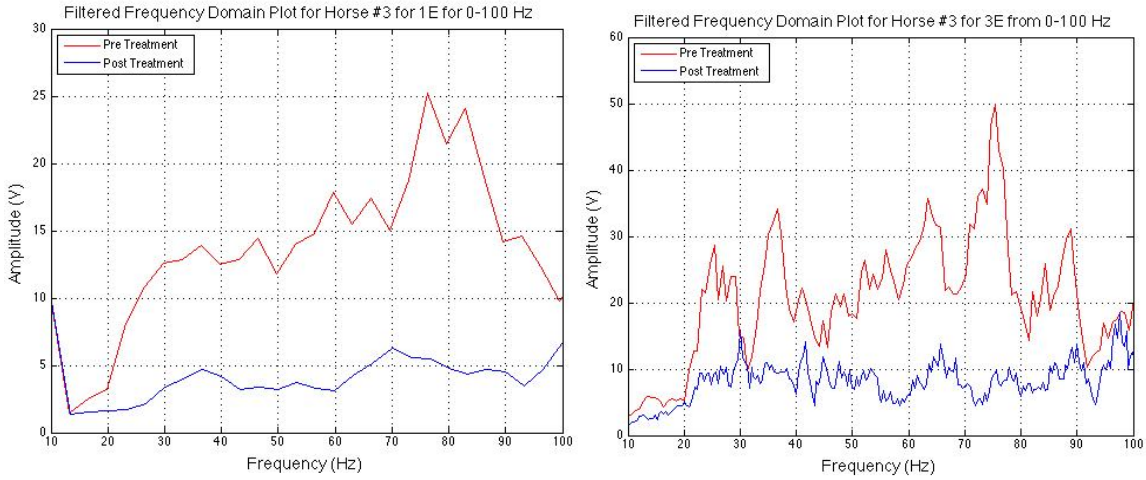

Figure 4.58: The areas under the frequency domain curve for the 1E (left) and 3E (right) files show a reduction in amplitudes from the pre treatment to the post treatment graphs, relating to a reduction in snoring loudness for Horse #3.

Table 4.8: This table shows the spectral density of the audio data represented by the areas under the curve in the frequency domain for the 1E and 3E audio files from 0-100 Hz and the percent differences calculated between the pre treatment and post treatment graphs.

Audio File	$\sum_{\omega=0}^{\omega=200} A_{1E}\Delta\omega$ A_{1E}=Audio Amplitude for 1E	1E %Difference between Pre and Post Treatment Audio	$\sum_{\omega=0}^{\omega=200} A_{3E}\Delta\omega$ A_{3E}=Audio Amplitude for 3E	3E %Difference between Pre and Post Treatment Audio
Horse #1: Pre Treatment	1.65E+03	41.46% decrease	1.93E+03	7.37% increase
Horse #1: Post Treatment	9.70E+02		2.07E+03	
Horse #2: Pre Treatment	1.22E+03	56.93% decrease	2.30E+03	53.80% decrease
Horse #2: Post Treatment	5.26E+02		1.06E+03	
Horse #3: Pre Treatment	1.29E+03	66.68% decrease	1.86E+03	60.48% decrease
Horse #3: Post Treatment	4.29E+02		7.36E+02	

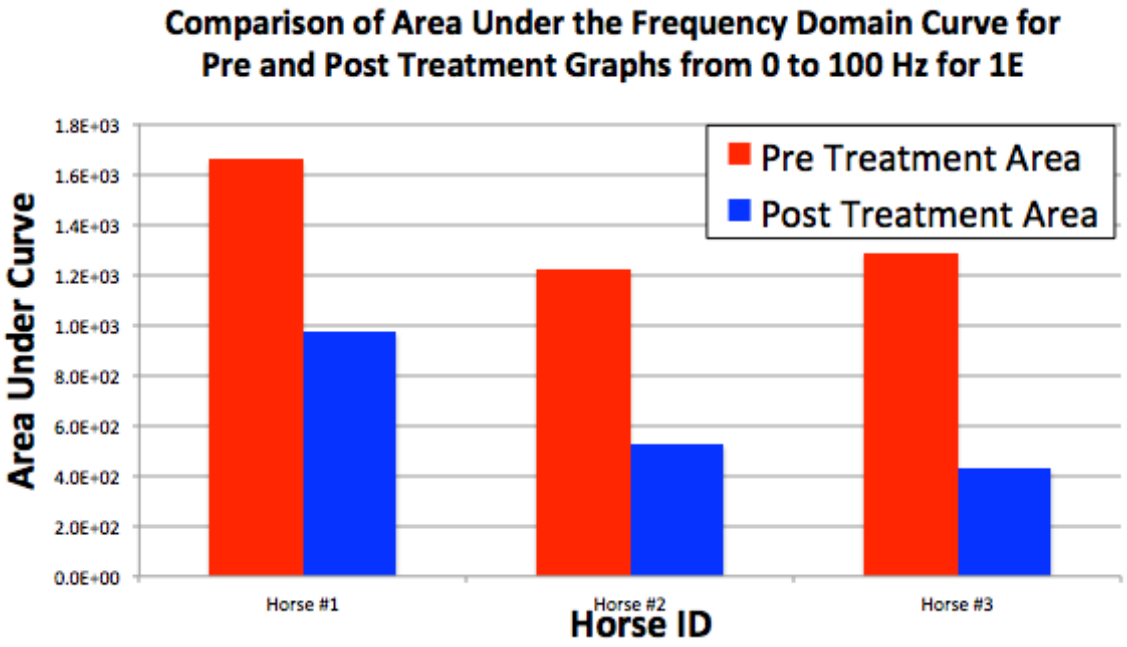

Figure 4.59: All three horses experienced a reduction in the amplitudes for the areas under the frequency domain curves, which represented spectral density, from 0-100 Hz for the 1E graphs, relating to a reduction in snoring loudness and palatal vibrations.

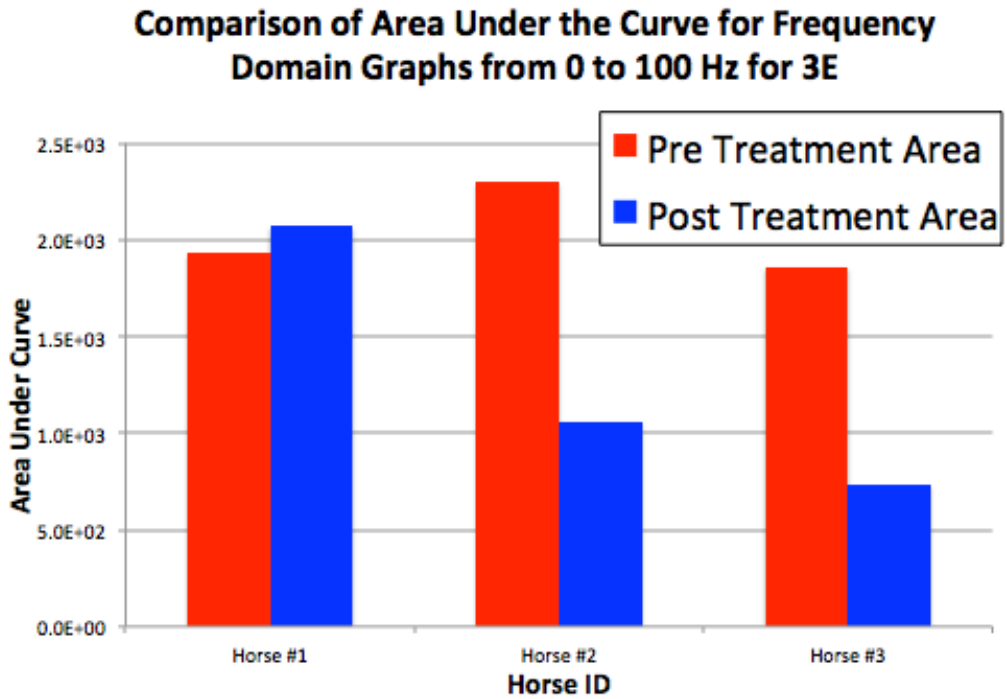

Figure 4.60: Two of the three horses experienced a reduction in the amplitudes for the areas under the frequency domain curves, which represented spectral density, from 0-100 Hz for the 3E graphs, relating to a reduction in snoring loudness and palatal vibrations. Horse #1 had a slight increase in the post treatment amplitudes.

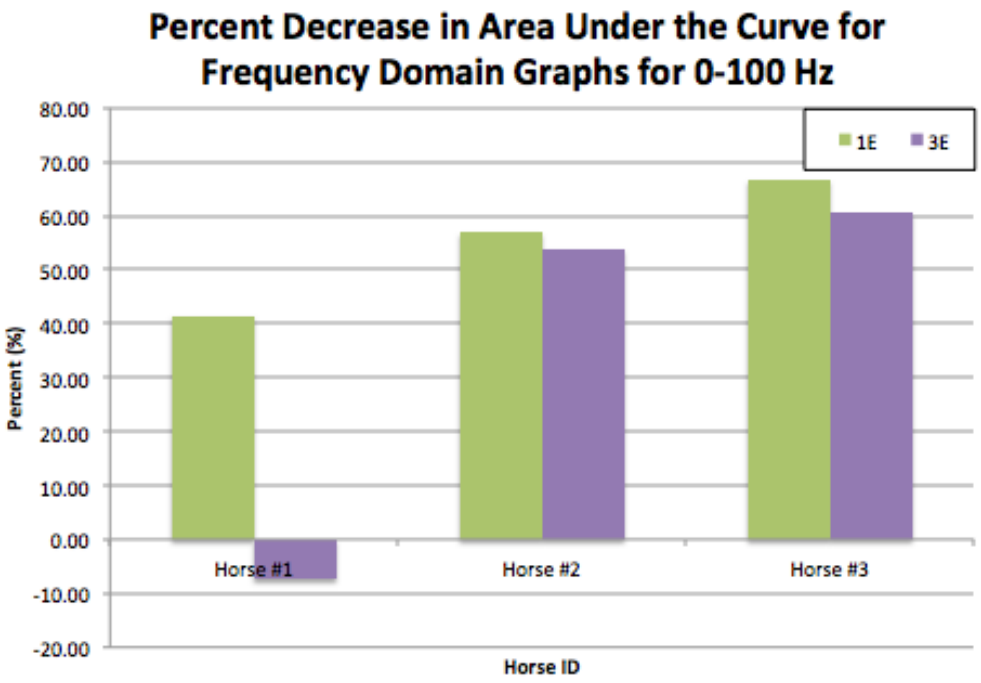

Figure 4.61: Comparing the percent differences in the amplitudes of the pre treatment and post treatment spectral densities for the 1E and 3E files from 0-100 Hz, shows an average 55% decrease for the 1E file and 35.6% decrease for the 3E files.

Finally, the 1E files were analyzed from 20 to 80 Hz in the 0-100 Hz frequency domain graphs to correspond with the previous study completed by Franklin et al. In this study, a common 'DDSP' peak was located at 41 ± 21Hz for the *in vitro* horses and at 53 ± 24 Hz for *in vivo*, as shown in Figure 4.62 [55]. The frequency domain graphs were analyzed for all three horses to see if the 'DDSP' peak existed in the pre treatment audio graph, and to see if it disappeared in the post treatment audio graph. As shown in Figure 4.63, Horse #1 had two prominent peaks in the 40-50 Hz range and in the 60-70 Hz range in the pre treatment frequency domain curve, which could correspond with the 'DDSP' peak because both of these peaks fall near the average peak location from Franklin's study. In the post treatment curve, both of these peaks have disappeared for Horse #1. This supports the dynamic endoscope examination results because Horse #1 was cured of DDSP, therefore, any 'DDSP' peaks should be nonexistent in the post treatment frequency domain graph. Horse #2 had a medium peak around 35 Hz and a large peak around 70 Hz in the pre treatment frequency domain graph as shown in Figure 4.64. Both of these peaks disappear in the post treatment curve; however, a new, smaller amplitude peak appears around 60 Hz. Horse #2 was diagnosed with still having DDSP in the post treatment dynamic endoscope examination; therefore, the

appearance of a new peak in the post treatment curve corresponds with these results. Finally, for Horse #3, there was a prominent peak between 70-90 Hz in the pre treatment curve as shown in Figure 4.65. In the post treatment curve, all of the peaks are noticeably decreased from the pre treatment curve, including the potential 'DDSP' peak between 70-90 Hz, corresponding with the owner's reports that Horse #3 is no longer experiencing any DDSP symptoms.

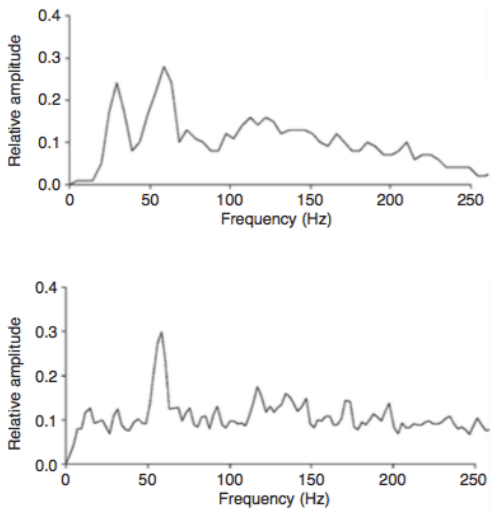

Figure 4.62: From the Franklin et al study, the top graph demonstrates the 'DDSP' peaks found for *in vitro* cadaveric horses, and the bottom graph shows the 'DDSP' peak found for the *in vivo* exercising study horses with DDSP [55].

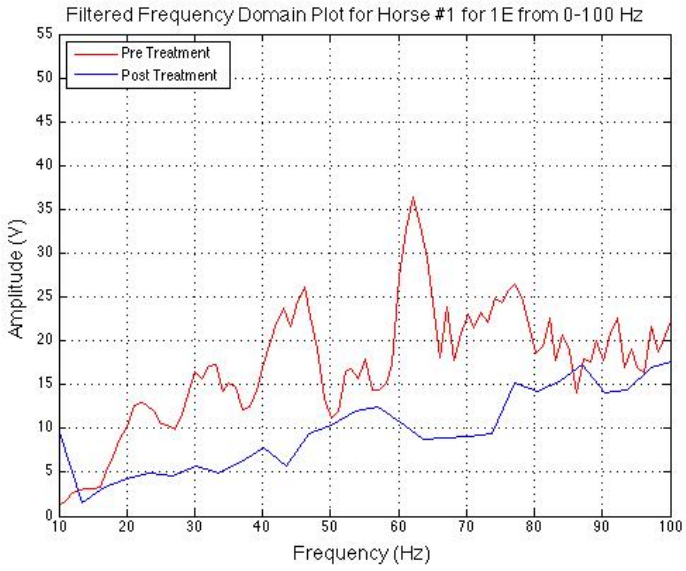

Figure 4.63: Horse #1 had two prominent peaks in the 20-80 Hz range in the pre treatment audio file that could be related to the 'DDSP' Peak. Both of these peaks disappeared in the post treatment curve, relating to a non DDSP dynamic endoscope diagnosis.

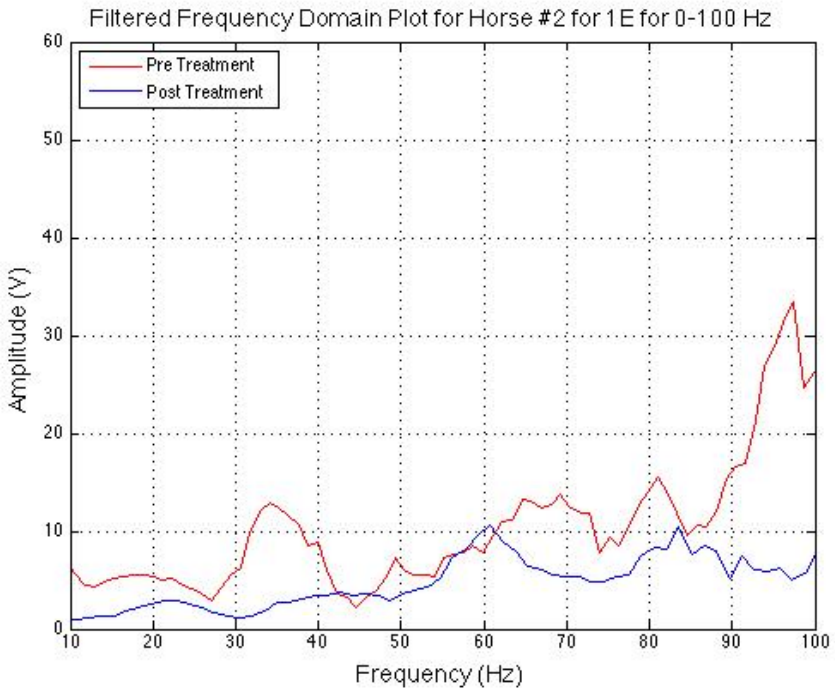

Figure 4.64: Horse #2 had two prominent peaks in the 20-80 Hz range in the pre treatment audio file that could be related to the 'DDSP' Peak. In the post treatment audio file, both of the original peaks disappeared, but a new 'DDSP' peak appeared, leading one to believe that the horse still experienced DDSP, as confirmed by the dynamic endoscope results.

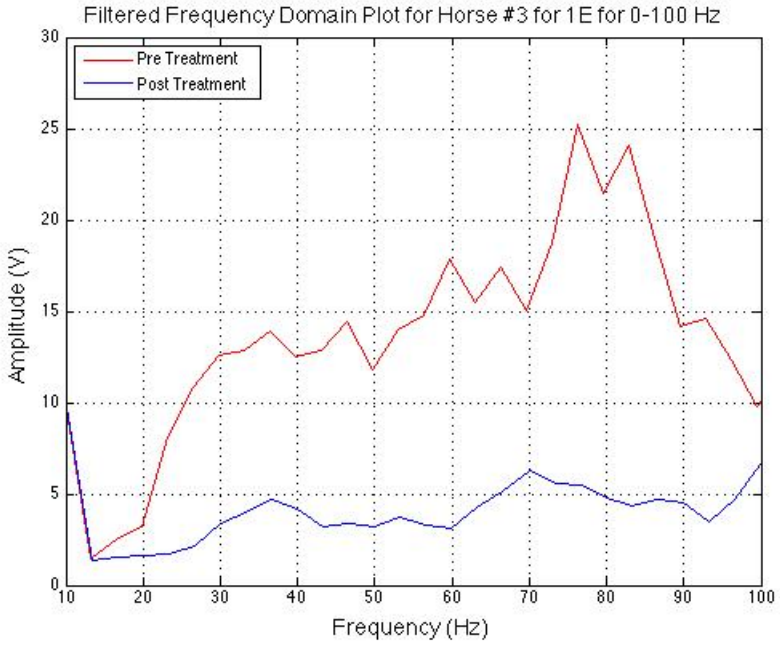

Figure 4.65: Horse #3 had a prominent peak in the pre treatment graph corresponding to a potential 'DDSP' peak. In the post treatment curve, all of the prominent peaks have disappeared, supporting the owner's report that Horse#3 no longer experiences any symptoms of DDSP.

4.1.7 Histological Analysis

The three soft palates from the safety phase horses were harvested upon completion of the *in vivo* study. Upon thawing, the three palates were observed and divided into six sections per palate as previously described. The soft palate from Horse #4, as shown in Figure 4.66, had two noticeable thickened and elevated 'pillow-like' regions around the injection site. When cutting into these areas, the tissue was a dark blue color, indicating that it had been crosslinked by the genipin reagent. This was most likely due to either the 'pillowing' or inflation effect of the soft palate that occurred during the injections or to an errant injection in which the needle was not fully inserted into tissue, causing the reagent to be injected closer to the respiratory mucosal layer. The palate from Horse #5 had a small area of necrosis, but otherwise looked normal as demonstrated in Figure 4.67. The necrotic area from palate of Horse #5 was crosslinked blue from the genipin treatment on the inside. Similarly, Horse #6's palate showed a large region of necrotic tissue on the surface of the soft palate encircled by a fibrotic encapsulation around the injection area, as seen in Figure 4.68. Inside of this necrotic tissue, the region had a small area of dark blue crosslinking, but otherwise it appeared to be non-crosslinked, unhealthy, damaged tissue.

Once all observations were complete, the palates were cut in half into left (L) and right (R) sections, and then three segments were cut from each half: top (T), middle (M), bottom (B) with the top closest to the epiglottis and the bottom closest to the hard palate. From each half, at least one of the segments was taken from a perceived untreated section as indicated by an apparent absence of blue coloration. This produced 18 segments total: 4LT, 4LM, 4LB (untreated), 4RT, 4RM, 4RB (untreated), 5LT, 5LM, 5LB (untreated), 5RT, 5RM, 5RB (untreated), 6LT (untreated), 6LM, 6LB, 6RT (untreated), 6RM, and 6RB. These samples were then fixed in 10% formalin for six days, then placed in 70% ethanol and shipped to IDEXX BioResearch Pathology Services for histological analysis.

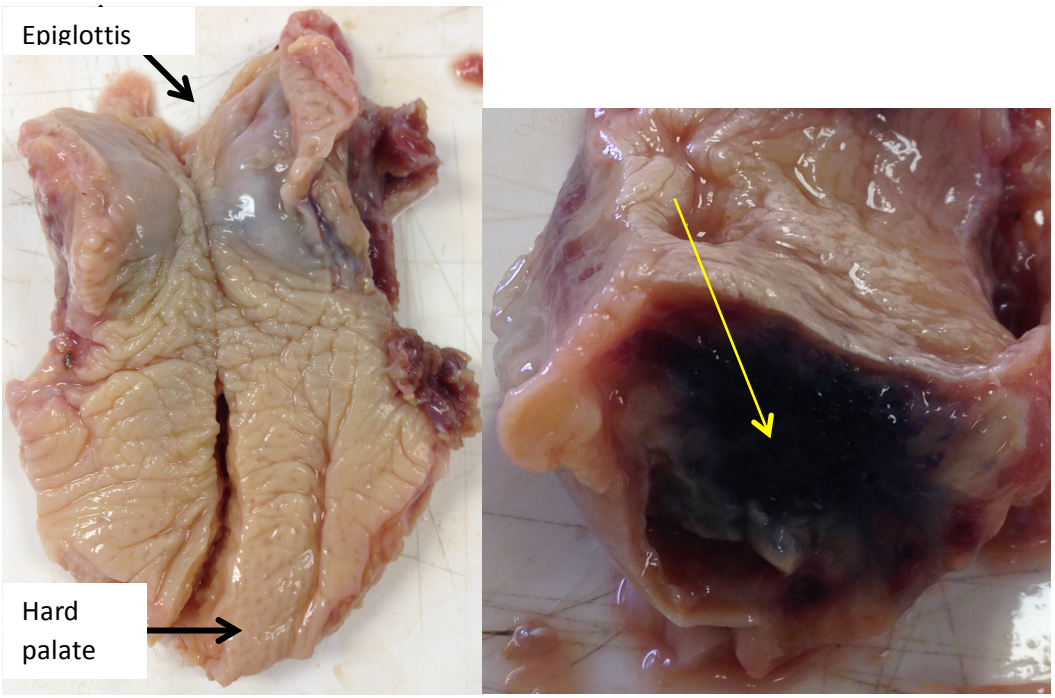

Figure 4.66: The soft palate from Horse #4 showed two large regions of distended 'pillowed' tissue as demonstrated in the full soft palate picture on the left. Upon cutting into these regions, it was discovered that the inside tissue was a dark blue color as shown by the yellow arrow, indicating that it had been crosslinked by the genipin treatment as shown in the picture on the right.

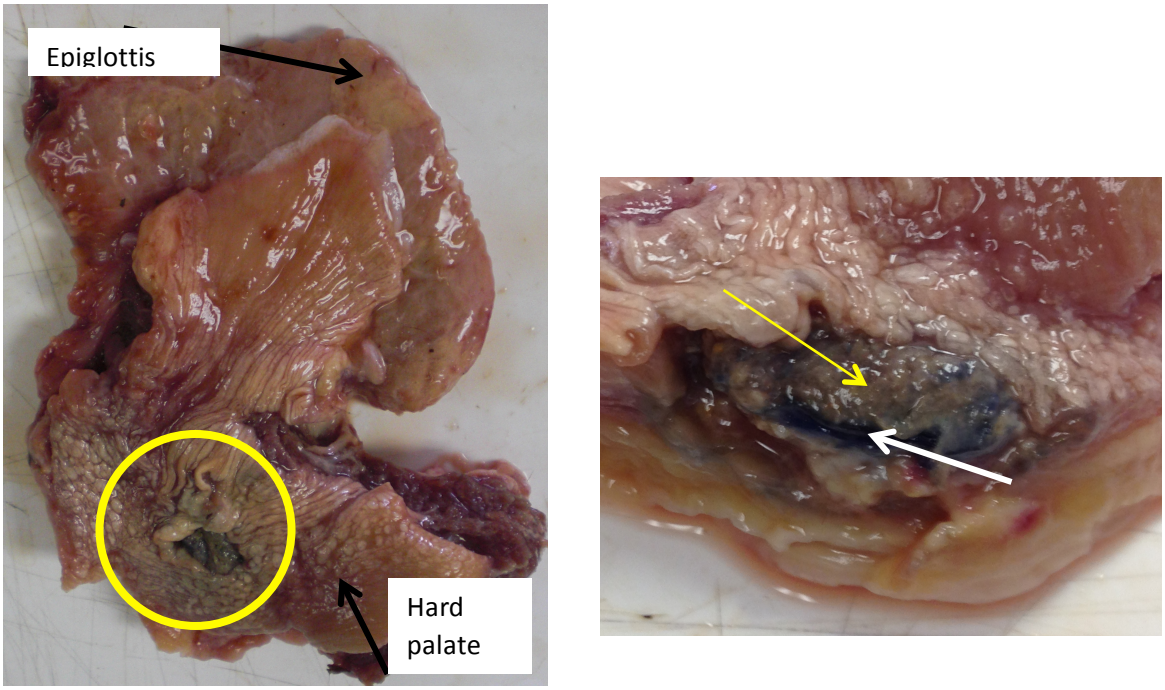

Figure 4.67: The soft palate from Horse #5 had a small necrotic region in the top area as highlighted by the yellow circle in the picture on the left. Inside this region, the tissue was crosslinked blue as pointed out by the white arrow surrounded by a small pocket of apparent light gray necrotic tissue as shown by the yellow arrow in the picture on the right.

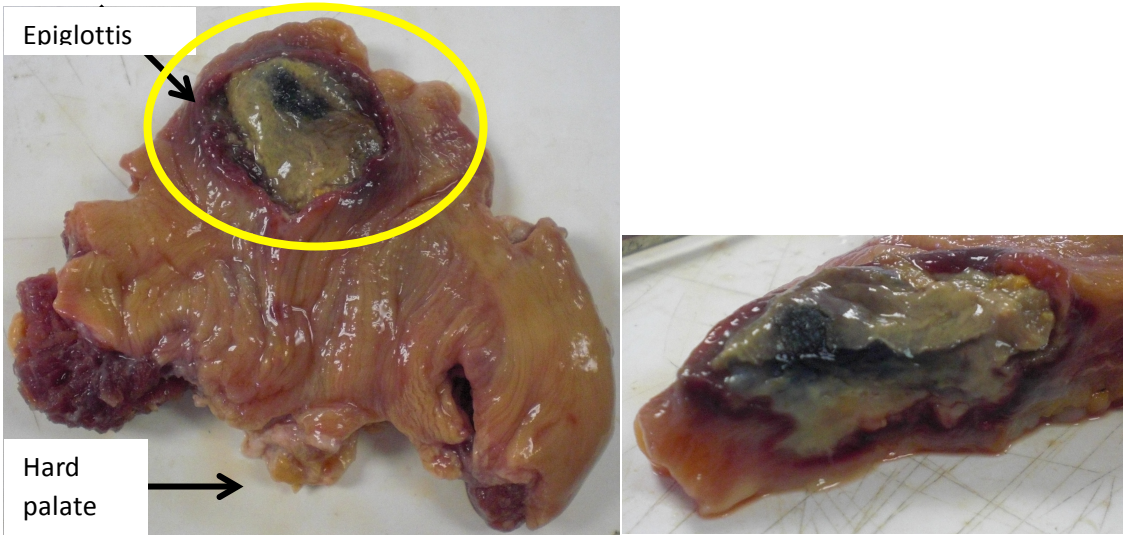

Figure 4.68: The soft palate from Horse #6 had a large region of gray necrotic tissue surrounded by a fibrotic encapsulation as seen in yellow circle in the picture on the left. Inside of this region, the tissue had some evidence of blue crosslinking, but it also had evidence of damaged tissue as seen in the picture on the right.

Dr. Cynthia Besch-Williford, a licensed veterinary pathologist, completed the histological analysis. Each sample was processed for paraffin infiltration, blocked, sectioned, stained with H&E and examined microscopically. A few of the samples were too large to fit in one cassette, so they were bisected and placed into two cassettes. Observed microscopic changes were described to the extent and grade of inflammation using terms including minimal, mild, moderate, and marked.

Overall, there was no specific trend in the severity or extent of inflammatory infiltrates related to the treated sections. However, the inflammatory response was linked to the extent of tissue necrosis. Two untreated samples, 4RB and 6LT, had tissue damage, fibroplasia and inflammatory responses similar to the treated tissues, suggesting to Dr. Besch-Williford that the crosslinking reagent had migrated to these regions despite the lack of any blue coloration. It is not likely that Dr. Besch-Williford came to the correct conclusion in this regard, being unfamiliar with the direct link between genipin penetration and the presence of blue coloration. In all samples, there was a moderate to extensive region of tissue disruption and necrosis in the middle or the core of the soft palate with abundant neutrophils associated with regions of tearing and lesions as shown in Figures 4.69 and 4.70. These results were most likely due to the consistently observed expansion, or pillowing of the tissue during the injections to accommodate the two 1 mL volumes of reagent (or 1.5 mL in the case of Horse #5) plus any aberrant amount of air used to push the reagent into the tissue, which caused the

tissue to be disrupted. Figure 4.71 demonstrated expanded vessels in the submucosa, caused by edema formed from mechanical disruption or tissue freezing. Bacteria colonized the necrotic region on the exterior of the soft palate from Horse #6, with encysted *Sarcocystis* bradyzoites also observed in the viable muscle as seen in Figure 4.72. The inflammation and fibroplastic responses of this tissue were most likely increased as a result of the bacteria present. Summaries of inflammation and fibroplasia scores for each section are listed in Table 4.9, and detailed histological analysis descriptions from IDEXX are listed in Appendix C4.

Based on the disruptive reagent delivery technique, it is unclear to what extent the tissue disruption, inflammatory response and scar tissue formation was due to the mechanics of the injections or due to the genipin reagent. By the presence of tissue disruption, inflammatory and fibroplastic responses in the control regions of the soft palate that had not been contacted by the genipin crosslinker, it is clear that the injection technique itself contributed to these histological observations. Additionally, the inadvertent creation of fibrotic tissue as a result of the disruptive delivery technique could have assisted in stiffening the soft palate, thus preventing dorsal displacement of the soft palate and causing a reduction in snoring. Due to the effects of the adverse reagent delivery technique, the relative contribution of the genipin agent itself has yet to be fully determined. Also, the histologic results are at a single, seven-day time point post injection and may not adequately reflect the long-term responses of the treatment and fibrotic tissue formation.

Table 4.9 Relative scores of inflammation and fibroplasia for each sample with 0=no significant change noted, 1=minimal, 2=mild, 3=moderate, and 4=marked.

Sample ID	Group	Inflammation Severity	Inflammation Extent	Central Tissue Necrosis	Fibroplasia
4LT	Treated	4	3	4	2
4LM	Treated	3	3	2	2-3
4LB	Control	0	0	0	0
4RT	Treated	4	4	4	2-3
4RM	Treated	4	4	4	3
4RB	Control	4	4	4	3
5LT	Treated	4	4	4	3
5LM	Treated	4	4	4	3
5LB	Control	0	0	0	0
5RT	Treated	3	4	3	2-3
5RM	Treated	3	4	2	2-3
5RB	Control	0	0	0	0
6LT	Control	2	2	1	1
6LM	Treated	4	3	4	2-3
6LB	Treated	4	4	4	3
6RT	Control	0	0	0	0
6RM	Treated	4	4	4	3
6RB	Treated	4	4	4	3

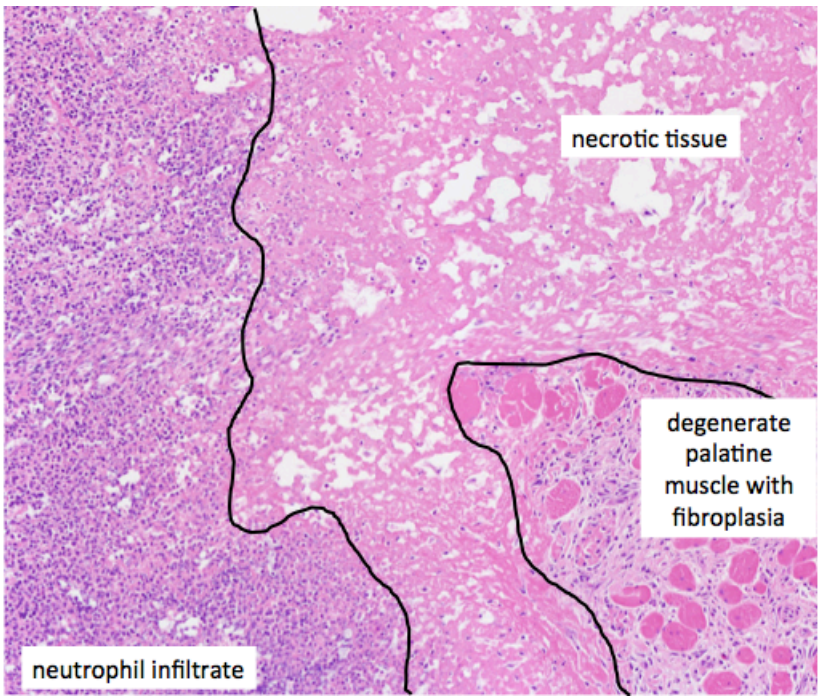

Figure 4.69: An image taken at 20X magnification from sample 4LM shows abundant neutrophils in the core of the biopsy with a mild to moderate zone of necrotic tissue. In this sample, degenerated palatine muscle with fibroplasia is also evident.

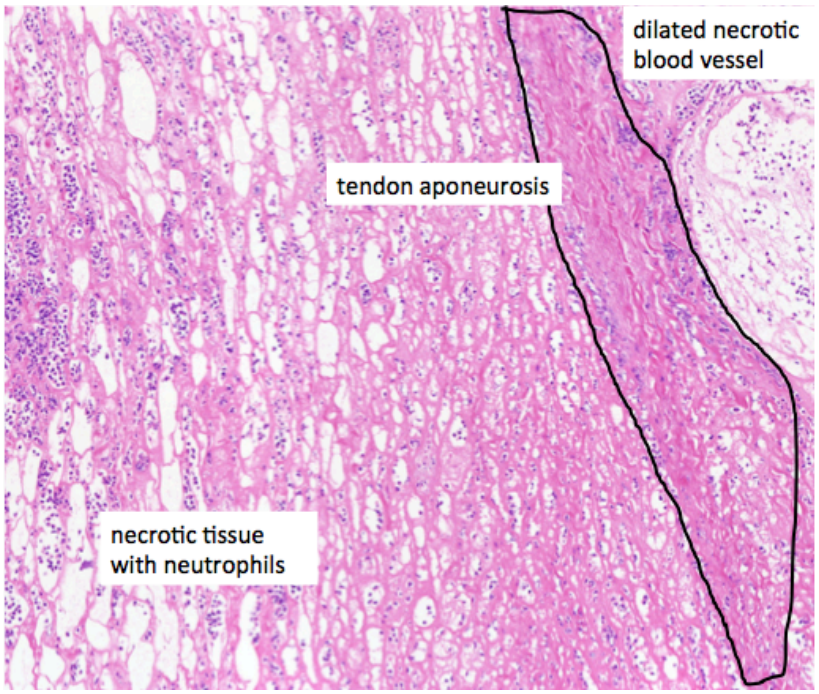

Figure 4.70: The 20x magnification image of sample 4RT showed an extensively necrotic core with distended blood vessels. The surrounding tissue had an abundant amount of neutrophil infiltrates

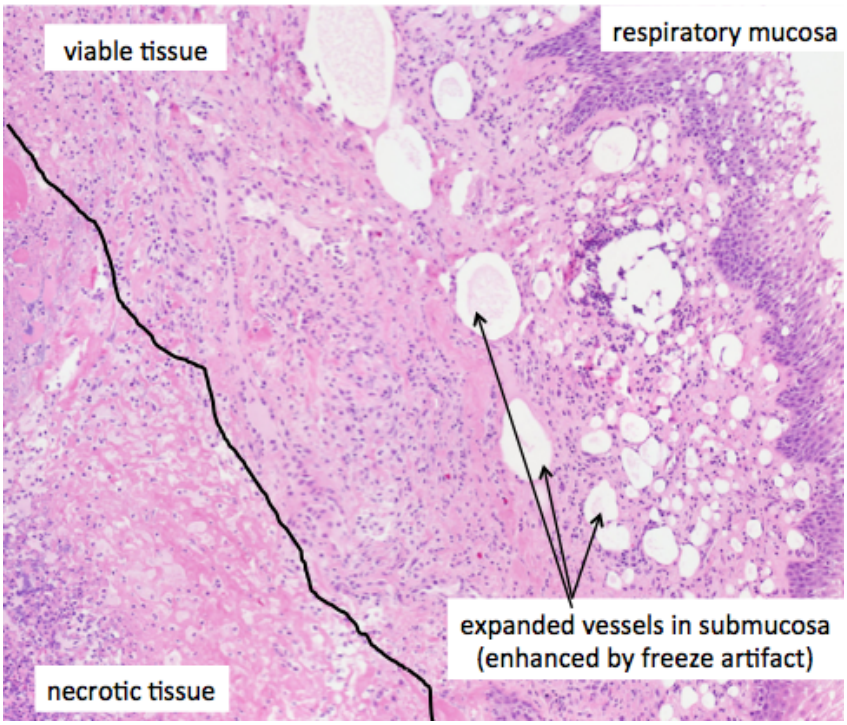

Figure 4.71: The connective tissue fibrils of the 4LT sample at 20x magnification were widely separated from edema, perhaps secondary to mechanical disruption, or tissue freezing as indicated by the arrows in the picture. Otherwise, the sample had necrotic collagenous stroma that was moderately infiltrated with neutrophils.

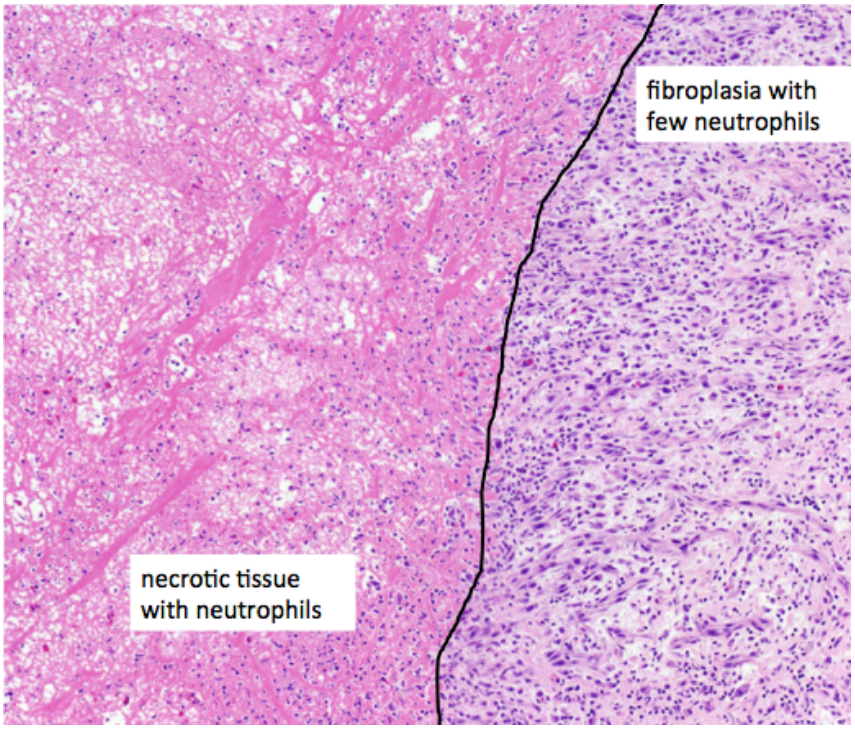

Figure 4.72: The 20x magnification image of the 6LM sample showed an extensively necrotic core surrounded by a region of fibroplasia. This sample had a few neutrophils present as well.

4.2 Soft Palate Mechanical Testing Study

The soft palate mechanical testing study examined the effects of the genipin treatment in cadaveric equine samples on the mechanical properties of the soft palate. The results of the hysteresis, stress relaxation, and tensile loading to failure tests were summarized in this section. Additionally, statistical analysis for each sample were completed and described.

4.2.1 Sample Preparation

Twelve cadaveric equine soft palates were obtained from Conboy Enterprises, Inc. in Lexington, KY. Each palate was thawed for 24 hours and extracted from the surrounding tissue. Then, two to four sections were cut from each palate following the Figure 3.10 from Chapter 3 with two top sections cut closest to the edge contacting the epiglottis and with two bottom sections cut closest to the hard palate. Palates #5, #6, and #9 only had two sections cut from it, and Palate #1 only had three sections cut from it due to size and quality issues with the individual palate specimens. The remaining palates had four sections cut from them. The palate sections were then divided into 3 test groups. The control group had 14 total samples, with 8 top sections and 6 bottom sections. The buffer group had 12 total samples, with 6 top sections and 6 bottom sections. The genipin group had 17 total samples, with 9 top sections and 8 bottom sections.

Each sample was then treated with the appropriate reagent or left untreated based on their specific test group based on Figure 3.11 from Chapter 3. The reagents were delivered into the middle of the sample at an approximately 30-degree angle from the horizontal. The best way to ensure even coverage of the reagent, based on trial and error injection tests, was to insert the needle slightly toward one end but adjacent to the halfway point of the length of the sample, and then dispense the reagent as the needle was being pulled out. The needle was inserted to about half of the depth of the tissue, then the reagent was injected with even pressure at a rate of approximately 0.1 mL per second as the needle was being slowly extracted. This method allowed the reagent to cover a larger cross-sectional area and helped to prevent any expansion of the tissue to accommodate the liquid. If the entire reagent volume was injected entirely in one location, then the tissue would expand like a ‘pillow’ to accommodate the extra fluid. As noted, in the histology results from the *in vivo* study, the ‘pillowing’ effect was associated

with tearing and lesions within the tissue leading to neutrophil invasion and necrotic tissue in and around the injected area, so the 'pillowing' effect was avoided in the mechanical testing study. The injection time and location on the soft palate were noted for each sample. After incubation, the samples were necked down to approximately 1 cm wide, which was about half of the starting width of each sample. The length, width and depth of the entire sample and necking region were measured using a ruler and recorded. For the genipin samples, the area of blue visible on the outside surface of the sample was also measured using a ruler and recorded. In most of the top samples, the genipin reagent covered the entire cross-sectional area of the necking region based on observations of the outside edges of the specimen. In thicker samples, the volume of genipin injected was not sufficient to cover the entire cross-sectional area of the tissue; therefore, the blue crosslinked region would be located more towards the top layer of the samples only. All pertinent information and testing notes for the soft palate mechanical testing study is included in Table 4.10 in Appendix D1.

4.2.2 Mechanical Testing

Each sample first underwent the hysteresis test. For all samples, a load of 10 N was applied, and then the sample was displaced ± 3 mm from the starting point for 20 cycles. One sample, SP8BLB, underwent the hysteresis test twice because the 10 N preload was not applied in the first one. Using the time (s), stroke (mm), and load (N) values recorded from the tensile testing machine, the 1st cycle hysteresis, 20th cycle hysteresis, change in hysteresis and hysteresis ratio were calculated. Additionally, the 1st and 20th cycle hysteresis curves, as well as the entire hysteresis graph, were plotted for each specimen. Example 1st cycle, 20th cycle, and entire hysteresis curves for a control, buffer and genipin sample are shown in Figures 4.73 – 4.78. In general, based on the graphs, the genipin treated experienced a trend of more hysteresis in the 1st cycle, but the difference was not statistically significant. Additionally, the genipin treated samples experienced a larger change in hysteresis over the course of the 20 cycles, but the difference was not statistically significant. The hysteresis test parameter results for all individual samples are shown in Table 4.11 in Appendix D2.

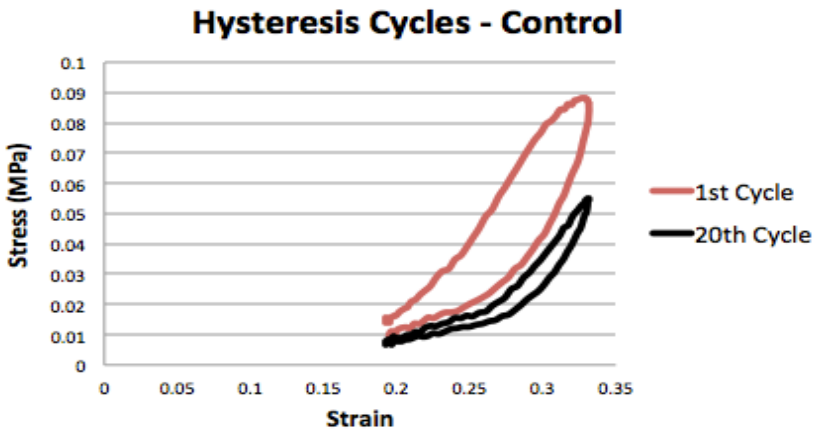

Figure 4.73: The 1st and 20th cycles for the hysteresis curve for the control sample show a reduction in the area between the curves for the two cycles.

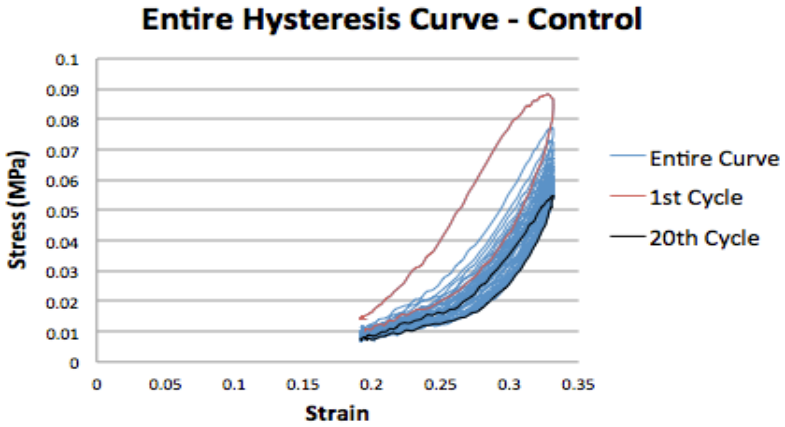

Figure 4.74: The entire hysteresis curve for the control samples demonstrates where the 1st and 20th cycle are in relation to the rest of the curve. It also demonstrates the reduction in maximum stress as the cycle number increases.

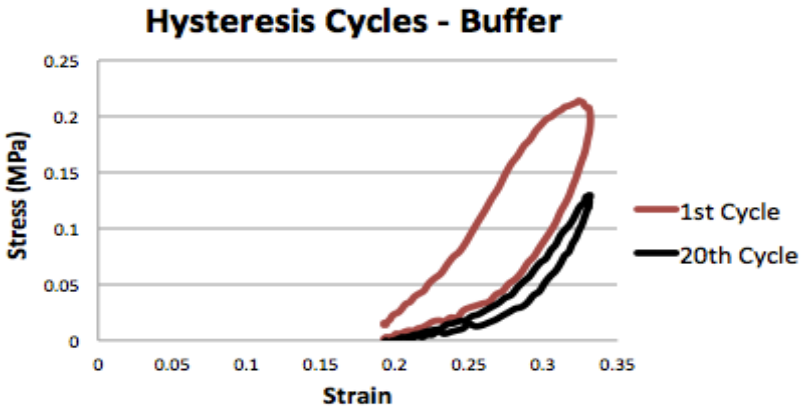

Figure 4.75: The 1st and 20th cycles for the hysteresis curve for the buffer sample show a large difference in the area between the curves for the two cycles.

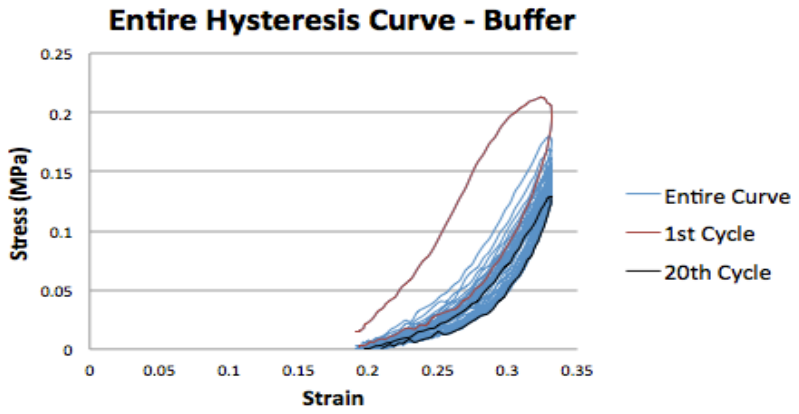

Figure 4.76: The entire hysteresis curve for the buffer samples demonstrates where the 1st and 20th cycle are in relation to the rest of the curve. It also demonstrates the reduction in maximum stress as the cycle number increases.

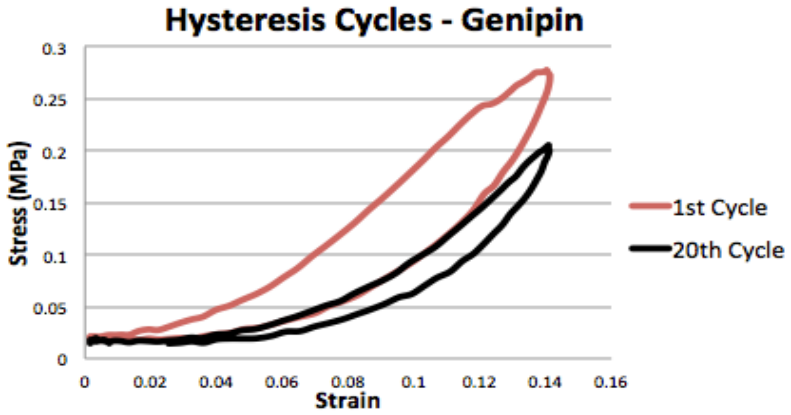

Figure 4.77: The 1st and 20th cycles for the genipin sample show a smaller difference in the area between the curve compared to the buffer and control samples.

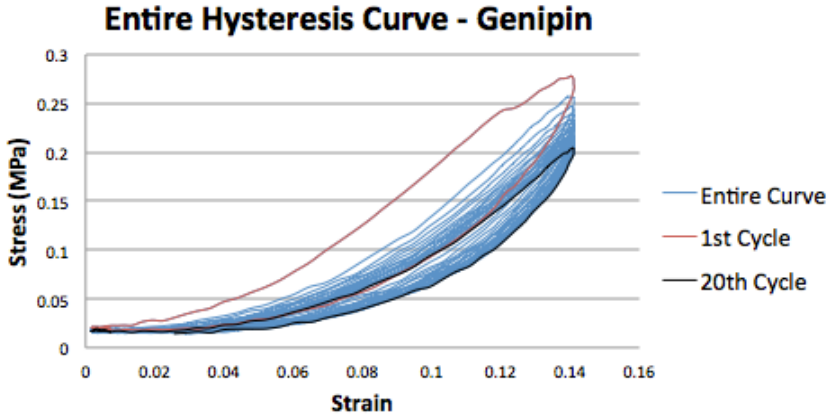

Figure 4.78: The entire hysteresis curve for the genipin samples demonstrates where the 1st and 20th cycle are in relation to the rest of the curve. It also demonstrates a longer toe region when applying load during cyclical loading for the genipin samples.

Next, each sample underwent the stress relaxation test, where the sample was preloaded with 10 N and held at a constant deformation for 5 minutes. One sample, SP3TRB, underwent the stress relaxation test twice because the first set of data was not recorded. Using the time (s), stroke (mm), and load (N) values recorded from the tensile testing machine, the minimum stress, maximum stress, stress relaxation, relaxation modulus, and normalized relaxation modulus were calculated, and the respective graphs were plotted. Examples of stress relaxation graphs for the control, buffer and genipin samples are shown in Figure 4.79. Based on the figure, the buffer specimen appears to have a larger stress relaxation, however, the differences between the three groups was not statistically significant as further discussed below in Section 4.2.3.

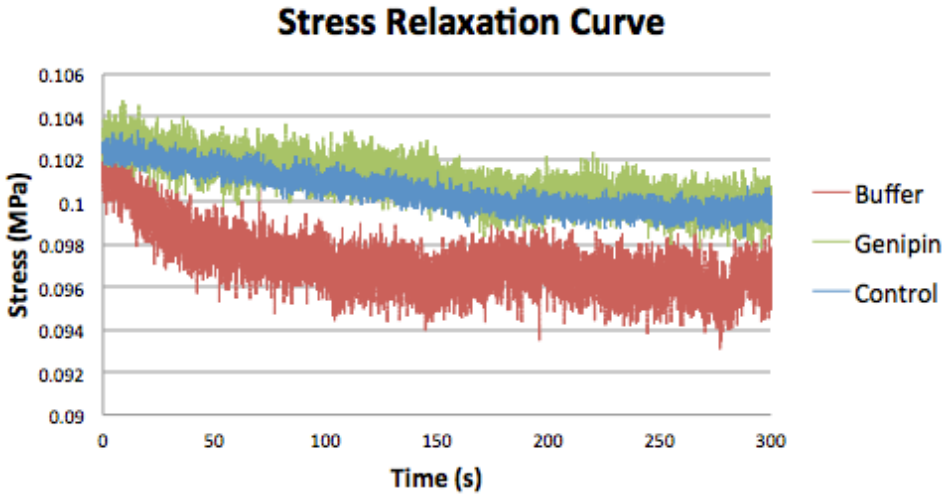

Figure 4.79: Typical stress relaxation curves for the buffer, genipin, and control groups.

Also, the relaxation modulus and normalized relaxation modulus were calculated for each sample. The normalized relaxation modulus was calculated by dividing the individual sample strain by the average strain for that test group. The averages for the control group, buffer group and genipin group were 0.2771 MPa, 0.3027 MPa, 0.2355 MPa, respectively. The normalized relaxation modulus in general showed an increase for the genipin and buffer treated samples as shown in Figure 4.80, but the differences were not statistically significant. The stress relaxation test results for individual samples are shown in Table 4.11 in Appendix D2.

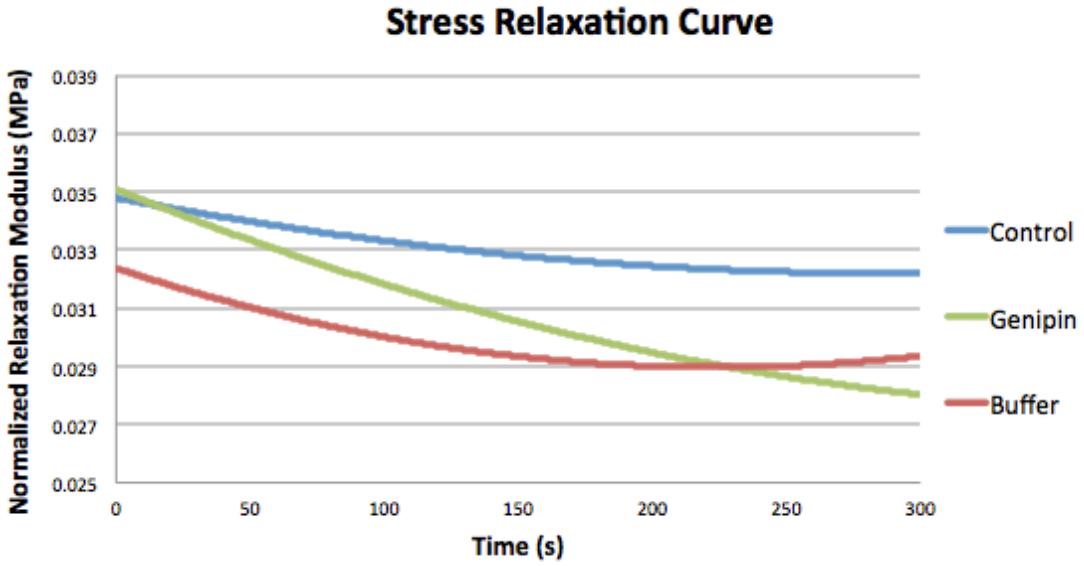

Figure 4.80: The normalized relaxation modulus, which was normalized to the individual averages for each test group, displayed an increase for the genipin and buffer treated samples, although the differences were not statistically significant.

Finally, each sample underwent a tensile load to failure test at a rate of 1 mm/second. During the SP4TLG sample's tensile test, the tissue slipped out of the grips during the early loading phase before any failure was observed, thus requiring the test to be repeated. In general, the samples failed diagonally along the outer layer fibers in the middle of the sample for 34 of the 44 samples, or 77% of the time. The remaining samples failed outside of the middle region, closer to the grips. Using the time (s), stroke (mm), and load (N) values recorded from the TestResources system, tensile stress and strain parameters were determined. Then, the stress-strain curve was plotted, and from that, the toe region slope, Young's Modulus, yield stress, yield strain, toughness, energy, and resilience were calculated. Examples of stress strain curves for the control, buffer and genipin samples are shown in Figures 4.81-4.83. In general, the different treatment groups all had similar stress-strain profiles, with a defined toe region, linear region and yield point. The tensile test results for individual samples are shown in Table 4.11 in Appendix D2.

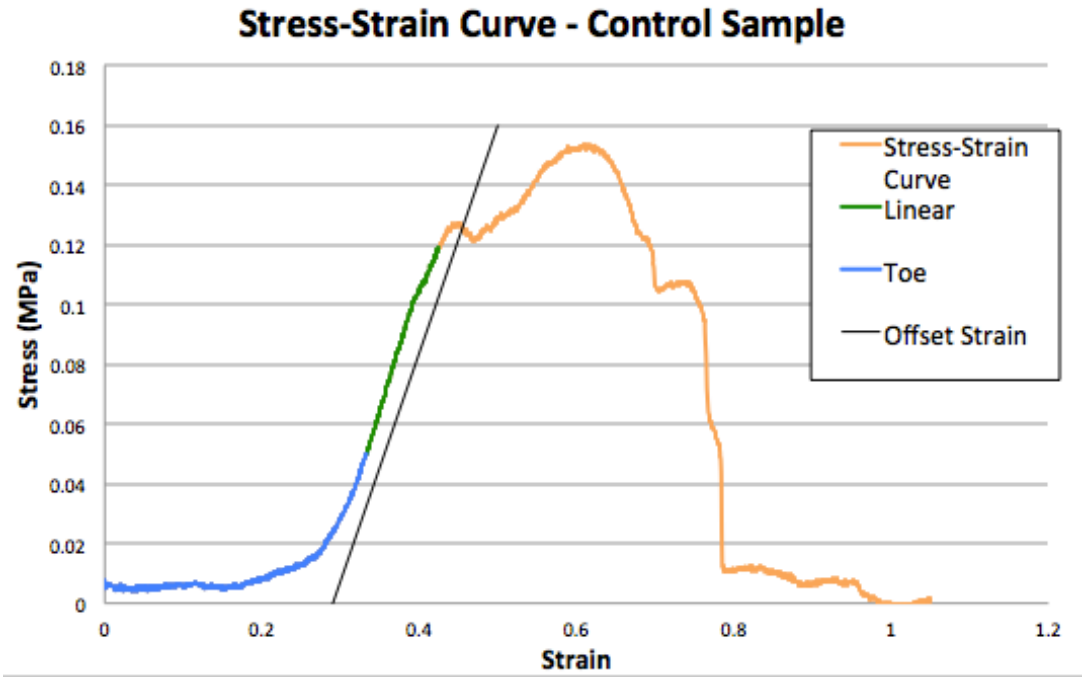

Figure 4.81: The stress strain curve allowed many important parameters to be calculated for each test group. This sample stress strain curve for the control group shows an obvious yield point at the intersection of the curve and the offset strain line.

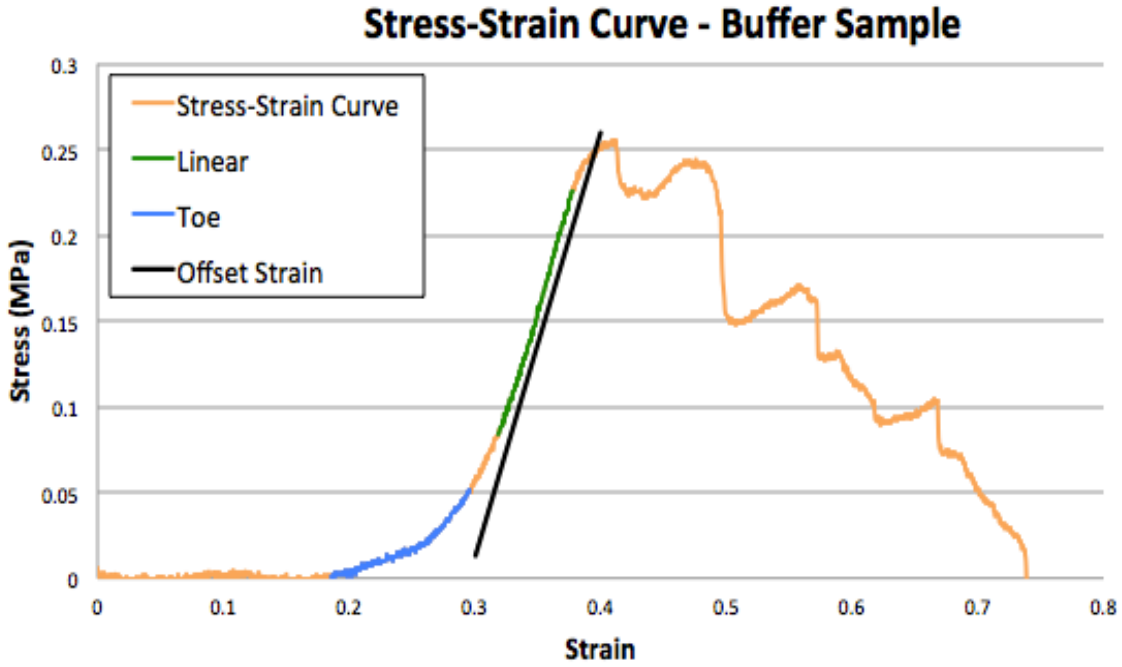

Figure 4.82: The stress strain curve allowed many important parameters to be calculated for each test group. This sample stress strain curve for the buffer group highlights the toe region and linear region, as well as the offset strain line, that were used to calculate the respective slopes and yield point.

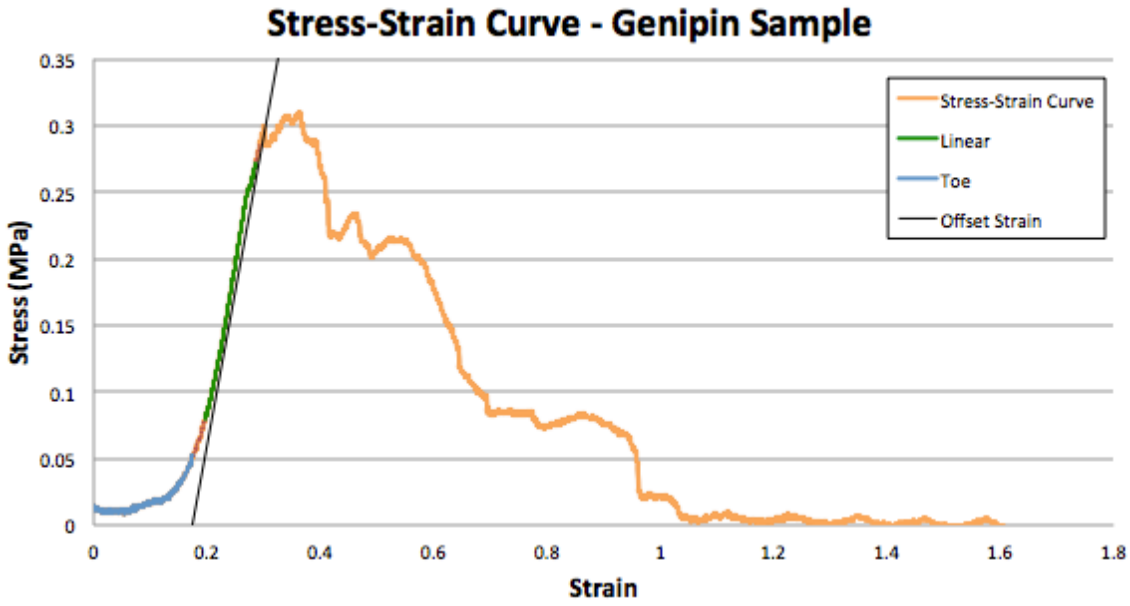

Figure 4.83: The stress strain curve allowed many important parameters to be calculated for each test group. This sample stress strain curve for the genipin group demonstrates how the maximum point on the graph is usually not equal to the yield point, as shown by the offset strain line intersection with the stress strain curve.

4.2.3 Mechanical Testing Analysis

Once all of the parameters were determined for each sample, the outliers were removed using the three-sigma rule, meaning that any sample with results more than three standard deviations away from the mean in a specific parameter was considered to be an outlier for that category. Any sample that had five category outliers was considered to be an overall outlier, and removed from the data set. There were five outliers in total: SP1TLG, SP7TLG, SP12BLG, SP3TRB, and SP10TRC. The three genipin samples, SP1TLG, SP7TLG, and SP12BLG, all failed above the blue, crosslinked region, meaning the tensile testing data did not test the genipin treated area. The buffer sample, SP3TRB, was an outlier because the stress relaxation test was repeated twice, leading to different mechanical testing results because of the collagen fibers were more relaxed. The control sample, SP10TRC, was a very flimsy and unhealthy sample. This left 12 samples in the control group, with 6 tops and 6 bottoms; 11 samples in the buffer group with 5 tops and 6 bottoms; and 14 samples in the genipin group with 8 tops and 6 bottoms. A summarized chart of the samples in each group and their values for all parameters is included in Table 4.12 in Appendix D3.

All of the viscoelastic and elastic-plastic parameter averages and standard deviations were calculated for each test group, as well as for the separated top samples and bottom samples. The top samples data was analyzed separately from the bottom samples because the thickness of the soft palate varies significantly when moving from the free end of the soft palate toward the hard palate. Therefore, the thinner top samples cut closest to the free end of the palate had a larger density of crosslinking treatment compared to the thicker bottom samples cut closer to the hard palate because the collagen content decreases when moving from the epiglottis to the hard palate, causing there to be a large variation in the results among test groups. Separating the top and bottom samples allowed for smaller standard deviations for each parameter. The averages and standard deviations for each group with the outliers removed are summarized in Table 4.13 in Appendix D4.

Using the averages for each parameter, the percent differences were determined. First, the percent differences between the control group and buffer group were calculated to see if injection of the buffer alone had any effect on the mechanical properties of the soft palate, as summarized in Table 4.14. Any statistically significant percent difference greater than 25% were noted in red. The percent differences between the buffer group and genipin group were calculated to determine the effect of the genipin treatment on the mechanical properties of the soft palate. Any statistically significant percent difference greater than 25% were highlighted in red, as summarized in Table 4.15. Some differences were expected between the buffer-only treated samples and the control samples due to the dramatically increased hydration in these samples. Using these differences, the effect of the genipin injection could be deduced based on the effects of the increased hydration caused by the injection of the solvent on the mechanical properties.

For the statistical analysis, either a *t*-test or Mann-Whitney U non-parametric test were completed based on whether the variance of the sample groups could be considered the same, as determined by the F-test. To complete the F-test, first the critical F-value (F_{crit}) was determined for each comparison using an F-table. Then, the F value was calculated. If the F value was less than the F_{crit} value, then the variances were considered to be the same and the *t*-test was used. If not, then the Mann Whitney U test was used. The F_{crit} values for each comparison are shown in Table 4.16, and the individual F values for each parameter are listed in Table 4.17 in Appendix D5. All F

values that are larger than the F_{crit} value for that comparison are highlighted in red. Based on the results of the F-test, the *t*-test could be applied to the buffer versus control comparison for the overall samples and the top only samples, and to the buffer versus genipin comparison for the tops only samples because the variances were assumed to be the same with an alpha of 0.05. For the remaining comparisons, the Mann-Whitney U non-parametric test was completed because the variances could not be assumed to be the same based on the failure of the F-test with an alpha of 0.05. Statistically significant parameters are marked with an asterisk (*) in Tables 4.14 and 4.15. Individual p-values for each parameter are shown in Table 4.18 in Appendix D6.

Table 4.14: COMPARISON OF BUFFER-ONLY GROUP TO CONTROL GROUP – The percent differences for the buffer samples compared to the control samples for each parameter were broken down into the top samples only, bottom samples only and overall samples. The results were reported based on how the buffer group average relates to the control group average. Statistically significant results with a p value less than 0.05 with α=0.05 are marked with an asterisk and highlighted in red (*).

Parameter	Top Samples Only	Bottom Samples Only	Overall Samples
Cross Sectional Area	14.64 % decrease	22.90 % decrease	18.57 % decrease
Ultimate Tensile Stress	6.40 % decrease	65.88 % increase*	16.24 % increase
Ultimate Tensile Strain	6.49 % decrease	33.08 % increase	11.14 % increase
Yield Strain	3.24 % increase	12.14 % increase	7.10 % increase
Yield Stress	4.48 % increase	34.54 % increase	14.02 % increase
Young's Modulus	4.42 % decrease	11.35 % increase	0.26 % decrease
Resilience	20.11 % decrease	276.07 % increase	49.67 % increase
Toe Region Modulus	17.28 % increase	30.61 % decrease	6.55 % decrease
Toughness	56.17 % decrease	140.94 % increase*	35.29 % decrease
Energy to Failure	58.63 % decrease	92.34 % increase	34.49 % decrease
1st Cycle Hysteresis	4.44% increase	17.66% increase	8.52% increase
Change in Hysteresis	9.48 % increase	16.63 % increase	11.38 % increase
Hysteresis Ratio	13.94 % decrease	4.47 % decrease	10.09 % decrease
Stress Relaxation	19.39 % increase	48.98 % increase	29.98 % increase
Relaxation Modulus	24.36 % increase	30.22 % increase	26.69 % increase
Normalized Relaxation Modulus	78.16% increase	42.26% increase	58.32% increase

Table 4.15: COMPARISON OF GENIPIN AND BUFFER-ONLY INJECTED GROUPS – The percent differences for the genipin samples compared to the buffer samples for each parameter were broken down into the top samples only and overall samples. The results were reported based on how the genipin group average relates to the buffer group average. Statistically significant results with a p value less than 0.05 with α=0.05 are marked with an asterisk and highlighted in red(*).

Parameter	Top Samples Only	Overall Samples
Cross Sectional Area	11.95 % decrease	20.49 % decrease
Ultimate Tensile Stress	51.67 % increase*	31.20 % increase
Ultimate Tensile Strain	32.89 % decrease	30.88 % decrease*
Yield Strain	34.57 % decrease	30.65 % decrease
Yield Stress	53.04 % increase*	42.69 % increase*
Young's Modulus	63 % increase*	56.02 % increase*
Resilience	6.43 % decrease	27.51 % decrease
Toe Region Modulus	118.34 % increase	118.33 % increase
Toughness	11.99 % increase	9.71 % increase
Energy to Failure	6.60 % increase	6.99 % decrease
1st Cycle Hysteresis	10.31% increase	23.41% increase
Change in Hysteresis	1.08 % decrease	14.88 % increase
Hysteresis Ratio	30.20 % increase	23.24 % increase
Stress Relaxation	4.09 % increase	9.19 % increase
Relaxation Modulus	74.10 % increase	71.54 % increase
Normalized Relaxation Modulus	96.28% increase	69.61% increase

When comparing the buffer samples to the control samples, it was expected that an increase in hydration would have an effect on the mechanical properties of the buffer-

only treated samples, however, there should not be many parameters with a statistically significant difference of more than 25%. Based on the results summarized in Table 4.14, the tops only buffer treated group and the overall buffer treated group had no parameters that had statistically significant differences from the control group. Since the tops only and the overall category did not have any statistically significant differences between the buffer treated samples and the control samples, it proves that the buffer treatment alone does not have any significant effect on the mechanical properties of the soft tissue for these test groups, despite the increase in hydration. This means that when the buffered genipin reagent is injected into the soft palate, the crosslinking affect caused by the genipin is presumed to be the primary contributor towards any changes in the mechanical properties.

On the other hand, the bottom only group had two parameters with statistically significant differences between the buffer treated group and the control group. Due to the statistically significant differences for two of the parameters, the bottom only group was determined to demonstrate a change in the mechanical properties when treated with the buffer only group. An effect by the buffer only treatment could be evident in the bottom only samples due to the large variation in the collagen content compared to the tops only samples. Additionally, the thicker samples may have retained more of the injected water, causing an increase in hydration that had an effect on the tissue's properties. Finally, since the bottom samples were thicker, the volume of genipin reagent injected may not have been able to adequately cover the entire cross-sectional area of the tissue compared to the thinner samples. Therefore, the bottom only samples were not used to compare the effect of the genipin treatment on the soft palate.

Finally, the genipin samples were compared to the buffer samples to determine the effect of the genipin treatment on the mechanical properties of the soft palate. Again, only the tops-only and the overall groups were statistically analyzed due to the bottoms-only group showing significant effects caused by a variety of reasons, as previously explained. The tops-only groups had statistically significant differences from the buffer treated samples in three parameters: ultimate tensile stress, yield stress and Young's modulus. The overall group had statistically significant differences for three categories as well: ultimate tensile strain, yield stress, and Young's Modulus.

None of the parameters from the hysteresis test demonstrated a statistically significant difference between the genipin treated samples and the buffer treated

samples. Similarly, the stress relaxation test did not produce any parameters with statistically significant differences. Consequently, there was no measurable effect of the genipin crosslinker on the viscoelastic properties of the soft palate.

The tensile test produced three parameters with statistically significant differences between the genipin treated group and the buffer treated group. Ultimate tensile stress ($p=0.021$) and strain ($p=0.006$) had statistically significant results for the tops only group and the overall group, respectively. The increase in ultimate tensile stress shows an increase in strength for the genipin treated samples, which is supported by a previous study that crosslinked spinal discs with genipin and demonstrated a statistically significant 20.7% increase in ultimate tensile strength ($p=0.036$) [19]. Another study that treated equine tendons produced statistically significant results in the ultimate tensile stress ($p<0.0001$) and strain ($p=0.01$) for genipin treated tissues [71]. The decrease in ultimate tensile strain showed an increase in stiffness. Both of these results enhance the soft palate, making it stronger and stiffer, and thus better able to resist displacement. Similarly, Young's modulus had a statistically significant ($p=0.026$ for tops-only and $p=0.014$ for overall) increase, demonstrating that the treated tissue is stiffer due to the genipin crosslinking, which was supported by an increase Young's modulus for the genipin treated samples in the tendon study ($p<0.0001$) [71].

As previously mentioned, yield stress and strain are important parameters in soft tissue applications because they mark the point at which the material begins to plastically deform, resulting in permanent deformation or injury to the tissue. The yield stress showed a statistically significant ($p=0.017$ for tops-only and $p=0.049$ for overall) increase in the strength of the genipin treated tissue for both the tops only and overall groups. This result was supported by previous studies that utilized genipin to crosslink spinal discs, which showed a statistically significant increases in yield stress ($p=0.012$) [19-20]. Yield strain was not statistically significant, but appeared to trend more than 25% lower for both the tops-only and overall groups.

Also, the statistically significant increase in yield stress without a statistically significant change in resilience suggests that there was no increase in the brittleness of the tissue compared to the buffer-only samples. The percent differences for resilience supported this because they were all less than 15%, showing that the energy required to plastically deform the genipin treated tissues was not statistically different than the control samples. Similar studies conducted in the tendon and intervertebral disc showed

statistically significant increases in the resilience (p=0.01 and p=0.019, respectively), meaning that genipin typically increases the resilience in tissues with a higher percentage of collagen content [19-20,71]. Since the soft palate has less collagen present, it makes sense that the resilience would not necessarily be as affected by the genipin treatment. Similarly, the energy required to permanently deform the tissue increased, but it was not statistically significant meaning that the toughness of the soft palate tissue was not affected by the genipin treatment. This was supported by similar tests in the disc that showed an increase in toughness, without statistical significance (p=0.170), meaning that genipin does not negatively affect the toughness of the tissue [19-20]. Based on these results, the genipin treatment created statistically significant differences in the ultimate tensile stress, ultimate tensile strain, yield stress and Young's modulus categories, exhibiting an increase in strength and stiffness of the soft palate.

5. Conclusions

Snoring and OSA are sleep disorders caused, in part, by mechanical degradation of the soft palate due to accumulated damage from snoring. Some current treatments focus on preventing snoring and OSA by increasing stiffness through fibrotic tissue formation, even though fibrosis formation leads to inferior mechanical properties. A genipin reagent was used as a treatment for the soft palate to prevent snoring and deformations and to also improve the mechanical properties by crosslinking the native collagen fibers. The genipin treatment was tested using a pilot equine *in vivo* study and a soft palate mechanical testing study.

The success of the pilot equine *in vivo* study relied upon the results of the respiratory audio recording, the dynamic endoscope examinations and the owner's reports. At least one of the horses was diagnosed as no longer having DDSP, and no longer shows any symptoms associated with the disorder. Another horse did not have a post treatment dynamic endoscope examination completed; however, based on the audio analysis and the owner's update, the horse is no longer experiencing any DDSP symptoms, including snoring, palatal displacements, or exercise intolerance. The final horse was diagnosed with DDSP still, but has showed improvements in exercise tolerance and snoring loudness. Histological results showed no specific inflammatory infiltrate trends. However, there was evidence of adverse responses due to errant injections, such as the necrotic tissue on the mucosal surface and the tearing and lesions due to the 'pillowing' of the soft palate during transnasal endoscopic injections.

The histology samples also had an appearance of fibroplasia, which could mean that the effective treatment of the DDSP horses may be due to a combination of the inadvertent fibroplastic response to the over-extension of the soft palate during injection and of the mechanical effects of the genipin treatment.

Future *in vivo* studies should focus on reduced injection volumes and alternative delivery methods to avoid errant injections and the over-extension of the soft palate during injections. Using the 1-meter long endoscope proved to be difficult to inject the soft palate due to issues with controlling the endoscope and clearly seeing the injection site. New possibilities for delivery methods include using coated sutures to release the genipin and to avoid errant injections, or using reduced injection volumes and multiple injection sites to avoid the 'pillowing' effect. Also, a video endoscope could be used to make viewing the injection area easier. Likewise, a larger *in vivo* study should be completed to test the effectiveness of the genipin treatment at different volumes and concentrations. Eventually, the genipin treatment should be tested in human trials to test the efficacy of the genipin injections for snoring and OSA applications.

The soft palate mechanical testing study produced statistically significant results in four categories for the genipin treated samples compared to the buffer treated samples, with an increase in ultimate tensile stress, yield stress, and Young's modulus and a decrease in yield strain. These results demonstrate an increase in tissue strength and stiffness, leading to an increase in tissue stability. The location of the samples in relation to the hard palate proved to have an effect on the results of the mechanical tests. The samples taken closer to the epiglottis produced statistically significant improvements in the mechanical properties due to their higher collagen content compared to the samples closer to the hard palate, thus indicating that the preferred treatment location is closer to the free edge of the soft palate near the epiglottis.

Future research should focus on standardizing the reagent delivery method. There is a large learning curve when it comes to injecting the reagent uniformly throughout the entire cross-section of the sample. Therefore, research should be done to determine the ideal injection angle, pressure and location. Similarly, the appropriate volume of the reagent to administer should be determined based on the cross-sectional area of the specific sample since the thickness of the soft palate increases from the free edge near the epiglottis to the hard palate. Finally, the mechanical testing study should

be repeated with human soft palates to determine the effects of the genipin treatment on human soft palate mechanical properties.

Overall, the *in vivo* study and mechanical testing study supported the hypothesis by showing reduction of aberrant vibrations and displacements while also improving the mechanical properties of the soft palate. The reduction in snoring loudness and palatal displacement in the *in vivo* study agreed with the increase in tissue stiffness from the mechanical testing study. The increase in tissue strength suggests that the stability of the tissue was increased by the genipin treatment. The histology results suggested that the microstructural and compositional integrity could be conserved with proper reagent delivery. This was further supported by the maintenance of the viscoelastic properties of soft palate as demonstrated by the hysteresis and stress relaxation tests. In essence, the genipin treatment demonstrated an increase in tissue strength, stiffness and stability based on the results from the *in vivo* study and the mechanical testing study, suggesting that genipin-based treatments should be further evaluated, and could become an effective and safe treatment for snoring and OSA applications.

APPENDIX A1: Dr. Sprayberry's questions and answers for *in vivo* study

Answers by Dr. Kim Sprayberry in bold

General Questions:

1. What needs to be done to obtain the DDSP horses?
    - **What is necessary is to contact either trainers or veterinarians in the Illinois/Indiana/Missouri region who have horses with DDSP and would be willing to transport them to the study center.**
    - **I do not know many trainers or vets in those areas, and the few contacts I do have, have not been able to summon up any affected horses.**
2. What needs to be done to obtain the thoroughbreds?
    - **Same answer: the Thoroughbreds are the DDSP horses, and we need to contact people in the area of the contract researcher so we can enroll some horses. The problem is that this is a region of the country where racehorses are less numerous than in Kentucky, and I do not have many contacts there.**

Pre-Treatment Exam:

1. Can this be done at the horse's barn prior to sending the horse to Missouri or does this need to be completed at Missouri?
    - **A horse with DDSP would likely have already had an endoscopic exam to confirm the diagnosis. So yes, this pretreatment exam COULD be done at the horse's home barn. However, for the purposes of recording 'before' and 'after' pictures and comparing, it would be more uniform and repeatable if the B & A photos were done with the same equipment.**
2. What does the exam all need to include?
    a. Endoscopic exam? **Yes.**
    b. General exam? **Yes.**
    c. Record breathing? **Yes, although the abnormal breathing heard with DDSP typically is only audible during exercise, not at rest.**
3. Can their regular veterinarian complete this exam or do all exams need to be completed by you?
    - **Any veterinarian with an endoscope can do this. The only caveat is if we are going to be using B&A images to judge or score results. Then we'd run into a confounding factor with image variability stemming from different scopes, light sources, and other factors.**

Transportation:

1. Is there a certain company you recommend to transport the horses to Missouri?
    - **Not really; any company or individual with experience in hauling horses should be fine.**

Timeframe:

1. Approximate dates of study that would work for you?
    - **I can spend 2 days at a time, and would most easily be available for this beginning mid July. I am teaching summer school in the first session, meaning I'll be tied up from mid June until mid July. After that, I am very flexible and relatively uncommitted. I will also be in Lexington for 3-5 days sometime in late July or early August.**
2. How many days would you want the horses there before the study?
    - **Just 1.**
3. Any health requirements?
    a. Shots required? **No**
    b. Coggins? **Only as required for transport across state lines.**
    c. Health Certificate? **Ditto**

Breathing Recording:

1. Should the horse's breathing be recorded just during exercise or during both exercise and rest?
    - **Both**
2. How long to record the horse's breathing during exercise? i.e. is 5 minutes sufficient or do you suggest shorter or longer?
    - **5 minutes should be sufficient. We may find that a trainer will relate that his/her horse only begins making the noise after being on the track for 10 minutes, and in this regard, horses can vary among individuals. But most horses are on the track for no more than 10 minutes in the mornings, and that is when the abnormal sound associated with DDSP are heard.**
3. How strenuous should the horse be exercising? i.e. walk, jog, lope, gallop, etc.
    - **Galloping**
4. Does the breathing recording need to be completed within a certain timeframe? Does a week before study work or would a day before the study be sufficient?
    - **Either interval would be fine**
5. Do you think a microphone attached to the halter/bridle be sufficient data to record DDSP frequency?
    - **The best way of objectively confirming that any given horse has DDSP is to have a dynamic endoscope in place while the horse is galloping and record real-time images of the laryngeal abnormality. This equipment is increasingly in use.**

APPENDIX A2: Digital voice recorder specifications

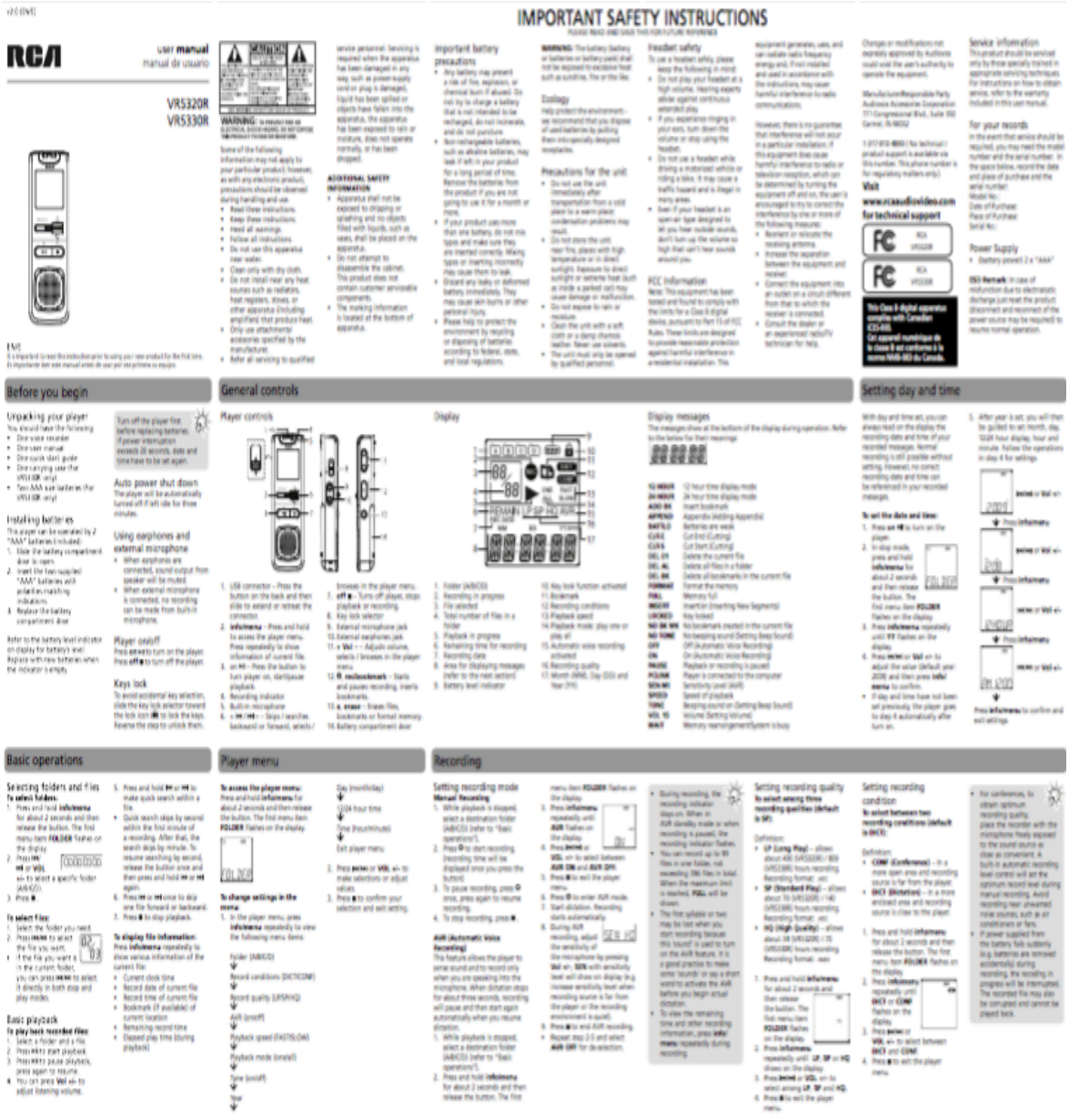

IMPORTANT SAFETY INSTRUCTIONS

RCA

user manual
manual de usuario

VR5320R
VR5330R

Before you begin

General controls

Setting day and time

Basic operations

Player menu

Recording

Erasing files and bookmarks

Erasing mode

To erase files or bookmarks while playback is stopped:

1. Press ■ once.
2. Press **MENU** to select one of the erasing options.
   - Delete the current file (**DEL ONE**)
   - Delete all files in the current folder (**DEL ALL**)
   - Format the memory of the player (**FORMAT**) (**Caution! All data inside the memory will be erased**)
   - Delete all bookmarks in the current file (**DEL BK**)
3. With one of the above options selected, press and hold ► for about 3 seconds to confirm your selection and start the deletion.

- File numbers that come after erased one will be moved forward by one automatically.
- Press ■ to cancel erasing all files. The undeleted files are saved automatically.

- Formatting the internal memory may be required when:
  1. The flash memory becomes unstable after performing many times on file creation and deletion.
  2. To ensure the file system compatibility (i.e. file system FAT12 for applications).
- You may also format the player when connected to a PC by right-clicking on the player's drive name or letter and select "Format" from the menu. Make sure you select FAT or FAT32 as the file system.

Editing

CAUTION

- The edit function does not operate when battery power is too low.
- Make sure **PLAY ALL** files is not selected. Inserting new segments, adding appendix and cutting cannot be performed when **PLAY ALL** files is selected.
- After editing a message, **WAIT** may be displayed. Do not power off the player until **WAIT** disappears. Otherwise, the memory which is rearranging could not be read or released until the player is formatted.

Editing mode

To insert bookmarks, new segments or appendix to a recorded file:

1. Select the desired file and start playback.
2. Press ⏻ during playback to enter editing mode. Playback is paused.
3. Press **MENU** to select one of the editing options:
   - Insert an interruption point (bookmark) into the current file for quick reference (**ADD BK**)
   - Insert a new segment into the current file (**INSERT**)
   - Insert an appendix at the end of the current file (**APPEND**)
4. With one of the above options selected, press ⏻ again to confirm your selection and start the editing.
- Refer to the following sections for details.

Bookmark

To create bookmarks:

- Once ⏻ is pressed (refer to step 4 in the section "Editing mode"), the bookmark icon flashes and a newly created bookmark number shows on the display.
- You can create up to 20 bookmarks in a file. When the maximum limit is reached, **FULL** will be shown.
- The minimum interval between bookmarks is 3 seconds.

To skip to a bookmark anytime during playback:

1. During playback, press **rd** to go to the bookmark (if available).
2. Press **rd** again to go to the next bookmark.

To delete all bookmarks created in the current file:

Refer to section "Erasing files and bookmarks".

Insert

To insert a new segment into the current file:

1. Once ⏻ is pressed (refer to step 4 in the section "Editing mode"), the pause mode is released and the **REC** icon shows. The recording of a new segment is started from where the pause mode is released.
2. Press ■ to stop the recording of new segment.
- Do not power off the player if **WAIT** appears on the display.

Append

To insert an appendix at the end of the current file:

1. Once ⏻ is pressed (refer to step 4 in the section "Editing mode"), the **REC** icon shows and the recording of appendix is started.
2. Press ■ to stop the recording of the appendix.
- Do not power off the player if **WAIT** appears on the display.

Cut

To erase unwanted parts from the current file:

1. Start playback of the desired file.
2. Press ► to mark the start of the unwanted part, **CUT1** shows on display.
3. Press ► to mark the end of the unwanted part, **CUT2** shows on display.
4. Press ► again to confirm cutting within 3 seconds. Otherwise, the cutting operation will be canceled.
- You may also press ■ to cancel the cutting operation.
- Do not power off the player if **WAIT** appears on the display.

- Insert, Append and Cut will only update the recorded time length, without changing recording time and date.
- All bookmarks will be deleted after Insert, Append or Cut is performed.

Advanced operations

Play one/all

To play a specific file or all files in a folder:

1. Press and hold **mic/menu** for about 2 seconds and then release the button. The first menu item **FOLDER** flashes on the display.
2. Press **mic/menu** repeatedly until **ONE** or **ALL** flashes on display.
3. Press **prev** or **VOL** +/- to select between **ONE** and **ALL**.
4. Press ■ to exit the player menu.
- If **ONE** is selected, the player will stop after the selected file is played. If **ALL** is selected, the player will stop after all files in a folder are played.

Advanced operations

Tones

To activate or deactivate the beep sound when any key is pressed (except during playback and recording):

1. Press and hold **mic/menu** for about 2 seconds and then release the button. The first menu item **FOLDER** flashes on the display.
2. Press **mic/menu** repeatedly until **TONE** or **NOTONE** shows on display.
3. Press **next** or **VOL** +/- to set beep sound ON/OFF.
4. Press ■ to exit the player menu.

Speed

To adjust the playback speed:

1. Press and hold **mic/menu** for about 2 seconds and then release the button. The first menu item **FOLDER** flashes on the display.
2. Press **mic/menu** repeatedly until **SPEED** shows on display.
3. Press **next** or **VOL** +/- to select among **FAST**, **SLOW** and no speed indication (normal speed).
4. Press ■ to exit the player menu.
- The above operations can also be done during playback.

Connecting to computer

Computer system requirements

- PC with Windows® 7, Windows Vista® or Windows® XP (Service Pack 1 or higher) or Windows® 2000 (Service Pack 3 or higher). Mac OS is NOT supported.
- 20MB free hard disk space for software
- USB port 1.1 or 2.0
- Installed sound card

Mac OS version (i.e. Mac OS X version 10.4.11 or later) can support the mass storage mode only for listening audio files (recorded in HQ mode – "WAV" format) through the Mac audio program (eg. QuickTime).

Connecting to computer

Connect the player before launching the Digital Voice Manager.

1. Extend the USB connector on the player and connect it to your computer's USB port.
2. **PCLINK** shows on the player's display. The player appears as a removable drive in your computer.

Installing Digital Voice Manager

1. Connect the player with the computer as instructed in the previous section.
2. Open My Computer and double-click the player's drive icon. Double-click **rcaDVM_setup.exe** to start the Digital Voice Manager installation.
3. The RCA Detective application is installed with the Digital Voice Manager application and will open the Digital Voice Manager application automatically when you connect the player to your computer.

- When the player is in Menu mode, during playback or recording, a connection between the player and the computer will not be established. Quit the above modes before connecting to the computer.
- Data transfer is possible even if no batteries are installed in the player.
- Do not disconnect the USB connection during files transfer.
- The Digital Voice Manager software can also be downloaded from **www.rcaaudiovideo.com**.

Using Digital Voice Manager

The RCA Digital Voice Manager can perform playback, organize your bookmarks of the recorded files and create self-executable voice file from the recorded files.

Launching the software

1. To launch the software, click **Start**, select **All Programs**, select **RCA Digital Voice Recorder**, then select **RCA Digital Voice Manager**.
- If RCA Detective feature is selected during installation of Digital Voice Manager, the application will open automatically once you connect the player to your computer.
2. All the drives in the computer except the removable Digital Voice Recorder are shown in the top while the removable Digital Voice Recorder is shown in the bottom.

Playback and editing operations

3. Adjust the volume on the right of the toolbar.

- Click the corresponding buttons in the toolbar to fast backward/forward, skip to a specific time in the file and stop playback of a recorded file.
- To adjust the playback speed, click **Normal Speed** and select desired speed from the pull down menu.
- To skip to a bookmark, select **Play** from the menu at the top, then select **Goto Bookmark** and select your desired bookmark.
- To edit bookmarks, click the corresponding buttons to add or clear the bookmarks.

2. To play the recorded files, highlight the file and click the **PLAY/PAUSE** button on the left of the toolbar.

Creating and playing self-executable file

You can play the created file independently without the Digital Voice Management software.

1. Highlight a recorded file, click .
2. Select the destination folder from the pop up window and click **Save**.
3. Go to the destination folder and double-click the created file.
4. Click **Play** to start playback. Adjust the volume on the right.

Creating wave file

Self-executable file may be blocked by some e-mail filters. When recordings are made in LP or SP quality, you may wish to create wave file if you want to send your recorded messages by e-mail.

1. Highlight a recorded file, click .
2. Select the destination folder from the pop up window and click **Save**.
3. The created file could be found in the destination folder.

Using Digital Voice Manager

Transfer Files with Digital Voice Manager

Your player is associated with a drive letter. You can copy the voice files you want to transfer to your player to the A:\VOICE folder in the drive.

Your files can be found in these folders in the player once it is disconnected from the computer.

You can also copy the voice files you want to transfer from the A:\VOICE folder in the drive to your computer.

Using your player as a file storage device

The player can function as a detachable data storage device. You can take along your favorite pictures and documents wherever you go. Simply cut-and-paste or drag-and-drop files to or from it via USB connection, the player will appear as a removable drive in Windows.

Do not rename, delete and transfer (drag-and-drop) voice files to your player directly in Windows Explorer. Use the Digital Voice Manager to rename, delete and transfer voice files.

Help – For detailed explanation on using Digital Voice Manager, click the Help icon on the toolbar.

Disconnecting from computer

After you have copied files to or from the player, you can disconnect the player from the computer.

1. Click the icon from the System Tray and select **Unplug or Eject hardware**. Select the drive corresponding to your player.
2. The **Stop a Hardware device** screen will appear. Select the player to be stopped again for confirmation and click **OK**.
3. Now you can disconnect the player from the computer. If you want to go back to USB mode for file transfer at this stage, you need to unplug and connect the player to the PC again.

Troubleshooting tips

Player doesn't turn on

- Check that batteries are properly inserted and not exhausted.
- Make sure battery compartment door is properly closed.
- Make sure LOCK function is not activated.

Display keeps flashing when player is off

- You may not have set the time. Refer to section "Setting date and time".

Cannot record

- This player does not record mp3 format.
- Make sure LOCK function is not activated.
- Make sure memory is not full.
- You have recorded 99 files in one folder. Try record in a new folder.
- You may have formatted the player with incorrect file system (e.g. NTFS or MAC format). Refer to section "Erasing files and bookmarks" and format the player again.

Incorrect recording date and time during playback

- You may have not set the date and time before recording. Refer to section "Setting date and time".

No sound from speaker during playback

- Make sure volume is not set to 0.
- Headphones should not be connected.

Cannot edit

- Make sure **PLAY ALL** function is not activated.

Cannot activate the player after pressing on keys

- Remove the batteries to reset the player.

Recordable time becomes shorter

- You may have set the recording quality to "High Quality", refer to section "Setting Recording Quality".
- Delete the Digital Voice Manager setup software from the player to free up more memory space.

Cannot perform playback

- This player does not play mp3 format.
- Make sure you have selected folder with recorded messages.
- Make sure LOCK function is not activated.
- Make sure the file is playable, which must be of WAV PCM or designated MCA format. Other formats (e.g. mp3, wma) cannot be shown in the player for playback.

Cannot erase recorded file(s)

- Make sure you follow each step under section "Erasing files and bookmarks" carefully.

Cannot stop recording when AVR ON

- If AVR ON sensitivity is set to HIGH, recording may not be stopped in noisy environment. Try setting the sensitivity to LOW.

Cannot keep the saved setting

- If the batteries are removed, saved settings may be removed.

Cannot open recorded files in the computer

- You must use the provided DMM software to open the files. To download the software, go to www.rcaaudiovideo.com
- On a Mac computer, only .WAV file on the player can be played directly via application such as QuickTime.

Warranty information

12 Month Limited Warranty
Applies to RCA Voice Recorders

AUDIOVOX ACCESSORIES CORP. (the Company) warrants to the original retail purchaser of this product that should this product or any part thereof, under normal use and conditions, be proven defective in material or workmanship within 12 months from the date of original purchase, such defect(s) will be repaired or replaced with reconditioned product (at the Company's option) without charge for parts and repair labor.

To obtain repair or replacement within the terms of this Warranty, the product is to be delivered with proof of warranty coverage (e.g. dated bill of sale), specification of defect(s), transportation prepaid, to the Company at the address shown below.

This Warranty does not extend to the elimination of externally generated static or noise, to correction of antenna problems, to customers instruction or breakdown or internal service, to units incurred for installation, removal or reinstallation of product, to computers caused by computer viruses, spyware or other malware, to loss of media, files, data or content, or to damage to tapes, discs, removable memory devices or cards, speakers, accessories, computers, computer peripherals, other media players, home networks or vehicle electrical systems.

This Warranty does not apply to any product or part thereof which, in the opinion of the Company, has suffered or been damaged through alteration, improper installation, mishandling, misuse, neglect, accident, or by removal or defacement of the factory serial number/bar code label(s). THE EXTENT OF THE COMPANY'S LIABILITY UNDER THIS WARRANTY IS LIMITED TO THE REPAIR OR REPLACEMENT PROVIDED ABOVE AND, IN NO EVENT, SHALL THE COMPANY'S LIABILITY EXCEED THE PURCHASE PRICE PAID BY PURCHASER FOR THE PRODUCT.

This Warranty is in lieu of all other express warranties or liabilities. ANY IMPLIED WARRANTIES, INCLUDING ANY IMPLIED WARRANTY OF MERCHANTABILITY, SHALL BE LIMITED TO THE DURATION OF THIS WRITTEN WARRANTY. ANY ACTION FOR BREACH OF ANY WARRANTY HEREUNDER INCLUDING ANY IMPLIED WARRANTY OF MERCHANTABILITY MUST BE BROUGHT WITHIN A PERIOD OF 24 MONTHS FROM DATE OF ORIGINAL PURCHASE. IN NO CASE SHALL THE COMPANY BE LIABLE FOR ANY CONSEQUENTIAL OR INCIDENTAL DAMAGES FOR BREACH OF THIS OR ANY OTHER WARRANTY, for person or representation is authorized to assume for the Company any liability other than expressed herein in connection with the sale of this product.

Some states do not allow limitations on how long an implied warranty lasts or the exclusion or limitation of incidental or consequential damage so the above limitations or exclusions may not apply to you. This Warranty gives you specific legal rights and you may also have other rights which vary from state to state.

Recommendations before returning your product for a warranty claim:

- If your product is capable of storing content (such as an mp3 player, voice recorder, camcorder, digital photo frame, etc), it is recommended to make periodic backup copies of content stored on the product. If applicable, before shipping a product, make a back up copy of content or data stored on the device. Also, it is advisable to remove any personal content which you would not want exposed to others. IT IS LIKELY THAT CONTENTS AND DATA ON THE DEVICE WILL BE LOST DURING SERVICE AND REFORMATTING. AUDIOVOX ACCEPTS NO LIABILITY FOR LOST CONTENT OR DATA, OR FOR THE SECURITY OF ANY PERSONAL CONTENT OR DATA ON THE RETURNED DEVICE. Product will be returned with factory default settings, and without any pre-loaded content which may have been installed in the original purchased product. Consumer will be responsible for reloading data and content. Consumer will be responsible to restore any personal preference settings.
- Properly pack your unit. Include any remotes, memory cards, cables, etc. which were originally provided with the product. However DO NOT return any removable batteries, even if batteries were included with the original purchase. We recommend using the original carton and packing materials. Ship to:

Audiovox Electronics Corp.
Attn: Service Department
150 Marcus Blvd.
Hauppauge N.Y. 11788

1-631-645-4994

For Canada Customers, please ship to:
Audiovox Return Center
c/o Genco
6685 Kennedy Road,
Unit#1, Door 15,
Mississauga, Ontario
L5T 3A6

Illustrations contained within the publication are for representation only and subject to change.

The descriptions and characteristics given in this document are given as a general indication and not as a guarantee. In order to provide the highest quality product possible, we reserve the right to make any improvement or modification without prior notice.

Visit http://www.audiovox.com to find the best accessories for your products.

APPENDIX A3: *in vivo* study consent form

AGREEMENT FOR EXPERIMENTAL EQUINE TREATMENT

AND OWNER'S INFORMED CONSENT

This **AGREEMENT FOR EXPERIMENTAL EQUINE TREATMENT AND OWNER'S INFORMED CONSENT** (referred to as "Agreement and Consent") is between:

_____, having an address of_____

(referred to as "Owner");

Orthopeutics, LP, a Kentucky limited liability company, having an address of 1501 Bull Lea Rd. #103, Lexington, KY 40511 (referred to singly as "Orthopeutics" and collectively with Sinclair Research Center, LLC as "Orthopeutics-Sinclair"); and

Sinclair Research Center, LLC, a Missouri biomedical research facility at the University of Missouri, having an address of 562 Missouri DD, Auxvasse, MO 65231 (referred to singly as "Sinclair" and collectively with Orthopeutics, LP as "Orthopeutics-Sinclair").

Owner, Orthopeutics, and Sinclair are referred to collectively as the "Parties". The Effective Date of this Agreement and Consent is the date it is signed by the Parties.

BACKGROUND

NEXT stands for Nonsurgical Exogenous crosslink Therapy. NEXT, sometimes referred to herein as NEXT Technology is a chemically made device formed following injection of a crosslinking agent into the soft palate of an animal, such as a horse, which interacts with the native proteins (e.g., collagen) causing the tissue to reduce its flaccidity and vibration and to increase its strength, resilience, toughness and fatigue resistance. Strengthening the soft palate may help horses diagnosed with dorsal displacement of the soft palate (DDSP), which involves a form of awake snoring and apnea.

The therapeutic effect of NEXT Technology typically begins within 30 minutes of application, and provides mechanical stabilization of the tissue within 24 hours of application.

Orthopeutics' spin out company, Equinext, LLC holds a worldwide exclusive license for NEXT technology for all animal applications. With potential commercialization benefits for Equinext, Orthopeutics-Sinclair are conducting the second stage of a First in Equine (FIE) study of the effects of NEXT on horses (referred to as the "Study").

Owner voluntarily elects to have the horse identified in Schedule 1 (referred to as "Horse") participate in the Study for the treatment of DDSP and the soft palate. Orthopeutics has determined that the Horse fits the NEXT treatment protocol, and Orthopeutics-Sinclair are willing to enroll the Horse in the Study subject to the agreements and Informed Consent expressed herein.

Accordingly, the Parties agree and state as follows:

1	1501 Bull Lea Road, Suite 103, Lexington, KY 40511-1285 Phone: 512.818.8468 Email: thedman@orthopeutics.com

AGREEMENTS

1. Orthopeutics-Sinclair in their sole discretion, may remove the Horse from the Study at any time. Owner may remove the Horse from the Study with a 14-day notice to Orthopeutics-Sinclair.

2. Owner shall be responsible for all normal and typical veterinary-related costs incurred before, during, and after the Horse's participation in the Study.

3. It is the Owner's sole responsibility, before agreeing to allow the Horse's participation in the Study, to obtain professional input from the Horse's veterinarian about whether NEXT Technology is reasonably likely to promote healing effects on the soft palate of the Horse, and whether the likely benefit justifies participation when weighed against possible adverse outcomes or side effects.

4. Owner shall follow the recommendations provided by the Horse's veterinarian regarding care, evaluation, and rehabilitation following the administration of NEXT Technology, including but not limited to periodic clinical and endoscopic evaluations, and other types of pre-operative and post-operative evaluations as appropriate. Owner, not Orthopeutics-Sinclair, shall be responsible for the costs of all forms of care, evaluation, and rehabilitation contemplated by this paragraph.

5. Orthopeutics-Sinclair may use any and all clinical or laboratory data related to the Horse and the NEXT Technology for any purpose, provided that the Horse's and the Owner's identity are kept confidential. Owner shall maintain the confidentiality of all clinical and non-clinical outcomes in association with the NEXT Technology, unless otherwise made public by Orthopeutics within its sole discretion according to this paragraph.

6. ORTHOPEUTICS-SINCLAIR DISCLAIM ANY AND ALL EXPRESS AND IMPLIED WARRANTIES IN CONNECTION WITH NEXT TECHNOLOGY AND THE AGENTS USED IN NEXT THERAPY, INCLUDING BUT NOT LIMITED TO THE IMPLIED WARRANTIES OF MERCHANTABILITY AND OF FITNESS FOR A PARTICULAR PURPOSE.

7. Liability of Orthopeutics-Sinclair, if any, is limited to the cost of the agents utilized in the NEXT Technology on the Horse, and Owner's recovery and remedies are limited to such cost. All further liability for all actual, direct, indirect, special, compensatory, and punitive damages, including but not limited to lost profits and consequential damages, which may occur for any reason are expressly disclaimed by mutual agreement of the Parties.

8. For the duration of this study, owner agrees to not utilize any other alternative treatment therapies on the Horse. Owner agrees to follow after care instructions and rehabilitation program as provided by Orthopeutics-Sinclair.

9. Owner understands that the Horse must be shipped to the Sinclair Research Center in Missouri and acknowledges the inherent risks that are involved in shipping and transporting horses. These risks may include but are not limited to, illness, disease, trauma, injury, or death of the Horse. Owner understands that Orthopeutics-Sinclair and the associated transporting company do not provide insurance. Owner hereby holds Orthopeutics, Sinclair, and the transporting

1501 Bull Lea Road, Suite 103, Lexington, KY 40511-1285
Phone: 512.818.8468 Email: thedman@orthopeutics.com

company harmless for any liability that could incur for property damage or bodily injury to any horse and/or patrons while loading, transporting, unloading or handling the Horse.

10. In the event that the horse requires veterinary care while in transport, Orthopeudics-Sinclair will immediately notify Owner. If the Owner cannot be reached, Orthopeudics-Sinclair will contact the first available licensed veterinarian. Owner shall be responsible for all fees listed by said veterinarian, with no liability to Orthopeudics, Sinclair, or the transporting company.

11, This Agreement and Informed Consent shall be governed by the laws of the Commonwealth of Kentucky, without regard to Kentucky's or any other state's rules concerning conflicts of law. The Parties agree that Kentucky Courts shall have jurisdiction over them personally as well as over the subject matter of any dispute that arises in connection with this Agreement and Informed Consent. Any lawsuit filed in connection with this Agreement must be commenced in Fayette County, Kentucky.

INFORMED CONSENT

1. The experimental nature of NEXT Technology has been fully explained to Owner and/or Owner's agent. Further, Owner is aware that potential risks, side effects, and adverse complications of NEXT Technology (referred to as "Complications") may include, without limitation, lack of repair, deterioration of condition, soft palate damage, infection, inflammation, and bleeding. However, the possibility of other unexpected responses including the possible need to euthanize the animal is not excluded. Owner is aware that Complications may be either anticipated or unanticipated, and may be either immediately known or not immediately knowable. While it is expected that Complications, if any, will be minimal, no guarantees or warranties of any kind are being provided regarding the outcome of the Study and/or the effects of NEXT Technology on the Horse.

2. Owner understands that NEXT Technology on the Horse may include mild sedation, injection of a local anesthetic, and one or more injections of Genipin, and consents to same.

3. The Parties acknowledge that Owner's decision to allow the Horse to participate in the Study is entirely voluntary.

4. By signing below, I, as the Owner or the Owner's agent, acknowledge that I have read this Agreement and Informed Consent in its entirety, I have been provided with a description of the NEXT Technology, I have had the opportunity to ask further questions of Orthopeutics-Sinclair, and that the risks of potential Complications have been explained to my satisfaction. I give informed consent to the administration of NEXT Technology to the Horse in connection with the Study.

1501 Bull Lea Road, Suite 103, Lexington, KY 40511-1285
Phone: 512.818.8468 Email: thedman@orthopeutics.com

Signatures

IN WITNESS WHEREOF, the parties have accepted and agreed to the above by and through their authorized agents as of the Effective Date:

On Behalf of Owner,

_____ :

_____

Name: _____

Title: _____

Date: _____

On Behalf of

Orthopeutics, LP**:**

_____

Name: _____

Title: _____

Date: _____

On Behalf of:

Sinclair Research Center, LLC:

_____

Name: _____

Title: _____

Date: _____

1501 Bull Lea Road, Suite 103, Lexington, KY 40511-1285
Phone: 512.818.8468 Email: thedman@orthopeutics.com

1. **SCHEDULE 1**

Information about horse:

Name:_____ Discipline:_____

Breed:_____ Sex: Mare Gelding Stallion Age:_____

Veterinarian:_____ Vet phone:_____ Email:_____

Date of DDSP ("Snoring") Onset:_____ Frequency of Displacement:_____

Loudness of "Snoring": _____

Previous Health Conditions/Surgeries: _____

Work Level of Horse:____ Pasture (no work) ____ light work ____ moderate work ____ full work (1 hr/5 days wk)

Purchase price of horse: _____

Declared Value of Horse:_____ Insured: Yes No

Has insurance company been contacted? Yes No

If insured, please provide following information:

Insurance Co:_____ Phone:_____ Contact:_____

Owner Information:

Name/Address:_____

_____

_____

Cell phone:_____ Email:_____

Information provided by:_____ Date:_____

1501 Bull Lea Road, Suite 103, Lexington, KY 40511-1285
Phone: 512.818.8468 Email: thedman@orthopeutics.com

APPENDIX A4: *in vivo* study donation form

AGREEMENT FOR DONATION OF EQUINE FOR EXPERIMENTAL EQUINE TREATMENT

This **AGREEMENT FOR DONATION OF AN EQUINE FOR EXPERIMENTAL EQUINE TREATMENT** (referred to as "Agreement") is between:

_____, having an address of _____ (referred to as "Owner"); and

Orthopeutics, LP, a Kentucky limitied liability company, having an address of 1501 Bull Lea Rd. #103, Lexington, KY 40511 (referred to as "Orthopeutics").

Owner and Orthopeutics are referred to collectively as the "Parties." The Effective date of this Agreement is the date it is signed by the Parties.

AGREEMENTS

1. Owner voluntarily donates the horse identified in Schedule 1 (referred to as "Horse") to Orthopeutics to be used in the study for the treatment of dorsal displacement of the soft palate (DDSP) in equines (referred to as "Study") at Sinclair Research Center at the University of Missouri (referred to as "Sinclair").

2. The Owner relinquishes all rights and responsibilities pertaining to the Horse to Orthopeutics.

3. The Owner acknowledges that the Horse will be used for scientific research as a part of the Study, including but not limited to, anesthesia, soft palate injections, sound recordings, or endoscope examinations.

4. Orthopeutics will be responsible for ensuring humane care of the Horse throughout the study.

5. The Owner acknowledges that the Horse will be humanely euthanized at the conclusion of the study by licensed veterinarians at Sinclair.

6. Owner acknowledges that there will be no money compensation for the donation of the Horse to Orthopeutics for the Study.

1501 Bull Lea Road, Suite 103, Lexington, KY 40511-1285
Phone: 512.818.8468 Email: thedman@orthopeutics.com

SIGNATURES

IN WITNESS WHEREOF, the parties have accepted and agreed to the above by and through their authorized agents as of the Effective Date:

On Behalf of Owner,

_____:

_____

Name: _____

Title: _____

Date: _____

On Behalf of

Orthopeutics, LP:

_____

Name: _____

Title: _____

Date: _____

1501 Bull Lea Road, Suite 103, Lexington, KY 40511-1285
Phone: 512.818.8468 Email: thedman@orthopeutics.com

1. **SCHEDULE 1**

Information about horse:

Name:_____ Discipline:_____

Breed:_____ Color: _____ Sex: Mare Gelding Stallion Age:_____

Veterinarian:_____ Vet phone:_____ Email:_____

Previous Health Conditions/Surgeries:
_____

Work Level of Horse:____ Pasture (no work) ____ light work ____ moderate work ____ full work (1 hr/5 days wk)

Purchase price of horse: _____

Declared Value of Horse:_____ Insured: Yes No

Has insurance company been contacted? Yes No

If insured, please provide following information:

Insurance Co:_____ Phone:_____ Contact:_____

Owner Information:

Name/Address:_____

_____

_____

Cell phone:_____ Email:_____

Information provided by:_____ Date:_____

1501 Bull Lea Road, Suite 103, Lexington, KY 40511-1285
Phone: 512.818.8468 Email: thedman@orthopeutics.com

APPENDIX A5: Veterinary transcript for DDSP horses

Hello Dr. [INSERT VET NAME HERE],

I am a graduate student in the Department of Biomedical Engineering at the University of Kentucky. I am currently working on an *in vivo* study on dorsal displacement of the soft palate, or DDSP, in horses. The study consists of injecting the soft palate with a natural substance to stiffen it and decrease vibrations, thus reducing the frequency of soft palate displacement. The study is being funded by a National Institute of Health SBIR Phase 1 grant.

I am actively searching for three horses with DDSP to be used in our study in the next couple of weeks. The DDSP horses in the study would be transported to the Sinclair Research Center in Missouri. The study would consist of an initial exam, including recording their breathing noises while running and an endoscopic evaluation. Then, the horse will be sedated and their soft palates injected using a transendoscopic injection needle. Finally, a post exam, similar to the initial exam, would be completed. The horses would then be returned to their owners at the end of the study. Licensed veterinarians at Sinclair Research Center would monitor the horses throughout the study.

Do you know of any horses that would be good candidates for the study? If you do not, do you know of anyone that could possibly help me?

Please feel free to email me or call me with any questions or concerns. I look forward to hearing from you.

Thank you,

Stephanie Hunt

APPENDIX A6: Reagent calculations for *in vivo* study

Genipin Calculations: 100 mM

$$\frac{100\ mmol}{1L} x \frac{1\ mol}{1000\ mmol} x \frac{226.22\ g}{1\ mol} x \frac{1L}{1000\ mL} x \frac{2\ mL}{1\ bottle} = 0.045244 \frac{g}{bottle} = 45.24 \frac{mg}{bottle}$$

Buffer Calculations: 10% DMSO, 45 mM EPPS-P

22.5 mL EPPS-P

22.5 mL Distilled Water

5 mL DMSO

$$100\ mM\ EPPS - P x \frac{22.5\ mL\ EPPS-P}{1\ bottle} x \frac{1\ bottle}{50\ mL} = 45\ mM\ EPPS - P$$

APPENDIX A7: Respiratory audio analysis Matlab codes


```
%%get sound files

%Pre Injection Sound
xpre=BHPre_3E_1;

%Post Injeciton Sound
xpost=BHPost_3E_1;
fs=fs;

%-----------------------------------------

%Length of file
Npre=length(xpre);
Npost=length(xpost);

%Time
tpre=(0:Npre-1)/fs;
tpost=(0:Npost-1)/fs;

%-------------------------------------------------
%%Time Domain - Normalized graph

%Both Time Domain in one Window
figure
a=1;
b=[1/4 1/4 1/4 1/4];
x=xpre(:,1);
xx=filter(b,a,x);
y=xpost(:,1);
yy=filter(b,a,y);
subplot(2,1,1);
plot(tpre,xx,'r');
xlim([0 5]);
xlabel('Time (s)','FontSize',14);
ylabel('Amplitude (V)','FontSize',14);grid on;
title('Pre Treatment Time Domain for Horse #1 for 3E','FontSize',14);
subplot(2,1,2);
plot(tpost,yy,'b');
xlim([0 5]);
xlabel('Time (s)','FontSize',14);
ylabel('Amplitude (V)','FontSize',14);grid on;
title('Post Treatment Time Domain for Horse #1 for 3E','FontSize',14);

%-------------------------------------------------
%%Spectrogram

%Pre and Post Spectrogram in one figure
figure
subplot(2,1,1)
spectrogram(xpre,1024,3/4*1024,[],fs,'yaxis');
xlabel('Time(s)','FontSize',14);
ylabel('Frequency (Hz)','FontSize',14);
title('Pre Treatment Spectrogram for Horse #1 for 3E','FontSize',14);
subplot(2,1,2)
spectrogram(xpost,1024,3/4*1024,[],fs,'yaxis');
grid on;
xlabel('Time(s)','FontSize',14);
ylabel('Frequency (Hz)','FontSize',14);
title('Post Treatment Spectrogram for Horse #1 for 3E','FontSize',14);
```

```
%--------------------------------------------------
%%Frequency Domain

%Pre Sound
XPRE=fft(xpre);
magXPRE=abs(XPRE);
fpre = fs/Npre .* (0:Npre-1);

%entire pre graph
figure
subplot(2,1,1)
plot(fpre,magXPRE,'r');
grid on;
ylim([0 150]);
xlim([10 4000]);
xlabel('Frequency (Hz)','FontSize',14);
ylabel('Amplitude (V)','FontSize',14);
title('Pre Treatment Frequency Domain for Horse #1 for 3E','FontSize',14);

%Post Sound
XPOST=fft(xpost);
magXPOST=abs(XPOST);
fpost = fs/Npost .* (0:Npost-1);

%entire post graph
subplot(2,1,2)
plot(fpost,magXPOST,'b');
grid on;
ylim([0 150]);
xlim([10 4000]);
xlabel('Frequency (Hz)','FontSize',14);
ylabel('Amplitude (V)','FontSize',14);
title('Post Treatment Frequency Domain for Horse #1 for 3E','FontSize',14);

%--------------------------------------------------
%Filter Frequency Domain

%Pre Frequency
a=1;
b=[1/4 1/4 1/4 1/4];
x=magXPRE(:,1);
y=filter(b,a,x);
figure
subplot(2,1,1)
plot(fpre,x,'k',fpre,y,'m');
xlim([10 4000]);
ylim([0 150]);
xlabel('Frequency (Hz)','FontSize',14);
ylabel('Amplitude (V)','FontSize',14);grid on;
legend('Original data','Filtered Data',2);
title({'Comparison of Original and Filtered Frequency Domain', 'for Pre Treatment Audio from↙
Horse #1 for 3E'},'FontSize',14);

%Post Frequency
a=1;
b=[1/4 1/4 1/4 1/4];
x=magXPOST(:,1);
y=filter(b,a,x);
```

```
subplot(2,1,2)
plot(fpost,x,'k',fpost,y,'m');
xlim([10 4000]);
ylim([0 150]);
xlabel('Frequency (Hz)','FontSize',14);
ylabel('Amplitude (V)','FontSize',14);grid on;
legend('Original data','Filtered Data',2);
title({'Comparison of Original and Filtered Frequency Domain', 'for Post Treatment Audio from↙
Horse #1 for 3E'},'FontSize',14);

%Area Under the Curve Calculations

%Pre Frequency
a=1;
b=[1/4 1/4 1/4 1/4];
x=magXPRE(:,1);
y=filter(b,a,x);
BHPrearea100=trapz(fpre(10:500),y(10:500))
BHPrearea200=trapz(fpre(10:1000),y(10:1000))
BHPrearea500=trapz(fpre(10:2500),y(10:2500))

figure
subplot(2,1,1)
plot(fpre,y,'red')
hold on;
area(fpre(10:2500),y(10:2500),'FaceColor','cyan')
hold on;
area(fpre(10:1000),y(10:1000),'FaceColor','green')
hold on;
area(fpre(10:500),y(10:500),'FaceColor','yellow')
hold off;
xlim([10 700]);
ylim([0 150]);
xlabel('Frequency (Hz)','FontSize',14);
ylabel('Amplitude (V)','FontSize',14);grid on;
legend(char({'Pre Treatment', 'Frequency Domain'}),'AUC 0-500','AUC 0-200','AUC 0-↙
100','Location','northeastoutside');
title('Pre Treatment Calculated Area Under Curve for Horse #1 for 3E','FontSize',14);

%Post Frequency
a=1;
b=[1/4 1/4 1/4 1/4];
x=magXPOST(:,1);
y=filter(b,a,x);

BHPostarea100=trapz(fpost(10:300),y(10:300))
BHPostarea200=trapz(fpost(10:600),y(10:600))
BHPostarea500=trapz(fpost(10:1500),y(10:1500))

subplot(2,1,2)
plot(fpost,y,'blue')
hold on;
area(fpost(10:1500),y(10:1500),'FaceColor','cyan')
hold on;
area(fpost(10:600),y(10:600),'FaceColor','green')
hold on;
area(fpost(10:300),y(10:300),'FaceColor','yellow')
xlim([10 700]);
ylim([0 150]);
```

```
xlabel('Frequency (Hz)','FontSize',14);
ylabel('Amplitude (V)','FontSize',14);grid on;
legend(char({'Post Treatment', 'Frequency Domain'}),'AUC 0-500','AUC 0-200','AUC 0-↙
100','Location','northeastoutside');
title('Post Treatment Calculated Area Under Curve for Horse #1 for 3E','FontSize',14);

%%High Amplitude - 500-4000 Hz
a=1;
b=[1/4 1/4 1/4 1/4];
x=magXPRE(:,1);
y=filter(b,a,x);
xx=magXPOST(:,1);
yy=filter(b,a,xx);
figure
plot(fpre,y,'r',fpost,yy,'b');
xlim([500 4000]);
ylim([0 100]);
xlabel('Frequency (Hz)','FontSize',14);
ylabel('Amplitude (V)','FontSize',14);grid on;
legend('Pre Treatment','Post Treatment',2);
title('Filtered Frequency Domain Plot for Horse #1 for 3E from 500-4000 Hz','FontSize',14);

%Low Amplitude - 0-500 Hz
figure
plot(fpre,y,'r',fpost,yy,'b');
xlim([10 500]);
ylim([0 100]);
xlabel('Frequency (Hz)','FontSize',14);
ylabel('Amplitude (V)','FontSize',14);grid on;
legend('Pre Treatment','Post Treatment',2);
title('Filtered Frequency Domain Plot for Horse #1 for 3E from 0-500 Hz','FontSize',14);

%Low Amplitude - 0-200 Hz
figure
plot(fpre,y,'r',fpost,yy,'b');
xlim([10 200]);
ylim([0 100]);
xlabel('Frequency (Hz)','FontSize',14);
ylabel('Amplitude (V)','FontSize',14);grid on;
legend('Pre Treatment','Post Treatment',2);
title('Filtered Frequency Domain Plot for Horse #1 for 3E from 0-200 Hz','FontSize',14);

%Low Amplitude - 0-100 Hz *corresponds with 'DDSP Peak'
figure
plot(fpre,y,'r',fpost,yy,'b');
xlim([10 100]);
ylim([0 100]);
xlabel('Frequency (Hz)','FontSize',14);
ylabel('Amplitude (V)','FontSize',14);grid on;
legend('Pre Treatment','Post Treatment',2);
title('Filtered Frequency Domain Plot for Horse #1 for 3E from 0-100 Hz','FontSize',14);

%-----------------------------------------------------------------------
%-----------------------------------------------------------------------
%%get sound files

%Pre Injection Sound
xpre=THPre_3E_1;
```

```
%Post Injeciton Sound
xpost=THPost_3E_1;
fs=fs;

%Length of file
Npre=length(xpre);
Npost=length(xpost);

%Time
tpre=(0:Npre-1)/fs;
tpost=(0:Npost-1)/fs;

%--------------------------------------------------
%%Time Domain - Normalized Graph

%Both Time Domain Graphs in one window
figure
a=1;
b=[1/4 1/4 1/4 1/4];
x=xpre(:,1);
xx=filter(b,a,x);
y=xpost(:,1);
yy=filter(b,a,y);
subplot(2,1,1);
xlim([0 3.5]);
plot(tpre,xx,'r');
xlabel('Time (s)','FontSize',14);
ylabel('Amplitude (V)','FontSize',14);grid on;
title('Pre Treatment Time Domain for Horse #2 for 3E','FontSize',14);
subplot(2,1,2)
plot(tpost,yy,'b');
xlim([0 3.5]);
xlabel('Time (s)','FontSize',14);
ylabel('Amplitude (V)','FontSize',14);grid on;
title('Post Treatment Time Domain for Horse #2 for 3E','FontSize',14);


%--------------------------------------------------
%%Spectrogram

%Both Spectrogram on one graph
figure
subplot(2,1,1)
spectrogram(xpre,1024,3/4*1024,[],fs,'yaxis');
xlabel('Time(s)','FontSize',14);
ylabel('Frequency (Hz)','FontSize',14);
title('Pre Treatment Spectrogram for Horse #2 for 3E','FontSize',14);
subplot(2,1,2)
spectrogram(xpost,1024,3/4*1024,[],fs,'yaxis');
grid on;
xlabel('Time(s)','FontSize',14);
ylabel('Frequency (Hz)','FontSize',14);
title('Post Treatment Spectrogram for Horse #2 for 3E','FontSize',14);

%--------------------------------------------------
%%Frequency Domain

%Pre Sound
XPRE=fft(xpre);
```

```
magXPRE=abs(XPRE);
fpre = fs/Npre .* (0:Npre-1);

%Entire Graph
figure
subplot(2,1,1)
plot(fpre,magXPRE,'r');
grid on;
ylim([0 150]);
xlim([10 4000]);
xlabel('Frequency (Hz)','FontSize',14);
ylabel('Amplitude (V)','FontSize',14);
title('Pre Treatment Frequency Domain for Horse #2 for 3E','FontSize',14);

%Post Sound
XPOST=fft(xpost);
magXPOST=abs(XPOST);
fpost = fs/Npost .* (0:Npost-1);

%Entire Graph
subplot(2,1,2)
plot(fpost,magXPOST,'b');
grid on;
ylim([0 150]);
xlim([10 4000]);
xlabel('Frequency (Hz)','FontSize',14);
ylabel('Amplitude (V)','FontSize',14);
title('Post Treatment Frequency Domain for Horse #2 for 3E','FontSize',14);

%------------------------------------------------

%Filter Frequency Domain

%Pre Frequency
a=1;
b=[1/4 1/4 1/4 1/4];
x=magXPRE(:,1);
y=filter(b,a,x);
figure
subplot(2,1,1)
plot(fpre,x,'k',fpre,y,'m');
xlim([10 4000]);
ylim([0 150]);
xlabel('Frequency (Hz)','FontSize',14);
ylabel('Amplitude (V)','FontSize',14);grid on;
legend('Original data','Filtered Data',2);
title({'Comparison of Original and Filtered Frequency Domain','for Pre Treatment Audio from↙
Horse #2 for 3E'},'FontSize',14);

%Post Frequency
a=1;
b=[1/4 1/4 1/4 1/4];
x=magXPOST(:,1);
y=filter(b,a,x);
subplot(2,1,2)
plot(fpost,x,'k',fpost,y,'m');
xlim([10 4000]);
ylim([0 150]);
xlabel('Frequency (Hz)','FontSize',14);
```

```
ylabel('Amplitude (V)','FontSize',14);grid on;
legend('Original data','Filtered Data',2);
title({'Comparison of Original and Filtered Frequency Domain','for Post Treatment Audio from↙
Horse #2 for 3E'},'FontSize',14);

%Area Under the Curve Calculations

%Pre Frequency
a=1;
b=[1/4 1/4 1/4 1/4];
x=magXPRE(:,1);
y=filter(b,a,x);
THPrearea100=trapz(fpre(10:378),y(10:378))
THPrearea200=trapz(fpre(10:756),y(10:756))
THPrearea500=trapz(fpre(10:1890),y(10:1890))

figure
subplot(2,1,1)
plot(fpre,y,'red')
hold on;
area(fpre(10:1890),y(10:1890),'FaceColor','cyan')
hold on;
area(fpre(10:756),y(10:756),'FaceColor','green')
hold on;
area(fpre(10:378),y(10:378),'FaceColor','yellow')
xlim([10 700]);
ylim([0 150]);
xlabel('Frequency (Hz)','FontSize',14);
ylabel('Amplitude (V)','FontSize',14);grid on;
legend(char({'Pre Treatment','Frequency Domain'}),'AUC 0-500','AUC 0-200','AUC 0-↙
100','Location','northeastoutside');
title('Pre Treatment Calculated Area Under Curve for Horse #2 for 3E','FontSize',14);

%Post Frequency
a=1;
b=[1/4 1/4 1/4 1/4];
x=magXPOST(:,1);
y=filter(b,a,x);
THPostarea100=trapz(fpost(10:327),y(10:327))
THPostarea200=trapz(fpost(10:654),y(10:654))
THPostarea500=trapz(fpost(10:1635),y(10:1635))

subplot(2,1,2)
plot(fpost,y,'blue')
hold on;
area(fpost(10:1635),y(10:1635),'FaceColor','cyan')
hold on;
area(fpost(10:654),y(10:654),'FaceColor','green')
hold on;
area(fpost(10:327),y(10:327),'FaceColor','yellow')
xlim([10 700]);
ylim([0 150]);
xlabel('Frequency (Hz)','FontSize',14);
ylabel('Amplitude (V)','FontSize',14);grid on;
legend(char({'Post Treatment','Frequency Domain'}),'AUC 0-500','AUC 0-200','AUC 0-↙
100','Location','northeastoutside');
title('Post Treatment Calculated Area Under Curve for Horse #2 for 3E','FontSize',14);
```

```
%High Amplitude - 500-4000 Hz
a=1;
b=[1/4 1/4 1/4 1/4];
x=magXPRE(:,1);
y=filter(b,a,x);
xx=magXPOST(:,1);
yy=filter(b,a,xx);
figure
plot(fpre,y,'r',fpost,yy,'b');
xlim([500 4000]);
ylim([0 150]);
xlabel('Frequency (Hz)','FontSize',14);
ylabel('Amplitude (V)','FontSize',14);grid on;
legend('Pre Treatment','Post Treatment',2);
title('Filtered Frequency Domain Plot for Horse #2 for 3E from 500-4000 Hz','FontSize',14);

%Low Amplitude - 0-500 Hz
figure
plot(fpre,y,'r',fpost,yy,'b');
xlim([10 500]);
ylim([0 150]);
xlabel('Frequency (Hz)','FontSize',14);
ylabel('Amplitude (V)','FontSize',14);grid on;
legend('Pre Treatment','Post Treatment',2);
title('Filtered Frequency Domain Plot for Horse #2 for 3E from 0-500 Hz','FontSize',14);

%Low Amplitude - 0-200 Hz
figure
plot(fpre,y,'r',fpost,yy,'b');
xlim([10 200]);
ylim([0 150]);
xlabel('Frequency (Hz)','FontSize',14);
ylabel('Amplitude (V)','FontSize',14);grid on;
legend('Pre Treatment','Post Treatment',2);
title('Filtered Frequency Domain Plot for Horse #2 for 3E from 0-200 Hz','FontSize',14);

%Low Amplitude - 0-100 Hz *corresponds with 'DDSP Peak'
figure
plot(fpre,y,'r',fpost,yy,'b');
xlim([10 100]);
ylim([0 150]);
xlabel('Frequency (Hz)','FontSize',14);
ylabel('Amplitude (V)','FontSize',14);grid on;
legend('Pre Treatment','Post Treatment',2);
title('Filtered Frequency Domain Plot for Horse #2 for 3E from 0-100 Hz','FontSize',14);

%-----------------------------------------------------------------------
%-----------------------------------------------------------------------
%%get sound files

%Pre Injection Sound
xpre=MVPre_3E_1;

%Post Injeciton Sound
xpost=MVPost_3E_1;
fs=fs;

%Length of file
Npre=length(xpre);
```

```
Npost=length(xpost);

%Time
tpre=(0:Npre-1)/fs;
tpost=(0:Npost-1)/fs;

%--------------------------------------------------
%%Time Domain - Normalized Graph

%Both Time Domain on one graph
a=1;
b=[1/4 1/4 1/4 1/4];
x=xpre(:,1);
xx=filter(b,a,x);
y=xpost(:,1);
yy=filter(b,a,y);
figure
subplot(2,1,1);
plot(tpre,xx,'r');
xlim([0 2.5]);
xlabel('Time (s)','FontSize',14);
ylabel('Amplitude (V)','FontSize',14);grid on;
title('Pre Treatment Time Domain for Horse #3 for 3E','FontSize',14);
subplot(2,1,2);
plot(tpost,yy,'b');
xlim([0 2.5]);
xlabel('Time (s)','FontSize',14);
ylabel('Amplitude (V)','FontSize',14);grid on;
title('Post Treatment Time Domain for Horse #3 for 3E','FontSize',14);

%--------------------------------------------------
%%Spectrogram

%Both on one graph
figure
subplot(2,1,1)
spectrogram(xpre,1024,3/4*1024,[],fs,'yaxis');
xlabel('Time(s)','FontSize',14);
ylabel('Frequency (Hz)','FontSize',14);
title('Pre Treatment Spectrogram for Horse #3 for 3E','FontSize',14);
subplot(2,1,2)
spectrogram(xpost,1024,3/4*1024,[],fs,'yaxis');
grid on;
xlabel('Time(s)','FontSize',14);
ylabel('Frequency (Hz)','FontSize',14);
title('Post Treatment Spectrogram for Horse #3 for 3E','FontSize',14);


%--------------------------------------------------
%%Frequency Domain

%Pre Sound
XPRE=fft(xpre);
magXPRE=abs(XPRE);
fpre = fs/Npre .* (0:Npre-1);

%entire graph
figure
subplot(2,1,1)
```

```
plot(fpre,magXPRE,'r');
grid on;
ylim([0 80]);
xlim([10 4000]);
xlabel('Frequency (Hz)','FontSize',14);
ylabel('Amplitude (V)','FontSize',14);
title('Pre Treatment Frequency Domain for Horse #3 for 3E','FontSize',14);

%Post Sound
XPOST=fft(xpost);
magXPOST=abs(XPOST);
fpost = fs/Npost .* (0:Npost-1);

%entire graph
subplot(2,1,2)
plot(fpost,magXPOST,'b');
grid on;
ylim([0 80]);
xlim([10 4000]);
xlabel('Frequency (Hz)','FontSize',14);
ylabel('Amplitude (V)','FontSize',14);
title('Post Treatment Frequency Domain for Horse #3 for 3E','FontSize',14);

%-------------------------------------------------------------------------
%Filter Frequency Domain

%Pre Frequency
a=1;
b=[1/4 1/4 1/4 1/4];
x=magXPRE(:,1);
y=filter(b,a,x);
figure
subplot(2,1,1)
plot(fpre,x,'k',fpre,y,'m');
xlim([10 4000]);
ylim([0 80]);
xlabel('Frequency (Hz)','FontSize',14);
ylabel('Amplitude (V)','FontSize',14);grid on;
legend('Original data','Filtered Data',2);
title({'Comparison of Original and Filtered Frequendy Domain','for Pre Treatment Audio from↙
Horse #3 for 3E'},'FontSize',14);

%Post Frequency
a=1;
b=[1/4 1/4 1/4 1/4];
x=magXPOST(:,1);
y=filter(b,a,x);
subplot(2,1,2)
plot(fpost,x,'k',fpost,y,'m');
xlim([10 4000]);
ylim([0 80]);
xlabel('Frequency (Hz)','FontSize',14);
ylabel('Amplitude (V)','FontSize',14);grid on;
legend('Original data','Filtered Data',2);
title({'Comparison of Original and Filtered Frequendy Domain','for Post Treatment Audio from↙
Horse #3 for 3E'},'FontSize',14);

%Area Under the Curve Calculations
```

```
%Pre Frequency
a=1;
b=[1/4 1/4 1/4 1/4];
x=magXPRE(:,1);
y=filter(b,a,x);
MVPrearea100=trapz(fpre(10:134),y(10:134))
MVPrearea200=trapz(fpre(10:268),y(10:268))
MVPrearea500=trapz(fpre(10:670),y(10:670))

figure
subplot(2,1,1)
plot(fpre,y,'red')
hold on;
area(fpre(10:670),y(10:670),'FaceColor','cyan')
hold on;
area(fpre(10:268),y(10:268),'FaceColor','green')
hold on;
area(fpre(10:134),y(10:134),'FaceColor','yellow')
xlim([10 700]);
ylim([0 60]);
xlabel('Frequency (Hz)','FontSize',14);
ylabel('Amplitude (V)','FontSize',14);grid on;
legend(char({'Pre Treatment','Freqeuncy Domain'}),'AUC 0-500','AUC 0-200','AUC 0-↙
100','Location','northeastoutside');
title('Pre Treatment Calculated Area Under Curve for Horse #3 for 3E','FontSize',14);


%Post Frequency
a=1;
b=[1/4 1/4 1/4 1/4];
x=magXPOST(:,1);
y=filter(b,a,x);
MVPostarea100=trapz(fpost(10:250),y(10:250))
MVPostarea200=trapz(fpost(10:500),y(10:500))
MVPostarea500=trapz(fpost(10:1250),y(10:1250))

subplot(2,1,2)
plot(fpost,y,'blue')
hold on;
area(fpost(10:1250),y(10:1250),'FaceColor','cyan')
hold on;
area(fpost(10:500),y(10:500),'FaceColor','green')
hold on;
area(fpost(10:250),y(10:250),'FaceColor','yellow')
xlim([10 700]);
ylim([0 60]);
xlabel('Frequency (Hz)','FontSize',14);
ylabel('Amplitude (V)','FontSize',14);grid on;
legend(char({'Post Treatment','Freqeuncy Domain'}),'AUC 0-500','AUC 0-200','AUC 0-↙
100','Location','northeastoutside');
title('Post Treatment Calculated Area Under Curve for Horse #3 for 3E','FontSize',14);

%High Frequency - 500-4000 Hz
a=1;
b=[1/4 1/4 1/4 1/4];
x=magXPRE(:,1);
y=filter(b,a,x);
xx=magXPOST(:,1);
yy=filter(b,a,xx);
```

```
figure
plot(fpre,y,'r',fpost,yy,'b');
xlim([500 4000]);
ylim([0 60]);
xlabel('Frequency (Hz)','FontSize',14);
ylabel('Amplitude (V)','FontSize',14);grid on;
legend('Pre Treatment','Post Treatment',2);
title('Filtered Frequency Domain Plot for Horse #3 for 3E from 500-4000 Hz','FontSize',14);

%Low Frequency - 0-500 Hz
figure
plot(fpre,y,'r',fpost,yy,'b');
xlim([10 500]);
ylim([0 60]);
xlabel('Frequency (Hz)','FontSize',14);
ylabel('Amplitude (V)','FontSize',14);grid on;
legend('Pre Treatment','Post Treatment',2);
title('Filtered Frequency Domain Plot for Horse #3 for 3E from 0-500 Hz','FontSize',14);

%Low Frequency - 0-200 Hz
figure
plot(fpre,y,'r',fpost,yy,'b');
xlim([10 200]);
ylim([0 60]);
xlabel('Frequency (Hz)','FontSize',14);
ylabel('Amplitude (V)','FontSize',14);grid on;
legend('Pre Treatment','Post Treatment',2);
title('Filtered Frequency Domain Plot for Horse #3 for 3E from 0-200 Hz','FontSize',14);

%Low Frequency - 0-100 Hz *corresponds with 'DDSP Peak'
figure
plot(fpre,y,'r',fpost,yy,'b');
xlim([10 100]);
ylim([0 60]);
xlabel('Frequency (Hz)','FontSize',14);
ylabel('Amplitude (V)','FontSize',14);grid on;
legend('Pre Treatment','Post Treatment',2);
title('Filtered Frequency Domain Plot for Horse #3 for 3E from 0-100 Hz','FontSize',14);
```

APPENDIX A8: ImageJ Protocol

1. Open ImageJ
2. Import image
3. Select image from the menu bar → color → split channels
4. Using the green channel, select image → adjust → threshold
5. Use the default values, then press okay.
6. Select analyze → analyze particles

The output will provide the count of the red squares, the area, and the percent area of red squares.

APPENDIX B1: Reagent calculations for mechanical testing study

Genipin Reagent: 50 mM

$$\frac{50\ mmol}{1L} x \frac{1\ mol}{1000\ mmol} x \frac{226.22\ g}{1\ mol} x \frac{1L}{1000\ mL} x \frac{2\ mL}{1\ vial} = 0.0226 \frac{g}{vial} = 22.6 \frac{g}{vial}$$

Saline Buffer: 0.9% NaCl

$$\frac{4.5\ g\ NaCl}{500\ mL} x \frac{1000\ mL}{1\ vial} = 9 \frac{g}{vial}$$

Saline-Phosphate Buffer: 50 mM tri-sodium phosphate

$$\frac{50\ mmol}{1L} x \frac{1\ mol}{1000\ mmol} x \frac{380.12\ g}{1\ mol} x \frac{1\ L}{1000\ mL} x \frac{1000\ mL}{1\ vial} = 19.01 \frac{g}{vial}$$

APPENDIX B2: Soft palate extraction protocol

Soft Palate Extraction

1. Soft palates will arrive with trachea and surrounding tissues.

2. Locate the epiglottis. Flip the epiglottis tip below the notch of the soft palate.

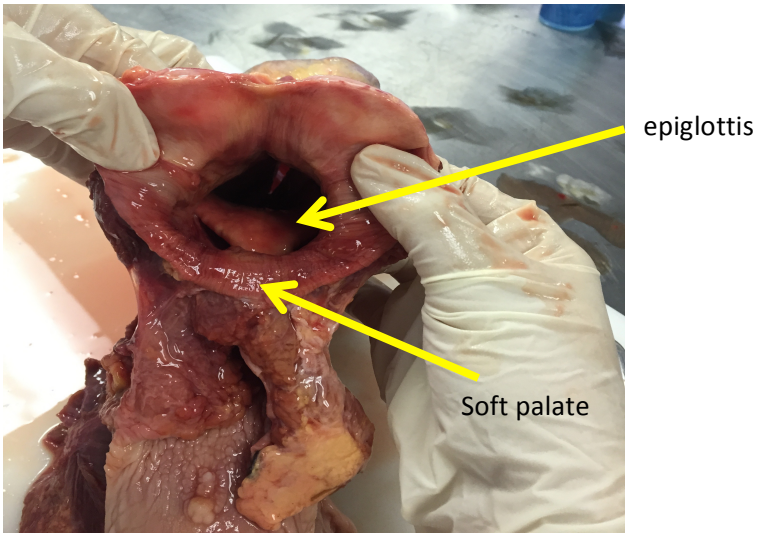

3. Cut the tissue directly above the soft palate along the median.

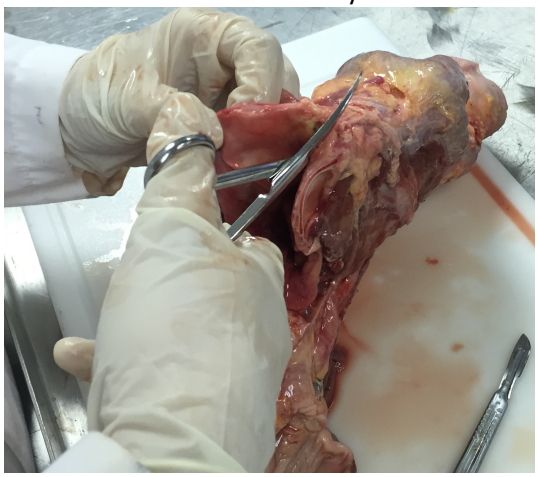

4. Open the tissue you just cut to expose the epiglottis, soft palate and larynx.

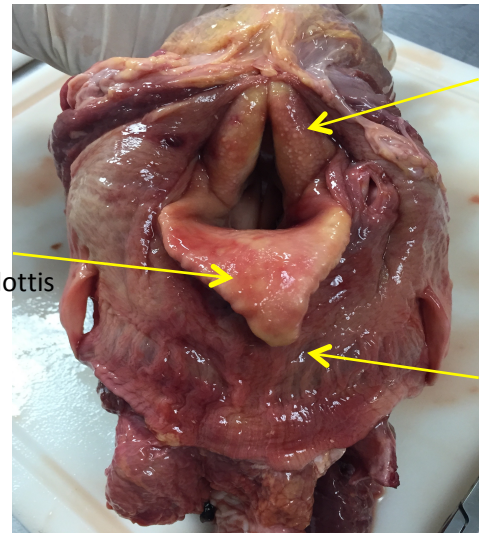

5. Cut along the outer edges of the soft palate to separate the excess tissue. The tissue along the edge of the soft palate will be very thin and transparent – this is a good place to cut along to ensure the entire palate is included.

6. Cut along the bones below the epiglottis to remove the pant legs.

7. Trim any excess tissue from soft palate.

APPENDIX B3: Mechanical testing protocol

Mechanical Testing Protocol

Hysteresis Test

1. Load Sample
2. Preload 10 N
3. Set up program
    a. Show Cycling Panel: Axial: Stroke, Mean: ht of sample, Amplitude: 3 mm, Freq: 0.5, Phase:0, Cycles:20, Sine, mean down
4. Set up DAQ file at a sampling rate of 50 Hz
5. Start recording
6. Start cycle
7. Stop recording
8. Export data

Stress Relaxation Test

1. Load Sample
2. Preload 10 N
3. Create program
    a. Step 1: ramp up to 10 N, rate 1 mm/s
    b. Step 2: hold 300 s
    c. Step 3: Idle
4. Set up DAQ file. Change DAQ Rate to 25 Hz
5. Start Recording
6. Start cycle
7. Stop recording
8. Export data

Tensile Test

1. Load sample
2. Return displacement to 0 and wait 30 seconds
3. Set up function generator
    a. Axial mode: stroke, target point: 39, ramp 1mm/s
4. Set up DAQ at a sampling rate of 50 Hz
5. Start recording
6. Start ramp
7. Stop recording
8. Export data

APPENDIX B4: Hysteresis Parameter Calculations

Hysteresis Calculations:

First, the starting point was used to offset the stroke data to find the absolute displacements. For example, if the starting point was 42 mm, the stroke data was offset by 42 mm. Then, strain was calculated by dividing the displacement by the gauge length. Next, stress in MPa was calculated by dividing the load by the cross-sectional area of the sample. Finally, stress in Pa was calculated by raising the stress in MPa values to the sixth power.

Once the strain and stress in Pa were calculated, the hysteresis graphs were plotted. First, the cyclical loading was plotted with load on the y-axis and time on the x-axis to determine the location of the 1st and 20th cycles. The 1st cycle was determined to be from the first local minimum to the second local minimum as shown in red in Figure 1. The 20th cycle was determined to be from the 19th local minimum to the 20th local minimum.

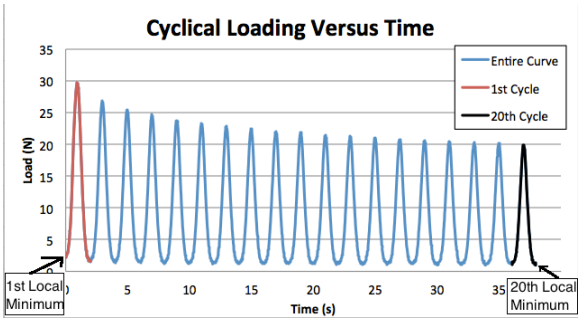

Figure 1: Hysteresis Cycles shown as load versus time to determine location of 1st and 20th cycles.

Then, the corresponding local minimum points were extracted and graphed to create the individual cycle hysteresis curves with stress on the y-axis and strain on the x-axis. For the 1st cycle, the stress and strain were plotted from corresponding values at the 1st local minimum point to the 2nd local minimum point as shown in Figure 2. For the 20th cycle, the stress and strain were plotted from corresponding values at the 19th local minimum point to the 20th local minimum point as shown in Figure 3.

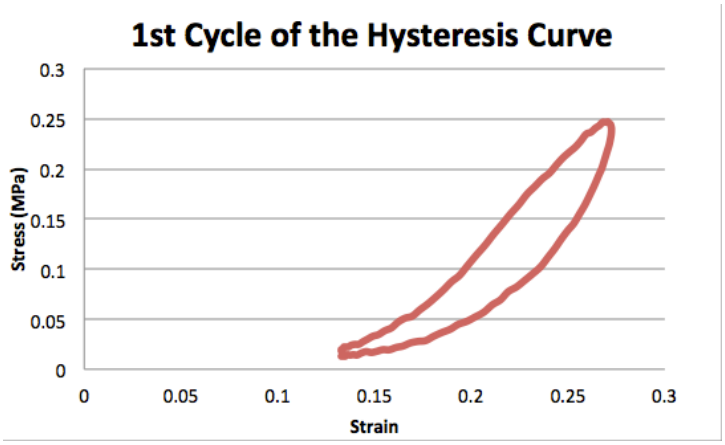

Figure 2: 1st cycle hysteresis curve

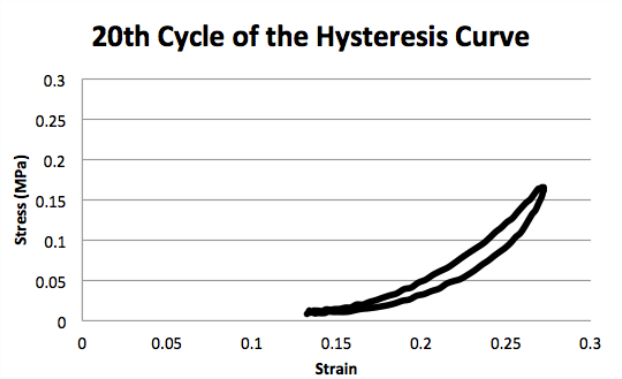

Figure 3: 20th Cycle hysteresis curve

Then, the entire hysteresis cycle was plotted with strain on the x-axis and stress on the y-axis as shown in Figure 4. The 1st and 20th cycle curves were highlighted in red and black respectively.

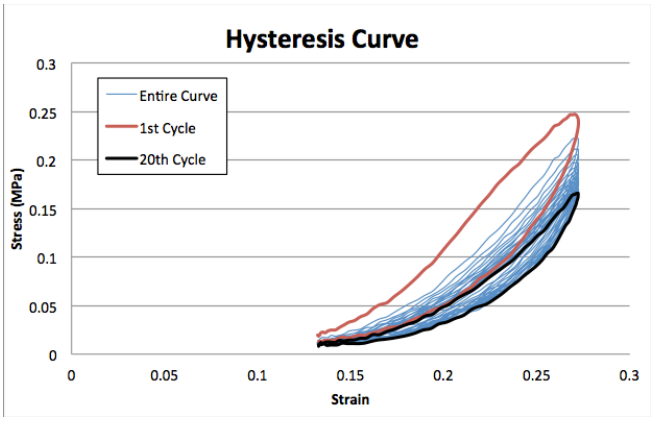

Figure 4: Hysteresis Curve for all Cycles

Finally, the hysteresis for each point was calculated using the equation below.

$$Individual\ Hysteresis = \left(\frac{Stress\ Point\ 1 + Stress\ Point\ 2}{2}\right) * (Strain\ 2 - Strain\ 1)$$

Once all of the individual hysteresis points were calculated, the total hysteresis for the cycle up and the total hysteresis for the cycle down were calculated for the 1st curve. The total hysteresis for the cycle up was calculated by adding together all of the individual hysteresis values from the 1st local minimum to the 1st cycle maximum. The total hysteresis for the cycle down was calculated by adding together all of the individual hysteresis values form the 1st cycle maximum to the 2nd local minimum. Then the difference between the cycle up total hysteresis and the cycle down hysteresis was calculated to determine the area between the curves. This was repeated for the 20th cycle.

APPENDIX B5: Stress relaxation parameter calculations

The stress relaxation graphs were analyzed for the relaxation force and for the relaxation modulus. First, the stress relaxation graph was plotted with time on the x-axis and stress in MPa on the y-axis as shown in Figure 1. From this graph, the maximum and minimum stresses were determined. Then the relaxation force was calculated by calculating the difference between the maximum and minimum.

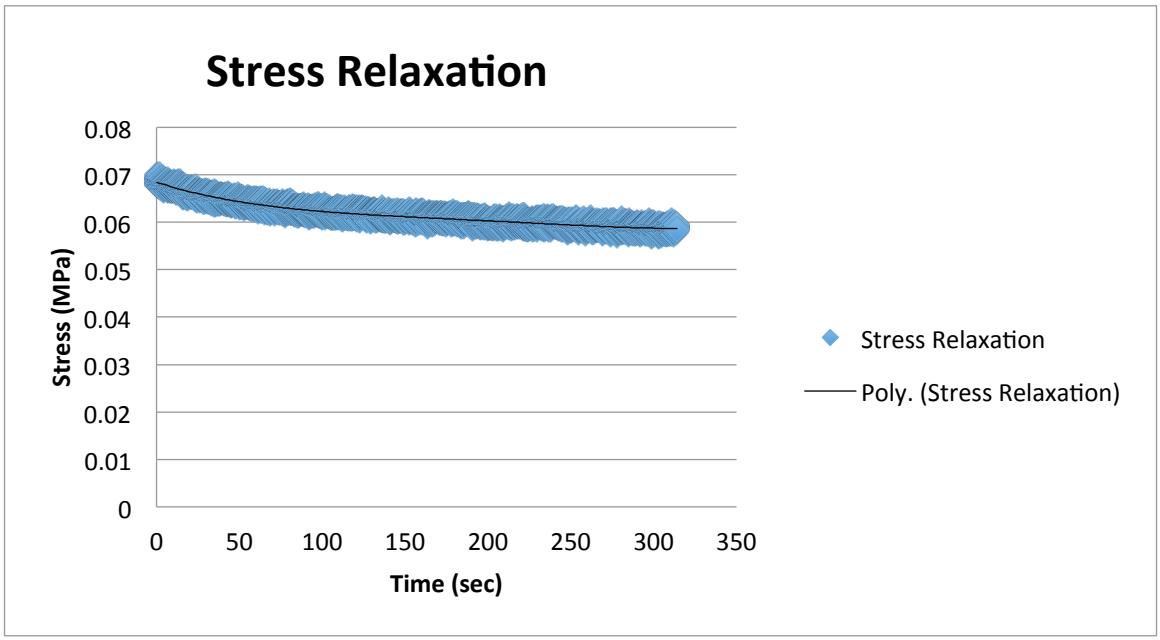

Figure 5: Stress Relaxation Graph

Finally, the stress relaxation modulus was calculated at each point using Equation 1. Then, the maximum and minimum relaxation modulus values were determined, and the relaxation modulus difference was calculated by subtracting the minimum value from the maximum value.

$$Relaxation\ Modulus = \frac{\sigma(t)}{\varepsilon} \text{ (Equation 1)}$$

APPENDIX B6: Tensile test parameter calculations

Tensile Test

Goal: Find the Peak Stress, Strain, Toughness, Energy to Peak, Toe Region Slope, Young's Modulus and Yield Point.

1. Using the stroke data offset the values by the starting point. For example, if all data starts at -42mm, offset the values by 42 mm.
2. Find the strain by dividing the offset stroke by the length.
3. Find the stress by dividing the load by the cross sectional area.
4. Find the peak stress by finding the absolute maximum stress.
5. The strain at peak is determined by finding the strain at the absolute peak stress value.
6. Plot the stress vs. strain graph.
7. Plot the toughness values from the start of the graph to the final non zero point. Add a trendline with the equation and R^2 value. The trendline should be raised to the 3^{rd} power.
8. Determine the toughness by dividing each part of the toughness equation by the strain raised to the respective power and adding them together.
9. Calculate the energy for the entire curve by multiplying the toughness by the cross sectional area.
10. Locate the toe region by highlighting from the first non-zero value in the stress region to 0.05 MPa.
11. Plot the toe region and add a trendline with the equation and R^2 value. The equation should be raised to the 2^{nd} power.
12. Find the slope of the toe region by taking the derivative of the equation.
13. Find the start of the linear region by adding 50 points onto the end of the toe region. Take the end of the linear region to be about 150-200 points from the beginning, unless there is an obvious break from linearity in the graph.
14. Plot the linear region and trendline with the equation and R^2 value. The Young's Modulus is the slope of the linear region.
15. To determine the yield point, first find the offset strain line by taking the linear region equation and offsetting it by .02.
16. Plot the offset strain line and determine the point of intersection with the curve. The y value of the intersection point is the yield point.
17. Find resilience by calculating the area under the curve to the yield point.

APPENDIX C1: Bright Humor's dynamic endoscope diagnoses

Pre Treatment:

Natanya M. Nieman, DVM
3241 Pisgah Pike
Versailles, KY 40383
(859)537-5000

BRIGHT HUMOR
Scope report

March 23, 2014-
Left arytenoid completely paralyzed and thickened, partially scarred up out of the airway (previous tieback surgery that was released. Dorsal displacement of the soft palate-displaced 90% of the exam. Epiglottis is moderately flaccid and of normal size.

Previous surgeries:
Tie Back
Tie Back Release
Tie Forward
Laser edge of soft palate

Post Treatment:

Rood and Riddle Equine Hospital
P.O. Box 12070
Lexington, Kentucky 40580
(859) 233-0371

Patient Evaluation Form

Patient: Bright Humor Date Evaluated: 11-4-14

Owner: Natanya Nieman

Referring Veterinarian:

Diagnosis: Upper airway evaluation

Diagnostic Procedures and Finds:
Upper airway endoscopy at rest and during exercise

Prognosis:

Surgery: Date of Surgery:

Treatment:

Recommendations and Instructions:

On resting endoscopy the left arytenoid does not move and a left ventriculocordectomy has been performed. The corniculate process of the left arytenoid is mildly thickened. The horse did not displace his soft palate during resting endoscopy. The overground endoscope was positioned in his upper airway and his upper airway function was evaluated while he was lunged. He did not displace his soft palate during exercise (walk, trot, & canter). He did have intermittent epiglottic entrapment. He did not make any abnormal respiratory noise during exercise.

Please let me know if you have any questions

Brett Woodie

Releasing Veterinarian

Dispensed:

Released To

APPENDIX C2: Talladega Hall's dynamic endoscope diagnoses

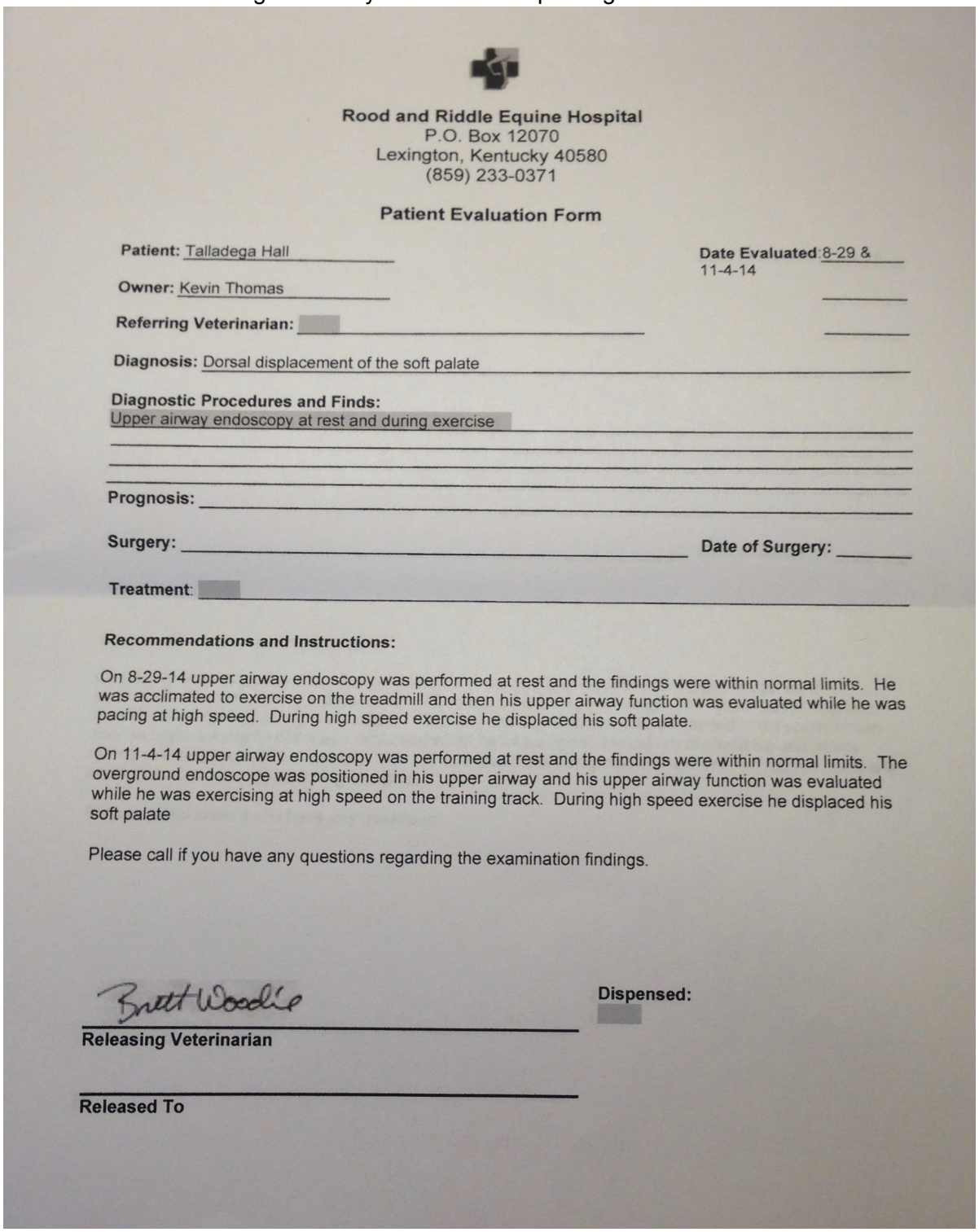

Rood and Riddle Equine Hospital
P.O. Box 12070
Lexington, Kentucky 40580
(859) 233-0371

Patient Evaluation Form

Patient: Talladega Hall

Date Evaluated: 8-29 & 11-4-14

Owner: Kevin Thomas

Referring Veterinarian:

Diagnosis: Dorsal displacement of the soft palate

Diagnostic Procedures and Finds:
Upper airway endoscopy at rest and during exercise

Prognosis:

Surgery: **Date of Surgery:**

Treatment:

Recommendations and Instructions:

On 8-29-14 upper airway endoscopy was performed at rest and the findings were within normal limits. He was acclimated to exercise on the treadmill and then his upper airway function was evaluated while he was pacing at high speed. During high speed exercise he displaced his soft palate.

On 11-4-14 upper airway endoscopy was performed at rest and the findings were within normal limits. The overground endoscope was positioned in his upper airway and his upper airway function was evaluated while he was exercising at high speed on the training track. During high speed exercise he displaced his soft palate

Please call if you have any questions regarding the examination findings.

Brett Woodie

Releasing Veterinarian

Dispensed:

Released To

APPENDIX C3: Post treatment clinical observations

Table 4.3: Post treatment clinical observations from *in vivo* study for each horse

Study ID	Study Day	Time	Clinical Observations
1	1	13 hr post	clearing throat repeatedly but not excessive
		15 hr post	slight teeth grinding and licking
2	0	1 hr post	still slightly sedated
	1	25 hr post	slight clear nasal discharge bilaterally, breathing normally
		28 hr post	licking occasionally
		29 hr post	twitching lips and licking occasionally
	3	59 hr post	laying down
		68 hr post	mild mucoid nasal discharge from both nares
3	0	1 hr post	still slightly sedated
		2 hr post	licking/chewing
	1	21 hr post	mild hypersalivation, reduced appetite
		22 hr post	eating normally
		23 hr post	mild hypersalivation, licking side of stall, breathing normally
		24 hr post	occasional licking
		25 hr post	mild hypersalivation, licking back of stall, breathing normally
		28 hr post	slight clear nasal discharge from right nostril, breathing normally, eating well
	2	43 hr post	some feed remaining
4	0	11 hr post	smacking continuously
		12 hr post	continues to smack
	1	14 hr post	clearing throat repeatedly but not excessive
		15 hr post	constantly chewing and licking, no respiratory difficulty
		16 hr post	small amount licking
		19 hr post	clearing throat repeatedly
	2	43 hr post	laying down
5	0	1 hr post	still slightly sedated
		11 hr post	good amount of smacking and tongue movement in and out, cleared throat several times
	2	55 hr post	chewing
		57 hr post	chewing
6	1	13 hr post	laying down quietly
		16 hr post	laying down quietly

IDEXX BioResearch

HISTOPATHOLOGY REPORT

4LT 1-2 Two sections through the treated palate 4LT are examined. The biopsy has intact mucosa on both the respiratory and oral sides. The core of the biopsy is necrotic and connective tissue fibrils are widely separated. The separation may be from edema or from expansion associated with tissue freezing. Few muscular fascicles adjacent to the necrotic core retain their striations and are diffusely basophilic. Surrounding the necrotic core is a marked zone of abundant neutrophils, many of which have degenerated into basophilic smears (degenerated chromatin). In the palatine muscles adjacent to the necrotic core, neutrophil infiltrates widely separate muscle fibers within fascicles. Muscle fibers are swollen and most retain striations. Some myofibers have granular cytoplasm with large clear vacuoles. The vacuoles may be from freezing artifact as similar cytoplasmic vacuoles are observed in the control palate sections. Outside of the neutrophils, a wide zone of the collagenous stroma is necrotic.

Between the necrotic core and the viable submucosa of the oral mucosal epithelium is a moderate band of spindloid cells with plump nuclei interpreted to be fibroblasts and mild amounts of irregular bands of collagen. Mild numbers of eosinophils infiltrate the viable submucosa and a few small lobules of mucous glands are observed. The stratified epithelium of the oral mucosa is unremarkable.

On the respiratory side, the necrotic collagenous stroma is moderately infiltrated with neutrophils. In the submucosa are variably-sized clear spaces lined with a simple endothelium and filled with a minimal amount of flocculent eosinophilic material. These clear spaces may represent vessels (lymphatic and /or vascular) that may have expanded because of freezing. Also in the submucosa are mild to moderate numbers of eosinophils. The respiratory mucosa is mildly infiltrated with granulocytes and cilia are not observed. The lack of cilia may be associated with the transition of respiratory to oral mucosa.

4LM 1-2 Two sections through the treated palate 4LM are examined. The biopsy has intact mucosa on both the respiratory and oral sides. The core of the biopsy contains abundant neutrophils. Surrounding the core of neutrophils is a mild to moderate zone of necrotic collagenous stroma.

Neutrophil infiltrates occasionally extend through the necrotic stroma and surround degenerated lobules of mucous glands on the oral side. Between the necrotic stroma and the viable submucosa of the oral mucosa is a moderate band of spindloid cells with plump nuclei interpreted to be fibroblasts and abundant dense irregular collagen. In some regions, collagenous fibers are separated by pale eosinophilic material (suggestive of edema or freezing artifact). The submucosa is infiltrated with mild to moderate numbers of neutrophils and lymphocytes that extend to the basal cells of the mucosa. Few inflammatory cells infiltrate mildly edematous rete pegs of the mucosa.

Many muscle fascicles adjacent to the necrotic stroma on the respiratory side have myofibers with single cytoplasmic vacuoles (freezing artifact). A minor number of muscle fascicles contain small myofibers separated by mild numbers of spindloid cells and mild amounts of irregular collagenous fibers, which are changes associated with fibroplasia. Many of the small myofibers have central plump nuclei, a change associated with muscle hyperplasia or repair. Between the regenerating muscle and the submucosa are moderate bands of plump spindloid cells or fibroblasts, with occasional mitotic figures, with moderate amounts of irregular collagen fibrils. Between the regions of fibroplasia and the mucosa are numerous lobules of mucous glands that have an edematous interstitial stroma. In the submucosa are variably-sized clear spaces lined with a simple endothelium and filled with a minimal amount of flocculent eosinophilic material. These clear spaces may represent vessels (lymphatic and /or vascular) that may have expanded because of freezing. Also in the submucosa are mild to moderate numbers of eosinophils. The respiratory mucosa contains small vacuoles that separate epithelial cells.

4LB 1-2 Two sections of the control palate 4LB are examined. No significant lesions are observed. The pseudostratified columnar ciliated epithelium on the respiratory side of the palate is intermittently folded to form glandular-like pockets. The submucosa is moderately populated with tubuloalveolar mucous glands in a well-vascularized stroma of fine collagenous fibrils. Around the base of the mucous glands

and diffusely within the stroma are mild infiltrates of lymphocytes and plasma cells. Deep to the submucosa are moderately-sized arteries and bands of dense collagen, tendons and fascicles of the palatine skeletal muscles. Skeletal myofibers occasionally contain cytoplasmic clear vacuoles which are most likely a consequence of ice crystal formation associated with freezing. Toward the oral side of the palate, abundant large lobules of mucous glands are adjacent and occasionally separate the muscular fascicles. Glandular lobules are separated from each other by thick bands of dense connective tissue. Closer to the mucosal surface and within the dense collagenous stroma of the submucosa are multiple lymph nodules, each with multiple germinal centers. Interspersed between lymphoid nodules are smaller bands of skeletal muscle and cross-section of ducts – likely from the mucous glands. The oral mucosa is slightly folded and composed of acanthotic non-keratinized stratified squamous epithelium with prominent rete pegs.

4RT 1-2 Two sections through the treated palate 4RT are examined. The biopsy has mostly intact mucosa on both the respiratory and oral sides. The core of the biopsy is extensively necrotic. Vessels in the necrotic core are distended and contain fibrillar eosinophilic material which may represent fibrin. Surrounding the necrotic core are abundant infiltrates of neutrophils. Outside of the zone of neutrophils, a wide zone of the collagenous stroma is necrotic.

Between the necrotic stroma and the viable submucosa of the oral mucosal epithelium is a mild band of spindloid cells with plump nuclei interpreted to be fibroblasts and mild amounts of dense collagen. The submucosa is infiltrated with mild numbers of eosinophils and lymphocytes. The mucosa is unremarkable.

On the respiratory side, neutrophil infiltrates widely separate muscle fibers within many fascicles. Muscle fascicles contain swollen and fragmented myofibers separated by moderate numbers of spindloid cells (fibroblasts) and mild amounts of collagenous fibers, which are changes associated with fibroplasia. Between the injured muscle and the submucosa are degenerated mucous glands, moderate infiltrates of plump fibroblasts, mild deposits of irregular collagen and mild to moderate infiltrates of eosinophils and lymphocytes. Neutrophil infiltrates within the necrotic stroma extend to the submucosa in many regions. The submucosa is mildly edematous. In a few regions of the submucosa are variably-sized clear spaces lined with a simple endothelium and filled with a minimal amount of flocculent eosinophilic material. These clear spaces may represent vessels (lymphatic and /or vascular) that may have expanded because of freezing. In the respiratory mucosa are minimal inflammatory cells. Cilia are not observed.

4RM 1-2 Two sections through the treated palate 4RM are examined. The biopsy has mostly intact mucosa on both the respiratory and oral sides. The core of the biopsy is extensively necrotic. Vessels in the necrotic core are distended and contain fibrillar eosinophilic material which may represent fibrin. Surrounding the necrotic core are abundant infiltrates of neutrophils. Outside of the zone of neutrophils, a wide zone of collagenous stroma is necrotic.

Between the necrotic stroma and the viable submucosa of the oral mucosal epithelium is a moderate band of spindloid cells with plump nuclei interpreted to be fibroblasts and moderate amounts of dense irregular collagen. Lobules of mucous glands are degenerated with loss and attenuation of glandular epithelium. The submucosa is edematous and infiltrated with moderate numbers of eosinophils and lymphocytes. Occasional inflammatory cells are within the mucosa and occasional mitoses are observed in basal epithelial cells.

Neutrophil infiltrates widely separate muscle fibers within many fascicles on the respiratory side. Muscle fascicles contain swollen and fragmented myofibers separated by moderate numbers of spindloid cells (fibroblasts) and mild deposits of irregular collagen, which are changes associated with fibroplasia. Many muscle fascicles adjacent to the necrotic stroma contain small myofibers with central plump nuclei, a change associated with muscle hyperplasia or repair. Between the regenerating muscle and the submucosa are moderate bands of plump fibroblasts with moderate irregular collagen deposits.

Between the regions of fibroplasia and the mucosa are numerous lobules of mucous glands. Neutrophil infiltrates of the necrotic stroma extend to the submucosa in many regions. In most of the biopsy, the submucosa is mildly edematous and moderately infiltrated with lymphocytes, neutrophils and few eosinophils. The respiratory mucosa is mildly infiltrated with granulocytes and cilia are not observed. The lack of cilia may be associated with the transition of respiratory to oral mucosa.

4RB 1-2 Two sections through the control palate 4RB are examined. The biopsy has mostly intact mucosa on both the respiratory and oral sides. The core of the biopsy is extensively necrotic which may be from carryover from the treated sites. Vessels in the necrotic core are distended and contain fibrillar eosinophilic material which may represent fibrin. Surrounding the necrotic core are abundant infiltrates of neutrophils.. Outside of the abscess, a wide zone of the collagenous stroma is necrotic.

Between the necrotic stroma and the viable submucosa of the oral mucosal epithelium is a moderate band of spindloid cells with plump nuclei interpreted to be fibroblasts and moderate deposits of dense irregular collagen. Lobules of mucous glands are degenerated with loss and attenuation of glandular epithelium. The submucosa is edematous and infiltrated with moderate numbers of eosinophils and lymphocytes. Occasional inflammatory cells are within the mucosa and occasional mitoses are observed in basal epithelial cells.

On the respiratory side, necrosis of the stroma with moderate neutrophil infiltrates extends to the submucosa in many regions. Neutrophil infiltrates widely separate muscle fibers within many fascicles. Muscle fascicles contain swollen and fragmented myofibers separated by moderate numbers of spindloid cells (fibroblasts) and mild amounts of collagenous fibers, which are changes associated with fibroplasia. Many muscle fascicles adjacent to the necrotic stroma contain small myofibers with central plump nuclei, a change associated with muscle hyperplasia or repair. Between the regenerating muscle and the submucosa are moderate bands of plump fibroblasts with moderate irregular collagen deposits. Between the regions of fibroplasia and the mucosa are numerous lobules of mucous glands within an edematous interstitial stroma. The submucosa is mildly edematous and moderately infiltrated with lymphocytes, neutrophils and few eosinophils. The respiratory mucosa is mildly infiltrated with granulocytes.

5LT One section through the treated palate 5LT is examined. The biopsy has a limited amount of mucosa on the respiratory and oral sides. The core of the biopsy is extensively necrotic. Within the necrotic tissue are scattered bacterial colonies. Moderate to marked infiltrates of neutrophils surround the necrotic core. Outside of the neutrophilic zone, a wide zone of the collagenous stroma is necrotic.

Between the necrotic stroma and the viable submucosa of the oral mucosal epithelium are moderate bands of spindloid cells with plump nuclei interpreted to be fibroblasts and moderate amounts of dense collagen. These bands of fibroplasia frequently surround foci of necrotic stroma and extend up to the level of the mucous glands. Mild infiltrates of neutrophils are among the fibroblasts at the interface of the necrotic stroma and many small blood vessels are observed within the fibroplastic tissue. The submucosa and oral mucosa are within normal limits.

On the respiratory side, necrosis of stroma and muscular fascicles with moderate to marked neutrophil infiltrates extend to the submucosa and occasionally to the base of the mucosa. Some mucous glands are degenerated and infiltrated with mild numbers of lymphocytes and plasma cells. Muscle fascicles contain swollen and fragmented myofibers separated by moderate numbers of spindloid cells and mild amounts of collagenous fibers, which are changes associated with fibroplasia. On the periphery of the necrotic tissue, muscle fasicles are separated by moderate amounts of dense and fine collagen fibrils with fewer and smaller spindloid cells (interpreted to be fibrocytes) and minimal inflammatory cell infiltrates. This expanded stroma may represent artifactual separation associated with freezing. The mucous glands in this region are mildly infiltrated with lymphocytes and plasma cells. In the submucosa are multiple variably-sized clear spaces lined with a simple endothelium and rarely filled with a minimal amount of flocculent eosinophilic material. These clear spaces may represent vessels (lymphatic and

/or vascular) that may have expanded because of freezing. The submucosa has mild to moderate numbers of lymphocytes that often extend to the base of the mucosa. The respiratory mucosa occasionally contains small vacuoles that separate epithelial cells. No cilia are observed.

5LM One section through the treated palate 5LM is examined. The biopsy has a limited amount of mucosa on the respiratory and oral sides. The core of the biopsy is extensively necrotic at one margin. Surrounding the necrotic core are mild to moderate infiltrates of neutrophils. Outside of the neutrophilic zone are multiple regions of necrotic collagenous stroma.

Between the necrotic stroma and the viable submucosa of the oral mucosal epithelium are moderate bands of spindloid cells with plump nuclei interpreted to be fibroblasts and moderate amounts of dense irregular collagen. Mild infiltrates of neutrophils are among the fibroblasts at the interface of the necrotic stroma and many small blood vessels are observed within the fibroplastic tissue. Mucous glands in the region with the most inflammation and fibroplasia have mild interstitial edema. The submucosa in the region of inflammation has mild numbers of infiltrating eosinophils, plasma cells and lymphocytes. The oral mucosa is unremarkable.

On the respiratory side, collagenous stroma and muscular fascicles are necrotic with moderate to marked neutrophil infiltrates. Neutrophilic infiltrates extend from the necrotic tissue to the submucosa and base of the mucosa. Some mucous glands in this region are moderately to markedly degenerated and infiltrated with mild numbers of neutrophils, lymphocytes and plasma cells. Muscle fascicles contain swollen and occasionally fragmented myofibers separated by moderate numbers of spindloid cells, interpreted to be fibroblasts, mild to moderate amounts of irregular collagen and mild infiltrates of neutrophils and occasionally eosinophils. On the periphery of the necrotic tissue, muscle fasicles are separated by moderate amounts of dense and fine irregular collagen fibrils with fewer and smaller spindloid cells (interpreted to be fibrocytes) and minimal inflammatory cell infiltrates. This expanded stroma may represent artifactual separation of normal stroma associated with freezing. Mild interstitial infiltrates of lymphocytes and plasma cells are observed in the mucous glands in this region. In the submucosa are multiple variably-sized clear spaces, most of which are lined with a simple endothelium. These clear spaces may represent vessels (lymphatic and /or vascular) that may have expanded because of freezing. The submucosa has mild to marked numbers of lymphocytes that often extend to the base of the mucosa. The respiratory mucosa occasionally contains small vacuoles that separate epithelial cells. No cilia are observed.

5LB One section of the control palate 5LB is examined. No significant lesions are observed. The surface epithelium on the respiratory side of the palate is intermittently folded to form glandular-like pockets and overlays multiple large submucosal lymphoid nodules, each composed of lymphoid aggregates with prominent germinal centers. The epithelium overlying the nodules is a simple low columnar epithelium while that of the infolded regions is pseudostratified and columnar. Between and beneath the lymphoid nodules are mucous glands in a well-vascularized stroma of fine irregular collagenous fibrils. Around the base of the mucous glands and diffusely within the stroma are mild infiltrates of lymphocytes and plasma cells. Deep to the mucous glands is a broad band of dense regular collagen populated with medium-sized arteries and multiple small clusters of lymphocytes. Beneath this layer is a fascial plane composed of mild amounts of collagen surrounding arteries, nerves and clusters of adipose tissue. The core of the biopsy contains a moderate band of large dense collagenous fascicles interpreted to be the tendon aponeurosis. Between the tendon aponeurosis and the oral side of the palate are abundant lobules of mucous gland. Few bands of collagen associated with ductal structures extend from the submucosa into the glands. Closer to the mucosal surface and within the dense collagenous stroma of the submucosa are multiple lymph aggregates and ducts. The oral mucosa is slightly folded, nonkeratinized stratified squamous epithelium with prominent rete pegs.

5RT 1-2 Two sections through the treated palate 5RT are examined. One portion of the biopsy (5RT1) is interpreted to be within normal limits and is not described. Changes are observed on section 5RT2. The

core of the biopsy is necrotic with moderate neutrophilic infiltrates at one margin. Outside of the neutrophilic zone are multiple regions of necrotic collagenous stroma.

Between the necrotic stroma and the viable submucosa of the oral mucosal epithelium are moderate bands of spindloid cells with plump nuclei interpreted to be fibroblasts and moderate amounts of dense irregular collagen. Mild to moderate infiltrates of neutrophils are among the fibroblasts at the interface of the necrotic stroma and many small blood vessels are observed within the fibroplastic tissue. Mucous glands in the region with the most inflammation and fibroplasia have mild interstitial fibrosis, edema (or freezing artifact) and mild infiltrates of lymphocytes and plasma cells. The submucosa in the region of inflammation has minimal numbers of infiltrating eosinophils, plasma cells and lymphocytes. The oral mucosa is unremarkable.

On the respiratory side, collagenous stroma and muscular fascicles are necrotic with moderate to marked neutrophil infiltrates. Neutrophilic infiltrates extend from the necrotic tissue to the submucosa and base of the mucosa. Some mucous glands in this region are mildly to moderately degenerated and infiltrated with mild numbers of neutrophils, lymphocytes and plasma cells. Muscle fascicles contain few myofibers separated by moderate numbers of spindloid cells, interpreted to be fibroblasts, mild to moderate amounts of irregular collagen and mild infiltrates of neutrophils and occasionally eosinophils. Many muscle fascicles adjacent to the necrotic stroma contain small myofibers with central plump and peripheral nuclei, a change associated with muscle hyperplasia or repair. Between the regenerating muscle and the submucosa are moderate bands of fibroblasts with moderate irregular dense collagen deposits. Mild interstitial infiltrates of lymphocytes and plasma cells are observed in the mucous glands in this region. In the submucosa are multifocal variably-sized clear spaces, most of which are lined with a simple endothelium. These clear spaces may represent vessels (lymphatic and /or vascular) that may have expanded because of freezing. The submucosa has mild diffuse to marked focal numbers of lymphocytes that often extend to the base of the mucosa. The respiratory mucosa occasionally contains small vacuoles that separate epithelial cells. No cilia are observed.

5RM 1-2 Two sections through the treated palate 5RM are examined. One portion of the biopsy (5RM2) is interpreted to be within normal limits and is not described. Changes are observed on section 5RM1. The core of the biopsy is mildly necrotic with moderate to marked neutrophilic infiltrates at one margin. Outside of the neutrophilic zone are multiple regions of necrotic stroma.

Between the necrotic stroma and the viable submucosa of the oral mucosal epithelium are moderate bands of spindloid cells with plump nuclei interpreted to be fibroblasts and moderate amounts of dense irregular collagen. Mild to moderate infiltrates of neutrophils are among the fibroblasts at the interface of the necrotic stroma and many small blood vessels are observed within the fibroplastic tissue. Mucous glands in the region with the most inflammation and fibroplasia have mild interstitial fibrosis, edema (or freezing artifact) and mild infiltrates of lymphocytes and plasma cells. The submucosa in the region of inflammation has minimal numbers of infiltrating eosinophils, plasma cells and lymphocytes. The oral mucosa is unremarkable.

On the respiratory side, collagenous stroma and muscular fascicles are necrotic with moderate to marked neutrophil infiltrates. Neutrophilic infiltrates extend from the necrotic tissue to the submucosa and base of the mucosa. Some mucous glands in this region are mildly to moderately degenerated and infiltrated with mild numbers of neutrophils, lymphocytes and plasma cells. Many muscle fascicles adjacent to the necrotic stroma contain small myofibers with central plump and peripheral nuclei, a change associated with muscle hyperplasia or repair. Viable muscle fascicles frequently contain few myofibers separated by moderate numbers of spindloid cells, interpreted to be fibroblasts, mild to moderate amounts of irregular collagen and mild infiltrates of neutrophils and occasionally eosinophils. Between the regenerating muscle and the submucosa are moderate bands of plump fibroblasts with moderate irregular collagen deposits. Mild interstitial infiltrates of lymphocytes and plasma cells are observed in the mucous glands in this region. In the submucosa are multifocal variably-sized clear

spaces, most of which are lined with a simple endothelium. These clear spaces may represent vessels (lymphatic and /or vascular) that may have expanded because of freezing. The submucosa also has mild diffuse to marked aggregates of lymphocytes that often extend to the base of the mucosa. No cilia are observed on respiratory mucosal epithelia.

5RB One section of the control palate 5RB is examined. No significant lesions are observed. The oral mucosa is slightly folded nonkeratinized stratified squamous epithelium with prominent rete pegs. The submucosa contains dense collagenous stroma with multiple lymph aggregates and ducts of mucous glands. Few bands of collagen associated with ductal structures extend from the submucosa into the glands. Between the submucosa are abundant lobules of mucous glands. No respiratory mucosa is present in the section.

6LT One section of the control palate 6LT is examined. The pseudostratified columnar ciliated epithelium on the respiratory side of the palate is absent in half of the section. The submucosa is moderately populated with tubuloalveolar mucous glands in a well-vascularized stroma of fine collagenous fibrils. In the region missing the mucosa, the submucosa contains several foci of necrotic stroma surrounded by and infiltrated with mild numbers of neutrophils. It is likely this is carryover damage from the treated portions of the same soft palate. Around the base of the mucous glands and diffusely within the stroma are mild infiltrates of lymphocytes and plasma cells. Deep to the submucosa are moderately-sized arteries and bands of dense collagen, tendons and abundant fascicles of skeletal muscle. Toward the oral side of the palate are many large lobules of mucous glands. Glandular lobules are separated from each other by small bands of dense connective tissue. Closer to the mucosal surface and within the dense collagenous stroma of the submucosa are multiple cross-sections of ducts – likely from the mucous glands. The oral mucosa is occasionally folded and composed of acanthotic non-keratinized stratified squamous epithelium with prominent rete pegs.

6LM One section through the treated palate 6LM is examined. The biopsy has mostly intact mucosa on the oral side. No mucosa is observed on the respiratory side. The core of the biopsy is extensively necrotic. Vessels in the necrotic core are distended and contain fibrillar eosinophilic material which may represent fibrin. Within the necrotic area are moderate numbers of coccobacillary bacterial colonies. Surrounding the necrotic core are abundant infiltrates of neutrophils. Outside of the neutrophil infiltrates, a wide zone of the collagenous stroma is necrotic.

Between the necrotic stroma and the viable submucosa of the oral mucosal epithelium is a mild band of spindloid cells with plump nuclei interpreted to be fibroblasts and mild amounts of dense irregular collagen. The submucosa is infiltrated with mild numbers of eosinophils and lymphocytes. Multifocal lymphoid nodules with lymphoid aggregates and germinal centers are observed. The mucosa is unremarkable.

Neutrophil infiltrates and collagen fibrils widely separate muscle fibers within many fascicles adjacent to the necrotic core on the respiratory side. Muscle fibers are small, most retain striations and have central nuclei consistent with regeneration. Some muscle fascicles contain myofibers separated by moderate numbers of fibroblasts and mild deposits of irregular collagen fibers, which are changes associated with fibroplasia. There is minimal submucosa and no respiratory mucosa present in the section.

In the palatine muscles distant from the treatment site is an intracytoplasmic cyst filled with banana-shaped protozoal organisms consistent with *Sarcocystis*. No inflammation was associated with the presence of the encysted protozoa.

6LB 1-2 Two sections through the treated palate 6LB are examined. The biopsy has a small portion of intact mucosa on the respiratory side and a limited amount of oral mucosa. The core of the biopsy is extensively necrotic. Within the necrotic tissue are multiple mineralized foci and coccobacillary bacterial colonies. Surrounding the necrotic core are abundant infiltrates of neutrophils. Outside of the zone of neutrophils is a wide zone of necrotic collagenous stroma. On the respiratory side is a broad region of

diffuse basophilia (representing degeneration) of muscle, fascia and mucosa. A small portion of viable respiratory mucosa is on one section.

Between the necrotic stroma and the viable submucosa of the oral mucosal epithelium is a moderate band of spindloid cells with plump nuclei interpreted to be fibroblasts and moderate amounts of dense irregular collagen. Some lobules of mucous glands are degenerated with loss and attenuation of glandular epithelium. The submucosa is infiltrated with mild numbers of eosinophils and lymphocytes. Occasional inflammatory cells are within the mucosa.

On the respiratory side, collagenous stroma and muscular fascicles are necrotic with moderate to marked neutrophil infiltrates. Neutrophilic infiltrates extend from the necrotic tissue to the submucosa and base of the mucosa. In this area, muscle fascicles are separated by moderate numbers of fibroblasts and mild deposits of irregular collagen which are changes associated with fibroplasia. Many myofibers in fascicles adjacent to the necrotic stroma are absent and some are small with central plump nuclei, a change associated with muscle hyperplasia or repair. Between the regenerating muscle and the submucosa are moderate bands of plump fibroblasts with moderate irregular collagen deposits. Between the regions of fibroplasia and the mucosa are numerous lobules of mucous glands, some with degenerated glandular epithelium, and all with moderate interstitial infiltrates of lymphocytes, neutrophils and few eosinophils. The submucosa is mildly edematous and moderately infiltrated with lymphocytes, plasma cells, neutrophils and few eosinophils. The respiratory mucosa is mildly infiltrated with granulocytes.

6RT One section of the control palate 6RT is examined. No significant lesions are observed. The pseudostratified columnar ciliated epithelium on the respiratory side of the palate is intermittently folded to form glandular-like pockets. The submucosa is moderately populated with tubuloalveolar mucous glands in a well-vascularized stroma of fine collagenous fibrils. Around the base of the mucous glands and diffusely within the submucosa are minimal infiltrates of lymphocytes, plasma cells and occasional eosinophils. Deep to the submucosa are moderately-sized arteries and bands of dense collagen, tendons and abundant fascicles of skeletal muscle. Skeletal myofibers occasionally contain cytoplasmic clear vacuoles which are most likely a consequence of ice crystal formation associated with freezing. Toward the oral side of the palate, abundant large lobules of mucous glands are adjacent to and occasionally separate the muscular fascicles. Glandular lobules are separated from each other by thick bands of dense connective tissue. Closer to the mucosal surface and within the dense collagenous stroma of the submucosa is an aggregate of lymphocytes, smaller bands of skeletal muscle and cross-section of ducts – likely from the mucous glands. The oral mucosa is slightly folded and composed of acanthotic non-keratinized stratified squamous epithelium with prominent rete pegs.

6RM 1-2 Two sections through the treated palate 6RM are examined. One portion of the biopsy (6RM2) is interpreted to be within normal limits and is not described. Changes are observed on section 6RM1. The core of the biopsy is extensively necrotic. Within the necrotic tissue are multiple mineralized foci and coccobacillary bacterial colonies. Surrounding the necrotic core are abundant infiltrates of neutrophils. Outside the zone of neutrophils on the respiratory side is a broad region of diffuse basophilia (representing degeneration) of muscle, fascia and portions of mucosa.

Between the necrotic stroma and the viable submucosa of the oral mucosal epithelium is a large region of stroma composed of spindloid cells with plump nuclei interpreted to be fibroblasts and moderate amounts of dense irregular collagen. In this area are a few muscle fascicles with mild to moderate interstitial infiltrates of plump fibroblasts, mild amounts of irregular collagen fibrils and mild infiltrates of plasma cells and lymphocytes. Between the fibroplastic regions and mucosa is abundant regular collagenous stroma with a single lobule of mucous glands. Stroma and submucosa are infiltrated with minimal numbers of eosinophils and lymphocytes.

On the respiratory side, collagenous stroma and muscular fascicles are necrotic with moderate to marked neutrophil infiltrates. Neutrophilic infiltrates extend from the necrotic tissue to the submucosa

and base of the mucosa. In this area, muscle fascicles are separated by moderate numbers of spindloid cells or fibroblasts and mild deposits of irregular collagenous fibers. Many myofibers in fascicles adjacent to the necrotic stroma are absent and some are small with central plump nuclei, a change associated with muscle hyperplasia or repair. Between the regenerating muscle and the submucosa are moderate bands of plump fibroblasts with moderate irregular collagen deposits. Between the regions of fibroplasia and the mucosa are numerous lobules of mucous glands, some with degenerated glandular epithelium, and all with mild interstitial infiltrates of lymphocytes, neutrophils and few eosinophils. The submucosa is mildly edematous and moderately infiltrated with lymphocytes, plasma cells, neutrophils and few eosinophils. The respiratory mucosa shows the transition from pseudostratified columnar to stratified squamous epithelium in this region. The mucosa is mildly infiltrated with granulocytes.

In the palatine muscles distant from the treatment site is an intracytoplasmic cyst filled with banana-shaped protozoal organisms consistent with *Sarcocystis*. No inflammation was associated with the presence of the encysted protozoa.

6RB One section through the treated palate 6RB is examined. The core of the biopsy is extensively necrotic. Within the necrotic tissue are multiple mineralized foci. Surrounding the necrotic core are abundant infiltrates of neutrophils. Outside the zone of neutrophils on the respiratory side is a broad region of diffuse basophilia (representing degeneration) of muscle, fascia and portions of mucosa.

Between the necrotic stroma and the viable submucosa of the oral mucosal epithelium is a large region of stroma composed of spindloid cells with plump nuclei interpreted to be fibroblasts and moderate amounts of dense irregular collagen. In this area are a few muscle fascicles with mild to moderate interstitial infiltrates of plump spindloid cells, mild amounts of collagenous fibers and mild infiltrates of plasma cells and lymphocytes. Between the fibroplastic regions and mucosa is abundant regular collagenous stroma. Stroma and submucosa are infiltrated with mild numbers of plasma cells, lymphocytes and minimal numbers of eosinophils.

On the respiratory side, necrosis of the stroma with moderate neutrophil infiltrates partially extends to the submucosa only in the region with viable mucosa. In this area, muscle fascicles are separated by moderate numbers of fibroblasts and mild to moderate deposits of irregular collagenous fibers. Many myofibers in fascicles adjacent to the necrotic stroma are absent and some are small with central plump nuclei, a change associated with muscle hyperplasia or repair. Between the regions of fibroplasia and the mucosa are numerous lobules of mucous glands, one with degenerated glandular epithelium and the others with mild interstitial infiltrates of lymphocytes, neutrophils and few eosinophils. The submucosa is moderately infiltrated with lymphocytes, plasma cells, neutrophils and few eosinophils. The respiratory mucosa shows the transition from pseudostratified columnar to stratified squamous epithelium in this region. The mucosa is mildly infiltrated with granulocytes.

APPENDIX D1: Mechanical testing study notes

Table 4.10: Mechanical testing study sample notes

Patient #	Date Received	Date Thawed	Injection Type	Date Injected	Qty Injected	Time Injected	Top (cm)	Side (cm)	Notes	Date Tested	Time Tested	Length (cm)	Width (cm)	Depth (cm)	Length (cm)	Width (cm)	Depth (cm)	Gage Length	Blue Area	Notes
SPTest1G	17-Jun	30-Jun	GENIPIN	30-Jun	0.5 ml	6:30 PM			Test Sample	1-Jul	8:45 AM	8	3	1				50	1 x 1 cm square	tore to left side, slightly lower than middle
SP1TLG	17-Jun	6-Jul	GENIPIN	7-Jul	0.5 ml	6:30 PM	3	3	bad sample, black/orange spot on palate	8-Jul	12:00 PM	8	3.5	1	1.5	1.5	1	45	-	delay b/t of tensile test technical difficulties, broke in middle, some blue on top only
SP1BLG	17-Jun	6-Jul	GENIPIN	7-Jul	0.5 ml	6:30 PM	4	2	bad sample, black/orange spot on palate	8-Jul	12:20 PM	8	3.5	0.5	1	1	0.5	45		delay b/t of tensile test tech difficulties, tore in middle, no noticable blue on outside
SP1TNC	17-Jun	6-Jul	CONTROL	7-Jul	N/A	6:00 PM	N/A	N/A	palate poorly cut- only one section, bad sample	8-Jul	11:40 AM	7.5	4	0.5	1	0.5	0.5	45	N/A	delay b/t of tensile test tech difficulties, tore in middle
SP1TLB	17-Jun	13-Jul	BUFFER	14-Jul	0.5 ml	6:00 PM		5	very deep notch	15-Jul	8:10 AM	10	2.5	0.5	1	1	0.5	45	N/A	tore high close to grip, may have torn in the grip
SP1BLB	17-Jun	13-Jul	BUFFER	14-Jul	0.5 ml	6:00 PM	4	3		15-Jul	8:30 AM	8.5	3	0.5	1.5	1	0.5	45	N/A	tore diagonally along the fibers on the top membrane, tore in middle
SP2TNG	17-Jun	13-Jul	GENIPIN	14-Jul	0.5 ml	6:30 PM	3	3	small sample, deep notch, visible bubble at injection site	15-Jul	8:45 AM	7	2.5	0.5	1	1	0.5	45	1.5 x 2 cm square front and back	tore in middle
SP2BRG	17-Jun	13-Jul	GENIPIN	14-Jul	0.5 ml	6:30 PM	4	3	small sample, missing part on right side, small bubble at injection site	15-Jul	9:30 AM	8	2	0.5	1	1	0.5	45	1 x .5 cm front and back, off centered	small tear on front about 1/2 cm circle, tore high, 1-2 large white fibers were last to tear, a few blue fibers present
SP3TLC	17-Jun	13-Jul	CONTROL	14-Jul	N/A	6:30 PM	N/A	N/A	small notch.	15-Jul	9:50 AM	6.5	2.5	0.5	1	1	0.5	45	N/A	very pale white, small tears during hysteresis test on edge
SP3BLC	17-Jun	13-Jul	CONTROL	14-Jul	N/A	6:30 PM	N/A	N/A	very thick sample --> fatty like	15-Jul	10:10 AM	7.5	3.5	1	1	1	1	45	N/A	thicker, bottom layer separating, top layer tore in grips, bulk of material tore in middle
SP3TRB	17-Jun	13-Jul	BUFFER	14-Jul	0.5 ml	6:30 PM	2.5	3	small notch, small sample, bubble formed at injection site	15-Jul	10:50 AM	5	3	0.5	1	1	0.5	42	N/A	*moved crosshead down. Stress relax test repeated twice b/c forgot to record, tore slightly higher than middle, larger tissue tore first then membrane tore. No tensile test video
SP3BRB	17-Jun	13-Jul	BUFFER	14-Jul	0.5 ml	6:30 PM	3	1.5	thick sample --> fatty like, small bubble formation at injection site.	15-Jul	10:30 AM	6	3	0.5	1	1	0.5	42	N/A	small tear near grips, tore in middle diagonally along fibers
SP4TLG	17-Jun	20-Jul	GENIPIN	21-Jul	0.5 ml	6:00 PM	5.5	3	dragged needle while applying slow and steady pressure for injection, small bubble at injection site	22-Jul	8:25 AM	10	2	0.5	1	1	0.5	45	1.5 cm circle, front and back	blue fibers after tear: 50-60%, slipped during 1st tensile test, small rip during that test. Tensile test repeated
SP4BLG	17-Jun	20-Jul	GENIPIN	21-Jul	0.5 ml	6:00 PM	5.5	3	thicker at bottom of sample, dragged needle while applying slow and steady pressure	22-Jul	8:45 AM	8	2	0.5	1	1	0.5	42	2 x 1 cm oval, front and back	tore in middle, blue fibers after tear: 70-80%
SP4TNC	17-Jun	20-Jul	CONTROL	21-Jul	N/A	6:00 PM	N/A	N/A	very thin, deep notch	22-Jul	9:05 AM	7.5	2	0.5	3.25	1	0.5	42	N/A	failed near grips
SP4BRC	17-Jun	20-Jul	CONTROL	21-Jul	N/A	6:00 PM	N/A	N/A	small sample (part of soft palate missing), thicker at bottom	22-Jul	10:15 AM	5	2.5	0.5	6.75	1	0.5	42	N/A	failed diagonally along fibers
SP5BLB	20-Jul	30-Jul	BUFFER	31-Jul	0.5 ml	6:45 PM	2.5	3	only one sample from soft palate side b/c soft palate was split on part leg, very wrinkled, injected via drag and inject method	22-Jul	10:30 AM	8.5	4	0.5	1.5	1	0.5	42	N/A	one strand did not break until almost full distance
SP5TNG	20-Jul	30-Jul	GENIPIN	31-Jul	0.5 ml	6:45 PM	3.5	3	only one sample from soft palate side b/c mucous layer was separating from palate at the bottom, drag and inject method applied, very thin sample, some may have leaked through tissue	22-Jul	10:50 AM	8	3.5	0.5	1.5	1	0.5	42	1 cm square on back, none on front, small blue spot on bottom	genipin appeared to have leaked out, blue fibers at end: 10%, broke low close to the grips, pulled fibers from grips first, did not break in injection region.
SP6TLC	20-Jul	27-Jul	CONTROL	28-Jul	N/A	6:00 PM	N/A	N/A	forgot to take pictures. Nothing notable about palate	29-Jul	8:15 AM	10	2.8	1	1	1	1	42	N/A	tore in middle
SP6BLC	20-Jul	27-Jul	CONTROL	28-Jul	N/A	6:00 PM	N/A	N/A	forgot to take pictures. Nothing notable about palate	29-Jul	8:30 AM	7.5	3	0.7	1.2	1	0.7	42	N/A	tore high
SP6TRB	20-Jul	27-Jul	BUFFER	28-Jul	0.5 ml	6:00 PM	5	3	hole in side of soft palate that ended up being at location of cut between samples, bubble at injection site, slow and steady injection, dragged injection	29-Jul	8:50 AM	9	2.5	0.5	1	0.5	0.5	42	N/A	failed in middle
SP6BRB	20-Jul	27-Jul	BUFFER	28-Jul	0.5 ml	6:00 PM	6	3	hole in soft palate on edge of sample, thicker at bottom, bottom layer coming off, small oval bubble at injection site, slow and steady injection, dragged injection	29-Jul	9:15 AM	10	2	0.5	1	1	0.5	42	N/A	very narrow palate (width), failed in middle-diagonally along main fibers
SP7TLG	20-Jul	27-Jul	GENIPIN	28-Jul	0.5 ml	6:30 PM	6	3	very dark color, wide v, large injection bubble	29-Jul	10:25 AM	11	2.5	0.5	1	1	0.5	42	2.5 x 1 cm oval/rect. Front and back	dark gray palate, failed in middle, about 75% blue fibers at end, last fiber was not blue
SP7NLG	20-Jul	27-Jul	GENIPIN	28-Jul	0.5 ml	6:30 PM	5	3	very dark color, very short palate, very thick, no injection bubble	29-Jul	10:45 AM	6	3.5	0.8	1	1	0.5	42	2 x 1 cm rect. Front only	tore high, above blue area, %blue=0
SP7TRC	20-Jul	27-Jul	CONTROL	28-Jul	N/A	6:30 PM	N/A	N/A	very dark color, wide v	29-Jul	11:00 AM	12.5	2	0.6	1	0.8	0.6	42	N/A	tore in middle, large fiber breakerear clamps on top layer first about halfway through test
SP7BRC	20-Jul	27-Jul	CONTROL	28-Jul	N/A	6:30 PM	N/A	N/A	very dark color, thick sample	29-Jul	11:20 AM	8.5	3	0.8	1	1	0.8	42	N/A	necking of top fiber layer is slightly wider, tore in middle, tear in top layer first
SP8TLB	20-Jul	30-Jul	BUFFER	31-Jul	0.5 ml	5:50 PM	5	3	very large bubble, thin sample, healthy color	1-Aug	8:25 AM	11.5	2	0.5	1	1	0.5	42	N/A	tore diagonally along fibers in middle
SP8BLB	20-Jul	30-Jul	BUFFER	31-Jul	0.5 ml	5:50 PM	3	1.5	slight bubble formed just above injection site, healthy color	1-Aug	8:40 AM	7.5	3.2	0.7	1	1	0.7	42	N/A	hysteresis done twice (forgot to set preload value) tore in middle, 1 fiber held on for a long time
SP8TNG	20-Jul	30-Jul	GENIPIN	31-Jul	0.5 ml	5:25 PM	5	3	very large bubble, very thin, healthy color	1-Aug	9:00 AM	11	2	0.4	1	1	0.4	42	2.2x2 cm, all blue when cut, front and back, edge to edge	%blue:100% at end, tore in middle
SP8BRG	20-Jul	30-Jul	GENIPIN	31-Jul	0.5 ml	5:25 PM	2.5	3	small bubble at 3 cm	1-Aug	9:15 AM	6.5	1	0.7	1	1	0.7	42	2 x 1.5 cm off centered circle, front and back	tore below blue area, %blue=0
SP9TLC	20-Jul	30-Jul	CONTROL	31-Jul	N/A	5:45 PM	N/A	N/A	small palate (foal sized?), only 2 samples total	1-Aug	9:30 AM	7.5	3	0.7	1	1	0.7	42	N/A	tore in middle
SP9TRB	20-Jul	30-Jul	BUFFER	31-Jul	0.5 ml	5:50 PM	4	1.2	small palate (foal size?), only 2 samples total, slight bulge at injection site	1-Aug	9:45 AM	6.5	2.5	1	1	1	1	42	N/A	tore in middle, layers tore first from inside clamps
SP10TLG	20-Jul	30-Jul	GENIPIN	31-Jul	0.5 ml	6:15 PM	3	3	black spots on palate, horrible smell, slight bubble at injection site	1-Aug	10:00 AM	9	2.5	0.5	1	1	0.5	42	2x2 front and back, more prominent in front	tore in middle, top blue layer tore off first, %blue=50%
SP10BLG	20-Jul	30-Jul	GENIPIN	31-Jul	0.5 ml	6:15 PM	2	3	black spots on palate, horrible smell, very short and very thick	1-Aug	10:15 AM	6.5	3	0.8	1	1	0.8	42	2x2 oval/rect, diagonal shaped, front and back, small blue spot at bottom	%blue=50%, layers tore apart from within clamps first
SP10TRC	20-Jul	30-Jul	CONTROL	31-Jul	N/A	6:15 PM	N/A	N/A	very smelly, black spots on palate	1-Aug	10:30 AM	10	1.5	0.5	1	1	0.5	42	N/A	very flimsy and narrow, difficult to neck down, tore in middle
SP10BRC	20-Jul	30-Jul	CONTROL	31-Jul	N/A	6:15 PM	N/A	N/A	very smelly, black spots on palate	1-Aug	10:45 AM	6	3	0.7	1	1	0.7	42	N/A	tore in middle, top layer tore first, stress relax and hysteresis in one file
SP11TLC	29-Jul	3-Aug	CONTROL	4-Aug	N/A	5:35 PM	N/A	N/A	very flimsy, healthy apperance	5-Aug	8:25 AM	9.5	2.2	0.4	1	1	0.4	42	N/A	tore in two layers- top layer tore first in middle, bottom layer tore slightly lower than middle
SP11BLC	29-Jul	3-Aug	CONTROL	4-Aug	N/A	5:35 PM	N/A	N/A	very thick and short, healthy apperance	5-Aug	8:40 AM	6.5	3.5	0.7	1	1	0.7	42	N/A	very thick and short, difficult to get into grips, tore in middle diagonally, two large strands held onto until the end
SP11TRG	29-Jul	3-Aug	GENIPIN	4-Aug	0.5 ml	5:45 PM	5	3	very flimsy, healthy apperance, small bubble at injection site	5-Aug	9:00 AM	10	2.5	0.5	1	1	0.5	42	1 1/2 x 2 front and back oval, necked area completely blue	tore in middle, 1 strand on top layer was not blue, %blue fibers=80%
SP11BRG	29-Jul	3-Aug	GENIPIN	4-Aug	0.5 ml	5:45 PM	4	3	thicker, healthy apperance , no bubble formation	5-Aug	9:25 AM	8	2	0.6	1	1	0.6	42	2x2 cm diagonal square on front and back	top layer tore below the blue area, bottom layer tore in middle blue area. %blue=50%
SP12TLG	29-Jul	3-Aug	GENIPIN	4-Aug	0.5 ml	6:15 PM	6	3	very dark and unhealthy looking, black spots on palate, bubble at 5 cm	5-Aug	10:35 AM	10	2.2	0.5	1	1	0.5	42	2.8x1.5 diagonal square on front and back	very dark pallate, difficult to see blue on back, tore in middle, 80% blue fibers
SP12BLG	29-Jul	3-Aug	GENIPIN	4-Aug	0.5 ml	6:15 PM	4	3	very dark and unhealthy looking, very thick	5-Aug	11:00 AM	6.5	3	1	1	1	1	42	2x1cm diagonal on front only	tore in middle, top tore behed blue and fibers were all pink, bottom tore in blue area. %blue=50%
SP12TRB	29-Jul	3-Aug	BUFFER	4-Aug	0.5 ml	6:00 PM	6	3	very dark with black spots, thin specimen, slight bulge at 5 cm	5-Aug	11:20 AM	9.3	2.5	0.5	1	0.5	0.5	42	N/A	tore in middle, 1 layer tore first from clamps, very dark palate
SP12BRB	29-Jul	3-Aug	BUFFER	4-Aug	0.5 ml	6:00 PM	4.5	3	very dark with black spots, very thick, no bubble formation	5-Aug	11:40 AM	6.5	3	0.8	1	1	0.8	42	N/A	tore in middle, good tensile test

APPENDIX D2: Mechanical testing study raw data

Table 4.11: Raw data from mechanical testing study for each individual sample

	Palate #	Date	% Blue Fibers at failure	Length mm	Width mm	Thickness mm	Cross Section mm^2	Ulitmate Tensile Stress mpa	Strain at Ultimate Tensile Stress	Yield Point Strain	Yield Point Stress mpa	Young's Modulus - Linear Region mpa	Resilience J/m^3
CONTROL	SP1TRC	7/8/15		45	40	5	200						
2	SP3TLC	7/15/15		45	25	5	125	0.3680264	0.749704	0.46	0.1750264	1.3318	0.202242623
3	SP3BLC	7/15/15		45	35	10	350	0.11035086	0.227113	0.22711333	0.11035086	0.8632	0.010484364
4	SP4TRC	7/22/15		42	20	5	100	0.263514	0.476467	0.46932857	0.256943	2.4464	0.02285769
5	SP4BRC	7/22/15		42	25	5	125	0.2277216	0.326950	0.33072381	0.2244784	2.1341	0.01792581
6	SP6TLC	7/29/15		42	28	10	280	0.16726107	0.481340	0.48424048	0.16670107	1.283	0.013767576
7	SP6BLC	7/29/15		42	30	7	210	0.14155238	0.385902	0.38065476	0.13964429	1.359	0.011361698
8	SP7TRC	7/29/15		42	20	6	120	0.51384583	0.487314	0.33721429	0.34179	2.6766	0.145335239
9	SP7BRC	7/29/15		42	30	8	240	0.17888375	0.556300	0.48188333	0.14773375	1.0336	0.03373816
10	SP9TLC	8/1/15		42	25	10	250	0.153648	0.609419	0.45446429	0.1248064	0.7626	0.055667221
11	SP10TRC	8/1/15		42	15	5	75	1.11024	0.251757	0.19250476	0.958868	8.722	0.14223771
	SP10BRC	8/1/15		42	30	7	210	0.17202429	0.410605	0.29810238	0.15756095	1.3885	0.04951773
	SP11TLC	8/5/15		42	22	4	88	0.55899773	0.300621	0.29254524	0.51584318	4.7109	0.034229829
	SP11BLC	8/5/15		42	35	7	245	0.1434698	0.475198	0.45082381	0.1379347	1.0316	0.01713889
			AVERAGE	42.6429	27.1429	6.7143	187.0000	0.3161	0.4414	0.3738	0.2660	2.2879	0.0582
			ST. DEV	1.2774	6.8147	2.0913	82.5917	0.2788	0.1476	0.1012	0.2364	2.2093	0.0630
BUFFER	SP2TLB	7/15/15		45	25	5	125	0.3642504	0.885338	0.71677556	0.2484248	1.6091	0.176233195
2	SP2BLB	7/15/15		45	30	5	150	0.22048733	0.654384	0.36366	0.17339533	1.5741	0.25863594
3	SP3TRB	7/15/15		42	30	5	150	0.11688867	0.329414	0.33509048	0.11029	1.2038	0.009497846
4	SP3BRB	7/15/15		42	30	5	150	0.32885067	0.485493	0.32965714	0.21459733	1.2841	0.08258872
5	SP5BLB	7/22/15		42	40	5	200	0.4264685	0.463781	0.31601667	0.247773	1.5189	0.092014677
6	SP6TRB	7/29/15		42	25	5	125	0.2836512	0.436807	0.38751667	0.243832	1.7975	0.038462633
7	SP6BRB	7/29/15		42	20	5	100	0.261479	0.430305	0.4	0.255185	1.9637	0.032365978
8	SP8TLB	8/1/15		42	20	5	100	0.255138	0.409195	0.39393571	0.246862	2.4646	0.0210602
9	SP8BLB	8/1/15		42	32	7	224	0.16688884	0.633140	0.54394286	0.14012723	1.1324	0.032769266
10	SP9TRB	8/1/15		42	30	7	210	0.15781762	0.358905	0.36085476	0.14976476	1.2153	0.014681915
11	SP12TRB	8/5/15		42	25	5	125	0.518708	0.329288	0.2899	0.4876104	3.4361	0.065184478
12	SP12BRB	8/5/15		42	30	8	240	0.21155	0.503024	0.47948095	0.2036425	1.223	0.028748284
			AVERAGE	42.5000	28.0833	5.5833	158.2500	0.2760	0.4933	0.4097	0.2268	1.7019	0.0710
			ST. DEV	1.1677	5.5179	1.0836	48.3681	0.1173	0.1613	0.1197	0.0958	0.6700	0.0752
GENIPIN	SP1BLG	7/8/15	minimal	45	35	5	175	0.18278	0.371998	0.28871333	0.17119714	1.3199	0.0390068
2	SP1TLG	7/8/15	minimal	45	35	10	350	0.07592943	0.296747	0.30838667	0.07266143	0.5478	0.01730633
3	SP2TRG	7/15/15		45	25	5	125	0.310544	0.363831	0.29251333	0.2861432	2.3202	0.054671746
4	SP2BRG	7/15/15		45	20	5	100	0.28809	0.424411	0.25775556	0.237171	2.2613	0.14119571
5	SP4TLG	7/22/15	50-60	45	20	5	100	0.486347	0.293109	0.27092667	0.463819	2.9275	0.05544
6	SP4BLG	7/22/15	70-80	42	20	5	100	0.283626	0.340588	0.33493095	0.280455	2.3176	0.025266773
7	SP5TRG	7/22/15	10	42	35	5	175	0.407752	0.487329	0.46399762	0.38104286	2.0994	0.0514932
8	SP7TLG	7/29/15	75	42	25	5	125	0.510244	0.438943	0.38466667	0.4754448	3.8168	0.087108173
9	SP7BLG	7/29/15	minimal	42	35	8	280	0.11273179	0.465300	0.40437143	0.09276143	0.6052	0.018199907
10	SP8TRG	8/1/15	100	42	20	4	80	0.46565125	0.269817	0.24298333	0.40545375	3.9628	0.039420044
11	SP8BRG	8/1/15	minimal	42	10	7	70	0.22234857	0.421598	0.40030476	0.21529	1.6624	0.028817463
12	SP10TLG	8/1/15	50	42	25	5	125	0.5663784	0.263874	0.20842381	0.4733216	4.0995	0.068486771
13	SP10BLG	8/1/15	50	42	30	8	240	0.24996125	0.427731	0.22091458	0.22091458	1.2468	0.03621215
14	SP11TRG	8/5/15	80	42	25	5	125	0.5431136	0.204895	0.1537881	0.426588	4.7819	0.054662708
15	SP11BRG	8/5/15	50	42	20	6	120	0.27553	0.332688	0.29170238	0.24668333	1.9126	0.034544733
16	SP12TLG	8/5/15	80	42	22	5	110	0.54319545	0.276352	0.23241905	0.45863273	3.4349	0.061227815
17	SP12BLG	8/5/15	50	42	30	10	300	0.12803567	0.415195	0.40942857	0.12680133	0.8106	0.015873338
			AVERAGE	42.8824	25.4118	6.0588	158.8235	0.3325	0.3585	0.3039	0.2961	2.3604	0.0488
			ST. DEV	1.4090	7.0981	1.8531	83.3766	0.1635	0.0819	0.0847	0.1388	1.2969	0.0308

Toe Region -Slope	Toughness - Entire Curve	Energy - Entire Curve	Cyclical Hysteresis (pa*e)		Change in Hysteresis	Hystresis Ratio	Min	Max	Stress Relaxation	Relaxation Modulus
mpa	mpa*strain	Joules	1st cycle	20th cycle	1st-20th	20/1	Mpa	Mpa	Mpa	Mpa
					0	#DIV/0!				
0.9972	5.007449783	28.16690503	0.0054213	0.00126623	0.00415507	0.23356575	0.0674352	0.0841784	0.0167432	0.044435184
5.6722	0.077395924	1.218985803	0.00202159	0.00069409	0.0013275	0.34333866	0.025224	0.02963286	0.004408857	0.041720698
0.9492	0.33916574	1.424496108	0.01052602	0.00075324	0.00977278	0.07155981	0.09041	0.107819	0.017409	0.043628383
2.1442	0.22570165	1.184933663	0.00918219	0.0012184	0.00796379	0.13269166	0.0752904	0.0848448	0.009554	0.037298059
5.593	0.452761496	5.324475193	0.0028672	0.00121229	0.00165491	0.4228132	0.03710821	0.03929	0.002181786	0.005846973
5.911	0.618956178	5.45919349	0.00485223	0.00091501	0.00393722	0.18857515	0.04436476	0.05152905	0.007164286	0.023590343
3.2902	5.468984479	27.56368177	0.00722487	0.00226314	0.00496173	0.31324301	0.08256083	0.09012	0.007559167	0.030862971
1.0714	0.31365863	3.16167899	0.0035201	0.00085315	0.00266695	0.24236527	0.03881375	0.04545375	0.00664	0.018469344
1.1998	0.590810541	6.203510681	0.00302699	0.00072394	0.00230305	0.23916168	0.0367244	0.041716	0.0049916	0.015301415
24.506	18.95910791	59.72118992	0.0123449	0.0048859	0.007459	0.39578287	0.129104	0.14409567	0.014990667	0.170010109
2.9596	0.33007206	2.911235569	0.00414695	0.00093929	0.00320766	0.2265014	0.0433281	0.04295238	0.005967143	0.028516241
13.5066	0.227478709	0.840761308	0.01041757	0.00442886	0.00598871	0.42513369	0.10776705	0.11687159	0.009104545	0.04292754
1.1954	0.13703524	1.41009262	0.00331113	0.00084969	0.00246144	0.25661632	0.03934694	0.04380327	0.004456327	0.012810824
5.3074	2.5191	11.1224	0.0061	0.0016	0.0045	0.2686	0.0629	0.0709	0.0086	0.0396
6.7409	5.2704	17.4028	0.0035	0.0014	0.0026	0.1082	0.0321	0.0361	0.0049	0.0412
3.6538	1.802022385	10.13637592	0.00747343	0.00153253	0.0059409	0.20506381	0.0666456	0.084484	0.0178384	0.029723279
1.7576	0.65245932	4.40410041	0.00615503	0.00091165	0.00524338	0.14811463	0.05696867	0.06996333	0.012994667	0.044975045
2.4936	0.063718976	0.401429549	0.00663155	0.00086908	0.00576247	0.13105232	0.05746933	0.06819667	0.010727333	0.03827115
3.2746	0.55628018	3.504565134	0.00629072	0.00122269	0.00506803	0.19436408	0.05843733	0.07039933	0.011962	0.058037397
3.521	0.880617557	7.397187479	0.00317604	0.00114901	0.00202703	0.36177441	0.0483805	0.0542255	0.005845	0.033208166
5.0036	1.883156153	9.886569803	0.00650406	0.00192521	0.00457885	0.29600127	0.0737608	0.0866864	0.0129256	0.044311491
2.8786	0.835688638	3.50989228	0.00805687	0.00171703	0.00633984	0.21311378	0.095676	0.108819	0.013143	0.041148054
8.0412	0.25407878	1.067130876	0.00968556	0.00167233	0.00801323	0.17266219	0.093118	0.103182	0.010064	0.030176898
0.6218	0.433509706	4.078459314	0.004385035	0.000813576	0.003571459	0.18553467	0.0433067	0.0494817	0.006175	0.013798667
2.0146	0.107533185	0.948442692	0.00370251	0.00103191	0.0026706	0.27870553	0.04310333	0.05039619	0.007292857	0.028038631
6.245	0.368002808	1.932014742	0.0069986	0.00189485	0.00510375	0.27074701	0.0777888	0.0873648	0.009576	0.057393756
1.0984	0.406534884	4.097871631	0.00374423	0.00084283	0.0029014	0.22510102	0.03650875	0.04328667	0.006777917	0.020310998
3.3837	0.6870	4.2803	0.0061	0.0013	0.0048	0.2235	0.0626	0.0730	0.0104	0.0366
2.1537	0.5961	3.2851	0.0020	0.0004	0.0017	0.0669	0.0193	0.0214	0.0036	0.0135
3.4988	0.45719802	3.600434408	0.00529066	0.00098368	0.00430698	0.18592765	0.04856	0.057276	0.008716	0.171525715
1.3742	0.08253711	1.299959483	0.00200218	0.0004233	0.00157888	0.21141955	0.02496629	0.03048686	0.005520571	0.027588873
3.8934	0.260762246	1.466787634	0.00602158	0.00163861	0.00438297	0.27212293	0.0781448	0.0887592	0.0106144	0.051637719
4.567	0.52080357	2.343616065	0.00934515	0.00154501	0.00780014	0.16532747	0.093878	0.104006	0.010128	0.023135676
11.5156	0.25904068	1.16568306	0.00843558	0.00190687	0.00652871	0.22605085	0.070481	0.107288	0.036807	0.127907999
2.9036	1.520331603	6.385392733	0.00688308	0.00243382	0.00444926	0.35359461	0.100486	0.108448	0.007962	0.031360144
1.3316	0.52205126	3.837076761	0.00609898	0.00159337	0.00450561	0.26125188	0.05252171	0.05902114	0.00699429	0.021392439
11.0728	5.120691013	26.88362782	0.00647345	0.00239754	0.00407591	0.37036511	0.0757296	0.083204	0.0074744	0.027325026
1.5316	0.698114677	8.2098286	0.00255586	0.00033647	0.00221939	0.13164649	0.02960679	0.03839893	0.008792143	0.030768167
8.2272	0.469282104	1.576787869	0.0114957	0.00283499	0.00866071	0.24661308	0.12612625	0.13665125	0.010525	0.059763057
1.272	0.226853733	0.666949975	0.01170408	0.0017923	0.00991178	0.15313463	0.12485429	0.14736	0.022505714	0.063866745
15.2316	0.572448461	3.00535442	0.00695574	0.00265164	0.0043041	0.38121609	0.0764688	0.0836576	0.0071888	0.068345129
2.3258	0.49221899	4.961567419	0.00342053	0.00108951	0.00233102	0.31852081	0.039495	0.04546042	0.005965417	0.018643453
23.842	0.231183918	1.21371557	0.00809808	0.00316115	0.00493693	0.39035796	0.0778168	0.0848624	0.0070456	0.095756202
4.144	0.294262553	1.483083267	0.00663853	0.00183862	0.00479991	0.27696192	0.07747	0.08535917	0.007889167	0.038924903
12.0744	0.474792905	2.193543221	0.00707158	0.0028294	0.00424218	0.4001086	0.08705545	0.09649273	0.009437273	0.076140417
1.604	0.178141628	2.244584513	0.00284171	0.00057305	0.00226866	0.20165675	0.02977467	0.03445233	0.004677667	0.017561396
6.4947	0.7283	4.2669	0.0065	0.0018	0.0048	0.2674	0.0714	0.0818	0.0105	0.0560
6.3321	1.1763	6.1739	0.0028	0.0009	0.0023	0.0883	0.0308	0.0341	0.0078	0.0426

APPENDIX D3: Summarized data with outliers removed

Table 4.12: Individual sample data with outliers removed from mechanical testing study

Averages without Outliers
Outlier = +/- 3 st.dev away from mean in more than 6 categories
Outliers: SP10TRC, SP3TRB,SP1TLG,SP7BLG, SP12BLG. SP1TRC removed because missing tensile data

		% Blue Fibers at failure	Cross Section mm^2	Ulitmate Tensile Stress mpa	Strain at Ultimate Tensile Stress	Yield Point Strain	Yield Point Stress mpa	Young's Modulus - Linear Region mpa	Resilience mpa*strain	Slope - Toe Region mpa
CONTROL TOPS	SP3TLC		125.0000	0.3680	0.7497	0.4600	0.1750	1.3318	0.2022	0.9972
	SP4TRC		100.0000	0.2635	0.4765	0.4693	0.2569	2.4464	0.0229	0.9492
	SP6TLC		280.0000	0.1673	0.4813	0.4842	0.1667	1.2830	0.0138	5.5930
	SP7TRC		120.0000	0.5138	0.4873	0.3372	0.3418	2.6766	0.1453	3.2902
	SP9TLC		250.0000	0.1536	0.6094	0.4545	0.1248	0.7626	0.0557	1.1998
	SP11TLC		88.0000	0.5590	0.3006	0.2925	0.5158	4.7109	0.0342	13.5066
		AVERAGE	160.5000	0.3375	0.5175	0.4163	0.2635	2.2019	0.0790	4.2560
		ST. DEV	82.5924	0.1728	0.1505	0.0805	0.1458	1.4320	0.0769	4.8824
CONTROL BOTTOMS	SP3BLC		350.0000	0.1104	0.2271	0.2271	0.1104	0.8632	0.0105	5.6722
	SP4BRC		125.0000	0.2277	0.3270	0.3307	0.2245	2.1341	0.0179	2.1442
	SP6BLC		210.0000	0.1416	0.3859	0.3807	0.1396	1.3590	0.0114	5.9110
	SP7BRC		240.0000	0.1789	0.5563	0.4819	0.1477	1.0336	0.0337	1.0714
	SP10BRC		210.0000	0.1720	0.4106	0.2981	0.1576	1.3885	0.0495	2.9596
	SP11BLC		245.0000	0.1435	0.4752	0.4508	0.1379	1.0316	0.0171	1.1954
		AVERAGE	230.0000	0.1623	0.3970	0.3616	0.1530	1.3017	0.0234	3.1590
		ST. DEV	72.8697	0.0403	0.1145	0.0958	0.0384	0.4563	0.0153	2.1528
CONTROL OVERALL		AVERAGE	195.2500	0.2499	0.4572	0.3889	0.2082	1.7518	0.0512	3.7075
		ST. DEV	82.6539	0.1506	0.1422	0.0890	0.1169	1.1170	0.0603	3.6428
BUFFER TOPS	SP2TLB		125.0000	0.3643	0.8853	0.7168	0.2484	1.6091	0.1762	3.6538
	SP6TRB		125.0000	0.2837	0.4368	0.3875	0.2438	1.7975	0.0385	5.0036
	SP8TLB		100.0000	0.2551	0.4092	0.3939	0.2469	2.4646	0.0211	8.0412
	SP9TRB		210.0000	0.1578	0.3589	0.3609	0.1498	1.2153	0.0147	2.0146
	SP12TRB		125.0000	0.5187	0.3293	0.2899	0.4876	3.4361	0.0652	6.2450
		AVERAGE	137.0000	0.3159	0.4839	0.4298	0.2753	2.1045	0.0631	4.9916
		ST. DEV	42.2197	0.1353	0.2283	0.1656	0.1259	0.8708	0.0662	2.3197
BUFFER BOTTOMS	SP2BLB		150.0000	0.2205	0.6544	0.3637	0.1734	1.5741	0.2586	1.7576
	SP3BRB		150.0000	0.3289	0.4855	0.3297	0.2146	1.2841	0.0826	3.2746
	SP5BLB		200.0000	0.4265	0.4638	0.3160	0.2478	1.5189	0.0920	3.5210
	SP6BRB		100.0000	0.2615	0.4303	0.4000	0.2552	1.9637	0.0324	2.8786
	SP8BLB		224.0000	0.1669	0.6331	0.5439	0.1401	1.1324	0.0328	0.6218
	SP12BRB		240.0000	0.2116	0.5030	0.4795	0.2036	1.2230	0.0287	1.0984
		AVERAGE	177.3333	0.2693	0.5284	0.4055	0.2058	1.4494	0.0879	2.1920
		ST. DEV	53.0911	0.0944	0.0929	0.0896	0.0439	0.3046	0.0881	1.2050
BUFFER OVERALL		AVERAGE	159.0000	0.2905	0.5082	0.4165	0.2374	1.7472	0.0766	3.4646
		ST. DEV	50.6557	0.1112	0.1603	0.1231	0.0928	0.6832	0.0762	2.2396
GENIPIN TOPS	SP2TRG		125.0000	0.3105	0.3638	0.2925	0.2861	2.3202	0.0547	3.8934
	SP4TLG	50-60	100.0000	0.4863	0.2931	0.2709	0.4638	2.9275	0.0554	11.5156
	SP5TRG	10	175.0000	0.4078	0.4873	0.4640	0.3810	2.0994	0.0515	1.3316
	SP7TLG	3/15/00	125.0000	0.51024	0.4389	0.3847	0.4754	3.8168	0.0871	11.0728
	SP8TRG	100	80.0000	0.4657	0.2698	0.2430	0.4055	3.9628	0.0394	8.2272
	SP10TLG	50	125.0000	0.5664	0.2639	0.2084	0.4733	4.0995	0.0685	15.2316
	SP11TRG	80	125.0000	0.5431	0.2049	0.1538	0.4266	4.7819	0.0547	23.8420
	SP12TLG	80	110.0000	0.5432	0.2764	0.2324	0.4586	3.4349	0.0612	12.0744
		AVERAGE	120.6250	0.4792	0.3248	0.2812	0.4213	3.4304	0.0591	10.8986
		ST. DEV	27.3127	0.0850	0.0967	0.0998	0.0644	0.9230	0.0140	6.9255
GENIPIN BOTTOMS	SP1BLG	minimal	175.0000	0.1828	0.3720	0.2887	0.1712	1.3199	0.0390	3.4988
	SP2BRG		100.0000	0.2881	0.4244	0.2578	0.2372	2.2613	0.1411	4.5670
	SP4BLG	70-80	100.0000	0.2836	0.3406	0.3349	0.2805	2.3176	0.0253	2.9036
	SP8BRG	minimal	70.0000	0.2223	0.4216	0.4003	0.2153	1.6624	0.0288	1.2720
	SP10BLG	50	240.0000	0.2500	0.4277	0.2209	0.2209	1.2468	0.0362	2.3258
	SP11BRG	50	120.0000	0.2755	0.3327	0.2917	0.2457	1.9126	0.0345	4.1440
		AVERAGE	134.1667	0.2504	0.3865	0.2991	0.2286	1.7868	0.0508	3.1185
		ST. DEV	62.4833	0.0413	0.0438	0.0625	0.0364	0.4578	0.0445	1.2148
GENIPIN OVERALL		AVERAGE	126.4286	0.3811	0.3512	0.2889	0.3387	2.7260	0.0555	7.5643
		ST. DEV	44.1775	0.1354	0.0823	0.0834	0.1119	1.1189	0.0298	6.5088

Toughness - Entire Curve J/mm^3	Energy - Entire Curve Joules	1st Cycle Hysteresis Mpa	Change in Hysteresis Mpa	Hysteresis Ratio 20th/1st	Stress Relaxation Mpa	Relaxation Modulus Mpa	Normalized Relaxation Modulus Mpa
5007449.7830	28.1669	0.0054213	0.00415507	0.23356575	0.0167432	0.04443518	0.00027362
339165.7400	1.4245	0.01052602	0.00977278	0.071559811	0.017409	0.04362838	0.01208943
452761.4960	5.3245	0.0028672	0.00165491	0.422813198	0.002181786	0.00584697	0.0016202
5468984.4790	27.5637	0.00722487	0.00496173	0.313243006	0.007559167	0.03086297	0.00855213
590810.5410	6.2035	0.00302699	0.00230305	0.239161675	0.0049916	0.01530142	0.0042402
227478.7090	0.8408	0.01041757	0.00598871	0.425133692	0.009104545	0.04292754	0.01189522
2014441.7913	11.5873	0.0066	0.0048	0.2842	0.0097	0.0305	0.0064
2504289.1289	12.7836	0.0034	0.0029	0.1340	0.0062	0.0165	0.0051
77395.9240	1.2190	0.00202159	0.0013275	0.343338659	0.004408857	0.0417207	0.01156081
225701.6500	1.1849	0.00918219	0.00796379	0.132691656	0.009554	0.03729806	0.01033529
618956.1780	5.4592	0.00485223	0.00393722	0.18857515	0.007164286	0.02359034	0.00653688
313658.6300	3.1617	0.0035201	0.00266695	0.242365274	0.00664	0.01846934	0.00511786
330072.0600	2.9112	0.00414695	0.00320766	0.226501405	0.005967143	0.02851624	0.00790185
137035.2400	1.4101	0.00331113	0.00246144	0.256616321	0.004456327	0.01281082	0.00354988
283803.2803	2.5577	0.0045	0.0036	0.2317	0.0064	0.0271	0.0075
191248.6656	1.6675	0.0025	0.0023	0.0706	0.0019	0.0111	0.0031
1149122.5358	7.0725	0.0055	0.0042	0.2580	0.0080	0.0288	0.0070
1919411.1179	9.8885	0.0030	0.0026	0.1057	0.0047	0.0135	0.0041
1802022.3850	10.1364	0.00747343	0.0059409	0.205063806	0.0178384	0.02972328	0.00899823
1883156.1530	9.8866	0.00650406	0.00457885	0.296001267	0.0129256	0.04431149	0.01341457
254078.7800	1.0671	0.00968556	0.00801323	0.17266219	0.010064	0.0301769	0.00913555
107533.1850	0.9484	0.00370251	0.0027	0.278705527	0.007292857	0.02803863	0.00848823
368002.8080	1.9320	0.0069986	0.00510375	0.270747007	0.009576	0.05739376	0.017375
882958.6622	4.7941	0.0069	0.0053	0.2446	0.0115	0.0379	0.0115
881338.0815	4.7787	0.0021	0.0020	0.0530	0.0041	0.0127	0.0038
652459.3200	4.4041	0.00615503	0.00524338	0.148114631	0.012994667	0.04497505	0.01361545
556280.1800	3.5046	0.00629072	0.00506803	0.194364079	0.011962	0.0580374	0.01756986
880617.5570	7.3972	0.00317604	0.00202703	0.361774411	0.005845	0.03320817	0.01005322
835688.6380	3.5099	0.00805687	0.00633984	0.213113777	0.013143	0.04114805	0.01245689
433509.7060	4.0785	0.00438504	0.0036	0.185534665	0.006175	0.01379867	0.00417732
406534.8840	4.0979	0.00374423	0.0029014	0.225101022	0.006777917	0.020311	0.00614882
627515.0475	4.4987	0.0053	0.0042	0.2213	0.0095	0.0352	0.0107
199781.9073	1.4638	0.0018	0.0016	0.0737	0.0036	0.0163	0.0049
743625.7815	4.6330	0.0060	0.0047	0.2319	0.0104	0.0365	0.0110
590300.7523	3.1984	0.0021	0.0018	0.0632	0.0037	0.0141	0.0043
260762.2460	1.4668	0.00602158	0.00438297	0.272122931	0.0106144	0.05163772	0.0121622
259040.6800	1.1657	0.00843558	0.00652871	0.226050847	0.036807	0.127908	0.08600604
522051.2600	3.8371	0.00609898	0.00450561	0.261251881	0.00699429	0.02139244	0.00503855
5120691.01300	26.42640	0.00647345	0.00407591	0.37036511	0.0074744	0.02732503	0.00643585
469282.1040	1.5768	0.0114957	0.00866071	0.246613081	0.010525	0.05976306	0.01407596
572448.4610	3.0054	0.00695574	0.0043041	0.381216089	0.0071888	0.06834513	0.01609729
231183.9180	1.2137	0.00809808	0.00493693	0.390357961	0.0070456	0.0957562	0.0225534
474792.9050	2.1935	0.00707158	0.00424218	0.400108604	0.009437273	0.07614042	0.01793331
988781.5734	5.1107	0.0076	0.0052	0.3185	0.0120	0.0660	0.0225
1674787.7577	8.6639	0.0018	0.0016	0.0733	0.0101	0.0350	0.0263
457198.0200	3.6004	0.00529066	0.00430698	0.185927654	0.008716	0.17152572	0.04039935
520727.4310	2.3433	0.00934515	0.00780014	0.165327469	0.010128	0.02313568	0.00544913
1520331.6030	6.3854	0.00688308	0.00444926	0.353594612	0.007962	0.03136014	0.00738624
226853.7330	0.6669	0.01170408	0.00991178	0.153134633	0.022505714	0.06386675	0.0150426
492218.9900	4.9616	0.00342053	0.00233102	0.318520814	0.005965417	0.01864345	0.00439108
294262.5530	1.4831	0.00663853	0.00479991	0.276961918	0.007889167	0.0389249	0.00916796
585265.3883	3.2401	0.0072	0.0056	0.2422	0.0105	0.0579	0.0136
472591.6677	2.1679	0.0029	0.0027	0.0854	0.0060	0.0579	0.0136
815846.0655	4.3090	0.0074	0.0054	0.2858	0.0114	0.0626	0.0187
1280305.5785	6.5688	0.0023	0.0021	0.0850	0.0084	0.0443	0.0215

APPENDIX D4: Averages and standard deviations of data

Table 4.13: Averages and standard deviations for each parameter. The percent differences comparing each group are also listed.

		Cross Section	Ulitmate Tensile Stress	Strain at Ultimate Tensile Stress	Yield Point Strain	Yield Point Stress	Young's Modulus - Linear Region
CONTROL TOPS	AVERAGE	160.5000	0.3375	0.5175	0.4163	0.2635	2.2019
	ST. DEV	82.5924	0.1728	0.1505	0.0805	0.1458	1.4320
BUFFER TOPS	AVERAGE	137.0000	0.3159	0.4839	0.4298	0.2753	2.1045
	ST. DEV	42.2197	0.1353	0.2283	0.1656	0.1259	0.8708
GENIPIN TOPS	AVERAGE	120.6250	0.4792	0.3248	0.2812	0.4213	3.4304
	ST. DEV	27.3127	0.0850	0.0967	0.0998	0.0644	0.9230
CONTROL BOTTOMS	AVERAGE	230.0000	0.1623	0.3970	0.3616	0.1530	1.3017
	ST. DEV	72.8697	0.0403	0.1145	0.0958	0.0384	0.4563
BUFFER BOTTOMS	AVERAGE	177.3333	0.2693	0.5284	0.4055	0.2058	1.4494
	ST. DEV	53.0911	0.0944	0.0929	0.0896	0.0439	0.3046
GENIPIN BOTTOMS	AVERAGE	134.1667	0.2504	0.3865	0.2991	0.2286	1.7868
	ST. DEV	62.4833	0.0413	0.0438	0.0625	0.0364	0.4578
CONTROL OVERALL	AVERAGE	195.2500	0.2499	0.4572	0.3889	0.2082	1.7518
	ST. DEV	82.6539	0.1506	0.1422	0.0890	0.1169	1.1170
BUFFER OVERALL	AVERAGE	159.0000	0.2905	0.5082	0.4165	0.2374	1.7472
	ST. DEV	50.6557	0.1112	0.1603	0.1231	0.0928	0.6832
GENIPIN OVERALL	AVERAGE	126.4286	0.3811	0.3512	0.2889	0.3387	2.7260
	ST. DEV	44.1775	0.1354	0.0823	0.0834	0.1119	1.1189

% Difference	Buffer vs Genipin	Cross Section	Ulitmate Tensile Stress	Strain at Ultimate Tensile Stress	Yield Point Strain	Yield Point Stress	Young's Modulus - Linear Region
TOPS	AVERAGE	11.95%	-51.67%	32.89%	34.57%	-53.04%	-63.00%
BOTTOMS	AVERAGE	24.34%	7.02%	26.85%	26.24%	-11.09%	-23.28%
OVERALL	AVERAGE	20.49%	-31.20%	30.88%	30.65%	-42.69%	-56.02%

% Difference	Control vs Buffer	Cross Section	Ulitmate Tensile Stress	Strain at Ultimate Tensile Stress	Yield Point Strain	Yield Point Stress	Young's Modulus - Linear Region
TOPS	AVERAGE	14.64%	6.40%	6.49%	-3.24%	-4.48%	4.42%
BOTTOMS	AVERAGE	22.90%	-65.88%	-33.08%	-12.14%	-34.54%	-11.35%
OVERALL	AVERAGE	18.57%	-16.24%	-11.14%	-7.10%	-14.02%	0.26%

Resilience	Slope - Toe Region	Toughness - Entire Curve	Energy - Entire Curve	1st Cycle Hysteresis	Δ Hysteresis	Hysteresis Ratio	Stress Relaxation	Relaxation Modulus	Normalized Relaxation Modulus
0.0790	4.2560	2.0144	11.5873	0.0066	0.0048	0.2842	0.0097	0.0305	0.0064
0.0769	4.8824	2.5043	12.7836	0.0034	0.0029	0.1340	0.0062	0.0165	0.0051
0.0631	4.9916	0.8830	4.7941	0.0069	0.0053	0.2446	0.0115	0.0379	0.0115
0.0662	2.3197	0.8813	4.7787	0.0021	0.0020	0.0530	0.0041	0.0127	0.0038
0.0591	10.8986	0.9888	5.1107	0.0076	0.0052	0.3185	0.0120	0.0660	0.0225
0.0140	6.9265	1.6748	8.6639	0.0018	0.0016	0.0733	0.0101	0.0350	0.0263
0.0234	3.1590	0.2604	2.3389	0.0045	0.0036	0.2317	0.0064	0.0271	0.0075
0.0153	2.1528	0.1904	1.6615	0.0025	0.0023	0.0706	0.0019	0.0111	0.0031
0.0879	2.1920	0.6275	4.4987	0.0053	0.0042	0.2213	0.0095	0.0352	0.0107
0.0881	1.2050	0.1998	1.4638	0.0018	0.0016	0.0737	0.0036	0.0163	0.0049
0.0508	3.1185	0.5853	3.2401	0.0072	0.0056	0.2422	0.0105	0.0579	0.0136
0.0445	1.2148	0.4726	2.1679	0.0029	0.0027	0.0854	0.0060	0.0579	0.0136
0.0512	3.7075	1.1491	7.0725	0.0055	0.0042	0.2580	0.0080	0.0288	0.0070
0.0603	3.6428	1.9194	9.8885	0.0030	0.0026	0.1057	0.0047	0.0135	0.0041
0.0766	3.4646	0.7436	4.6330	0.0060	0.0047	0.2319	0.0104	0.0365	0.0110
0.0762	2.2396	0.5903	3.1984	0.0021	0.0018	0.0632	0.0037	0.0141	0.0043
0.0555	7.5643	0.8158	4.3090	0.0074	0.0054	0.2858	0.0114	0.0626	0.0187
0.0298	6.5088	1.2803	6.5688	0.0023	0.0021	0.0850	0.0084	0.0443	0.0215

Resilience	Slope - Toe Region	Toughness - Entire Curve	Energy - Entire Curve	1st Cycle Hysteresis	Δ Hysteresis	Hysteresis Ratio	Stress Relaxation	Relaxation Modulus	Normalized Relaxation Modulus
6.43%	-118.34%	-11.99%	-6.60%	-10.31%	1.08%	-30.20%	-4.09%	-74.10%	-96.28%
42.14%	-42.27%	6.73%	27.98%	-36.07%	-33.59%	-9.43%	-10.73%	-64.27%	-27.83%
27.51%	-118.33%	-9.71%	6.99%	-23.41%	-14.88%	-23.24%	-9.19%	-71.54%	-69.61%

Resilience	Slope - Toe Region	Toughness - Entire Curve	Energy - Entire Curve	1st Cycle Hysteresis	Δ Hysteresis	Hysteresis Ratio	Stress Relaxation	Relaxation Modulus	Normalized Relaxation Modulus
20.11%	-17.28%	56.17%	58.63%	-4.44%	-9.48%	13.94%	-19.39%	-24.36%	-78.16%
-276.07%	30.61%	-140.94%	-92.34%	-17.66%	-16.63%	4.47%	-48.98%	-30.22%	-42.26%
-49.67%	6.55%	35.29%	34.49%	-8.52%	-11.38%	10.09%	-29.98%	-26.69%	-58.32%

APPENDIX D5: F-test results for each parameter

Table 4.16: Critical F values for each comparison for the mechanical testing study

Control vs Genipin	F Crit	Buffer vs Control	F Crit	Buffer vs Genipin	F Crit
Overall	2.53424325	Overall	2.71733144	Overall	2.56549741
Tops	3.58058032	Tops	4.38737	Tops	3.68749867
Bottoms	4.28386571	Bottoms	4.28386571	Bottoms	4.28386571

Table 4.17: F-test results for each individual parameter. Values that do not pass the test are highlighted in pink with red text.

F-Test	Determine whether t-test can be used or not				
Test: F-Test Control vs Genipin	Ulitmate Tensile Stress	Strain at Ultimate Tensile Stress	Yield Point Strain	Yield Point Stress	Young's Modulus - Linear Region
Overall	5.467	5.615	1.257	8.429	4.906
Tops only	4.127	8.548	3.525	7.571	3.829
Bottoms Only	13.972	0.044	1.792	12.287	3.38
Test: F-test Buffer vs Control	Ulitmate Tensile Stress	Strain at Ultimate Tensile Stress	Yield Point Strain	Yield Point Stress	Young's Modulus - Linear Region
Overall	0.531	0.651	0.384	0.433	0
Tops only	0.052	0.086	0.031	0.89	0.018
Bottoms Only	6.518	4.761	0.672	4.918	0.435
Test: F-test Buffer vs Genipin	Ulitmate Tensile Stress	Strain at Ultimate Tensile Stress	Yield Point Strain	Yield Point Stress	Young's Modulus - Linear Region
Overall	3.284	4.877	1.4	5.239	4.069
Tops only	3.149	3.077	1.722	4.349	3.129
Bottoms Only	4.794	4.754	2.438	5.733	2.18

Resilience	Slope - Toe Region	Toughness - Entire Curve	Energy - Entire Curve	1st Cycle Hysteresis	Δ Hysteresis (1st - 20th)	Hysteresis Ratio	Stress Relaxation	Relaxation Modulus	Normalized Relaxation Modulus
0.057	3.311	0.298	0.701	1.383	1.644	0.555	1.52	6.418	3.443
0.53	3.99	0.85	1.231	0.148	0.158	0.379	0.248	5.238	2.145
2.043	0.002	1.685	0.31	1.466	1.321	0.055	2.602	0.52	1.158

Resilience	Slope - Toe Region	Toughness - Entire Curve	Energy - Entire Curve	1st Cycle Hysteresis	Δ Hysteresis (1st - 20th)	Hysteresis Ratio	Stress Relaxation	Relaxation Modulus	Normalized Relaxation Modulus
0.795	0.036	0.54	0.733	0.187	0.261	0.502	1.81	1.775	5.448
0.132	0.094	0.942	1.281	0.027	0.049	0.381	0.334	0.676	3.255
3.12	0.922	6.093	2.942	0.399	0.475	0.062	3.562	1.19	1.78

Resilience	Slope - Toe Region	Toughness - Entire Curve	Energy - Entire Curve	1st Cycle Hysteresis	Δ Hysteresis (1st - 20th)	Hysteresis Ratio	Stress Relaxation	Relaxation Modulus	Normalized Relaxation Modulus
0.658	3.1334	0.331	0.573	0.863	0.956	1.194	0.995	4.729	2.474
0.238	3.119	0.702	0.398	0.086	0.091	0.978	0.163	3.742	1.514
1.889	0.712	1.492	1.119	0.954	0.777	0.111	1.604	1.423	0.772

APPENDIX D6: p-value results for each parameter

Table 4.18: p-value results for each parameter. The categories that failed the F-test were analyzed with the Mann-Whitney U non-parametric test, and those that passed were analyzed with the t-test. Statistically significant values with a p value < 0.05 at α = 0.05 are highlighted in red and pink.

Test: Mann- Whitney Buffer vs Control	Ulitmate Tensile Stress	Strain at Ultimate Tensile Stress	Yield Point Strain	Yield Point Stress	Young's Modulus - Linear Region
Bottoms Only	0.037	0.055	0.522	0.055	0.337

Test: t-test independent Buffer vs Control	Ulitmate Tensile Stress	Strain at Ultimate Tensile Stress	Yield Point Strain	Yield Point Stress	Young's Modulus - Linear Region
Overall	0.474	0.429	0.542	0.518	0.991
Tops only	0.825	0.776	0.863	0.89	0.898

Test: t-test independent Buffer vs Genipin	Ulitmate Tensile Stress	Strain at Ultimate Tensile Stress	Yield Point Strain	Yield Point Stress	Young's Modulus - Linear Region
Tops only	0.021	0.105	0.172	0.017	0.026

Test: Mann- Whitney Buffer vs Genipin	Ulitmate Tensile Stress	Strain at Ultimate Tensile Stress	Yield Point Strain	Yield Point Stress	Young's Modulus - Linear Region
Overall	0.09	0.006	0.298	0.049	0.014
Bottoms Only	0.873	0.004	0.055	0.423	0.15

Resilience	Slope - Toe Region	Toughness - Entire Curve	Energy - Entire Curve	1st Cycle Hysteresis	Δ Hysteresis (1st - 20th)	Hysteresis Ratio	Stress Relaxation	Relaxation Modulus	Normalized Relaxation Modulus
0.057	3.311	0.298	0.701	1.383	1.644	0.555	1.52	6.418	3.443
0.53	3.99	0.85	1.231	0.148	0.158	0.379	0.248	5.238	2.145
2.043	0.002	1.685	0.31	1.466	1.321	0.055	2.602	0.52	1.158

Resilience	Slope - Toe Region	Toughness - Entire Curve	Energy - Entire Curve	1st Cycle Hysteresis	Δ Hysteresis (1st - 20th)	Hysteresis Ratio	Stress Relaxation	Relaxation Modulus	Normalized Relaxation Modulus
0.795	0.036	0.54	0.733	0.187	0.261	0.502	1.81	1.775	5.448
0.132	0.094	0.942	1.281	0.027	0.049	0.381	0.334	0.676	3.255
3.12	0.922	6.093	2.942	0.399	0.475	0.062	3.562	1.19	1.78

Resilience	Slope - Toe Region	Toughness - Entire Curve	Energy - Entire Curve	1st Cycle Hysteresis	Δ Hysteresis (1st - 20th)	Hysteresis Ratio	Stress Relaxation	Relaxation Modulus	Normalized Relaxation Modulus
0.658	3.1334	0.331	0.573	0.863	0.956	1.194	0.995	4.729	2.474
0.238	3.119	0.702	0.398	0.086	0.091	0.978	0.163	3.742	1.514
1.889	0.712	1.492	1.119	0.954	0.777	0.111	1.604	1.423	0.772

REFERENCES

1. Hormann, K., & Verse, T. (2010). *Surgery for sleep- disordered breathing* (2.nd ed.). Berlin: Springer.
2. Strohl, K., Butler, J., & Malhotra, A. (2012). Mechanical Properties of the Upper Airway. *Comprehensive Physiology*. Retrieved October 26, 2015, from Pubmed.
3. Friedman, M. (2009). *Sleep apnea and snoring: Surgical and non-surgical therapy*. Edinburgh?: Saunders/Elsevier.
4. Johnson, J., Gluckman, J., & Sanders, M. (Eds.). (2002). *Management of obstructive sleep apnea*. London: Martin Dunitz ;.
5. Kotecha, B., & Hall, A. (2014). Role of surgery in adult obstructive sleep apnoea. *Sleep Medicine Reviews,* 405-413. Retrieved October 27, 2015, from Pubmed.
6. Fischer Y, Hafner B, Mann WJ. [Radiofrequency ablation of the soft palate (somnoplasty). A new method in the treatment of habitual and obstructive snoring]. *HNO* 2000;48:33-40
7. Lauretano AM, Khosla RK, Richardson G et al. Efficacy of laser-assisted uvulopalatoplasty. *Lasers Surg.Med.* 1997;21:109-16.
8. Blumen MB, Dahan S, Fleury B et al. Radiofrequency ablation for the treatment of mild to moderate obstructive sleep apnea. *Laryngoscope* 2002;112:2086-92.
9. Brietzke SE, Mair EA. Injection snoreplasty: investigation of alternative sclerotherapy agents. *Otolaryngol.Head Neck Surg.* 2004;130:47-57.
10. Brietzke SE, Mair EA. Injection snoreplasty: extended follow-up and new objective data. *Otolaryngol.Head Neck Surg.* 2003;128:605-15.
11. Brietzke SE, Mair EA. Injection snoreplasty: how to treat snoring without all the pain and expense. *Otolaryngol.Head Neck Surg.* 2001;124:503-10.
12. Marcoux M, Picandet V, Celeste C et al. Palatal sclerotherapy: a potentially useful treatment of intermittent dorsal displacement of the soft palate in juvenile standardbred racehorses. *Can.Vet.J.* 2008;49:587-91
13. Catalano P, Goh YH, Romanow J. Additional palatal implants for refractory snoring. *Otolaryngol.Head Neck Surg.* 2007;137:105-9.
14. Romanow JH, Catalano PJ. Initial U.S. pilot study: palatal implants for the treatment of snoring. *Otolaryngol.Head Neck Surg.* 2006;134:551-7.
15. Friedman M, Vidyasagar R, Bliznikas D et al. Patient selection and efficacy of pillar implant technique for treatment of snoring and obstructive sleep apnea/hypopnea syndrome. *Otolaryngol.Head Neck Surg.* 2006;134:187-96.

16. Schreuders PD, Salthouse TN, von Recum AF. Normal wound healing compared to healing within porous Dacron implants. *J.Biomed.Mater.Res.* 1988;22:121-35.
17. Fomin D, Nicola E, Oliver C et al. Collagen type analysis in the soft palate after surgical intervention with CO(2) laser and radiofrequency ablation. *Photomed.Laser Surg.* 2007;25:449- 54.
18. Hedman TP, Chuang SY, Syed BGD. Biomechanical benefits of crosslink augmentation in spinal discs. *Proceedings of IMECE* 2003;43256.
19. Chuang SY, Odono RM, Hedman TP. Effects of exogenous crosslinking on in vitro tensile and compressive moduli of lumbar intervertebral discs. *Clin.Biomech.* 2007;22:14-20.
20. Slusarewicz P, Zhu K, Kirking B et al. Optimization of Protein Crosslinking Formulations for the Treatment of Degenerative Disc Disease. *Spine* 2010;In Press.
21. Charulatha V, Rajaram A. Influence of different crosslinking treatments on the physical properties of collagen membranes. *Biomaterials* 2003;24:759-67.
22. Han B, Jaurequi J, Tang BW et al. Proanthocyanidin: a natural crosslinking reagent for stabilizing collagen matrices. *J.Biomed.Mater.Res.A* 2003;65:118-24
23. Slusarewicz P, Zhu K, Hedman TP. Kinetic Characterization and Comparison of Various Protein Crosslinking Reagents for Matrix Modification. *J.Mater.Sci.Mater.Med.* 2010;DOI: 10.1007/s10856-010-3986-8..
24. Sung HW, Liang IL, Chen CN et al. Stability of a biological tissue fixed with a naturally occurring crosslinking agent (genipin). *J.Biomed.Mater.Res.* 2001;55:538-46.
25. Tang SY, Sharan AD, Vashishth D. Effects of collagen crosslinking on tissue fragility. *Clin.Biomech.(Bristol., Avon.)* 2008;23:122-3.
26. Vasudev SC, Chandy T. Effect of alternative crosslinking techniques on the enzymatic degradation of bovine pericardia and their calcification. *J.Biomed.Mater.Res.* 1997;35:357-69.
27. Hawkins, J. (2014). Dorsal Displacement of the Soft Palate. In *Advances in equine upper respiratory surgery*. Somerset, NJ: Wiley.
28. Tan, R., Dowling, B., & Dart, A. (2004). High-speed treadmill videoendoscopic examination of the upper respiratory tract in the horse: The results of 291 clinical cases. *The Veterinary Journal,* 243-248. Retrieved October 27, 2015, from Pubmed

29. Priest, D., Cheetham, J., Regner, A., Mitchell, L., Soderholm, L., Tamzali, Y., & Ducharme, N. (2012). Dynamic respiratory endoscopy of Standardbred racehorses during qualifying races. *Equine Veterinary Journal,* 529-534. Retrieved October 27, 2015, from Pubmed.
30. Martin, B., Reef, V., Parente, E., & Sage, A. (2000). Causes of poor performance of horses during training, racing, or showing: 348 cases (1992-1996). *Journal of the American Veterinary Medical Association, 216*(4), 554-558. Retrieved October 27, 2015, from Pubmed.
31. Ferrucci, F., Zucca, E., Fabio, V., & Ferro, E. (2013). Treadmill Endoscopic Findings in 15 Racehorses Presented for Poor Performance. *Veterinary Research Communications Vet Res Commun,* 395-397. Retrieved October 27, 2015, from Pubmed.
32. Lane, J., Bladon, B., Little, D., Naylor, J., & Franklin, S. (2006). Dynamic obstructions of the equine upper respiratory tract. Part 1: Observations during high-speed treadmill endoscopy of 600 Thoroughbred racehorses. *Equine Veterinary Journal, 38*, 393-399. Retrieved October 27, 2015, from Pubmed.
33. Davidson, E., Martin, B., Boston, R., & Parente, E. (2010). Exercising upper respiratory videoendoscopic evaluation of 100 nonracing performance horses with abnormal respiratory noise and/or poor performance. *Equine Veterinary Journal,* 3-8. Retrieved October 27, 2015, from Pubmed.
34. Strohl, K., & Olson, L. (1987). Concerning the importance of pharyngeal muscles in the maintenance of upper airway patency during sleep. An opinion. *CHEST Journal CHEST,* 918-918. Retrieved October 30, 2015, from http://chestjournal.chestpubs.org/content/92/5/918.citation
35. Randerath, W., Sanner, B., & Somers, V. (Eds.). (2006). *Sleep Apnea: Current Diagnosis and Treatment* (Vol. 35). Reinhardt Druck.
36. Choi, J., Kim, S., & Cho, J. (2012). Efficacy of the pillar implant in the treatment of snoring and mild-to-moderate obstructive sleep apnea: A meta-analysis. *The Laryngoscope,* 269-276. Retrieved October 27, 2015, from Pubmed.
37. Lavigne, G., Cistulli, P., & Smith, M. (Eds.). (2009). *Sleep medicine for dentists: A practical overview*. Chicago, Illinois: Quintessence Pub.
38. Wang, Z., Rebeiz, E., & Shapshay, S. (2002). Laser soft palate “stiffening”: An alternative to uvulopalatopharyngoplasty. *Lasers Surg. Med. Lasers in Surgery and Medicine,* 40-43.

39. Fairbanks, D., & Fujita, S. (Eds.). (1994). *Snoring and obstructive sleep apnea* (2nd ed.). Philadelphia, PA: Lippincott Williams & Wilkins.
40. Beck, R., Odeh, M., Oliven, A., & Gavriely, N. (1995). The acoustic properties of snores. *European Respiratory Journal,* 2120-2128. Retrieved October 27, 2015, from Pubmed.
41. Acar, M., Yaz C , D., Muluk, N., Hanc , D., Seren, E., & Cingi, C. (2015). Is There a Relationship Between Snoring Sound Intensity and Frequency and OSAS Severity? *Annals of Otology, Rhinology & Laryngology*. Retrieved October 27, 2015, from Pubmed.
42. Azarbarzin, A., & Moussavi, Z. (2012). Snoring sounds variability as a signature of obstructive sleep apnea. *Medical Engineering & Physics,* 479-485.
43. Mitchell, C., & Heidorn, N. (2013, October 15). Dorsal Displacement of the Soft Palate in Horses. Retrieved October 27, 2015.
44. Beech, J. (1991). *Equine respiratory disorders*. Philadelphia, Pennsylvania: Lea & Febiger.
45. Allen, K., & Franklin, S. (2013). The effect of palatal dysfunction on measures of ventilation ... Retrieved October 27, 2015.
46. White III, N., & Moore, J. (1990). In *Current Practice of Equine Snoring*. Philadelphia, Pennsylvania: J.B. Lippincott Company.
47. Woodie, J., Ducharme, N., Hackett, R., Erb, H., Mitchell, L., & Soderholm, L. (2005). Can an external device prevent dorsal displacement of the soft palate during strenuous exercise? *Equine Veterinary Journal, 37*(5), 425-429.
48. Smith, J., & Embertson, R. (2005). Sternothyroideus Myotomy, Staphylectomy, and Oral Caudal Soft Palate Photothermoplasty for Treatment of Dorsal Displacement of the Soft Palate in 102 Thoroughbred Racehorses. *Veterinary Surgery,* 5-10. Retrieved October 27, 2015, from Pubmed.
49. Marcoux, M., Picandet, V., Celeste, C., Macieira, S., Morisset, S., Rossier, Y., . . . Jean, D. (2008). Palatal sclerotherapy: A potentially useful treatment of intermittent dorsal displacement of the soft palate in juvenile standardbred racehorses. *Canada Veterinary Journal, 49*, 587-591. Retrieved October 27, 2015, from Pubmed.
50. Woodie, J., Ducharme, N., Kanter, P., Hackett, R., & Erb, H. (2005). Surgical advancement of the larynx (laryngeal tie-forward) as a treatment for dorsal

displacement of the soft palate in horses: A prospective study 2001-2004. *Equine Veterinary Journal, 37*(5), 418-423. Retrieved October 27, 2015, from Pubmed.

51. Barakzai, S., Johnson, V., Baird, D., Bladon, B., & Lane, J. (2004). Assessment of the efficacy of composite surgery for the treatment of dorsal displacement of the soft palate in a group of 53 racing Thoroughbreds (1990-1996). *Equine Veterinary Journal, 36*, 175-179. Retrieved October 27, 2015, from Pubmed.
52. Muñoz, J., Marcoux, M., Picandet, V., Theoret, C., Perron, M., & Lepage, O. (2008). Histological and biomechanical effects of palatal sclerotherapy in the horse using sodium tetradecyl sulfate. *The Veterinary Journal,* 316-321. Retrieved October 27, 2015, from Pubmed.
53. Alkabes, K., Hawkins, J., Miller, M., Nauman, E., Widmer, W., Dunco, D., . . . Gautam, R. (2010). Evaluation of the effects of transendoscopic diode laser palatoplasty on clinical, histologic, magnetic resonance imaging, and biomechanical findings in horses. *American Journal of Veterinary Research, 71*(5), 575-582. Retrieved October 27, 2015, from Pubmed.
54. Derksen, F., Holcombe, S., Hartmann, W., Robinson, N., & Stick, J. (2000). Spectrum analysis of respiratory sounds in exercising horses with experimentally induced laryngeal hemiplegia or dorsal displacement of the soft palate. *American Journal of Veterinary Research,* 659-664. Retrieved October 27, 2015, from Pubmed.
55. Franklin, S., Usmar, S., Lane, J., Shuttleworth, J., & Burn, J. (2003). Spectral analysis of respiratory noise in horses with upper airway disorders. *Equine Veterinary Journal, 35*(3), 264-268. Retrieved October 27, 2015, from Pubmed.
56. Franklin, S., Price, C., & Burn, J. (2004). The displaced equine soft palate as a source of abnormal respiratory noise during expiration. *Equine Veterinary Journal, 36*(7), 590-594. Retrieved October 27, 2015, from Pubmed.
57. Slusarewicz, P., Zhu, K., & Hedman, T. (2010). Kinetic characterization and comparison of various protein crosslinking reagents for matrix modification. *J Mater Sci: Mater Med Journal of Materials Science: Materials in Medicine,* 1175-1181. Retrieved October 27, 2015, from Pubmed.
58. Sung, H., Chang, W., Ma, C., & Lee, M. (2003). Crosslinking of biological tissues using genipin and/or carbodiimide. *Journal of Biomedical Materials Research J. Biomed. Mater. Res.,* 427-438.

59. Charulatha, V. (2002). Influence of different crosslinking treatments on the physical properties of collagen membranes. *Biomaterials,* 759-767. Retrieved October 27, 2015, from Pubmed.
60. Sung, H., Liang, I., Chen, C., Huang, R., & Liang, H. (2001). Stability of a biological tissue fixed with a naturally occurring crosslinking agent (genipin). *Journal of Biomedical Materials Research J. Biomed. Mater. Res.,* 538-546. Retrieved October 27, 2015, from Pubmed.
61. Sung, H., Chang, Y., Liang, I., Chang, W., & Chen, Y. (2000). Fixation of biological tissues with a naturally occurring crosslinking agent: Fixation rate and effects of pH, temperature, and initial fixative concentration. *Journal of Biomedical Materials Research,* 77-87. Retrieved October 27, 2015, from Pubmed.
62. Novobrace™ | Tendonitis, Desmitis and soft tissue injury treatment for horses. (n.d.). Retrieved October 27, 2015.
63. Huang, L., Sung, H., Tsai, C., & Huang, D. (1998). Biocompatibility study of a biological tissue fixed with a naturally occurring crosslinking reagent. *Journal of Biomedical Materials Research J. Biomed. Mater. Res.,* 568-576. Retrieved October 27, 2015, from Pubmed.
64. Tsai, C., Huang, R., Sung, H., & Liang, H. (2000). In vitro evaluation of the genotoxicity of a naturally occurring crosslinking agent (genipin) for biologic tissue fixation. *Journal of Biomedical Materials Research J. Biomed. Mater. Res.,* 58-65. Retrieved October 27, 2015, from Pubmed.
65. Mcgann, M., Bonitsky, C., Jackson, M., Ovaert, T., Trippel, S., & Wagner, D. (2015). Genipin crosslinking of cartilage enhances resistance to biochemical degradation and mechanical wear. *Journal of Orthopaedic Research J. Orthop. Res.,* 1571-1579. Retrieved October 27, 2015, from Pubmed.
66. Photoshop RGB Color and Color Channels Tutorial. (2012, October 2). Retrieved October 27, 2015, from http://www.photoshopessentials.com/essentials/rgb/
67. BME 332: Ligament/Tendon Structure-Function. (n.d.). Retrieved October 27, 2015, from http://www.umich.edu/~bme332/ch10ligten/bme332ligamenttendon.htm
68. Interpretation of stress strain curves and mechanical properties of materials. (n.d.). Retrieved October 27, 2015, from http://www.tiniusolsen.com/pdf/Pamphlet4.pdf

69. Roylance, D. (2001, August 23). Stress-strain curves. Retrieved October 27, 2015, from http://ocw.mit.edu/courses/materials-science-and-engineering/3-11-mechanics-of-materials-fall-1999/modules/ss.pdf
70. Two-sample t-test Using SPSS. (n.d.). Retrieved October 27, 2015, from http://www.stattutorials.com/SPSS/TUTORIAL-SPSS-two-sample-t-test.htm
71. Fessel, G., Cadby, J., Wunderli, S., Weeren, R., & Snedeker, J. (2013). Dose- and time-dependent effects of genipin crosslinking on cell viability and tissue mechanics – Toward clinical application for tendon repair. *Acta Biomaterialia,* 1897-1906. Retrieved November 15, 2015, from Pubmed.

VITA

Stephanie Louise Hunt

Birthplace: North Huntingdon, PA

Education:

B.S. in Biosystems Engineering, December 2013

University of Kentucky, Lexington, KY

Professional Positions:

- *Everburn Manufacturing,* Lexington, KY, Jan. 2014 – Present
  - Design Engineer
- *University of Kentucky*, Lexington, KY, Aug. 2013 – Dec. 2013
  - Undergraduate Research Assistant, Department of Biosystems Engineering
- *Gluck Equine Research Center*, Lexington, KY, Jan. 2010 – May 2013
  - Undergraduate Research Assistant, Department of Veterinary Science

Awards & Scholarships:

Margaret Ingles SWE Fellowship, Oct. 2014 – April 2015

USEC, INC. Fellowship, Oct. 2014 – April 2015

Professional Conference Abstracts & Presentations:

- *10th Annual CCTS Spring Conference*, Poster Presentation, Lexington, KY; March 2015
- *Society for Biomaterials, 2015 Annual Meeting,* Poster Presentation, Charlotte, NC; April 2015
- *2015 BMES Annual Meeting*, Podium Presentation, Tampa, FL; October 2015
- *2015 BMES Midwest Conference,* Poster Presentation, Akron, OH; November 2015